

**EVALUATING HUMAN HEALTH IMPACTS OF PRODUCTS FROM A LIFE CYCLE  
PERSPECTIVE: METHOD AND CASE STUDIES**

by

**Shen Tian**

BS in Environmental Sciences, Peking University, 2007

BA in International Relations, Peking University, 2007

MS in Environmental Sciences, Carnegie Mellon University, 2008

MS in Civil and Environmental Engineering, University of California, Davis, 2010

Submitted to the Graduate Faculty of  
the Swanson School of Engineering in partial fulfillment  
of the requirements for the degree of  
Doctor of Philosophy

University of Pittsburgh

2018

UNIVERSITY OF PITTSBURGH  
SWANSON SCHOOL OF ENGINEERING

This dissertation was presented

by

Shen Tian

It was defended on

November 13, 2018

and approved by

Radisav Vidic, PhD, Professor  
Department of Civil and Environmental Engineering

Eric Beckman, PhD, Professor  
Department of Chemical and Petroleum Engineering

Vikas Khanna, PhD, Associate Professor  
Department of Civil and Environmental Engineering

Dissertation Director:  
Melissa M. Bilec, PhD, Associate Professor  
Department of Civil and Environmental Engineering

Copyright © by Shen Tian

2018

**EVALUATING HUMAN HEALTH IMPACTS OF PRODUCTS FROM A LIFE CYCLE  
PERSPECTIVE: METHOD AND CASE STUDIES**

Shen Tian, Ph.D.

University of Pittsburgh, 2018

The human health impacts of products, especially those that may have consumer exposure, is a crucial aspect in product safety assessment. Existing life cycle assessment (LCA) is well established to evaluate products by traditional environmental metrics, such as global warming potential. However, a holistic and comprehensive approach is needed to study the human health impact of products along their life cycle and understand their fate, transport and distribution in the environment.

This dissertation illustrated how human health impact assessment (HHIA) could be conducted at product level from a life cycle perspective. This work showed that when advanced environmental engineering modeling tools are combined with LCA in product safety assessment, our understandings of chemical exposure and associated human health risks can be improved.

In this research, a method was developed to integrate high resolution air dispersion modeling and LCA to conduct HHIA, using publicly available inventory data. In particular, this method was applied to Methylene Diphenyl Diisocyanate (MDI), a chemical commonly used in building and construction products. It was found that the additional inhalation human health risks were three orders of magnitude lower than the United States Environmental Protection Agency (USEPA)'s risk management threshold.

Besides manufacturing stages, this research also evaluated the indoor air quality impact of the spray polyurethane foam (SPF) through industrial hygiene (IH) measurement, lab chamber testing and multi-media mass transfer modeling. The IH study revealed that MDI emitted from SPF decayed rapidly in the indoor environment. Two mass transfer models were employed to study the emission and distribution of Tris(1-Chloro-2-Propyl) Phosphate (TCPP), a flame retardant in SPF, and quantify its human health risks in the indoor environment. Verified by field measurements, the modeling results showed that TCPP was removed from indoor air primarily through indoor-outdoor ventilation, followed by the sorption into indoor diffusional sinks such as drywall. A screening level risk characterization revealed that in this SPF renovated house, TCPP time weighted average ingestion exposure of the most sensitive population (1-2 years old) was below ( $0.6 \mu\text{g}/\text{kg BW}/\text{day}$ ) the threshold set by USEPA ( $10 \mu\text{g}/\text{kg BW}/\text{day}$ ). The modeling approach is transferable to study other indoor pollutants.

## TABLE OF CONTENTS

<b>NOMENCLATURE.....</b>	<b>xviii</b>
<b>ACKNOWLEDGEMENTS .....</b>	<b>xx</b>
<b>1.0 INTRODUCTION.....</b>	<b>1</b>
1.1 PRODUCT SAFETY AND SUSTAINABILITY IN THE CHEMICAL INDUSTRY: FOCUSES ON CHEMICAL EXPOSURE.....	1
1.2 RESEARCH GOALS AND OBJECTIVES .....	3
1.3 BROADER IMPACTS .....	5
1.4 INTELLECTUAL MERIT .....	7
<b>2.0 BACKGROUND AND LITERATURE REVIEW .....</b>	<b>8</b>
2.1 CHEMICAL SAFETY REGULATIONS AND HHIA TOOLS .....	8
2.2 LCA AND HHRA: TWO POWERFUL METHODS IN HHIA .....	11
2.2.1 Life Cycle Assessment .....	11
2.2.2 Human health risk assessment.....	13
2.2.3 Previous work towards harmonizing LCA and HHRA for HHIA .....	14
2.2.3.1 Existing models in assessing human health impacts in LCA and HHRA....	16
2.2.3.2 Regionalization in LCA .....	19

2.2.3.3	Main obstacles in harmonizing existing tools for HHIA .....	22
2.3	<b>PRODUCT EMISSION AND INDOOR AIR QUALITY WITH FOCUS ON SVOCs</b> .....	29
2.3.1	Definition of SVOCs and their presence in the indoor environment .....	29
2.3.1.1	SVOCs in building and construction materials .....	30
2.3.1.2	OPFRs in the indoor environment.....	32
2.3.2	SVOCs measurement methods.....	35
2.3.3	SVOCs multi-media modeling .....	40
2.4	<b>INFORMATION OF CASE STUDY PRODUCTS AND CHEMICALS</b> .....	43
2.4.1	Methylene Diphenyl Diisocyanate and Spray Polyurethane Foam.....	44
2.4.1.1	Application and chemical properties.....	44
2.4.1.2	Environmental fate of MDI in air.....	45
2.4.1.3	Human health effects and exposure threshold of MDI .....	47
2.4.2	Tris(1-Chloro-2-Propyl) Phosphate.....	48
2.4.2.1	Application and chemical properties.....	48
2.4.2.2	TCPP presence in the indoor environment.....	49
2.4.2.3	Human health effects and exposure threshold of TCPP.....	50
<b>3.0</b>	<b>INTEGRATING SITE-SPECIFIC DISPERSION MODLEING INTO LIFE CYCLE ASSESSMENT: FOCUS ON INHALATION RISKS IN CHEMICAL PRODUCTION</b> .....	<b>52</b>
3.1	<b>INTRODUCTION</b> .....	<b>53</b>
3.1.1	The chemical industry and chemical management regulations.....	53

3.1.2	Existing methods to evaluate human health impacts of far-field chemical emissions.....	54
3.1.3	Previous work to evaluate the human health impacts of far-field chemical emissions.....	57
3.1.4	Objectives.....	59
3.1.5	Case study: cradle-to-gate production of MDI.....	59
3.2	<b>METHODS</b> .....	60
3.2.1	Scope of the case study (Step 1).....	61
3.2.2	Developing a regionalized LCI (Step 2) .....	64
3.2.3	Performing air dispersion modeling (Step 3a) .....	64
3.2.4	Calculating inhalation risks of site-specific unit processes (Step 3b).....	66
3.2.5	Calculating inhalation risks of non-site specific unit processes (Step 4).....	67
3.2.6	Combine the risk characterization values of all unit processes (Step 5).....	68
3.2.7	Identifying inhalation risk hotspots and patterns in GIS (Step 6).....	68
3.3	<b>RESULTS</b> .....	69
3.3.1	Site-specific unit processes .....	69
3.3.2	Non-site specific unit processes .....	74
3.3.3	Total inhalation risks of cradle-to-gate MDI production .....	76
3.4	<b>DISCUSSION</b> .....	76
3.4.1	Comparisons between HEM-3/AERMOD and USEtox .....	76
3.4.2	Impact of emission compartments in USEtox.....	78
3.4.3	Relative unit process contribution to the inhalation risks .....	79

3.4.4	Limitation of this study .....	81
3.5	CONCLUSIONS.....	83
<b>4.0</b>	<b>AN INDOOR AIR QUALITY EVALUATION IN A RESIDENTIAL RETROFIT PROJECT USING POLYURETHANE FOAM .....</b>	<b>86</b>
4.1	INTRODUCTION .....	87
4.1.1	Indoor air quality and spray polyurethane foam .....	87
4.1.2	Chemicals evaluated and their criteria values .....	89
4.2	METHODS AND MATERIALS.....	91
4.2.1	Building information and insulation material applied.....	91
4.2.2	Analytical methods and sampling procedure .....	92
4.2.2.1	Airborne MDI.....	93
4.2.2.2	Aldehydes.....	95
4.2.2.3	Blowing agent and flame retardant .....	96
4.2.2.4	Airborne particles.....	96
4.2.2.5	TCCP accumulation onto building materials.....	97
4.2.2.6	Air changes per hour .....	98
4.2.2.7	Sampling schedule.....	99
4.3	RESULTS AND DISCUSSION.....	101
4.3.1	Airborne MDI.....	101
4.3.2	Aldehydes.....	104
4.3.3	Blowing agent and flame retardant .....	107

4.3.4	Airborne particles .....	109
4.3.5	TCPP accumulation onto building materials.....	110
4.3.6	Air changes per hour .....	117
4.4	LIMITATIONS AND FUTURE STUDIES .....	117
4.5	CONCLUSIONS.....	119
4.6	ACKNOWLEDGEMENT .....	120
<b>5.0</b>	<b>INDOOR FATE OF FLAME RETARDANTS IN A RESIDENTIAL BUILDING RENOVATED WITH SPRAY POLYURETHANE FOAM: MODEL PARAMETERIZATION AND RESULT INTERPRETATION .....</b>	<b>121</b>
5.1	INTRODUCTION .....	121
5.1.1	SVOCs and OPFRs .....	121
5.1.2	TCPP in the indoor environment and multi-media models.....	122
5.1.3	Objective and scope .....	124
5.2	METHODS AND MATERIALS.....	125
5.2.1	Field measurements.....	125
5.2.2	Mass balance .....	125
5.2.3	IECCU model.....	126
5.2.4	Chamber testing.....	129
5.2.4.1	House dusts collection and preparation.....	129
5.2.4.2	Chamber testing systems .....	131
5.2.4.3	Sampling schedule and procedure.....	133

5.2.4.4	Extraction and analytical methods .....	133
5.2.4.5	Quality assurance and control .....	133
5.2.4.6	SVOC modeling parameterization and TCPP mass balance in the test chamber.....	134
5.2.5	IECCU Modeling software and parameterization.....	137
5.2.5.1	Building and environment.....	137
5.2.5.2	Sources .....	138
5.2.5.3	Sinks.....	139
5.2.5.4	Settled dusts.....	140
5.2.5.5	Airborne particles.....	141
5.2.5.6	Modeling scenarios .....	142
5.3	RESULTS AND DISCUSSION .....	143
5.3.1	Chamber testing.....	144
5.3.1.1	Chamber wall effects.....	144
5.3.1.2	TCPP diffusion coefficient in settled dusts ( $D_d$ ) .....	145
5.3.1.3	TCPP sorption rate .....	150
5.3.1.4	Direct contact with chamber wall.....	154
5.3.2	TCPP mass balance in the tested house .....	154
5.3.3	Modeled TCPP mass distribution in the tested house .....	156
5.3.4	Comparison between field measurements and IECCU modeling results .....	160
5.3.4.1	Airborne TCPP concentration .....	160

5.3.4.2	TCPP surface accumulation .....	162
5.3.5	Averaged TCPP exposure and risk characterization .....	164
5.4	CONCLUSIONS AND FUTURE STUDIES .....	167
<b>6.0</b>	<b>CONCLUSIONS .....</b>	<b>169</b>
6.1	INTEGRATION OF HIGH-RESOLUTION ENVIRONMENTAL MODELING TOOLS INTO LCA .....	169
6.2	CHEMICAL EMISSIONS IN PRODUCT USE PHASE .....	170
6.3	INDOOR MULTI-MEDIA MASS TRANSFER MODELING IN HUMAN HEALTH RISK ASSESSMENT .....	171
6.4	SUMMARY .....	173
6.5	RECOMMENDATIONS FOR FUTURE WORK .....	174
<b>APPENDIX A .....</b>		<b>177</b>
<b>APPENDIX B .....</b>		<b>179</b>
<b>BIBLIOGRAPHY .....</b>		<b>188</b>

## LIST OF TABLES

Table 1: Summary of recent LCIA methods.....	13
Table 2: Range of OPFRs concentration in various indoor media (Jayjock, Kroner et al. 2015, Wei, Li et al. 2015) .....	34
Table 3: Existing LCIA method/model in assessing human health impacts .....	56
Table 4: Classification of unit processes (based on ACC LCI, (American Chemistry Council 2011b)).....	63
Table 5: Unit processes and site-specific modeling/average stack parameters (U.S. Environmental Protection Agency 1999).....	66
Table 6: Chemical plants production capacity in relative high risk area.....	73
Table 7: Inhalation risks of unit processes without exact location (HAPs emitted to the continental air compartment) .....	75
Table 8: County level inhalation risk statistics (AERMOD) .....	77
Table 9: Inhalation risks of site-specific unit processes (if using USEtox) (Assume HAPs were emitted to the urban air compartment).....	78
Table 10: Inhalation risks of non-site specific unit processes (Assume HAPs were emitted to the urban air compartment).....	79
Table 11: HAPs mass distribution in different environmental compartments.....	83
Table 12: Criteria values for chemicals evaluated in this study, all units are in $\mu\text{g}/\text{m}^3$ .....	90
Table 13: Chemicals analyzed and were above LOQ.....	91
Table 14: Sampling media summary and sampling schedule.....	100
Table 15: Log-Log regression between airborne concentration and time. <sup>a</sup> .....	108
Table 16: Measured ACH50 and calculated ACH <sub>natural</sub> on each floor .....	117

Table 17: i-SVOC modeling parameters.....	135
Table 18: IECCU modeling parameters of building and environment .....	138
Table 19: IECCU modeling parameters of sources .....	139
Table 20: IECCU modeling parameters of sinks .....	140
Table 21: IECCU modeling parameters of settled dusts.....	141
Table 22: IECCU modeling parameters of airborne particles .....	142
Table 23: IECCU modeling scenarios .....	143
Table 24: TCPP mass balance in the 36 Liter test chamber .....	145
Table 25: Best fit TCPP diffusion coefficient ( $D_d$ ) within settled dusts.....	148
Table B1: Curve fitting residuals for all three tests .....	179
Table B2: Other IECCU modeling parameters.....	179

## LIST OF FIGURES

Figure 1: Research areas and gaps in LCA and HHRA.....	15
Figure 2: Micro-chamber (114 ml) used in studying SPF SVOC emissions (top and side view)	38
Figure 3: Small chamber (36 liters) used in studying SPF SVOC emissions.....	38
Figure 4: Chemical structure of the monomeric MDI (left) and polymeric MDI (right) .....	44
Figure 5: Chemical structure of TCPP.....	49
Figure 6: The system boundary of cradle-to-gate MDI production (modified based on (American Chemistry Council 2011b)).....	62
Figure 7: Census tract level inhalation of site-specific unit processes (Left: cancer risk, Right: non-cancer HI) .....	70
Figure 8: County level average inhalation of site-specific unit processes (Left: cancer risk, Right: non-cancer HI) .....	71
Figure 9: Distribution of inhalation risks associated with site-specific unit processes at county level (Left: Cancer risk, Right: Non-cancer Hazard Index).....	71
Figure 10: Site-specific plant locations and high cancer risks area .....	72
Figure 11: Site-specific plant locations and high non-cancer hazard index area.....	73
Figure 12: Inhalation risk distribution of census tracks within the highest county (Left: cancer risk, Right: Non-cancer HI) .....	74
Figure 13: Inhalation risk contribution by HAPs for non-site specific unit processes .....	75
Figure 14: Relative unit processes contribution to inhalation risks.....	80
Figure 15: First and second floor plan view of the residential home.....	93
Figure 16: Sampling equipment.....	95
Figure 17: TCPP accumulation samplers.....	98

Figure 18: SPF application first floor exterior façade (left) and second floor interior wall (right)	102
Figure 19: Airborne MDI concentration during application	102
Figure 20: Airborne MDI concentration after application	103
Figure 21: Airborne aldehydes concentration (during and after application)	106
Figure 22: Airborne Solstice™ LBA (a) and TCPP (b) concentration (During and after application)	108
Figure 23: Mean airborne concentration and confidence interval by particle	110
Figure 24: TCPP concentration ( $C_m$ , $\mu\text{g}/\text{m}^3$ ) in carpet and drywall, compared with Liu’s chamber study data (Liu, Allen et al. 2016a)	112
Figure 25: TCPP concentration ( $C_s$ , $\mu\text{g}/\text{m}^2$ ) in carpet and drywall by total exposed area	113
Figure 26: Averaged TCPP accumulation rate ( $R_m$ : $\mu\text{g}/\text{h}/\text{m}^3$ ), compared with Liu chamber study data.(Liu, Allen et al. 2016a)	115
Figure 27: TCPP surface specific averaged accumulation rate ( $R_s$ : $\mu\text{g}/\text{h}/\text{m}^2$ ) and comparisons with data in Liu (2016) (Liu, Allen et al. 2016a)	116
Figure 28: Schematic of the studied residential house	126
Figure 29: Schematic diagram for the MSS method and the local two-phase mass transfer theory	128
Figure 30: Dust samples and blank filter placed in the small chamber	130
Figure 31: Schematic of the two-chamber testing system	132
Figure 32: Micro-chambers (Source) and small chambers (connected with micro-chambers)	132
Figure 33: Comparison between i-SVOC modeling and measured results for 25-90 $\mu\text{m}$ dust	146
Figure 34: Comparison between i-SVOC modeling and measured results for 90-150 $\mu\text{m}$ dust	147
Figure 35: Comparison between i-SVOC modeling and measured results in Liu et al (Liu, Allen et al. 2016b)	148
Figure 36: Measured chamber air normalized TCPP sorption rates on settled dusts	151
Figure 37: Modeled chamber air normalized TCPP sorption rates on settled dusts	151
Figure 38: Modeled chamber air normalized TCPP sorption rates on settled dusts tested by Liu et al. (Liu, Allen et al. 2016b)	152

Figure 39: TCPP mass balance in the living area during the sampling period .....	155
Figure 40: TCPP mass balance in the attic during the sampling period .....	155
Figure 41: TCPP mass accumulated in each environmental media in the living area .....	157
Figure 42: TCPP mass distribution percentage in living area relevant to inhalation and ingestion exposure .....	158
Figure 43: TCPP mass accumulated in each environmental media in the attic .....	158
Figure 44: TCPP mass distribution percentage in attic relevant to inhalation and ingestion exposure .....	159
Figure 45: TCPP airborne concentration: modeled vs. measured.....	160
Figure 46: Modeled TCPP airborne concentration .....	162
Figure 47: TCPP accumulation on settled dusts and sinks: modeled vs. measured .....	163
Figure 48: Modeled TCPP surface accumulations (sink + settled dusts) .....	164
Figure 49: The averaged TCPP exposure level of different age groups .....	165
Figure B1: Modeled TCPP mass distribution in each indoor media in attic (HHH and LLL scenarios are listed in Figure 43) .....	183
Figure B2: Modeled TCPP mass distribution percentage in attic relevant to inhalation and ingestion exposure (HHH and LLL scenarios are listed in Figure 44).....	184
Figure B3: Modeled TCPP mass distribution in each indoor media in living area (HHH and LLL scenarios are listed in Figure 41) .....	185
Figure B4: Modeled TCPP mass distribution percentage in living area relevant to inhalation and ingestion exposure (HHH and LLL scenarios are listed in Figure 42).....	186
Figure B5: Modeled TCPP airborne concentration .....	187
Figure B6: Modeled TCPP surface accumulations (sink + settled dusts).....	187

## NOMENCLATURE

ACC	American Chemistry Council
ACH	Air Changes per Hour
CF	Characterization Factor
CTU	Comparative Toxic Unit
DALY	Disability Adjusted Life Years
DCP	Directory of Chemical Producers
EDIP	Environmental Design of Industrial Products
EIA	Environmental Impact Assessment
EUSES	European Union System for the Evaluation of Substances
HAPs	Hazardous Air Pollutants
HHIA	Human Health Impact Assessment
HHRA	Human Health Risk Assessment
HI	Hazard Index
IAQ	Indoor Air Quality
IECCU	Indoor Environmental Concentrations in buildings with Conditioned and Unconditioned zones
iFs	Intake Fractions
IH	Industrial Hygiene
LCA	Life Cycle Assessment
LCI	Life Cycle Inventory
LCIA	Life Cycle Impact Assessment
LOQ	Limit of Quantification
MDI	Methylene Diphenyl Diisocyanate
MSS	Modified State-Space

OPFRs	Organophosphate Flame Retardants
PNEC	Potential Non-Effect Concentration
RA	Risk Assessment
RCR	Risk Characterization Ratio
REACH	Registration, Evaluation, Authorization and Restriction of Chemicals
RfC	Reference Concentration
RfD	Reference Dose
SPF	Spray Polyurethane Foam
SVOCs	Semi-Volatile Organic Compounds
TCP	Tris(1-Chloro-2-Propyl) Phosphate
TRACI	Tool for the Reduction and Assessment of Chemical and other Environmental Impacts
USEPA	United States Environmental Protection Agency
VOC	Volatile Organic Compounds
WHO	World Health Organization

## **ACKNOWLEDGEMENTS**

This research would not be possible without my advisor, Professor Dr. Melissa Bilec. I would like to thank her for her patience, diligence, critical and constructive guidance and feedbacks during my entire Ph.D. career at the University of Pittsburgh. Under her direction, I trained and transformed myself from someone who has not much experience in academic writing to a veteran researcher who feels very comfortable in doing research independently. I also would like to thank all my committee members, Drs. Radisav Vidic, Eric Beckman and Vikas Khanna for their contributions in this work both academically and administratively.

I am also so grateful for my current employer, Covestro, to provide financial support for my study and the flexibility for my work/study/life balance. I want to specifically thank my former manager, mentor and true friend, Mr. George Pavlovich. He worked so hard within Covestro to get me this opportunity to continue my Ph.D. study at Pitt and supported me spiritly throughout the entire process. He is such a good mentor and manager who always thinks his employees first and put their career development and needs as the first priority. Without George, I would not be able to finish my study. There are quite a few other colleagues at Covestro who helped me in my Ph.D. time including Drs. Irene McGee, Janet Mostowy, Robert Skoglund, Mr. Chris Hazen, Scott Ecoff, John Sebroski, Jason Miller, Rich Peterman, Ms. Cathie Sayles and Dianna Kelly and other colleagues throughout Product Safety and Regulatory Affairs. I specifically want to thank my current manager Cathie for her continuous support on my research.

Outside Covestro, I had the great opportunity to collaborate and learn from other top researchers in this field, including but not limited to Drs. Zhishi Guo and Xiaoyu Liu and Mr. Mark Mason at the USEPA, Dr. Dustin Poppendieck at NIST and other colleagues with the ASTM D22.05 committee. Thank you all for your suggestions and recommendations to this research.

Last but not the least, I would like to thank my family for their support during my busiest time in the past two years, taking care of the two boys and sharing the responsibilities at home. With the joy brought by my two children, I was able to finish this work and continue working full time at Covestro. It is the strength and support that my family gave to me ensured the completion of my study.

I hope this work provides valuable information for the chemical industry and specifically for the product safety and sustainability community. It will be my greatest pleasure if this work will promote more sustainable products in the market place and help people live in a healthier life.

## **1.0 INTRODUCTION**

### **1.1 PRODUCT SAFETY AND SUSTAINABILITY IN THE CHEMICAL INDUSTRY: FOCUSES ON CHEMICAL EXPOSURE**

The chemical industry is the second largest manufacturing sector in the United States (US) on the value-added basis (Office of Energy Efficiency & Renewable Energy 2011), supplying nearly 15% of world's chemicals, accounting for 14% of US goods export (American Chemistry Council 2017) and producing more than 70,000 products among over 10,000 firms (International Trade Administration 2018). In 2017, the chemical industry generated \$397 billion to the US Gross Domestic Product (GDP), accounting for roughly 2% of the total (Bureau of Economic Analysis 2018). Chemical products are essential to everyday life. It was estimated that 96% of all manufactured goods are directly touched by the chemical industry (American Chemistry Council 2017).

Product safety, especially those products with potential chemical exposure to consumers, is a high priority for the chemical industry. There were many product safety related lawsuits which caused high attention from the public. The two most recent ones which had high publicity were the Johnson & Johnson baby powder case (Hsu 2018) and the Monsanto Roundup weed killer case (Reuters 2018), which were both ordered by the court to pay millions to billions of dollars to the plaintiffs. In order to determine whether a product is safe to use, deep knowledge and sophisticated tools in toxicology, exposure sciences and sustainable and environmental

engineering (SEE) are truly needed. In addition, a large quantity of measured or modeled data related to chemical hazard, manufacturing processes and product use patterns are required to use those tools. However, such data is often proprietary or not readily available.

There are many methods and tools to evaluate the human health impacts and risk of a product, such as life cycle impact assessment (LCA) and human health risk assessment (HHRA). However, each method and tool has its strengths and weaknesses (Tian and Bilec 2018). In order to evaluate the human health impacts of a product along its entire life cycle, multiple tools may be required. For example, to evaluate cradle-to-gate chemical emissions to the outdoor environment, LCA tools such as USEtox (Rosenbaum, Bachmann et al. 2008) can be combined with a classic environmental engineering tool, the American Meteorological Society/Environmental Protection Agency Model (AERMOD) (U.S. Environmental Protection Agency 2012a), to provide high resolution human health risk assessment and guide pollution prevention efforts (Tian and Bilec 2018).

Indoor near-field chemical exposure from building & construction products and consumer products is even more important than outdoor far-field exposure since in the US, people spend approximately 87% of their time indoor and 6% of time in vehicles (Klepeis, Nelson et al. 2001). In addition, human intake of chemicals is three orders of magnitude higher in the indoor environment than outdoors (Ilacqua, Hänninen et al. 2007, Nazaroff 2008). Many indoor models have been developed and applied in the past two decades to study the emission, transport and distribution of chemicals, especially the semi-volatile organic compounds (SVOCs) (Matoba, Yoshimura et al. 1998, Bennett and Furtaw 2004, Xu and Little 2006, Weschler and Nazaroff 2008, Xu, Cohen-Hubal et al. 2009, Zhang, Diamond et al. 2009, Clausen, Liu et al. 2010, Little, Weschler et al. 2012, Shin, McKone et al. 2013, Tian, Sebroski et al. 2017). However, many of

these models are more modeling shells which need the model users to have extensive knowledge in product emission characteristics and provide key modeling input parameters such as the Indoor Environmental Concentrations in Buildings with Conditioned and Unconditioned Zones (IECCU) and i-SVOC models developed by United States Environmental Protection Agency (USEPA). In order to use these models with confidence in product safety, sustainability and chemical exposure assessment, an approach to estimate a comprehensive list of modeling input parameters needs to be developed.

## **1.2 RESEARCH GOALS AND OBJECTIVES**

The overarching goal of this research is to propose a method to quantify the chemical exposure and human health impacts of products along their life cycle stages. This proposed method improves conventional LCA in the area of human health impact assessment (HHIA) from two aspects: 1) utilize high resolution SEE tools to increase geographical relevance for far-field chemical exposure and HHIA, and 2) apply product specific mass transfer models to address the near-field or indoor chemical exposure, often lacking in conventional LCA. This research applies the far-field air dispersion modeling and the near-field mass transfer modeling to evaluate chemical exposure along a product's manufacturing and use phases. By specifically studying methylene diphenyl diisocyanate (MDI) and spray polyurethane foam (SPF) insulation material, this research demonstrates the feasibility of applying the proposed method on building construction materials and potentially expanding it to any other products, especially those are used indoor. The work also provides the first-hand field measurement data to validate and compare modeling results.

The research increases our understandings of a product's far-field human health impacts at a refined geographical scale and expands current knowledge on the emission, transport and distribution of chemicals associated with installing and using a product in the near-field environment. Demonstrated in this dissertation, the combination of advanced SEE modeling tools and LCA techniques can advance product safety and sustainability assessment and prioritize risk mitigation strategies so that multi-stakeholders along a product's value chain can work together to design, manufacture and deliver safer and more sustainable products to the market place. The specific objectives of this research are:

- 1) Develop and test a method to integrate existing HHIA tools (high resolution air dispersion modeling and LCA) to evaluate far-field chemical exposure and risks with high geographical relevance, using publicly available data. Through a case study using MDI as an example, this method aims to improve conventional LCA by providing more insights of the human health risk spatial distribution and developing environmental impacts reduction strategies.
- 2) Quantify the near-field indoor air quality (IAQ) impacts of product emissions in a field study, using Industrial Hygiene (IH) methods to measure the airborne chemical concentrations found in a building and construction product (SPF) made of MDI. Evaluate the chemical concentrations in various indoor media in a residential building renovated with SPF.
- 3) Demonstrate a mathematical modeling approach to quantify product emissions mass distribution in the indoor environment, determine multi-pathway chemical exposure level and characterize human health risks of using a product (SPF) during its use phase. Summarize existing methods and propose new methods to generate key multi-media mass

transfer modeling parameters to study product emissions and IAQ, using an organophosphate flame retardant (Tris(1-Chloro-2-Propyl) Phosphate, TCPP) contained in SPF as an example. Discuss health risk mitigation strategies.

### **1.3 BROADER IMPACTS**

This research broadens the scope of product safety and sustainability assessment by adding both far-field and near-field exposure assessment to the conventional hazard only assessment and toxicity evaluation. Historically, product safety in the chemical industry often heavily focuses on the inherent toxicity of a product but lacks the ability to assess its human exposure due to limited exposure data available along the value chain. As a result, risk characterization is often qualitative and screening in nature that risk mitigation strategies are limited to eliminate hazards (American Chemistry Council 2011a). However, such strategies are not the most efficient way to manage the human health risks of a product because when human exposure is controlled, a product contains hazard chemical can be used safely. The overall benefit of using such products may be lost if product safety assessment is solely focused on hazards.

This research brings a new perspective in product safety assessment to raw material suppliers, product research and developers, product safety professionals and regulators. The entire project aligns well with the risk evaluation process defined in the amended Toxic Substances Control Act (TSCA) (U.S. Environmental Protection Agency 2017b) and the RISK 21 program managed by the Health and Environmental Sciences Institute (HSEI) (Health and Environmental Sciences Institute 2017). Both processes highlight the importance of conducting thorough exposure assessment of chemical substances in addition to hazard assessment.

Particularly, RISK21<sup>®</sup> emphasizes the need of estimating relevant product chemical exposure up front to prioritize and determine data needs. The case studies provide information on chemical and product specific emission data along the life cycle stages, methods to measure and estimate key indoor mass transfer modeling parameters and field monitoring validation for key indoor contaminants occurred during the product installation and use phase. The entire product safety community can benefit from this research by applying it to other chemicals and products.

The work pertaining to the development of a regionalized HHIA method by integrating site-specific air dispersion modeling and LCA provides a feasible approach to quantify human health risks at refined geographical scales. In addition, since this method only uses publicly available emission data along a product's supply chain, it can be expanded to other products in the chemical industry without collecting any sensitive proprietary data.

The near-field IAQ and mass transfer modeling studies were collaborated through the American Chemistry Council (ACC) and the American Society for Testing and Materials (ASTM). Governmental researchers from USEPA and National Institute of Standards and Technology (NIST) have provided valuable input to the work. Part of the outcome from this work was incorporated into the IECCU model. This part of the research expands our knowledge of the behavior of indoor pollutants, especially SVOCs. The approaches to quantify key modeling input parameters can be applied beyond the case study product and chemical to a broad spectrum of building construction materials and consumer products.

## **1.4 INTELLECTUAL MERIT**

This work not only develops a feasible approach to use publicly available data in far-field chemical exposure in HHIA but also demonstrates how to evaluate the near-field chemical exposure resulted during the application and use phase of a product. The novel method resolves a long-standing obstacle that proprietary data is needed to perform high resolution HHIA along a product's life cycle stages. The IAQ study and the mass transfer modeling study provide both first hand measurements and quantitative relationships to quantify many key IAQ parameters. A few of the mass transfer modeling parameters such as the settled dusts diffusion coefficient were first measured or derived by this research. This research is also the first to develop the values for a full list of modeling parameters required by IECCU and compared the modeling results with field measurements. Although significant future research is needed to expand our knowledge in product safety and HHIA, this work is among the first few studies to use the modern risk assessment techniques to promote comprehensive product safety and sustainability assessment.

## **2.0 BACKGROUND AND LITERATURE REVIEW**

This chapter starts with a review of chemical safety regulation history in the US and introduces a few regulatory tools commonly used in HHIA. Two of these tools are LCA and HHRA which are briefly summarized in Section 2.2. In the same subsection, previous work towards harmonizing LCA and HHRA for HHIA is reviewed and the main obstacles to harmonize these two tools are discussed. Section 2.3 introduces SVOCs, an emerging group of chemicals recently studied in the area of HHRA, especially on their indoor exposure to building occupants. Two key methods (chamber testing and multi-media modeling) to quantify human health risks resulted from SVOCs exposure are also included in this subsection. The last subsection of this chapter provides information on the case study product, SPF and two case study chemicals, MDI and TCPP.

### **2.1 CHEMICAL SAFETY REGULATIONS AND HHIA TOOLS**

The first federal regulations related to the chemical industry was the Federal Insecticide Act (FIA) of 1910 (The 61<sup>st</sup> United States Congress 1910). At the end of World War II, large quantity of pesticides such as Dichlorodiphenyltrichloroethane (DDT) was used in both agriculture and household. In 1947, the congress passed the Federal Insecticide, Fungicide, and

Rodenticide Act in 1947 to enhance FIA (The 80<sup>th</sup> United States Congress 1947). In 1962, with the publication of Silent Spring and growing concerns of the environmental and human health impacts of pesticide chemicals, the USEPA was formed in late 1970. To better manage all chemicals, the first comprehensive chemical management law, TSCA, was passed to regulate new and existing chemicals to prevent “unreasonable risk to health or to the environment” in 1976 (The 94<sup>th</sup> United State Congress 1976). Forty years later, congress started to amend TSCA, and the Frank R. Lautenberg Chemical Safety for the 21<sup>st</sup> century Act (LCSA) was passed to strengthen the chemical management framework in 2016 (The 114<sup>th</sup> United State Congress 2016). In LCSA, USEPA is required to use a three-stage process to evaluate the safety of existing chemicals, which includes prioritization, risk evaluation and risk management (U.S. Environmental Protection Agency 2018b). For each stage, qualitative and quantitative tools have been developed and applied to aid the evaluation process.

The prioritization step aims to designate a chemical substance to be either high or low priority. The high priority chemicals will be further evaluated in the three-stage process. USEPA has developed a few prioritization tools including the Stochastic Human Exposure and Dose Simulation Model – High Throughput (SHEDS-HT) model (Isaacs, Glen et al. 2014), the Exposure and Fate Assessment Screening Tool (E-FAST) (Versar 2007) and the Chemical Screening Tool for Exposures and Environmental Releases (ChemSTEER) (Office of Pollution Prevention and Toxics 2013). Besides the USEPA tool, chemical management agencies in Europe and research institutes around the globe also have developed prioritization tools for chemical human health assessment. For example, the European Centre for Ecotoxicology and Toxicology of Chemicals developed the Target Risk Assessment (TRA) tool is designed to evaluate both occupational and consumer health risks of chemicals. TRA has been identified by

the European Commission's Regulation on Registration, Evaluation, Authorization and Restriction of Chemicals (REACH) as a preferred tool in chemical HHRA. TRA tool is a screening tool in nature because it uses highly simplified and conservative exposure assessment algorithms. For instance, when a chemical is assessed for its occupational exposure through inhalation pathway, instead of quantitatively modeling the airborne concentration based on the chemical's emission mechanism, TRA assigns an airborne concentration based on the chemical's vapor pressure range. This simplification allows a wide range of chemicals with different vapor pressure to have the same exposure level through the inhalation pathway. The benefit of using a screening tool like TRA is the increasing speed of assessment which fits well with the prioritization stage. However, more advanced tools are needed for further refined assessment. Besides TRA, the United Nations Environment Programme (UNEP) has endorsed the USEtox as a scientific consensus model for characterizing human health impacts of chemicals. The characteristics, strength and weakness of each model has been thoroughly discussed by Egeghy et al. (Egeghy, Vallero et al. 2011).

In the risk evaluation step, higher tier tools are used to quantify the human health risks of chemicals under the conditions of use and determine if such risks are unacceptable to the general public or susceptible subpopulations. For exposure assessment in the risk evaluation step, higher tiered tools often require more information on chemical, physical properties and use information. For example, the two higher tiered models (i-SVOC and IECCU) used in this research require detailed knowledge on both of the targeted chemicals and the product contains such chemicals in order to simulate the chemical emission, transport and distribution in the indoor environment. In order to interpret results from these models with confidence, field studies to validate modeling results are often required.

## **2.2 LCA AND HHRA: TWO POWERFUL METHODS IN HHIA**

### **2.2.1 Life Cycle Assessment**

LCA is standardized according to ISO 14040 and 14044 and contains four basic steps: goal and scope definition, life cycle inventory analysis (LCI), life cycle impact assessment (LCIA) and interpretation (International Standard Organization 2006a, International Standard Organization 2006b). The common approach of an LCA is first to define the goal and scope of this study which includes functional unit, system boundary, data quality requirement and cut off criteria. The cut off criteria is used to determine which material, energy flow or environmental impact can be excluded from the study. Second, an LCI will be developed to identify and assess the environmental loads with the life cycle phases of the studied system. Third, a characterization model represents the environmental mechanism that is used to quantify the potential environmental or human health impacts caused by the derived LCI. Lastly, based on the LCIA results, conclusions and recommendations will be given to highlight the hotspots in terms of environmental impacts along the life cycle phases and how to improve the environmental performance if possible. The LCA steps are often iterative.

The earliest LCIA method development started in 1990s such as the critical volumes method (Guinee and Heijungs 1992, Guinée and Heijungs 1993) and Ecoscarcity (Finnvedcn and Lindfors 1996) in which only a few environmental impacts were assessed. The Institute of Environmental Sciences (CML) at the University of Leiden developed CML 1992 and PRE-

Consultants introduced Eco-indicator 95 as two of the LCIA methods which are still in use today. Entering the 21st century, over a dozen LCIA methods have been developed and they can be classified into three types: midpoint, endpoint and combined.

Examples of midpoint or problem oriented LCIA methods are CML 2001 (Guinée, Gorrée et al. 2001), Environmental Design of Industrial Products (EDIP) 2003 (Hauschild and Potting 2005) and the Tool for the Reduction and Assessment of Chemical and other Environmental Impacts (TRACI) (Bare 2011). This approach aims to reduce uncertainties and the amount of data needed in the modeling process; however, the environmental relevance may be reduced. This is because that the linkage between emissions and the impact indicator results increases when the LCIA method characterizes emissions closer to the endpoint of the cause-effect chain.

One example of endpoint or damage oriented LCIA methods is the Eco-Indicator 99 (EI99) by PRe Consultants (Goedkoop and Spriensma 2001). The endpoint approach attempts to quantifiably model the environmental damages or human health impacts caused by the emission inventory. While environmental relevance increases in the endpoint modeling approach, uncertainties are also increased due to the lack of quantifiable scientific information along the cause-effect chain.

More recent LCIA methods are the combined midpoint and endpoint methods such as ReCiPe (Goedkoop, Heijungs et al. 2008), IMPact Assessment of Chemical Toxics 2002+ (IMPACT2002+) (Jolliet, Margni et al. 2003) and IMPACT World+ (Jolliet 2014). Synergies exist between some of these methods. For instance, IMPACT2002+ and ReCiPe adopted the damage factor (Disability Adjusted Life Years or DALY) from EI99. Table 1 summarizes the number of impact categories of the most recent developed LCIA methods. The trend shows recent LCIA methods adopt the combined approach of both midpoint and endpoint indicator

results. These new LCIA methods can help LCA practitioners better understand the environmental mechanisms of each impact category and make comparisons at both stages of the cause effect chain.

**Table 1: Summary of recent LCIA methods**

<b>Method</b>	<b>Start Year</b>	<b>Latest Update</b>	<b>Number of IA Categories</b>	<b>Geographical Application</b>	<b>Type</b>
EDIP 2003	1997	2003	6	Europe	Midpoint
BEES	1998	2010	12	USA	Midpoint
EI99	1999	2000	9	Europe	Endpoint
CML	2001	2012	14	Europe	Midpoint
IMPACT2002+	2002	2012	10	Europe	Combined
TRACI 2	2002	2010	9	USA	Midpoint
USEtox	2008	2013	2	Worldwide	Midpoint
ReCiPe	2008	2010	12	Europe	Combined

Both midpoint and endpoint categories are counted and depend on impact category definition. BEES

= Building for Environmental and Economic Sustainability (Lippiatt, Greig et al. 2010)

### **2.2.2 Human health risk assessment**

HHRA is a tool to characterize the nature and magnitude of health risks to human and ecological receptors from chemical contaminants and other stressors that may be presented in the environment (U.S. Environmental Protection Agency 2016a). Risk assessment has been widely used in evaluating chemicals, nanotechnology, remediation of superfund site, environmental impact assessment (EIA) and planning. HHRA is one of the two most important branches of risk assessment (RA) which focuses on estimating the adverse health effects in humans potentially exposed to toxic chemicals. A typical HHRA includes the following four steps: First, the hazard identification process uses toxicokinetic and toxicodynamic studies to determine whether

exposure to a stressor can cause adverse health effects. Secondly, the dose-response assessment quantitatively links the amount and condition of exposure to a stressor(s) to the likelihood and severity of adverse health effects. Thirdly, exposure assessment studies how much of the stressor(s) people are exposed to and how many people are exposed. Lastly, the risk characterization step gives the numerical results of the additional human health risk caused by the stressor(s).

Both HHRA and LCA can be used to assess human health and ecological impacts of targeted system with similarities of these two tools. In terms of data demands of emissions inventory, application of the tools involves collecting the amount of chemicals emitted to the environment for a specified system. At the assessment level, most recent LCIA methods adopt some of the HHRA techniques at the global or regional level. For example, ReCiPe uses fate model at the European Union scale to calculate the environmental impacts of chemical releases. Similar fate models are also used in smaller scales (e.g. city level) in RA. A few LCIA methods such as EI99, ReCiPe and IMPACT2002+ adopt the Disability Adjusted Life Year (DALY) concept which is widely used in HHRA (World Health Organization 2018).

### **2.2.3 Previous work towards harmonizing LCA and HHRA for HHIA**

While Owens in 1997 pioneered the relation between LCA and RA via analysis of the mass-based accounting system of LCA, he also pointed out the limitations of existing impact assessment methods in terms of the loss of spatial, temporal, dose-response and threshold information (Owens 1997). Additionally, human health which is modeled as one single impact assessment category can oversimplify the problem and cannot assess actual adverse health effect and risk. Human health assessment in LCA often serves as a complementary tool for RA and

EIA. During the past 15 years, several groups or individuals have developed framework and models to bridge the gaps between LCA and RA (McKone, Hall et al. 1997, Olsen, Christensen et al. 2001, Citroth, Hagelüken et al. 2002a, Citroth, Hagelüken et al. 2002b, Bare 2011, Humbert, Marshall et al. 2011, Sleeswijk 2011). These efforts can be highlighted as exploring the opportunity to provide regionalized LCIA with RA techniques in assessing human health and other environmental impacts. Figure 1 demonstrates the unique features and common research areas of LCA and RA. A detailed discussion is included in this section.

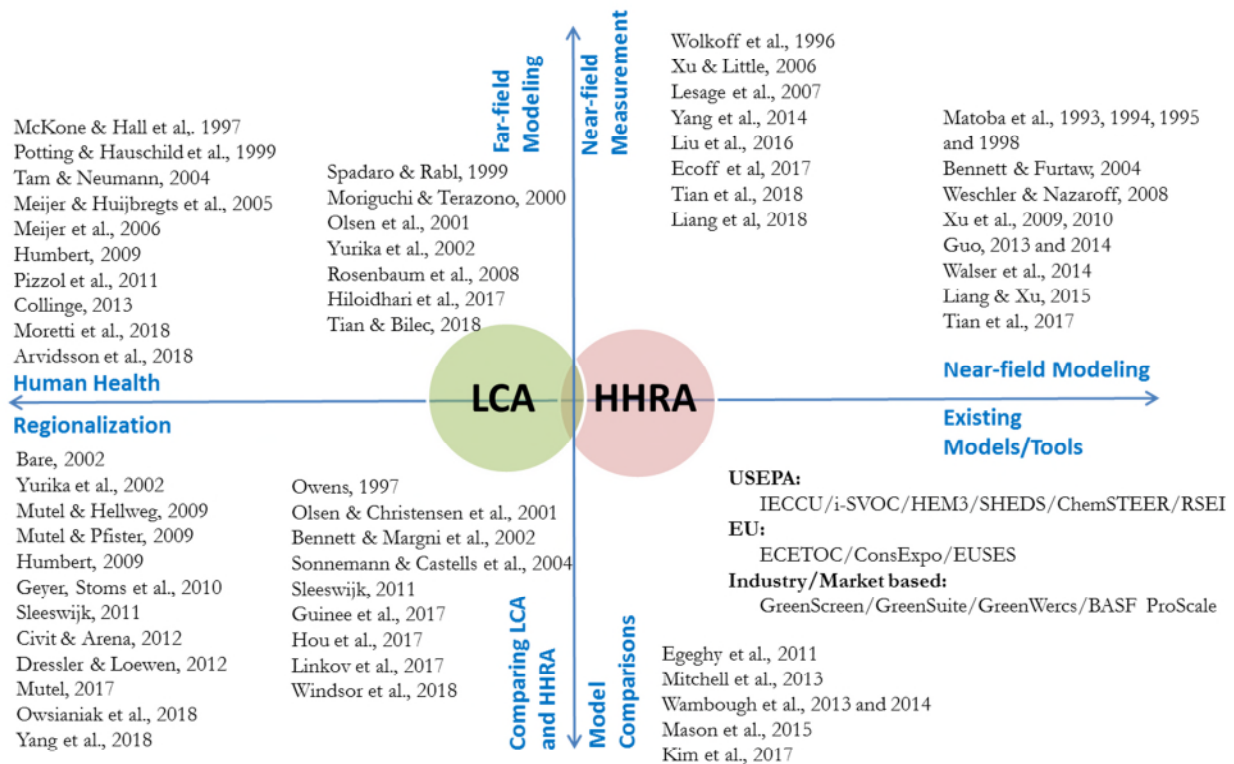


**Figure 1: Research areas and gaps in LCA and HHRA**

**2.2.3.1 Existing models in assessing human health impacts in LCA and HHRA** Human health assessment is a standard impact category listed in most LCIA methods and the main focus of HHRA. However, human health assessment is often not included in the LCAs conducted outside of academia since the uncertainties associated with the underlying human health models in LCIA are high (Hauschild, Huijbregts et al. 2008, Rosenbaum, Bachmann et al. 2008, Pizzol, Christensen et al. 2011, Rosenbaum, Huijbregts et al. 2011). In addition, human health is a site-dependent or site-specific impact category which cannot be well quantified in spatial and temporal generic models used in most current LCIA methods (Humbert, Manneh et al. 2009).

Multi-media and multi-pathways models (Mackay 2001) were recognized as a promising approach to calculate fate and exposure factors in LCA for the human health impact category (De Haes, Finnveden et al. 2002). Quite a few existing LCIA methods adopt this approach in evaluating the human health impacts of toxic substances at global, continental and regional scales. These models include Berkeley-Trent North America contaminant fate model (BETR North America) (MacLeod, Woodfine et al. 2001), BETR World (Toose, Woodfine et al. 2004), IMPACT North America (Humbert, Manneh et al. 2009), USES-LCA 2.0 (Zelm, Huijbregts et al. 2009) and GLOBOX (Wegener Sleeswijk and Heijungs 2010). These models use dozens to hundreds of parameters and mass balance equations to model global, continental and regional environmental conditions and study the partition of toxic chemicals emitted to various environmental compartments such as air, lake, river, ocean and land. In current practice, human health impacts in existing LCIA methods can be summarized as direct impact from toxic substances and indirect impact caused by other impact categories such as photochemical ozone creation. At the midpoint level, by using fate and exposure models at a given geographical level (e.g. Europe), existing LCIA methods characterize each toxic substance into a benchmark

chemical by assigning Characterization Factors (CFs) to each substance. For example, IMPACT 2002+ uses a western Europe based multimedia chemical fate and exposure model and calculates CFs in terms of chloroethylene emitted to air (Jolliet, Margni et al. 2003). At the endpoint level, a few other midpoint categories such as ozone depletion, photochemical oxidation and respiratory effect also contribute to human health at the endpoint category. With the WHO DALY approach to account the severity of each type of cancer or noncancer diseases, the midpoint indicator results from various impact categories can be quantified into human life years lost or disabled.

Quite a few models which were originally designed for RA purpose have been applied in LCIA to evaluate the human health impacts such as CalTox, USEtox and the European Union System for the Evaluation of Substances (EUSES). In the early development of LCIA, CalTox version 2.2 was adopted in the first version of USEPA's TRACI in 2002 (Bare 2002). CalTox model is a steady state, multimedia fate and multi-exposure model with fixed generic parameter for the United States. CalTox was originally developed for assessing human exposure and defining soil clean-up levels at uncontrolled hazardous waste site, and not for LCA purposes (McKone, Hall et al. 1997). In 2008, TRACI 2 switched to use USEtox to model human health impacts of chemical releases (even though USEtox is not U.S. specific). Building on USEtox, the Uniform System for the Evaluation of Substances adapted for LCA purposes 2.0 (USES-LCA 2.0) (Zelm, Huijbregts et al. 2009) is a multimedia fate, exposure and effect model to calculate both human and ecological toxicity developed in Europe based on the EUSES model, which is widely used for regulatory risk assessment purpose.

The recent research effort of HHIA in LCA is focusing on improving the calculation of intake fractions (iFs) by developing specific indoor exposure models and using GIS to include

meteorological and demographical information (Mutel and Hellweg 2009, Mutel, Pfister et al. 2011). iFs also known as exposure efficiency was first defined by Bennett (2002) as “the fraction of chemical mass emitted into the environment that eventually passes into a member of the population through inhalation, ingestion, or dermal exposure” (Bennett, Margni et al. 2002). Numerous indoor exposure models have been proposed in LCA since the indoor pollutant concentration is generally higher and chemical iFs in the indoor environment is up to three orders of magnitude higher than outdoor (Humbert, Marshall et al. 2011). Meijer et al. developed a methodology to calculate damages to human health by indoor pollutants emitted from building materials by using a conceptual Dutch reference dwelling (Meijer, Huijbregts et al. 2005a, Meijer, Huijbregts et al. 2005b). When the DALY approach was applied to calculate the damage factor, the contribution of carcinogenic effect was generally within one order of magnitude of non-carcinogenic effect. Compared to the rest of the life cycle phases of building materials, emissions emitted into the second floor of the Dutch reference dwelling may cause 20 times more damage.

Besides the indoor emissions from building materials, Meijer et al. also studied the human health impacts from outdoor traffic pollution using the Dutch reference dwelling (Meijer, Huijbregts et al. 2006). The results showed the human health damage due to indoor exposure to traffic pollutants and noise was in the same order of magnitude with the damage associated with the life cycle of dwellings. To compare the toxicity impacts from indoor and outdoor sources, Collinge et al. proposed a dynamic LCA framework to include indoor environmental quality metrics where he found the indoor pollution indicator results for cancer effect was one order of magnitude greater than outdoor source for an academic building located in the city of Pittsburgh (Collinge, Landis et al. 2013). Another important indoor exposure for industrial process happens

at the manufacturing plant or application site (e.g. solvent plant or indoor spray foam insulation application). However, very little studies have been done in this field. The regionalization in LCIA development for human health impacts is further reviewed in Section 2.2.3.2, as this area of background is critical to the proposed research.

**2.2.3.2 Regionalization in LCA** It is well known that spatial differentiation exists in process technology and affects the impact of environmental emissions. LCA has been criticized as a “site-generic” method since spatial information in both LCI and LCIA is not always included (Larry Barnthouse 1997, Owens 1997, Humbert, Manneh et al. 2009). In terms of LCI, the spatial differentiation is from available technologies, energy grid mix, political and economic conditions and transportation mode. Ciroth et al. showed the impact of geographical differentiation on the LCI to the same type of waste incinerator in Spain, Germany and Switzerland due to regional background energy supply (Ciroth, Hagelüken et al. 2002a, Ciroth, Hagelüken et al. 2002b). Regarding LCIA, the environmental impact from the same emission emitted to different locations may vary. A common issue in LCIA results is its limitation to express known environmental impacts with regionally specific clarity. For example, summer smog or photochemical ozone creation is determined by background airborne concentration of Volatile Organic Compounds (VOCs) and NO<sub>x</sub>, but most current LCIA methods only have an average CF at country scale. Shah and Ries studied the spatial and temporal resolution of photochemical precursors for LCA in the U.S. and found the CF of NO<sub>x</sub> has up to one and two orders of magnitude difference among the 50 states and DC (Shah and Ries 2009).

LCIA methods developed in Europe started to include spatial information into LCI and LCIA. For example, Hauschild and Potting classified LCIA into three types: “site-generic”, “site-dependent” and “site-specific” in the EDIP method (Hauschild and Potting 2005). Site-

generic LCIA assumes all emissions contribute to the same generic receiving environment, and no spatial differentiation is considered in the assessment. While site-dependent and site-specific LCIA employ a moderate to high spatial differentiation, respectively. In traditional LCIA methods, the site-generic global and continental scale models are common. Recently, however, LCA has moved towards the direction of developing a more site-dependent and site-specific models (Potting and Hauschild 1997, Tolle 1997, Potting, Schöpp et al. 1998, Shah and Ries 2009, Gallego, Rodríguez et al. 2010, Sala, Marinov et al. 2011, Sleeswijk 2011, Brown 2012, Dresen and Jandewerth 2012). Two aforementioned regionalization approaches, archetype regionalization and site-specific approach (Hauschild 2006, Potting, Hertel et al. 2006, Humbert, Manneh et al. 2009), are under development, but only the former one is being integrated in mainstream LCIA methods.

In archetype regionalization approach (or site-dependent characterization), specific emission location information is not needed. Geographical variability is identified as a few distinct categories with characteristics instead such as air emissions from high or low chimneys to high or low population density areas. Potting et al. first described the concepts although the word of “archetype” was not used (Potting and Hauschild 1997). Further, Hauschild et al. applied the archetype approach into EDIP method to derive site-dependent photochemical ozone formation CFs (Hauschild 2006). Similarly, Shah and Ries used a photochemical air quality modeling system (CAMx-MM5-SMOKE) to develop CFs for photochemical ozone creation in 50 U.S. states and DC (Shah and Ries 2009). Another example is that Gallego et al. studied the spatial characteristics of three ecosystems in northwest Spain and developed regional CFs for aquatic eutrophication (Gallego, Rodríguez et al. 2010). More thorough discussions about archetype regionalization can be found at Humbert et al. (Humbert, Manneh et al. 2009, Humbert, Marshall

et al. 2011). Humbert et al. (2009) developed the IMPACT North America which is a multimedia environmental fate and exposure model to calculate the iFs of emissions in the U.S. and Canada. They found the biggest difference of iFs can be six orders of magnitude between site-generic assessment and the site dependent archetype approach in a specific region such as Alaska. They also discovered in North America, two important archetypes in characterizing HH impact from emissions are population density and agriculture production rate for air and oral intake pathway, respectively. In addition to EDIP, current ReCiPe method adopts this approach in characterizing air, water and soil emissions even though a few archetypes are available to choose (Goedkoop, Heijungs et al. 2008). It is worthwhile to mention that not all archetype CFs are available in commercial LCA software.

In the site-specific approach, a high resolution model is often developed by using GIS (Kim and Dale 2009, Geyer, Lindner et al. 2010, Geyer, Stoms et al. 2010, Mutel, Pfister et al. 2011, Saad, Margni et al. 2011, Civit, Arena et al. 2012, Dressler, Loewen et al. 2012), instead of classifying geospatial characteristics into categories. Geyer et al. first modeled a regionalized LCI for foreground process (e.g. air emission from an agriculture product production in central valley), input them into GIS system and manually apply the CFs derived from a regionalized LCIA method (e.g. land use impact based on regional species richness). However, due to the difficulties of gathering spatially differentiated background data such as diesel production used in agriculture, LCA practitioners are often left with no options but to use the site genetic CFs in existing LCIA method (Mutel and Hellweg 2009). Normally the background processes are less sensitive to regionalization since energy supplies are spread out over the world and the spatial differences are more likely to be offset. Therefore, this “modeled LCI” approach is a compromise between the need of spatial differentiated LCIA results and the effort of collecting

data. However, it was only applicable to a few special cases such as land and water use. No study has been done for human health impacts using this approach. In addition, Mutel pointed out it is possible to miss important impacts along the supply chain without regionalizing the foreground processes (Mutel and Hellweg 2009). He proposed a buffering zone concept in GIS to include spatial uncertainties for foreground LCI, but the probability of the activity occurred in each buffered region is not totally objective.

Besides current method development in regionalization of fate and exposure models, there is a strong need for population specified exposure modeling. Children and elder citizens are more vulnerable than young adults to pollutants. This is because children have a higher chemical intake rate per body weight through both air and oral pathways and their organs are still under development. Although the variability in exposure factor is low among different age groups compared to several orders of magnitude differences in the spatial differentiation, it is worthwhile to develop an exposure model to combine the spatially differentiated iFs approach to protect vulnerable population such as children.

**2.2.3.3 Main obstacles in harmonizing existing tools for HHIA** Previous work reveals the obstacles to harmonize existing tools such as LCA and HHRA for HHIA.

***Complexity in supply chain and the lack of consistent prioritization process.***

A large number of raw materials and intermediates could be involved in a chemical's life cycle. For example, a total of 19 raw materials and intermediates are used to produce MDI, a raw material for many industrial and consumer products (American Chemistry Council 2011b). Along this supply chain, each raw material has hundreds of chemical emissions and the emission locations are often unknown. Even a single manufacturer often has the same type of raw material provided by different suppliers in different locations. Currently, manufacturers only track the raw

material suppliers instead of the manufacturing location of each shipment. As a result, it is impossible to conduct site specific HHRA for every chemical along the supply chain, due to the lack of geographical information and the complexity of the supply chain. A consistent and practical prioritization process is truly needed.

Fugacity based multi-media models were first brought to attention for its potential of studying chemical fate and transport in the environment and potential human exposure (Mackay 2001). Based on this approach, a few multi-media box models have been developed over the past two decades to study the fate and transport of chemicals in the environment (McKone, Hall et al. 1997, Georgopoulos and Liou 2006, Arnot 2009). For example, EUSES model has been used by the European Chemical Agency (ECHA) as screening level risk assessment tools (TSA Group Delft by 2008). However, each model often has its own strength in a particular area of chemical fate and exposure (Egeghy, Vallero et al. 2011). For instance, the Stochastic Human Exposure and Dose Simulation Model – High Throughput (Stochastic Human Exposure and Dose Simulation (SHEDS)-HT) primarily focuses on the near-field consumer exposure (Isaacs, Glen et al. 2014), while the USEtox model most commonly used in LCA focuses on the far-field environmental releases (Rosenbaum, Huijbregts et al. 2011). Recent research indicates the chemical near-field exposure is the most predictive to the overall human exposure to chemicals (Wambaugh, Setzer et al. 2013, Wambaugh, Wang et al. 2014). However, to fully evaluate the human health impacts of a chemical, a combined approach to address both near and far-field exposure from a chemical life cycle perspective is required and becoming an emerging research area (Isaacs, Glen et al. 2014, Jolliet, Ernstoff et al. 2015).

***Existing individual assessment tools alone does not meet the regulatory and market needs for chemical human health assessment***

Current chemical human health assessment has two primary goals. First, from the perspective of regulatory agencies such as USEPA, a quick but technically rigorous high throughput method is needed to screen large amount of chemicals and identify those high priority chemicals based on their toxicity and exposure potentials. To achieve this goal, USEPA has been working with the industry participants such as the ACC to develop methods and framework such as the ToxCast™ (U.S. Environmental Protection Agency 2018c) and ExpoCast™ program (Wambaugh, Setzer et al. 2013). In the EU, REACH regulation approves to use a tier one screening tool (TRA) to evaluate chemicals by their use pattern and potential exposure pathways with conservative assumptions (European Centre for Ecotoxicology and Toxicology of Chemicals 2004, European Centre for Ecotoxicology and Toxicology of Chemicals 2014). The high priority chemicals are further evaluated by higher tier methods which require more specific manufacturing and use pattern information instead of default values. Second, in addition to knowing where the human health hotspots are, both the regulatory agencies and general public are interested to quantify the human health risks which could be used to guide regional or local policy for human health risk mitigation. For example, one concern of the HHRA of building products and green building programs is burden shifting from one region or life cycle phase to another (Cellarius 2014, Pierce 2014). To avoid this, additional data collection such as chemical reaction kinetics and emission locations is required for a more comprehensive HHRA of chemicals.

To meet the above two goals, existing tools alone are not sufficient due to the complexity of chemical human health assessment. Two of the primary tools involved in HHIA are LCA and

HHRA are different in several aspects. First, LCA is a product-based tool which uses the concept of functional unit that includes all inputs and outputs to fulfill this function along a product's life cycle. All impacts are based on the studied functional unit. The midpoint and endpoint human health impact indicator results usually have their own units (e.g. Comparative Toxic Unit or CTU in USEtox and DALY for endpoint human health category in EI99, IMPACT 2002+ and ReCiPe). HHRA is a receptor-based tool which focuses on the human health impacts of one or several hazardous chemicals and one or several life cycle stages of these chemicals for targeted population (e.g., a specific location or an age group). Starting with certain production volume, HHRA transfers chemical emission rates into ambient concentrations with a fate and transport model, then applies an exposure model to calculate the human exposure dose and finally compare it to toxicological threshold (e.g. Integrated Risk Information System or IRIS) to derive hazardous quotient or risk characterization ratio (RCR). The risk characterization step usually gives a unitless numeric value for certain endpoint effects (e.g. one additional cancer case in a million people). Sleeswijk and Olsen et al. identified functional unit as a fundamental difference between LCA and HHRA (Olsen, Christensen et al. 2001, Sleeswijk 2011). This is because all emissions are allocated to one functional unit in LCA whereas emissions are evaluated based on their locations or temporal patterns in HHRA (e.g. SO<sub>2</sub> resulted from producing 1 kWh electricity vs. SO<sub>2</sub> from a coal power plant located in Pittsburgh). Second, LCA uses the principle which is often referred as "less is better" which means LCA assumes a linear relationship between human health impacts vs. chemical emissions. In contrast, RA uses the risk minimization principle as the basis which assumes only the emission over the environmental capacity will cause harm. This approach is commonly referred to as "only over the threshold" (Potting, Hauschild et al. 1999).

Due to the different focuses of LCA and HHRA, each tool alone cannot fulfill the two goals discussed above. For example, the screening level USEtox tool often used in LCA aggregates all relevant chemical releases together which aims to conduct efficient high throughput prioritization for the first goal. However, the loss of emission location information reduces the geographical relevance and may not be able to achieve the second goal. At the same time, traditional HHRA only focuses on the human health impacts of one or a few chemicals but ignores its origin and allocation throughout a product's life cycle phases. For example, the National-Scale Air Toxic Assessments identifies the top Hazardous Air Pollutants (HAPs) that contribute to regional or local human health impacts but it cannot track or allocate them to certain products or services (e.g., electricity generation) (ICF International 2011). Therefore, there is an emerging need for all parties involved to develop a systematic and practical method to meet the goals of chemical human health assessment, especially using more geographical and product specific information.

***A holistic method including the high throughput/tiered approach and utilizing existing tools with higher geographical and temporal resolution needs to be developed for chemical HHIA.***

In order to bridge the gaps of individual tools in assessing chemical human health impacts, there have been a few studies suggesting for using multiple tools. In 2004, Sonnemann proposed an integrated method to use LCA and RA for industrial processes which first uses traditional large scale LCIA models to identify a group of chemicals with an arbitrary 10% cut off rule based on the LCIA result. The site-specific impact assessment is then conducted for the selected chemicals (Sonnemann, Castells et al. 2004). However, the technical challenge is that this

method can be only used for a system (e.g., product or service) with a small amount of unit processes. When the human health impacts of each unit process are evenly distributed based on the traditional LCIA results, the number of unit process and associated chemicals which require site-specific assessment is too large. In addition, the methodology challenge is that by using traditional large scale LCIA models, the uncertainties embedded are carried over to the high priority chemical list. For example, if TRACI v2.1 were selected as the prioritization method, the uncertainty of USEtox causes heavy metals dominate the priority chemical list. Later on, Sleeswijk discussed that although existing tools such as LCA and RA cannot be fully integrated together due to LCA uses functional unit as the comparison basis while RA uses the ambient concentration of pollutants, these two tools can work together to assess human health impacts (Sleeswijk 2011). This research focuses on separating the areas by whether the threshold is exceeded and assess the environmental impacts separately. Sleeswijk introduced the concept of Sensitivity Factor (SF) and Threshold Factor (TF) which takes account the regional differences that SF and TF could be used to quantify the human health impacts in areas which are sensitive to this impact category and the human health threshold has been exceeded. However, no prioritization process was proposed in this work and the determination of SF and TF is subjective. More recently, outside the academia, individual companies such as BASF developed a framework called “Proscale” to use the TRA screening models in REACH to evaluate chemical human health impacts from a life cycle perspective (Kalberlah, Schwarz et al. 2015). The basic idea is to use TRA tool to look at individual chemical in a product by each life cycle phase and then calculate an overall human health score. The goal of this effort is to bring regulatory models and life cycle thinking together to rank products based on their human health impacts. Although the general approach is appreciated to look at chemical hazard and exposure for each life cycle

phase, the complex supply chain prevents doing that for every single chemical, its upstream raw material and downstream products. A screening and prioritization process are needed. In addition, Proscale simply multiplies a hazardous score which is derived from the Potential Non-Effect Concentration (PNEC) and an exposure score which is the RCR calculated from PNEC. The hazardous information was double counted and created methodological difficulties for this approach.

In summary, to better assess the chemical human health impacts from a life cycle perspective, there is an inevitable need to use more regional and temporal specific models to quantify the human health impacts for both far-field and near-field chemical exposure. Previous research has demonstrated the possibility of using existing tools such as LCA and HHRA together to achieve such goal. On one hand, with the improvement and increased efficiency of site-specific environmental fate, transport and exposure modeling (U.S. Environmental Protection Agency 2012a, EC/R Incorporated 2014), a combination of existing tools can better assess chemical human health impacts than using any individual one alone. On the other hand, HHIA should not be limited to far-field environmental chemical exposure but include near-field exposure, especially focusing on those vulnerable subpopulations. This research will be presented in chapter three aims to propose a practical and scientific rigorous approach to illustrate how existing tools could be used together for chemical HHIA.

## **2.3 PRODUCT EMISSION AND INDOOR AIR QUALITY WITH FOCUS ON SVOCS**

The relationship between IAQ and product emissions (or commonly called “off-gassing”) has been studied for decades and well characterized in the literature. However, the majority of these research studies focuses on the VOC, the emission mechanism, fate and transport of SVOCs in the indoor environment are still an emerging research area. Although many research studies exist in the area of VOCs and their impact on IAQ, this section primarily focuses on summarizing current SVOC research, specifically how SVOCs are measured and the development of recent indoor SVOC models.

### **2.3.1 Definition of SVOCs and their presence in the indoor environment**

SVOC is a class of chemical that can have meaningful abundance in both gas and condensed phases. The actual definition of SVOCs could vary by organizations and governmental authorities. WHO defines SVOCs by boiling point range (240 ~ 400 °C) (World Health Organization 1989) but a common approach in SVOC research is to define it by chemical vapor pressure ( $10^{-9}$  to 10 Pa) (Weschler and Nazaroff 2008, Xu and Zhang 2011). In comparison, VOCs have a higher but narrower vapor pressure range between 10 Pa to  $10^4$  Pa. SVOCs in the indoor environment can be grouped into the following categories by chemical class or use function: organophosphate flame retardants (OPFRs) and plasticizers, brominated flame retardants (BFRs), phthalate esters, synthetic musks, polycyclic aromatic hydrocarbons (PAHs), polychlorinated biphenyls, pesticides, polyfluorinated alkyl substances (PFASs), chlorinated paraffins, dechlorane and parabens.

SVOCs can be found in many indoor environmental media including air, airborne particles, settled dusts, sink materials such as building construction materials and consumer products such as electronics, cleaning products and furniture (Weschler and Nazaroff 2010, Liu and Little 2012, Liu, Allen et al. 2016a, Lucattini, Poma et al. 2018). The type and quantity of SVOCs presented in the indoor environment vary by product types and functions. Lucattini et al. did a literature review on SVOCs presence in indoor materials and products with a total of 259 publications. They reported the SVOC weight percentage ranges in each type of indoor material and media (Lucattini, Poma et al. 2018).

**2.3.1.1 SVOCs in building and construction materials** For building construction materials, three of the most common SVOC types are flame retardants in insulation foam and wall paper (Lazarov, Swinnen et al. 2016, Liu, Allen et al. 2016a), phthalate based plasticizers in vinyl flooring (Clausen, Xu et al. 2007, Xu, Cohen-Hubal et al. 2009, Xu, Liu et al. 2012, Liang and Xu 2014, Liang, Caillot et al. 2015) and polychlorinated biphenyl (PCBs) congeners based resin or soft agents in paint, adhesive and sealants (Andersson, Ottesen et al. 2004, Hu and Hornbuckle 2010, Liu, Guo et al. 2015, Liu, Guo et al. 2016a, Liu, Guo et al. 2016b).

Flame retardants found in insulation and wall paper include BFRs such as polybrominated diphenyl ethers (PBDEs), hexabromocyclododecane (HBCD) and OPFRs such as TCPP. OPFRs are relative newer flame retardants to replace BFRs in the past decade due to the phase out requirements (Dodson, Perovich et al. 2012, van der Veen and de Boer 2012, U.S. Environmental Protection Agency 2013a, U.S. Environmental Protection Agency 2017c). Kemmlein et al. reported TCPP was one of the most commonly emitted OPFRs in polyurethane (PU) foam application. The weight percentage of TCPP ranges from 5% in the polyisocyanurate insulating boards (PIR) to 20% in the one component PU foam. The authors also performed

emission studies using testing chambers (0.02 and 1 m<sup>3</sup>) and cells (0.001 m<sup>3</sup>). Depending on the sample type, area specific emission rates (SER) of TCPP varied from 20 ng/m<sup>2</sup>/h to 140 µg/m<sup>2</sup>/h (Kemmlin, Hahn et al. 2003).

Plasticizers are additives to enhance flexibility of plastics. Phthalates are a group of chemicals often used as plasticizers in vinyl flooring, carpet padding and PVC products. Common phthalates include dibutyl phthalate (DBP), di(2-ethylhexyl) phthalate (DEHP) and diisononyl phthalate (DINP). The weight percentage of plasticizers in polyvinyl flooring ranges from 13% (Clausen, Liu et al. 2012) to 30% (Cadogan and Howick 2000). Phthalates based plasticizers are not bounded chemically to the product material matrix. Plasticizer emissions from product occurs and have been studied using chamber testing methods (Carlsson, Nilsson et al. 1997, Hartmann, Bürgi et al. 2004, Clausen, Xu et al. 2007, Xu, Cohen-Hubal et al. 2009, Xu, Liu et al. 2012, Liang and Xu 2014). Xu et al. designed a special “sandwich” chamber with a 2-liter volume to test DEHP emission SER from vinyl flooring, which ranged from 0.14-0.18 µg/m<sup>2</sup>/h (Xu, Liu et al. 2012). Liang et al. conducted a similar test for vinyl flooring DEHP and DINP emissions and reported SERs of 3.2 and 2.7 µg/m<sup>2</sup>/h (Liang, Caillot et al. 2015). With the restriction on using phthalates in toys and children’s products, alternative plasticizers with higher molecular weight such as diisononyl cyclohexane-1,2-dicarboxylate (DINCH) and di(2-ethylhexyl)adipate (DEHA) were used (Weschler 2009).

Polychlorinated biphenyls have 209 congeners and different mixture of these congeners were sold under various commercial names, for example, the Aroclors marketed by Monsanto (Andersson, Ottesen et al. 2004, Guo, Liu et al. 2012a). PCBs were mainly used in caulk, paint, coating and fluorescent light ballasts, especially for buildings built or renovated between 1950 and 1979 (U.S. Environmental Protection Agency 2015b). In caulking materials, PCB may

account up to 30% of weight (Guo, Liu et al. 2012a). In plasters and paints, one of the PCB congener (PCB7) concentrations are up to  $2.9 \times 10^5$  ng/g and  $1.9 \times 10^6$  ng/g (Andersson, Ottesen et al. 2004). As the other two main SVOCs found in the indoor environment, PCBs have been widely tested in the past two decades in the laboratory and field (Vorhees, Cullen et al. 1999, Herrick, McClean et al. 2004, Kohler, Tremp et al. 2005, Robson, Melymuk et al. 2010, Guo, Liu et al. 2012b). In Guo's study conducted at the USEPA, caulk materials were reported to have up to 136 mg/g PCB with a mean of 50.3 mg/g and median of 42.6 mg/g. A linearly relationship was established between PCB congeners concentration in the caulk and the SER.

The common challenge faced by researchers in studying SVOC emissions from building and construction material is that the weight percentage of SVOCs in the product is often labeled as a trade secret therefore not mandatory to be reported (Lucattini, Poma et al. 2018). However, such information is crucial in SVOC emissions mechanism research and modeling. Due to the difficulties in SVOCs measurement, deriving the initial SVOCs content in a product such as SPF is a challenge (Sebroski, Miller et al. 2017). In order to advance our understanding of SVOC emissions and its IAQ impact, product transparency and disclosure are truly needed.

**2.3.1.2 OPFRs in the indoor environment** OPFRs are a group of chemicals which were used to replace BFRs. Common OPFRs include halogenated organophosphorus chemicals such as TCPP, Tris(2-chloroethyl) phosphate (TCEP), Tris(1,3-dichloro-2-propyl) Phosphate (TDCPP), and non-halogenated organophosphorus chemicals such as Triethyl phosphate (TEP) and Tripropyl phosphate (TPP). OPFRs have been evaluated for their presence in various indoor media including air (including airborne particles) (Sanchez, Ericsson et al. 2003, Hartmann, Bürgi et al. 2004, Marklund, Andersson et al. 2005, Saito, Onuki et al. 2007, Bradman, Castorina et al. 2014, Fromme, Lahrz et al. 2014, Yang, Ding et al. 2014), household dusts (Ingerowski, Friedle et al.

2001, Marklund, Andersson et al. 2005, Wensing, Uhde et al. 2005, Van den Eede, Dirtu et al. 2011, Brommer, Harrad et al. 2012, Fromme, Lahrz et al. 2014, Cowell, Stapleton et al. 2017, Wang, Wang et al. 2018), furniture (Stapleton, Klosterhaus et al. 2009, Cowell, Stapleton et al. 2017) and consumer products such as baby products (Stapleton, Klosterhaus et al. 2011), household products (Ingerowski, Friedle et al. 2001, International Agency for Research on Cancer 2015) and electronics (Kemmlin, Hahn et al. 2003, Saito, Onuki et al. 2007, Kajiwara, Noma et al. 2011).

Wei et al. and Jayjock et al. did thorough literature reviews on OPFRs presence in the indoor environment (Jayjock, Kroner et al. 2015, Wei, Li et al. 2015). Table 2 summarized their findings and additional literature reported common OPFRs concentration ranges in the indoor environment.

**Table 2: Range of OPFRs concentration in various indoor media (Jayjock, Kroner et al.**

**2015, Wei, Li et al. 2015)**

<b>Environmental media</b>	<b>TCPP</b>	<b>TCEP</b>	<b>TDCPP</b>	<b>TEP</b>	<b>TPP</b>
<b>Indoor air</b>			<b>ng/m<sup>3</sup></b>		
<i>Home</i>	nd <sup>a</sup> -2,660 <sup>b</sup>	nd <sup>c</sup> -6,000 <sup>d</sup>	nd <sup>a</sup> -61.4 <sup>b</sup>	nd <sup>a</sup> -511 <sup>b</sup>	nd <sup>c</sup> -17.5 <sup>b</sup>
<i>Office</i>	nd <sup>e</sup> -850 <sup>f</sup>	nd <sup>c</sup> -870 <sup>g</sup>	nd <sup>c</sup> -35.0 <sup>h</sup>	nd <sup>f</sup> -91.0 <sup>c</sup>	nd <sup>f</sup> -2.70 <sup>c</sup>
<i>School</i>	31.0 <sup>h</sup> -200 <sup>i</sup>	0.70 <sup>h</sup> -590 <sup>h</sup>	<0.30 <sup>h</sup> -1.70 <sup>h</sup>	-	<0.40 <sup>h</sup> -2.80 <sup>h</sup>
<i>Hotel</i>	69.0 <sup>h</sup>	2.20 <sup>h</sup>	<0.60 <sup>h</sup>	-	<0.30 <sup>h</sup>
<i>Daycare</i>	1.30 <sup>c</sup> -72.0 <sup>c</sup>	2.50 <sup>h</sup> -230 <sup>c</sup>	nd <sup>c</sup> -59.0 <sup>h</sup>	0.80 <sup>c</sup> -20.0 <sup>c</sup>	nd <sup>c</sup> -0.90 <sup>c</sup>
<i>Hospital</i>	1.00 <sup>g</sup> -750 <sup>g</sup>	2.20 <sup>e</sup> -350 <sup>g</sup>	<0.20 <sup>h</sup> -150 <sup>h</sup>	7.00 <sup>g</sup> -13.0 <sup>g</sup>	4.80 <sup>h</sup>
<i>prison</i>	570 <sup>h</sup>	17.0 <sup>h</sup>	6.00 <sup>h</sup>	-	<0.40 <sup>h</sup>
<b>Indoor dust</b>			<b>µg/g</b>		
<i>Home</i>	<0.01 <sup>j</sup> -462 <sup>k</sup>	<0.008 <sup>j</sup> -2,320 <sup>k</sup>	<0.009 <sup>j</sup> -864 <sup>k</sup>	<0.005 <sup>l</sup> -3.31 <sup>k</sup>	<0.005 <sup>l</sup> -1.13 <sup>k</sup>
<i>Office</i>	<0.01 <sup>j</sup> -120 <sup>c</sup>	<0.008 <sup>j</sup> -260 <sup>c</sup>	<0.009 <sup>j</sup> -91 <sup>c</sup>	nd <sup>c</sup> -0.10 <sup>c</sup>	-
<i>School</i>	2.90 <sup>m</sup> -50.0 <sup>m</sup>	1.60 <sup>m</sup> -94.0 <sup>m</sup>	0.84 <sup>m</sup> -5.70 <sup>m</sup>	-	-
<i>Hotel</i>	1.00 <sup>n</sup> -9.80 <sup>n</sup>	0.08 <sup>n</sup> -3.90 <sup>m</sup>	0.07 <sup>n</sup> -18.0 <sup>n</sup>	<0.02 <sup>n</sup> -0.09 <sup>n</sup>	-
<i>Store</i>	0.58 <sup>o</sup> -24.4 <sup>o</sup>	<0.08 <sup>o</sup> -5.46 <sup>o</sup>	<0.08 <sup>o</sup> -56.2 <sup>o</sup>	<0.05 <sup>o</sup> -0.37 <sup>o</sup>	-
<i>Daycare</i>	0.80 <sup>m</sup> -12.0 <sup>c</sup>	0.82 <sup>c</sup> -150 <sup>c</sup>	1.80 <sup>m</sup> -150 <sup>c</sup>	nd <sup>c</sup> -4.70 <sup>c</sup>	-
<i>Hospital</i>	2.30 <sup>c</sup> -5.30 <sup>c</sup>	0.56 <sup>c</sup> -2.10 <sup>c</sup>	1.00 <sup>c</sup> -3.80 <sup>c</sup>	-	-
<i>prison</i>	<0.01 <sup>m</sup> -134 <sup>m</sup>	<0.008 <sup>m</sup> -13.7 <sup>m</sup>	<0.005 <sup>m</sup> -620 <sup>m</sup>	-	-
<b>Indoor products</b>			<b>µg/g</b>		
<i>Baby products</i>	1,110 <sup>p</sup> -14,400 <sup>p</sup>	-	2,400 <sup>p</sup> -124,000 <sup>p</sup>	-	1,000 <sup>p</sup> -12,800 <sup>u</sup>
<i>Household Products</i>	0.90 <sup>q,v}</sup> -180,000 <sup>d,w}</sup>	-	4.5 <sup>q,v}</sup> -44,870 <sup>s,w}</sup>	<1.00×10 <sup>-4</sup> <sup>t,x}</sup> - 11 <sup>t,y}</sup> 1.8 <sup>t,z}</sup> - 3,230 <sup>t,w}</sup>	
<i>Electronics</i>	nd <sup>a</sup> -1,700 <sup>a}</sup>	nd <sup>a</sup> -13,000 <sup>a}</sup>	nd <sup>a</sup> -290 <sup>m}</sup>	3.00×10 <sup>-4</sup> <sup>t}</sup> -0.19 <sup>t}</sup>	0.56 <sup>t}</sup> -14,000 <sup>t}</sup>

nd = not detected; a: (Saito, Onuki et al. 2007); b: (Kanazawa, Saito et al. 2010); c: (Bergh, Torgrip et al. 2011); d: (Ingerowski, Friedle et al. 2001); e: (Hartmann, Bürgi et al. 2004); f: (Björklund, Isetun et al. 2004); g: (Staaf and Östman 2005); h: (Marklund, Andersson et al. 2005); i: (Mäkinen, Mäkinen et al. 2009); j: (Abdallah and Covaci 2014); k: (Araki, Saito et al. 2014); l: (Ali, Ali et al. 2013); m: (Marklund, Andersson et al. 2003); n: (Takigami, Suzuki et al. 2009); o: (Van den Eede, Dirtu et al. 2011); p: (Stapleton, Klosterhaus et al. 2011); q: (Nagase, Toba et al. 2003); s: (Stapleton, Sharma et al. 2012); t: (Kajiwara, Noma et al. 2011); u: (Ionas, Dirtu et al. 2014); v: Furniture cushion; w: PU foam; x: Curtain; y: Insulation board; z: Wall paper

### 2.3.2 SVOCs measurement methods

In order to measure product emissions and their impact on IAQ, researchers have developed chamber methods to quantify chemical emission rates from products. Compared to the field sampling studies, the primary advantage of these chamber methods is that they are conducted in a more controlled laboratories environment so researchers can control factors which may impact product emission rates and chemical's indoor fate and transport behavior. In addition, chamber tests often require less time and resources. However, the disadvantages of using chambers include the chamber wall sink effects and the difficulties in extrapolating chamber studies results to actual building. Due to SVOCs' low vapor pressure and high material-air partition coefficients, they tend to be absorbed onto the chamber walls and therefore may not be captured by air sampling techniques. The measured SVOCs concentration in the chamber air may be underestimated due this chamber wall effect. Another difficulty in using chamber test results to predict product's emission profile and its IAQ impact is that chamber tests often have different "external conditions" than the actual building. For example, the gas phase mass transfer coefficient is a function of ambient air velocity and dimensions of the products. Due to the volume differences between the chamber and actual building, air velocity can be quite different in the chamber vs. the actual room. Besides volume, the product loading factor (product surface area/chamber or room volume) can be different which may result that the emission factors derived from the chamber studies are not representative if the products were placed in an actual room.

There are a few types of chamber testing system developed in VOC and SVOC research in the past three decades. Each system has its own set of specifications which could be overwhelming. A brief description is summarized to introduce each system. The volume of these

chamber system varies from 35 milliliter (ml) to large chamber with a volume of 300 Liters (L) (Liang, Liu et al. 2018b). In certain cases, large room size spray booth is also used in SVOC research (Wood 2017). The early developed chambers include the Field and Laboratory Emission Cell (FLEC) and the Chamber for Laboratory Investigations of Materials, Pollution and Air Quality (CLIMAQ).

FLEC was developed initially for testing VOCs (Wolkoff, Clausen et al. 1991). It is a stainless-steel circular cell with a maximum test material surface area of  $1.77 \times 10^{-2} \text{ m}^2$ . Test material is placed on the bottom of a FLEC. Air is introduced into the chamber from two diagonally positioned inlets and leaves from the top center of the chamber, which provides a constant air flow over the tested materials. It has been applied to test VOC and SVOC emissions from carpet, paint, sealants (Wolkoff, Clausen et al. 1993), flooring adhesives (Yu and Crump 2003) and plasticizers (Clausen, Xu et al. 2007, Clausen, Liu et al. 2012) and furniture (Wolkoff 1996, Marć, Zabiegała et al. 2012).

CLIMAQ is made of panes of window glass, stainless steel and aluminum. The developers validated CLIMAQ by testing carpet, linoleum, wall paint and sealant simultaneously in the chamber (Gunnarsen, Nielsen et al. 1994) and compared results with four other chambers with volume ranged from a  $28 \text{ m}^3$  large booth to a 35 ml FLEC. They discovered the chemical measurement differences were up to one order of magnitude for the same tested product in different chambers. The possible reasons discussed for such differences include those environmental parameters which impact the emission rates such as specific ventilation rates and air velocity over the tested products and sink properties.

In recent development, micro-chamber and sandwich shape emission cells were developed and used to minimize the sink wall effects in product emission testing (Xu, Liu et al. 2012, Liang

and Xu 2014, Sebroski, Miller et al. 2017). Micro-chamber is a stainless chamber with a volume as small as 44 ml (Markes International 2018). An ASTM standard was developed to standardize the testing parameters such as air change rate and temperature for the micro-chamber (ASTM International 2017a). Katsumata developed a two-step method to use a micro-chamber with a volume of 390 ml to test SVOC emissions from various indoor materials. In order to minimize the chamber wall effect, the authors first collected the air when the material was in the chamber, then the material was removed and additional air volume was collected while the chamber was heated. They also validated their method through recovery rate and reproducibility tests (Katsumata, Murakami et al. 2008). Sebroski used a micro-chamber with a volume of 114 ml to study SPF emissions (shown in Figure 2) and compared with a 36-liter small scale chamber (shown in Figure 3). It was found that due to the higher air exchange rate and material loading factor, micro-chamber produced higher TCPP emissions compared to the 36-liter chamber but the difference was within one order of magnitude (Sebroski, Miller et al. 2017). Xu et al. developed a circular sandwich type of chamber which was designed to position the test material as the top and bottom of the chamber. This design maximized the surface area of the emission sources and at the same time minimized the chamber wall sink effects (Xu, Liu et al. 2012). The authors used this sandwich chamber to measure phthalate plasticizers from vinyl flooring materials. Compared to FLEC and CLIMAQ, the time to take the chamber wall to be saturated with the testing chemical reduced from 5 months to 1 months. The authors also further applied this special chamber to other building materials (Liang and Xu 2014).



**Figure 2: Micro-chamber (114 ml) used in studying SPF SVOC emissions (top and side view)**



**Figure 3: Small chamber (36 liters) used in studying SPF SVOC emissions**

Small scale chambers have volume up to 1 m<sup>3</sup> and the corresponding ASTM standard is the ASTM D5116-17 (ASTM International 2017c). The small chambers were originally designed for VOC testing but recent studies started to use them in SVOC research (Office of Chemical Safety and Pollution Prevention 2017, Liang, Liu et al. 2018a, Liang, Liu et al. 2018b). Liang et al. used two 53-liter small chambers in series to measure the parameters that control OPFR emissions. They used the first chamber as the source chamber to generate constant gas phase OPFRs and placed polyisocyanurate foam as samples in the second chamber to absorb OPFRs. With measured airborne OPFRs concentration and the amount of OPFRs absorbed onto the solid materials, the authors fitted their data to the degree of sorption saturation (DSS) model to estimate important IAQ modeling parameters such as the partition and diffusion coefficients for OPFRs. Similarly, Liu et al. used the same chamber system to test these key parameters for PCB congeners and OPFRs for more products found in the indoor environment such as clothing and building construction materials (Liu, Guo et al. 2014, Liu, Allen et al. 2016a).

A typical full-scale (large) chambers have a volume of 30 m<sup>3</sup> and the corresponding ASTM standard is the ASTM D6670 (ASTM International 2018). A full-scale chamber is not commercially available therefore not used as widely as the micro and small chambers in the SVOC research. The Center of Polyurethane Industry (CPI) has sponsored one study to evaluate VOC and SVOC emissions from high pressure applied SPF system in a laboratory spray booth (Wood 2017). Liang et al. used a full-scale chamber (4.8 m × 3.7 m × 3.0 m height) to study the phthalate emissions from flooring materials. They developed a fundamental mechanistic model to interpret the full-scale chamber measurement results and concluded that temperature and air mixing above the source are important factors that impact phthalate emission but air change rate is not (Liang, Caillot et al. 2015).

### 2.3.3 SVOCs multi-media modeling

Measuring SVOCs have posed a few significant challenges include low chemical volatility, strong chamber wall sorption effect and lab chemical contaminations (Guo 2013, Liu, Ye et al. 2013). In addition, SVOC emissions testing is often limited to a specific testing condition which may be quite different than the real indoor environment. Results from chamber studies may not be extrapolated to reflect the realistic indoor environment. Finally, SVOC testing requires significant time and resources commitment. To overcome these challenges, researchers extended VOC emission models, and many SVOC multi-media models have been developed as viable alternatives for chamber or field SVOCs testing. In the past two decades, over 15 multi-media models have been developed to study SVOC emission mechanisms and their fate and transport in the indoor environment. These models are often developed for a specific chemical class and validated through experimental studies. The multi-media models typically define an indoor environment into several “compartments” such as the source, sink, indoor air, airborne particle and settled dust. Depending on model assumptions, each compartment is represented based on different mass transfer models. The first type of model represents indoor sources and sinks using the fugacity concept. Matoba et al. developed a series of fugacity-based models to study emission, transport and distribution of pesticides used in the indoor environment and made these models available as Excel based software (Matoba, Ohnishi et al. 1993, Matoba, Ohnishi et al. 1994, Matoba, Ohnishi et al. 1995, Matoba, Yoshimura et al. 1998). Similarly, Bennett and Furtaw developed a dynamic mass balance compartment model which includes indoor air, sinks (carpet, flooring and wall) and six size fractions of particulate matter. They compared their model with field measured pesticide concentrations in air and carpet (Bennett and Furtaw 2004). Weschler et al. systematically studied SVOCs in the indoor environment by developing a steady

state fugacity-based model. Their model evaluated the influences of key modeling parameters that impact SVOC indoor behaviors such as the octanol-air partition coefficient (Weschler and Nazaroff 2008).

More recent model development focused on better describe the mass transfer mechanism of SVOC emission sources and indoor sinks. Xu and Little first extended a VOC mass transfer model to describe the emission mechanism of DEHP, a plasticizer, from vinyl flooring. In their model, a boundary layer was defined to separate the area immediately above the source material from the rest of bulk air in the indoor environment. SVOC concentration in this boundary layer is determined by the partition coefficient between source material and air, external convective mass transfer coefficient which is a function of air velocity, temperature and source material dimensions, and the SVOC sorption to indoor sinks such as airborne particles. The authors provided an analytical solution for the mass balance equations to calculate the bulk air SVOC concentration based on the initial SVOC concentration and physical properties (partition coefficient between source and air) of the source material and the external conditions (air properties and indoor sinks) (Xu and Little 2006). This model was further developed into a two-zone model to study the DEHP sorption on indoor surfaces such as human skin, carpet, wood and dust (Xu, Cohen-Hubal et al. 2009, Xu, Cohen-Hubal et al. 2010). Liang also used this model to study the influences of surface sorption and air flow on phthalate emissions from vinyl flooring in specially designed stainless steel and wood chambers (Liang and Xu 2015). Shortly after, Liang applied the same model in a large chamber test for vinyl floor phthalate emissions (Liang, Caillot et al. 2015). Additional research was conducted to evaluate the SVOC sink sorption mechanisms. Liu et al. applied the DSS model through chamber testing to characterize the sorption properties of polychlorinated biphenyl (PCB) congeners and OPFRs (Liu, Guo et al.

2014, Liu, Allen et al. 2016a). Similarly, Liang et al. conducted chamber tests to study OPFRs sorption onto impervious surfaces (chamber wall) and fitted the measured data with simplified Langmuir and Freundlich isotherms. They concluded the Freundlich isotherm fits better for OPFR sorption on impervious surfaces than the Langmuir isotherm.

The latest SVOC model development is centered in the Modified State-Space (MSS) method developed by Guo (Guo 2013, Guo 2014). MSS method was built on the State-Space (SS) method first introduced by Yan et al. into the indoor environmental modeling field (Yan, Zhang et al. 2009). The SS method divides a slab of material into a finite number of layers with the same thickness and chemical concentration in each layer is assumed to be uniform during the entire emission process. At the material surface layer, mass transfer process is determined by the fugacity difference at the interface, material-air partition coefficient and external convective mass transfer coefficient. Within the source, mass transfer is controlled by the fugacity difference between two adjacent layers and the solid phase mass transfer coefficient. Guo improved the SS method by making the following modifications: 1) introduced a local two-phase mass transfer theory to simulate mass transfer rate at the interface between solid material and air, and interface between the two solid materials (Lewis and Whitman 1924), as cited in (Guo 2014); 2) defined the thickness of the air exposed layer to be  $10^{-7}$ m for practical and computational purposes; and 3) for the interior layers, the thickness of the inner layer is twice of the outer layer. The MSS method has improved previous mass transfer models by transforming complex partial differential equations to a series discrete, ordinary differential equations which increased computational efficiency (Guo 2013). Moreover, the MSS method allows to model multiple sources, sinks and include chemical barriers, which better reflects the realistic indoor environment.

Among the most recent SVOC models, the MSS method is one of the few methods which have been integrated into a publicly available software, i-SVOC, by USEPA (U.S. Environmental Protection Agency 2013b). i-SVOC is a single zone multi-media model specifically designed to study the emission, fate and transport behavior for SVOCs. Tian et al. applied the i-SVOC software to study TCPP emission from SPF and compared the modeling results with data measured from field studies and micro-chamber tests. They concluded i-SVOC modeling results are highly sensitive to the source related input parameters such as the material-air partition coefficient (Tian, Sebroski et al. 2017).

## **2.4 INFORMATION OF CASE STUDY PRODUCTS AND CHEMICALS**

In this research, an organic chemical insulation material, SPF, was selected as the case study material to illustrate the quantitative approach to evaluate human health impacts of a product through its life cycle phases. For this case study product, two main chemical components were focused in this research. MDI accounts for 50% of the raw materials in weight to produce SPF and has been placed under USEPA's action plan to manage its human health risks (U.S. Environmental Protection Agency 2011b). Due to short half-life (about 15 hours by photochemical reaction in the atmosphere) of MDI in the environment (Tury, Pemberton et al. 2003), this research only evaluates its human health impacts in the cradle-to-gate and application phases. TCPP is a non-reactive flame retardant added to the SPF formulation and has a longer presence in the indoor environment than MDI. TCPP is selected as the case study chemical to evaluate the human health impacts of SPF during use phase.

## 2.4.1 Methylene Diphenyl Diisocyanate and Spray Polyurethane Foam

**2.4.1.1 Application and chemical properties** MDI is a very versatile chemical which is used in various industrial applications such as foam mattresses, pillows, shoe soles, carpet backing materials, insulation, binding agents and automotive parts. The most common type of MDI is the polymeric MDI mixture which is composed of MDI monomers (e.g., 2,4'-MDI or 4,4'-MDI) and high molecular weight polymeric MDI, as shown in Figure 4. The most common chemical reaction of MDI is the formation of polyurethane which was first discovered by Otto Bayer in the 1930s.

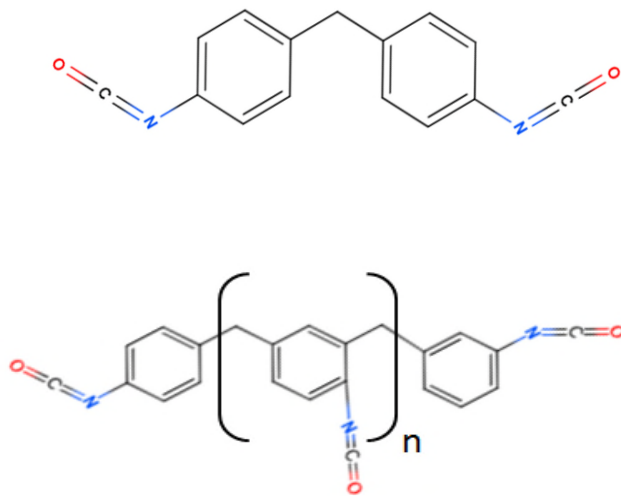


**Figure 4: Chemical structure of the monomeric MDI (left) and polymeric MDI (right)**

SPF is one type of insulation materials made of MDI and polyol. Due to its high performance in promoting energy efficiency, most recent data project SPF market will surpass 2.5 billion

USD by 2024 (Global Market Insights Inc 2017), which has the highest growth rate in the entire polyurethane foam sector (ReportsnReports 2018). SPF is often installed onsite in a newly built or renovated building by mixing the A side (polymeric MDI) and the B side (polyols, catalysts, flame retardants and blowing agents) and spraying these chemicals to a building cavity. When the A and B side chemicals meet together, chemical reaction occurs and forms polyurethane.

The physical and chemical properties of MDI are unique and have a high impact to its emission, transport and distribution in the outdoor and indoor environment. Vapor pressure is one of the key chemical properties that determine the environmental behavior of MDI. At the production temperature (about 200°C), monomeric MDI has a vapor pressure of 700 Pa but the final MDI product is often kept at 40 to 50°C that the vapor pressure is orders of magnitude lower ( $8.2 \times 10^{-3} - 2.5 \times 10^{-2}$  Pa) (International Isocyanate Institute 2003). At room temperature, pure MDI is a waxy solid with a white to yellow color. Pure MDI monomer has a vapor pressure of  $6.2 \times 10^{-4}$  Pa at 20°C while polymeric MDI's vapor pressure is essentially negligible. MDI is almost insoluble in water solubility and has a higher density than water. It has a melting point of 34 to 43°C, depending on specific monomers (e.g., 2,4'-MDI or 4,4'-MDI). MDI can react with many functional groups such as the hydroxyl (-OH) and amino (-NH) groups. The reaction kinetics are not only important for MDI's industrial applications but also impact its environmental behaviors.

**2.4.1.2 Environmental fate of MDI in air** MDI can be released into the environment through multiple pathways. During the cradle-to-gate manufacturing phase, MDI can be emitted to the outdoor air through equipment leaks or stack emissions. At downstream usage stages, MDI can be released to both industrial and residential indoor environment through various processes such

as foaming and spraying. The atmospheric chemistry of MDI is complex and an ongoing research but previous research findings are summarized herein.

Due to the low vapor pressure of MDI, atmospheric chemistry studies on MDI were conducted using para toluene isocyanate (PTI) and Toluene Diisocyanate (TDI) due to their similarity in chemical structure. Carter et al. studied the half-life of Para Toluene Isocyanate (PTI) through atmospheric photochemical reaction as a surrogate to MDI because MDI is “essentially a dimer of PTI” (Carter, Luo et al. 1999). They concluded that photochemical reaction with OH radical is the primary atmospheric removal mechanism of MDI in the outdoor environment. Tury et al. summarized Carter’s study and concluded that the half-life of MDI in the atmosphere is about 15 hours at the global average OH radical concentration (Tury, Pemberton et al. 2003). Besides the photochemical reaction, hydrolysis is another possible reaction to remove MDI from the atmosphere since MDI reacts with hydroxyl groups. However, previous research has proved that no matter MDI is present as vapor or airborne particles, hydrolysis is not a significant reaction to affect MDI fate in the atmosphere. Holdren et al. performed a chamber test to study the hydrolysis reaction of TDI in the atmosphere as a surrogate to MDI. They concluded that TDI vapor does not react with water vapor in the air (Holdren, Spicer et al. 1984). Hugo et al. studied the surface hydrolysis of MDI droplets and concluded that under a relative humidity of 40%~70%, a maximum of 10% MDI (as a droplet on a petri dish) reacted with water vapor in 24 hours (Hugo, Fishman et al. 2016).

In the indoor environment, when MDI is sprayed, the primary form of emission is an overspray aerosol (Lesage, Stanley et al. 2007). MDI airborne concentration resulted from spray application is highly influenced by the relative location to the emission source. Researchers surveyed SPF applicators at various indoor and outdoor locations and concluded that MDI

airborne concentration was higher at closer locations to the spray gun (Bilan, Hafladson et al. 1989, Crespo and Galán 1999). The indoor half-life of MDI is in order of days. Ecoff et al. reported that airborne MDI drops below the detection limit within 24 to 48 hours after spray application is finished (Ecoff, Tian et al. 2017). When MDI is not sprayed, MDI emitted to the air as a vapor, involves the formation of “condensation aerosols” which means vapor phase MDI condenses to nuclei in the air to form aerosols. However, this phenomenon only occurs when MDI vapor concentration is relatively high ( $\sim 100 \mu\text{g}/\text{m}^3$ ) such as in an occupational setting. It is different in residential settings. Skarping et al. have generated MDI vapor in an emission chamber and studied how MDI vapor interacted with room air. They concluded that when the total MDI concentration in the air was low ( $< 5 \mu\text{g}/\text{m}^3$ ), even with nuclei, the majority ( $>70\%$ ) of MDI remained in the gas phase during the first hour after MDI vapor was generated (Skarping, Karlsson et al. 2011).

**2.4.1.3 Human health effects and exposure threshold of MDI** MDI is not classifiable for cancer effect but is known as dermal and inhalation sensitizers and may cause contact dermatitis, skin and respiratory tract irritation and occupational asthma if exposed workers are not properly equipped with protection equipment (The National Institute for Occupational Safety and Health 1996, Krone and Klingner 2005). When uncured MDI is inhaled either as an aerosol or vapor, it can act as an agent to cause occupational asthma. In the early literature, isocyanates related asthma cases were extensively reported (The National Institute for Occupational Safety and Health 1978).

MDI exposure threshold values vary by organizations. The National Institute for Occupational Safety and Health (NIOSH) sets an 8-hour time weighted average recommended exposure level (REL) at  $50 \mu\text{g}/\text{m}^3$  and a ceiling level of  $200 \mu\text{g}/\text{m}^3$  (The National Institute for

Occupational Safety and Health 2007). In comparison, California Office of Environmental Health Hazard Assessment has a chronic reference exposure level at  $0.08 \mu\text{g}/\text{m}^3$  (Office of Environmental Health Hazard Assessment 2016).

## **2.4.2 Tris(1-Chloro-2-Propyl) Phosphate**

**2.4.2.1 Application and chemical properties** TCPP is an OPFR often used in polyurethane foam applications such as building insulations and refrigerator casings (Jayjock, Kroner et al. 2015). TCPP is one of the chemical to replace the phased-out PBDE flame retardants (U.S. Environmental Protection Agency 2013a). The typical weight % of TCPP in polyurethane foam is about 8-10% (European Commissions 2008). TCPP is also reported to be used in textiles as a plasticizer (Andresen, Grundmann et al. 2004, Agency for Toxic Substances and Disease Registry (ATSDR) 2009).

TCPP is a colorless liquid with a mild odor and has a solubility in water ranges from 1.2 g to 1.6 g/L (Hazardous Substance Data Bank (HSDB) 2013). The reported TCPP vapor pressure varies by one order of magnitude from  $1.4 \times 10^{-3}$  (European Commissions 2008) to  $2.0 \times 10^{-2}$  Pa (U.S. Environmental Protection Agency 2012b) at  $25^\circ\text{C}$  but all of them fall into the range of SVOCs. As a SVOC, TCPP has a relatively high molecular weight and high octanol-air partition coefficient ( $k_{oa}$ ) ranges from  $1.6 \times 10^8$  (U.S. Environmental Protection Agency 2012b) to  $4.8 \times 10^8$  (Wang, Zhao et al. 2017). These properties determine its fate and transport in the environment. For example, with a high  $k_{oa}$ , TCPP is lipophilic and tends to be partitioned in the indoor sinks with organic content such as flooring, carpeting and settled dusts more than the VOCs.

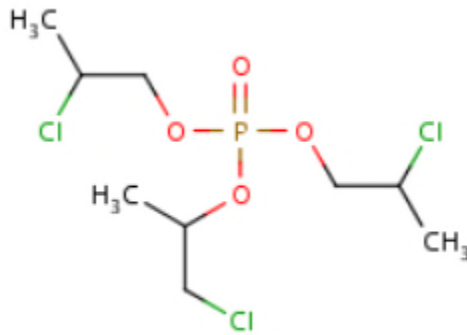


**Figure 5: Chemical structure of TCPP**

**2.4.2.2 TCPP presence in the indoor environment** TCPP can be present in different indoor environmental media: vapor phase, airborne particle, settled dust and accumulation onto indoor surfaces such as carpeting and flooring. Each environmental media contributes to the overall human exposure to TCPP through different exposure pathways (Agency for Toxic Substances and Disease Registry (ATSDR) 2009). TCPP in vapor phase and airborne particles can be inhaled (European Commissions 2008, Yang, Ding et al. 2014), TCPP in settled dust can be ingested by infants and young children (García, Rodríguez et al. 2007) and TCPP accumulated on indoor surfaces can be up taken by dermal contacts (National Research Council 2000).

Many previous research studies have measured the indoor airborne TCPP concentration in various settings, including houses, offices, schools, hospitals and retails. TCPP airborne concentration ranges from a few  $\text{ng/m}^3$  up to  $1,260 \text{ ng/m}^3$  found in Japanese houses (Saito, Onuki et al. 2007). Besides the true differences in airborne concentration, sampling techniques could contribute to such differences since among these studies, some use quartz fiber filter sampler (Carlsson, Nilsson et al. 1997) but others use solid phase extraction membranes (Tollbäck, Isetun et al. 2010) or cartridges (Marklund, Andersson et al. 2005).

TCPP found in the indoor environment is primarily emitted from various building construction materials, furniture and consumer products. Salthammer et al. reported TCPP emissions from polyurethane foam and recycled plastics used as flooring materials (Salthammer and Schripp 2015). Ingerowski et al. have measured high level of TCPP in furniture and household products with a range from 150,000 ng/g in wood coating to 180,000,000 ng/g in polyurethane foam fillers (Ingerowski, Friedle et al. 2001). TCPP can also be emitted from electronics such as television and laptop computers. Kajiwara et al. found up to 150 ng/g TCPP in the AC adaptor of a laptop (Kajiwara, Noma et al. 2011). Saito et al. reported computer monitors emit up to 1,700 ng/m<sup>2</sup>/hr using chamber testing methods (Saito, Onuki et al. 2007).

**2.4.2.3 Human health effects and exposure threshold of TCPP** Toxicological thresholds have not been systematically established for TCPP, largely due to the lack of toxicity studies with good data quality. There is no Reference Dose (RfD), Reference Concentration (RfC) or cancer assessment established for TCPP in the USEPA IRIS database (U.S. Environmental Protection Agency 2018a). For occupational exposure, no REL nor threshold value (TLV) was established by NIOSH or American Conference of Governmental Industrial Hygienists (ACGIH). Due to the lack of data, no minimum risk levels were reported in the Agency for Toxic Substances and Disease Registry (ATSDR) toxicological profile (Agency for Toxic Substances and Disease Registry (ATSDR) 2009). The USEPA alternative assessment classifies TCPP hazard profile as high in reproductive and developmental endpoints, moderate in carcinogenic and neurological endpoints and low in acute toxicity, genotoxicity, skin sensitization, eye and skin irritation. For the two high hazard endpoints, toxicological data were limited. One study conducted at TNO reported that rats fed with TCPP had decreased body weight, food consumption and number of pups delivered in mid and high dose parental animals and all dosed animals showed effects on

uterus (European Commissions 2008). There were two other studies with lower data quality did not show the same reproductive and developmental effects (Kawasaki, Murai et al. 1982, Freudenthal and Henrich 1999). Based on limited information, a screening level provisional RfD was established for subchronic and chronic exposure at 0.1 mg/kgBW/day and 0.01 mg/kgBW/day (U.S. Environmental Protection Agency 2012c).

In terms of human health risks, early literature concluded that TCPP has low risk due to low exposure (International Programme for Chemical Safety 1998). EU risk assessment report concluded that TCPP human health risk is limited to occupational dermal exposure during manufacturing phase in relation to effects on fertility and developmental toxicity while for other endpoints such as irritation, sensitization, mutagenicity and carcinogenicity, there is no need to apply risk reduction measures beyond those which are being applied already (European Commissions 2008). However, these assessments only address TCPP exposure to general population but did not evaluate human health risks associated with TCPP emitted from a specific product such as SPF.

### **3.0 INTEGRATING SITE-SPECIFIC DISPERSION MODELING INTO LIFE CYCLE ASSESSMENT: FOCUS ON INHALATION RISKS IN CHEMICAL PRODUCTION**

The following chapter contains material reproduced from an article published in the *Journal of the Air & Waste Management Association* with the citation:

Tian, S. and M. Bilec (2018). "Integrating site-specific dispersion modeling into life cycle assessment, with a focus on inhalation risks in chemical production." Journal of the Air & Waste Management Association: 1-15.

The article appears as published per the copyright agreement with Taylor & Francis, publisher of

*Journal of the Air & Waste Management Association*

Portions of the Supporting Information submitted with *Journal of the Air & Waste Management Association* appear in this chapter and the remaining portions appear in Appendix A.

## 3.1 INTRODUCTION

### 3.1.1 The chemical industry and chemical management regulations

In the U.S., the chemical industry supported 25% of the GDP and produced 15% of the world's chemicals in 2015 (American Chemistry Council 2016, Bureau of Economic Analysis 2016). According to the U.S. Environmental Protection Agency (USEPA), there are currently over 84,000 chemicals listed in the TSCA inventory (United States Government Accountability Office 2013). Federal and state agencies have set laws and regulations to manage hazard, exposure and risks along a chemical's supply chain. TSCA was passed to evaluate hazards and potential risks from new or existing chemicals in 1976. In 1986, Toxic Release Inventory (TRI) was created to address chemical releases from industrial facilities under the Emergency Planning and Community Right-to-Know Act. Under LCRA, the strengthened chemical management law framework (The 114<sup>th</sup> United State Congress 2016), USEPA has developed the ToxCast<sup>TM</sup> and ExpoCast<sup>TM</sup> programs to prioritize chemicals of concern (Wambaugh, Setzer et al. 2013, Isaacs, Glen et al. 2014, Wambaugh, Wang et al. 2014, Biryol, Nicolas et al. 2017, Bonnell, Zidek et al. 2018). To achieve the goal of environmental and human health protection, many tools have been developed by federal agencies and academia to assess the impact of chemicals (Centers for Disease Control and Prevention 2012). For example, ExpoCast used two far-field tools: the USEtox model and the Risk Assessment IDentification And Ranking (RAIDAR) Model to prioritize chemical exposure among 1,936 chemicals (Wambaugh, Setzer et al. 2013) However, each existing tool has its strength and weakness.

### **3.1.2 Existing methods to evaluate human health impacts of far-field chemical emissions**

HHRA and LCA are two methods that can be used to quantify chemical human health impacts. HHRA is a receptor-based method which evaluates the human health impacts of chemicals emitted to the environment for targeted population. HHRA often focuses on a chemical (e.g., is Bisphenol A safe?). Since it is a receptor driven method, HHRA is often conducted for individual life cycle phase separately. However, LCA considers the environmental and human health impacts from all life cycle emissions of a chemical. Another key distinction between HHRA and LCA, subsequently described, is the risk minimization principle. HHRA assumes only the risks over certain threshold (e.g., cancer risk: one in a million, non-cancer Hazard Index (HI): one) should be managed (U.S. Environmental Protection Agency 2005b).

LCA is another method to study the environmental and human health impacts of processes and products. Unlike HHRA, LCA defines a functional unit as the basis to collect the emission inventory released into the environment along life cycle phases and in the LCIA step, the toxic chemical emissions such as HAPs are characterized into human health endpoints, such as cancer and non-cancer. Depending on the geographical scale of the LCIA models, human health impacts can be evaluated at global, continental or regional levels. Some of the widely used LCIA models for HHIA are listed in Table 3. The more recent model development focuses on providing more geographical relevance by quantifying regional environmental characteristics. For example, USEtox 2.0 provides regionalized environmental conditions for 24 regions in the world (Rosenbaum, Huijbregts et al. 2011).

Although HHIA in LCIA has been improved by regionalizing the environmental compartments, research efforts are still desirable to overcome two major obstacles in order to assess the health risk of chemicals along their life cycle phases. First, disaggregated LCI data

with site-specific geographical information is lacking. In current LCI databases such as Gabi and Ecoinvent (Weidema, Bauer et al. 2013, Thinkstep 2014), the location of emissions is recorded at a large and often generic geographical scale, such as the continental air of North America, instead of a specific geographical coordinate. Except certain unit processes, most chemicals are produced in chemical plants which have geographical coordinates recorded in publicly available databases, such as EPA's TRI and National Emission Inventory (NEI). With the exact emission location, site-specific human health impacts can be assessed for a unit process using localized meteorological, terrestrial and demographical information. Second, current LCIA models assume that chemical distribution in each environmental compartment is homogeneous. However, in a real-world scenario, chemical concentrations vary both temporally and geographically. For example, USEtox assumes everyone in the entire continental compartment (a population of 998 million) has the same level of inhalation exposure. This approach fits the purpose of high throughput assessment but may neglect the temporal and geographical differences within each environmental compartment. For chemicals emitted into the air, it is expected that the inhalation risk is higher for people living closer to the emission source. With current LCIA methods and regionalization approaches, such differentiations may not be achieved. Therefore, the homogeneous environmental compartment assumptions may not be adequate for a comprehensive HHIA. A method is truly needed to derive site-specific LCI using public information and assess human health impacts at a finer geographical scale.

**Table 3: Existing LCIA method/model in assessing human health impacts**

<b>LCIA Method/HH Characterization Model</b>	<b>Last Update to HH CFs</b>	<b>Level of Regionalization</b>
TRACI 2/USEtox (Bare 2011)	2016	USEtox divides the world into 24 regions* and provides regionalized environmental landscape parameters for each region.
CML/USEtox (Rosenbaum, Bachmann et al. 2008, Rosenbaum, Huijbregts et al. 2011)	2010	
ReCiPe/USES-LCA 2.0 (Zelm, Huijbregts et al. 2009)	2015	USES-LCA 2.0 provides default environmental landscape parameters at three geographical scales (Global, Continental and Urban). ReCiPe provides different CFs based on “archetype LCIA” such as high vs. low population density areas and high vs. very high stress watersheds.
IMPACT North America (Humbert, Manneh et al. 2009)	2013	IMPACT North America divides the U.S. and Canada into 1° x 1° air cells, 523 watersheds and five coastal zones. Within each cell or zone, the “archetype LCIA” is used to differentiate high vs. low population density area and high vs. low agricultural production regions.
GLOBOX (Wegener Sleeswijk and Heijungs 2010)	2011	GLOBOX divides the world into 250 regions and provides default environmental landscape parameters.

Notes: \* With overlap (e.g., North America vs. USA & Southern Canada)

### **3.1.3 Previous work to evaluate the human health impacts of far-field chemical emissions**

There are approaches and case studies that combine HHRA and LCA to advance HHIA of chemicals (Sonnemann, Castells et al. 2004, Sleeswijk 2011, Walser, Juraske et al. 2014). In late 1990s, Spadaro and Rabl proposed a framework to calculate the endpoint impact of air pollutants by utilizing both short range (<50 km) and long range (>50km) air dispersion modeling. The calculated airborne concentration is coupled with population data, dose-response curves and monetary valuation to derive the “real damage” from air pollutants (Spadaro and Rabl 1999). In the early 2000s, researches adopted the iFs or similar concepts to increase the geographical relevance in LCIA (Moriguchi and Terazono 2000, Yurika, I. et al. 2002). For example, Yurika et al. applied the CALPUFF air dispersion model to evaluate the human health risk reduction from insulation materials in four U.S. regions. Moriguchi and Terazono used the Gaussian dispersion equations to develop an exposure per emission coefficient which can differentiate the amount of air emissions intake by population in different regions. Later in mid 2000s, Sonnemann proposed to combine the multi-media models with site-specific impact assessment to evaluate industrial processes. More recently, LCA and RA have been used together to study indoor chemical exposures (Hellweg, Demou et al. 2009, Walser, Juraske et al. 2014, Rosenbaum, Meijer et al. 2015). These studies have been thoroughly discussed by Harder et al. (Harder, Holmquist et al. 2015).

At the national level, the USEPA has published the National Air Toxics Assessment (NATA) since early 2000s to characterize nationwide chronic cancer risk and non-cancer HI of HAPs. NATA, essentially a national level HHRA, uses NEI data of point and mobile sources, applies air dispersion modeling to quantify the human health impacts of HAPs, and identifies risk hotspots throughout the country. The most recent NATA was published in 2015, using 2011 NEI data

which included 180 pollutants (Office of Air Quality Planning and Standards 2015). The USEPA has also created the Risk Screening Environmental Indicator (RSEI) model, integrating TRI data, chemical toxicity values, air dispersion modeling, and population census to calculate the relative hazard-based and risk-based scores for one facility. At the state level, a few authors quantified the human health risks of chemical emissions from manufacturing facilities, especially HAPs by analyzing the TRI and NEI datasets (Neumann, Forman et al. 1998, Morello-Frosch., Woodruff et al. 2000, Tam and Neumann 2004). Although these national and state level assessments have the potential to offer rich data sources for the often data-scarce LCA community, their goal is not to evaluate the human health impacts of one product but rather focus on one facility or an industry sector.

Previous work identified two major obstacles to combine tools in HHRA and LCA for human health assessment of chemicals. The most discussed is the different fundamental assumptions in HHRA and LCA regarding the human health impact. HHRA assumes that chemicals will only cause damage when the health risk exceeds a certain threshold, and therefore should be managed. LCA assumes a linear cause-effect relationship between chemical emissions and health impacts; therefore, more emissions will cause additional health damage. Walser et al. studied the human health impacts of printed magazines by conducting an LCA using the USEtox model and an HHRA for indoor chemical exposures (Walser, Juraske et al. 2014). They found the two methods did not necessarily identify the same health hotspots. The second obstacle is that HHIA in LCA is based on a functional unit, while HHRA often focuses on one facility or industry sector. Previous research discovered that the functional unit is one of the major differences between HHRA and LCA (Olsen, Christensen et al. 2001, Sleeswijk 2011). Therefore, any improvement to include site-specific modeling in HHRA and LCA should first develop a regionalized LCI based

on the selected functional unit and conduct the human health assessment with site specific environmental fate and transport tools.

### **3.1.4 Objectives**

One goal of this research was to develop a method to assess the human health impacts of chemicals and products along their life cycle phases with high geographical relevance by combining site-specific air dispersion modeling and LCA, using publicly available data. An approach to derive a regionalized LCI is described and can be used to bridge the gaps, lacking in current LCI databases. The outcome reveals the geographical pattern of health risks and prioritizes pollution reduction measures both along a chemical's life cycle phases and at a finer geographical scale. A case study of quantifying the inhalation risks of MDI is presented to demonstrate the development and application of this proposed method. The method is presented and immediately following each method subsection is case study information to better contextualize the method. For the purpose of this research, only chemicals listed as HAPs were included. Criteria air pollutants and other chemical emissions such as NO<sub>x</sub> and ammonia may be characterized to have human health impacts in traditional LCIA methods but are excluded from this assessment. Therefore, the results of this case study are not directly comparable with a conventional LCA.

### **3.1.5 Case study: cradle-to-gate production of MDI**

MDI was chosen as the case study material, since it is a chemical widely used in the production of many common products such as mattress foam, building insulation material, oriented strand

board, footwear, coating and sealants (American Chemistry Council 2015). MDI is produced worldwide by five major manufacturers with a capacity of 6.51 million tons/year, in which 1.27 million tons are produced in the U.S. (Afshar 2014). There are only three locations in the U.S. where MDI is produced. These locations are Baytown and Freeport in Texas and Geismar in Louisiana, but many other production sites are involved in producing the raw materials needed for MDI. In 2011, ACC published an LCI report which summarized the raw materials and emissions involved in cradle-to-gate MDI production (American Chemistry Council 2011b). In this report, LCI emissions were reported for each unit process, which made it possible to track the exact emission location by geocoding the raw material suppliers. MDI is also an important chemical from a regulatory perspective. USEPA had an action plan to address the concerns of ‘uncured’ MDI products in locations where the general population could be exposed (U.S. Environmental Protection Agency 2015a). The case study also aimed to show how human health assessment can be performed along a chemical’s cradle-to-gate life cycle phases that health risks (inhalation) can be addressed with high geographical relevance at the same time.

### **3.2 METHODS**

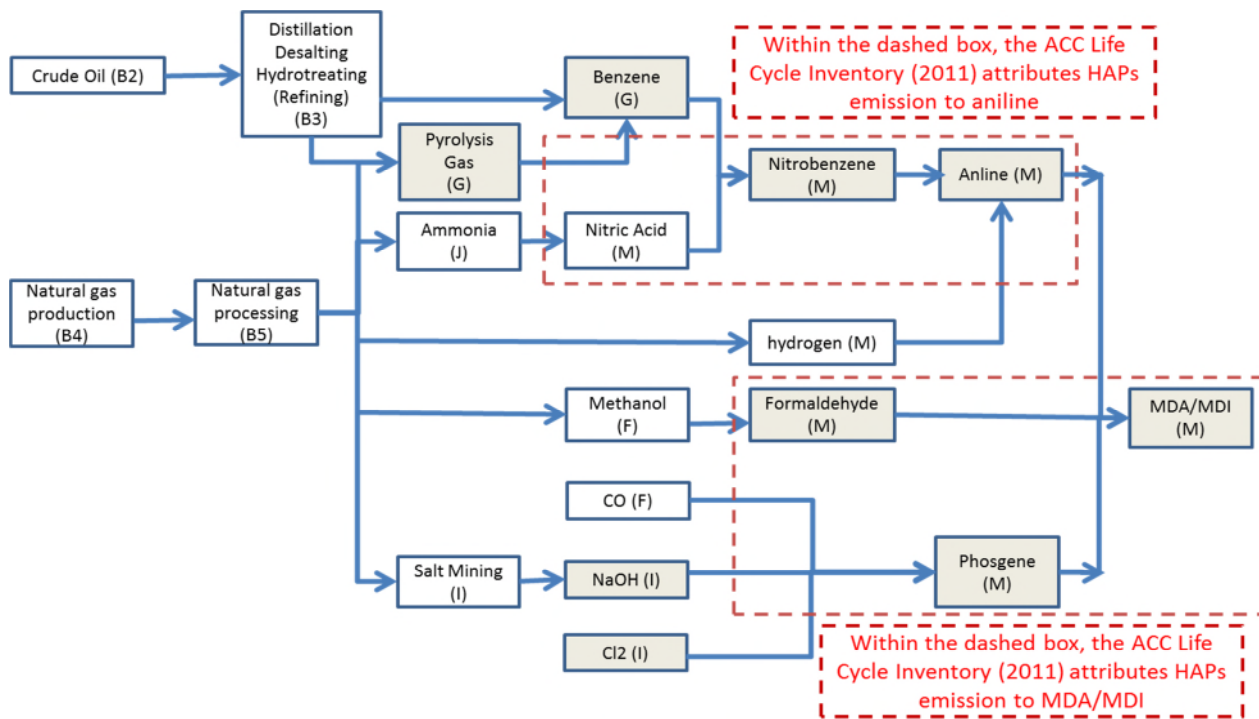
This section introduces a method that describes how publicly available datasets can be used to derive regionalized LCI, then apply site-specific air dispersion modeling to evaluate the human health risks of a case study chemical with a focus on inhalation pathway. The main steps can be summarized as: 1) Define the scope of the study and identify unit processes which emit Hazard Air Pollutants (HAPs); 2) Develop a regionalized LCI for the selected unit processes by geocoding manufacturing plants; 3) Perform air dispersion modeling (Step 3a) and calculate the

inhalation risks of the unit process for which exact manufacturing locations are known (site-specific unit process) (Step 3b); 4) Calculate the inhalation risks of unit processes for which the exact locations are unknown (non-site specific unit process) using the USEtox model (Step 4); 5) Combine the risks calculated to derive the total inhalation risks (Step 5); and 6) Identify risk hotspots and patterns (Step 6).

### **3.2.1 Scope of the case study (Step 1)**

The system boundary defined for this case study is “cradle-to-gate” which starts from raw material extraction and ends at the manufacturing plant where MDI is ready to be shipped, see Figure 6. The functional unit is 1,000 kg of MDI produced. The unit processes to be included and studied in future site-specific modeling were identified by the following steps. First, on-site (i.e., gate-to-gate) emissions were obtained from the ACC report (American Chemistry Council 2011b), as shown in Figure 6. It should be noted that the red dashed boxes indicate that gate-to-gate emissions of a few unit processes are aggregated together, since they are often co-produced at one plant. Second, unit processes that emit HAPs were identified based on the HAPs list (U.S. Environmental Protection Agency 2016b) as shown in Table 4 under “site-specific dispersion modeling (exact location is known).” Third, the Directory of Chemical Producers (DCP) was used to locate the manufacturers of the identified unit process (e.g., Benzene) (Stanford Research Institute 2011) for site-specific dispersion modeling. If the manufacturers could not be identified in the DCP, such as crude oil and natural gas, then they were excluded from site-specific modeling but included in the multi-media modeling. For cradle-to-gate MDI production, a total of five unit processes were identified for site-specific modeling and three unit processes were

identified for multi-media modeling as shown in Table 4. The remaining unit processes in this cradle-to-gate LCI do not have HAPs reported in the LCI developed by ACC.



The red dashed boxes indicate that gate-to-gate emissions of a few unit processes are aggregated together since they are often coproduced at one plant. The HAPs emission associated with each unit process or group of unit processes are listed in Table 4.

**Figure 6: The system boundary of cradle-to-gate MDI production (modified based on (American Chemistry Council 2011b))**

**Table 4: Classification of unit processes (based on ACC LCI, (American Chemistry Council 2011b))**

<b>Model Scenarios</b>	<b>Unit process</b>	<b>HAPs emitted</b>	<b>Total # of plants*</b>
Site-specific dispersion modeling (Exact location is known)	Cl <sub>2</sub> and NaOH	Benzene, CCl <sub>4</sub> , Cl <sub>2</sub> , Pb and Hg (II)	14
	Aniline	Pb	5
	Pyrolysis Gas (Olefins)	Cl <sub>2</sub>	3
	Benzene	Cl <sub>2</sub>	16
Non-site specific Multi-media modeling (Exact location is unknown)	MDA/MDI	Cl <sub>2</sub> , Formaldehyde, Methanol, Cl <sub>2</sub> and CCl <sub>4</sub>	4
	Crude oil production and processing	As (V), Benzene, Cl <sub>2</sub> , Cr (VI), Ethyl benzene, Ethylene	N/A.
	Natural gas production and processing	Dibromide, Hg (II), Ni (II), PAH as B(a)P, Sb (V), Toluene and Xylene	
Salt mining			
Not modeled	Ammonia	No HAPs emission reported at the manufacturing site	N/A.
	Methanol		
	Hydrogen		
	Carbon Monoxide		

Notes: \* Total number of plants which were included for site-specific modeling that covers 85% of the annual production capacity.

### **3.2.2 Developing a regionalized LCI (Step 2)**

In order to assess the inhalation risks of each unit process at the site-specific level, a regionalized LCI is required. The first step was geocoding the unit process identified in step 1. TRI is a publicly available database which contains the latitude and longitude coordinates of each plant (U.S. Environmental Protection Agency 2018d). The geocoded plant locations were entered into a Geographical Information System (ArcGIS) (Environmental Systems Research Institute 2015). For certain unit process (e.g., Benzene) which has multiple plants (may be owned by the same company) in the U.S., a cut off criteria was applied as described below. All plants were ranked by their production capacities from the highest to the lowest and the production capacities were summed. Only the plants (from the highest to the lowest production capacity) which contribute to the top 85% production capacity were included for site-specific modeling. For example, there were 36 plants in the U.S. that produce benzene, the top 16 of them accounted for over 85% of the total production capacity (Stanford Research Institute 2011). Therefore, the cut off criteria was set to include the top 16 plants (based on production capacity) in site-specific modeling. When two plants had the same capacity, the one in proximity to Houston, TX or Geismar, LA was selected as these two locations are the primary regions of MDI production. Individual plant capacity was also recorded for future analysis.

### **3.2.3 Performing air dispersion modeling (Step 3a)**

EPA's Human Exposure Model (HEM-3) with American Meteorological Society/Environmental Protection Agency Model (AERMOD) (SC&A Incorporated 2017) was used for site-specific air

dispersion modeling. AERMOD is different than LCIA models as it uses site-specific meteorological and geographical conditions to study the fate and transport of HAPs, while LCIA approaches largely assume the aforementioned conditions are homogeneous within one environmental compartment. AERMOD calculates the airborne HAPs concentration at a certain distance from the emission source. This concentration can be linked with a specific census block (i.e., receptor). The common trend is that the airborne concentration is higher at receptors which are closer to the emission sources. Key input files needed to perform such modeling include: emission, meteorological and surface terrain files.

In site-specific modeling, the amount of HAPs emitted from each unit process at an individual plant was calculated based on the functional unit (mt HAPs emitted per 1 mt MDI produced). All emissions were modeled as a point source located at the coordinates as previously geocoded in ArcGIS. One important component in the emission profile is the stack parameters. The NEI Standard Classification Code (SCC) average stack parameters were chosen for the unit processes as listed in Table 5. Meteorological and surface terrain files were obtained from weather stations closest to the manufacturing plant according to the station list provided by HEM-3. A total of 36 unique plants which produced one or more of the five unit processes listed in Table 5 were modeled.

**Table 5: Unit processes and site-specific modeling/average stack parameters (U.S. Environmental Protection Agency 1999)**

Unit Process	Average Stack Parameters			
	Height (m)	Diameter (m)	Exit velocity (m/s)	Exit Temperature (K)
Cl <sub>2</sub> and NaOH	10.68	0.92	8.94	318.61
Aniline	16.73	1.17	8.20	399.73
Pyrolysis Gas (Olefins)	25.10	1.31	4.75	409.72
Benzene	14.67	0.23	0.31	297.13
MDA/MDI	5.87	0.12	1.00	315.28

### 3.2.4 Calculating inhalation risks of site-specific unit processes (Step 3b)

Two human health endpoints (cancer and non-cancer) were evaluated based on the modeled average airborne concentration of each HAP at a specific census block and its toxicity values in the reference library of HEM-3 (SC&A Incorporated 2017). At a specific census block, the cancer risk of HAPs by inhalation pathway was expressed mathematically as Equation 1.

$$\text{Cancer risk} = \left( \sum_k^p \sum_j^n \sum_i^m \overline{C_{i,j}} \times URE_i \times EF_{i,k} \times PC_{k,j} \right) \times P_{MDI} \times 1.1 \frac{\text{ton}}{\text{mt}} \quad \text{Equation 1}$$

Where,

$\overline{C_{i,j}}$  ( $\mu\text{g}/\text{m}^3$  per ton of HAP) is the modeled yearly average airborne concentration of HAP  $i$  at a specific census block based on 1 ton HAP  $i$  emission from plant  $j$ .  $URE_i$  ( $\text{m}^3/\mu\text{g}$ ) is the inhalation cancer Unit Risk Estimate of HAP  $i$  that represents the upper-bound excess lifetime cancer risk estimated to result from continuous exposure to an agent at a concentration of  $1 \mu\text{g}/\text{m}^3$  in air (U.S. environmental Protection Agency 1996).  $EF_{i,k}$  (emission factor, mt HAP <sub>$i$</sub> /mt MDI) is the amount of HAP  $i$  emitted from unit process  $k$  per functional unit (1,000 kg MDI),  $PC_{k,j}$  (%) is

the plant  $j$ 's production capacity percentage among all plants which produces unit process  $k$ ,  $P_{MDI}$  (mt) is the total MDI production capacity in the U.S.,  $m$  is the number of HAPs emitted from unit process  $k$ ,  $n$  is the number of manufacturing plants which produces unit process  $k$ , and  $p$  is the number of unit processes identified for site-specific air dispersion modeling.

Similarly, non-cancer risk of HAPs by inhalation pathway can be expressed as Equation 2.

The non-cancer hazard index can be calculated as:

$$\text{Non-cancer Hazard Index (HI)} = \frac{\left( \sum_k^p \sum_j^n \sum_i^m \overline{C_{i,j}} \times EF_{i,k} \times PC_{k,j} \right) \times P_{MDI} \times 1.1 \frac{\text{ton}}{\text{mt}}}{RfC_i} \quad \text{Equation 2}$$

Where,

$RfC_i$  is the reference concentration for non-cancer endpoints by inhalation pathway for HAP  $i$ . For chemicals with multiple non-cancer endpoints, HEM-3 identifies all the targeted organs but only the RfC which results the highest HI is included in the toxicity value reference library.

An example calculation can be found in the Appendix A.

### 3.2.5 Calculating inhalation risks of non-site specific unit processes (Step 4)

For unit processes without exact production location as shown in Table 4, the USEtox model was used to provide screening level risk characterization. In this case study, the HAP emission rates (kg/day) of non-site specific unit processes were calculated based on the emission factor per functional unit and then scaled by annual MDI production capacity. The HAPs were assumed to be released into the continental air compartment. For example, a total of 0.037 kg benzene is emitted from all non-site specific unit processes per 1 metric ton of MDI produced. Based on the annual MDI production of 1.27 million metric tons in the U.S., the average daily benzene

emission is 129 kg. In the USEtox model, HAP emissions from non-site specific unit processes created an emission rate matrix containing an entry for the continental air compartment only. The emission rate matrix was then multiplied by the fate factor matrix which describes the HAPs fate and transport amongst different environmental compartments. The product of these two matrices was the HAPs mass in each compartment at steady state. Then the HAPs mass was divided by the air compartment volume defined in USEtox to calculate the steady state airborne concentration (Urban:  $5.76 \times 10^{10} \text{ m}^3$ , Continental:  $1.00 \times 10^{16} \text{ m}^3$  and Global:  $4.60 \times 10^{17} \text{ m}^3$ ). Following the Risk Assessment Guidance for Superfund (U.S. Environmental Protection Agency 1989), the inhalation risk of each HAPs was calculated using the steady state airborne concentration and the toxicity values provided in the reference library of HEM-3. For the same benzene example, USEtox calculated the steady state benzene concentration in continental air compartment at  $4.18 \times 10^{-5} \mu\text{g}/\text{m}^3$ . The corresponding cancer risk was  $3.26 \times 10^{-10}$  and non-cancer HI was  $1.39 \times 10^{-6}$ . Finally, the inhalation risk associated with non-site specific unit processes were calculated by adding the risk characterization values of all HAPs involved in USEtox modeling.

### **3.2.6 Combine the risk characterization values of all unit processes (Step 5)**

Finally, the total inhalation risks of the cradle-to-gate MDI production were calculated by adding the site-specific (Step 3b) and non-site specific (Step 4) risk characterization values.

### **3.2.7 Identifying inhalation risk hotspots and patterns in GIS (Step 6)**

In HEM-3, the modeled airborne concentration is at census block level, which is the smallest graphical unit in the census (United States Census Bureau 2015). However, due to model

uncertainties, it has been shown in previous studies that census block or tract level results should only be used to identify geographical patterns of human health risks instead of pinpointing any specific census block or tract (Office of Air Quality Planning and Standards 2015). Therefore, this research investigated the census tract level results to identify the geographical pattern of inhalation risks and used the total inhalation risk at the county level for risk characterization. The census block level results were averaged within each census tract to represent tract level results and plotted in ArcMap. Similarly, census tract results were averaged within each county to represent county level results.

### **3.3 RESULTS**

As described in the method Steps 4 and 5, inhalation risks associated with cradle-to-gate MDI production were calculated separately for the site-specific and non-site specific unit processes.

#### **3.3.1 Site-specific unit processes**

A total of 36 plants were included in the site-specific modeling, which covered the five unit processes listed in Table 5. All plants are located in the Gulf coast region including four states: Texas, Louisiana, Mississippi and Alabama. Out of the 36 plants, one plant covers three unit processes, four plants cover two unit processes, and the remaining plants cover only one unit process. The inhalation risks were first plotted at the census tract level in ArcGIS to illustrate the risk pattern in terms of plant locations (Figure 7). Then in Figure 8, the averaged census tract

result was chosen to represent the entire county. The color scheme only shows the absolute values of inhalation risks and does not correspond to any risk management threshold values.

Overall, for the five unit processes involved in site-specific modeling, the accumulated inhalation risks ranged from  $10^{-12}$  to  $10^{-9}$  for cancer risk and  $10^{-6}$  to  $10^{-3}$  for non-cancer HI. At the county level, the highest average cancer risk was  $1.70 \times 10^{-9}$  at Ascension Parish, LA and the highest average non-cancer HI was  $1.53 \times 10^{-3}$  at Iberville Parish, LA. The majority of the county level average inhalation risk was much lower than the highest values. As shown in Figure 9, the distribution of inhalation risk is skewed to the right for both cancer risk and non-cancer HI with the majority of counties lower than  $10^{-10}$  for cancer risk (45 out of 50) and  $10^{-4}$  for non-cancer HI (44 out of 59).

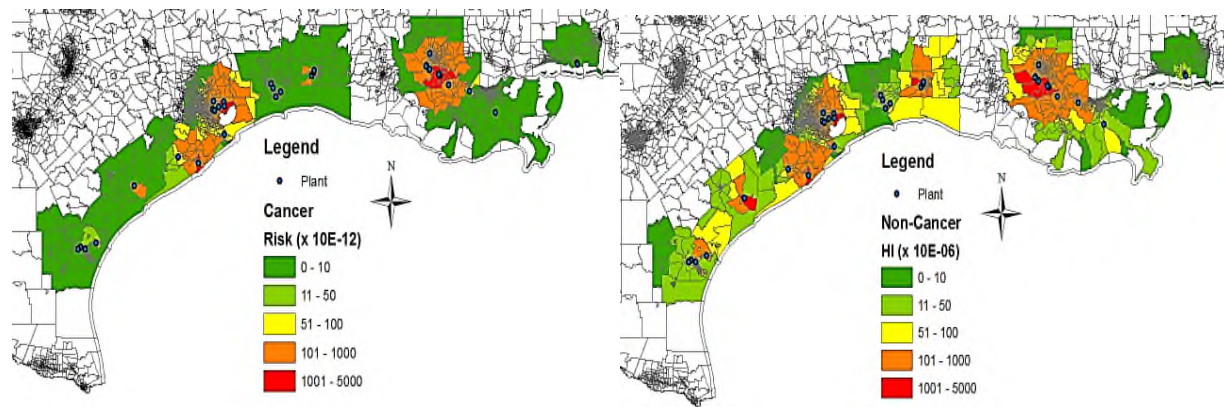


**Figure 7: Census tract level inhalation of site-specific unit processes (Left: cancer risk, Right: non-cancer HI)**

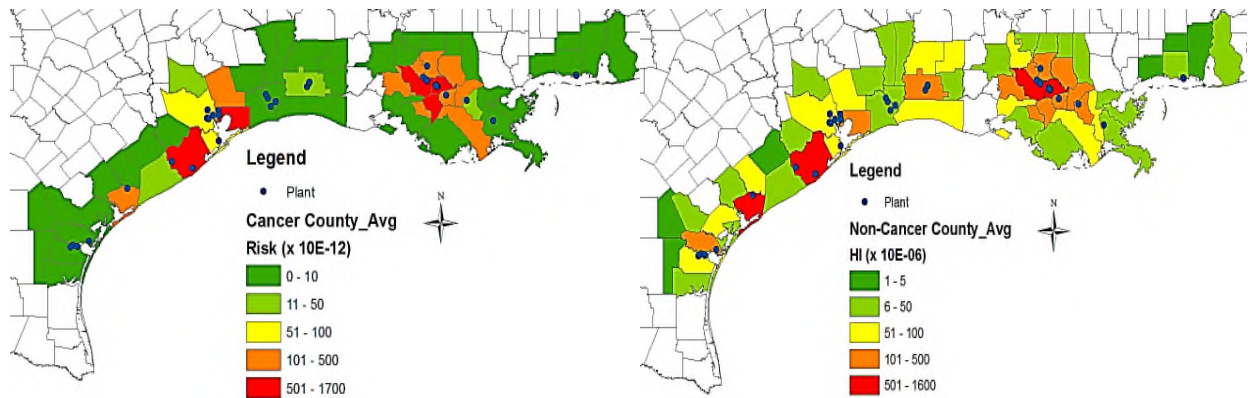


**Figure 8: County level average inhalation of site-specific unit processes (Left: cancer risk, Right: non-cancer HI)**

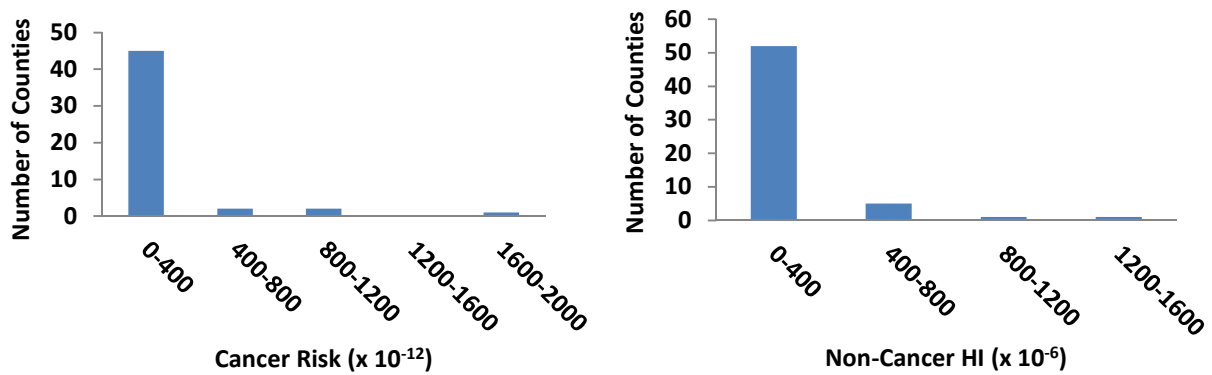


**Figure 9: Distribution of inhalation risks associated with site-specific unit processes at county level (Left: Cancer risk, Right: Non-cancer Hazard Index)**

In addition to the average inhalation risks shown at the county level, the census tract level map reveals the spatial distribution of inhalation risks. Figure 10 and Figure 11 demonstrate that higher potential inhalation risks occur in regions which have manufacturing plants with greater production capacities. Two regions with relatively higher risks were identified: Houston and Baton Rouge. Production capacities in these regions can be found in Table 6. The four counties (Harris, Chamber and Brazoria in TX and Ascension Parish in LA) in these two regions were among the highest cancer and non-cancer risk counties out of a total of 59 counties evaluated. Plant production capacity was an important factor to determine the potential inhalation risks and their spatial distribution. The majority of aniline, olefins and MDI were produced in these four counties as shown in Table 6. In comparison, Jefferson County had four plants which only supply 14.0% of aniline and 8.55% benzene and ranked at the 20<sup>th</sup> for cancer risk and the 21<sup>st</sup> for non-cancer HI out of the 59 counties evaluated.

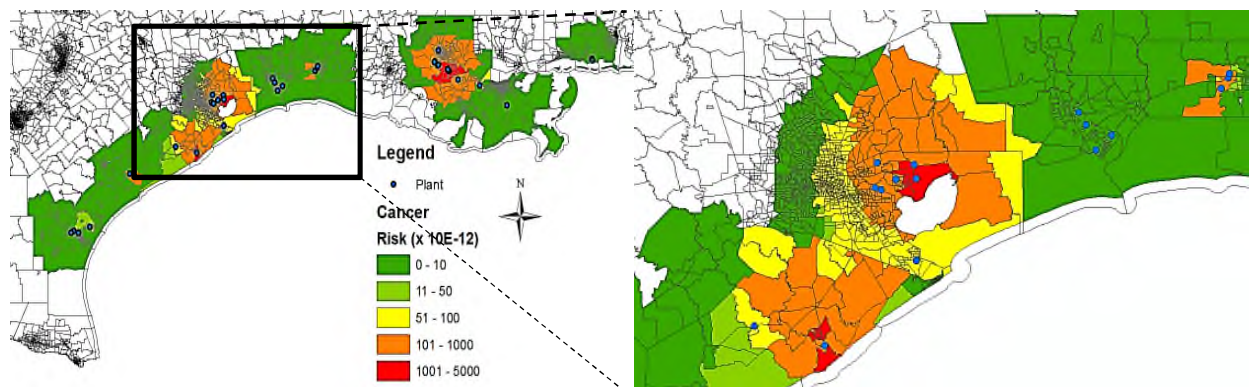


**Figure 10: Site-specific plant locations and high cancer risks area**

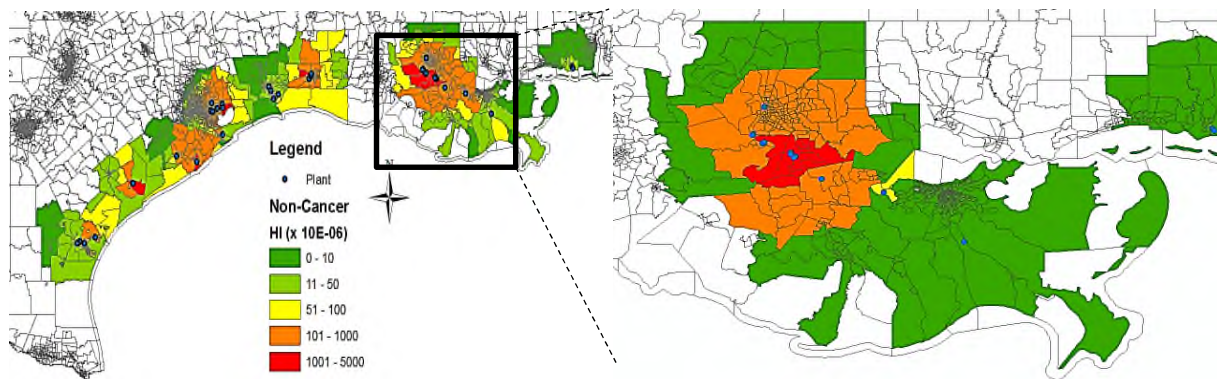


**Figure 11: Site-specific plant locations and high non-cancer hazard index area**

**Table 6: Chemical plants production capacity in relative high risk area**

Area	# of Plants	Production Capacity by Mass				
		Aniline	Benzene	Cl <sub>2</sub> /NaOH	Olefins	MDI
Houston	10	18.1%	37.1%	26.5%	48.2%	43.5%
Baton Rouge	7	55.3%	0	6.0%	46.3%	56.5%
Sum	17	73.4%	37.1%	32.5%	94.5%	100%

All the plants modeled by site-specific modeling are located in the Gulf coast which is known to be the petrochemical corridor of the U.S. However, the inhalation risks associated with MDI production varied among and within counties. The ratio between the highest and lowest county was 14,457 for cancer risk and 1,369 for non-cancer HI. Within the same county, inhalation risk pattern could have significant spatial variations. For example, the cancer risk of the highest census tract was about 20,000 times higher than the lowest one in Harris County as shown in Figure 12. Such spatial differentiation revealed the limitation of existing LCIA models which assume the homogeneity within each environmental compartment. The site-specific modeling results showed that the variation in the same environmental compartment was not negligible.

Therefore, the assumption that chemicals have a homogeneous steady state concentration in each environmental compartment may not be valid in cases where geographical variations are significant.

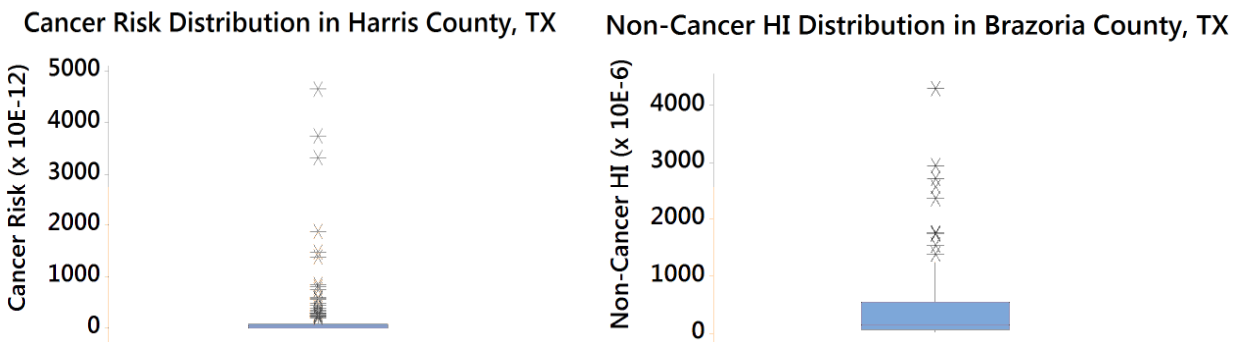


**Figure 12: Inhalation risk distribution of census tracks within the highest county (Left: cancer risk, Right: Non-cancer HI)**

### 3.3.2 Non-site specific unit processes

Site-specific modeling was not feasible for those unit processes with unknown production locations. Therefore, the USEtox model was used as an approach to assess inhalation risks associated with these unit processes as explained in step 5 of the method. Table 7 illustrates the total inhalation risks of non-site specific unit process in each modeled environmental compartment. Urban and continental air compartments (cancer:  $10^{-10}$ , non-cancer:  $10^{-6}$ ) had similar risk results which were one order of magnitude higher than the global air compartment (cancer:  $10^{-11}$ , non-cancer:  $10^{-7}$ ). Figure 13 illustrates the relative contribution of HAPs to the

inhalation risks. Benzene and Nickel compounds were the two major contributors in all compartments and Ethylene Dibromide accounts for about 21% of the total non-cancer HI in the global air compartment. The relative contribution of HAPs was similar in urban and continental air compartments.

**Table 7: Inhalation risks of unit processes without exact location (HAPs emitted to the continental air compartment)**

Environmental Compartment	Volume (m <sup>3</sup> )	Cancer Risk	Non-cancer HI
Urban Air	$5.76 \times 10^{10}$	$4.42 \times 10^{-10}$	$4.46 \times 10^{-6}$
Continental Air	$1.00 \times 10^{16}$	$4.61 \times 10^{-10}$	$4.65 \times 10^{-6}$
Global Air	$4.60 \times 10^{17}$	$2.13 \times 10^{-11}$	$1.52 \times 10^{-7}$

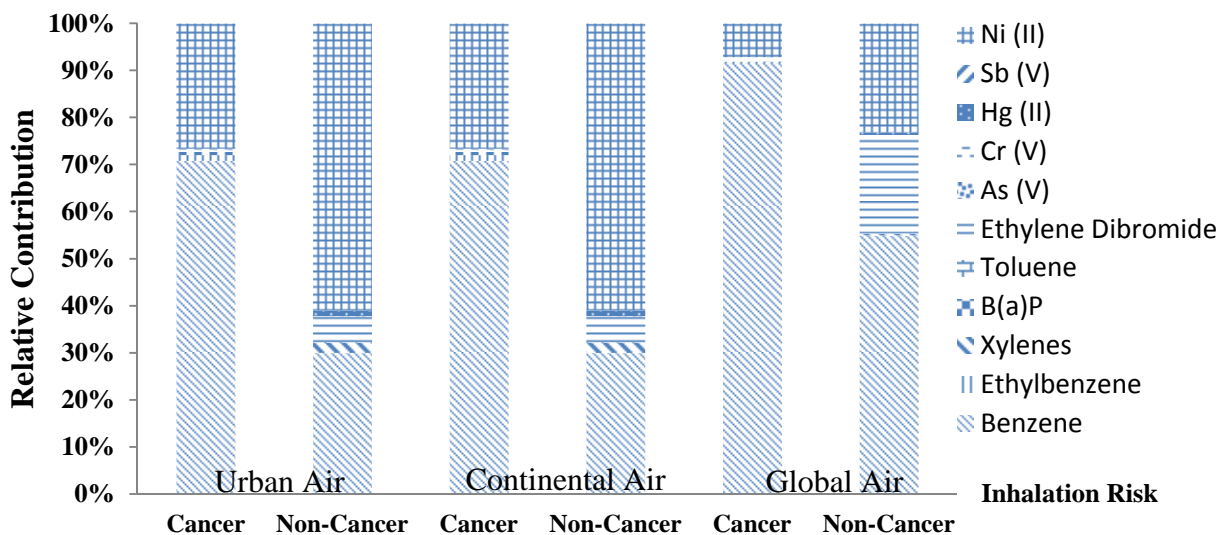


**Figure 13: Inhalation risk contribution by HAPs for non-site specific unit processes**

### **3.3.3 Total inhalation risks of cradle-to-gate MDI production**

Risk characterization results of site-specific and non-site specific were combined to derive the overall inhalation risks of cradle-to-gate MDI production. To be conservative, the highest risk of non-site specific unit processes among air compartments (continental air) and the highest county level risks of site-specific unit process (Ascension Parish and Iberville Parish) were combined. The combined overall inhalation risks are  $2.16 \times 10^{-9}$  for cancer risk and  $1.53 \times 10^{-3}$  for non-cancer HI. These levels were three orders of magnitude lower than the EPA risk management threshold values of  $10^{-6}$  for cancer risk and 1 for non-cancer HI (Office Of Air Quality Planning and Standards 1999).

## **3.4 DISCUSSION**

### **3.4.1 Comparisons between HEM-3/AERMOD and USEtox**

Two models were used to evaluate the unit processes in MDI production, depending on whether the exact production location is known. Comparing to the multi-media modeling (USEtox), the site-specific modeling (HEM-3/AERMOD) provides more information on the geographical distribution of inhalation risks. Table 8 illustrates the inhalation risks of the cradle-to-gate MDI production can vary significantly in terms of geographical locations. The highest averaged county level cancer risk at Ascension Parish, LA was 5 orders of magnitude higher than the lowest value at Wharton County, TX. Similarly, for non-cancer HI, this ratio was approximate 1,400 between the highest value at Iberville Parish, LA and the lowest value at Stephens County, TX.

**Table 8: County level inhalation risk statistics (AERMOD)**

<b>Scenarios</b>	<b>Cancer Risk</b>	<b>Non-Cancer HI</b>
Maximum	$1.70 \times 10^{-9}$	$1.54 \times 10^{-3}$
Median	$1.84 \times 10^{-12}$	$5.36 \times 10^{-5}$
Minimum	$5.30 \times 10^{-14}$	$1.12 \times 10^{-6}$

In order to demonstrate the differences between the two modeling approaches, a comparison was made by assuming all HAPs modeled in HEM-3/AERMOD (from site-specific processes) were emitted into the urban air compartment in USEtox. The mass of the HAPs that remained in three air compartments (Global, Continental and Urban) at steady state were calculated and converted to concentrations, using the volume of each environmental compartment. All the HAPs included in AERMOD were considered in USEtox except Cl<sub>2</sub>, which has not been characterized in the most recent version of USEtox.

Table 9 presents the results: for cancer risk, the urban, continental and global air compartment results in USEtox were within one order of magnitude of the maximum, median and minimum county level results in HEM-3/AERMOD, respectively. However, for non-cancer HI, only the urban air compartment result was within one order of magnitude of the maximum county level results in HEM-3/AERMOD. One possible reason of USEtox underestimating the non-cancer HI is the lack of CF of Cl<sub>2</sub>. Such results also illustrated that inhalation risks can vary significantly within the modeled domain (50 km radius from the source), when HAPs were evaluated using HEM-3/AERMOD. In fact, the USEtox model can only calculate one risk value per air compartment based on the steady state concentration. Without accounting for the geographical differences, assuming a homogeneous environmental compartment could potentially over or underestimate inhalation risks. Therefore, HEM-3/AERMOD can better characterize the

inhalation risk of emissions if the production location is available since in a real-world scenario, many factors may cause the homogeneous condition assumed in USEtox to be invalid. These factors are the relative location of the receptor to emission source, meteorological and terrain conditions in a specific region/site and removal mechanisms of chemicals such as dry and wet depositions. Due to the non-homogeneous nature of each environmental compartment, the lack of geographical granularity limits the use of USEtox beyond a high-throughput tool in human health assessment.

**Table 9: Inhalation risks of site-specific unit processes (if using USEtox) (Assume HAPs were emitted to the urban air compartment)**

<b>Environmental Compartment</b>	<b>Cancer Risk</b>	<b>Non-cancer HI</b>
Urban Air	$1.99 \times 10^{-9}$	$5.42 \times 10^{-4}$
Continental Air	$1.14 \times 10^{-12}$	$8.98 \times 10^{-8}$
Global Air	$3.25 \times 10^{-13}$	$1.64 \times 10^{-9}$

### 3.4.2 Impact of emission compartments in USEtox

This research demonstrates the possibility of tracking exact emission locations of unit processes using publicly available data. However, such data is not always available for all unit processes. In this case study, natural gas, crude oil and salt production were not included in the DCP. The selection of the emission compartment in USEtox could impact risk characterization of the non-site specific unit processes. If the HAPs of the aforementioned three unit processes were emitted to the urban air compartment (Table 10) instead of the continental air compartment (Table 7), inhalation risks in urban air compartment were increased by four orders of magnitude for both

cancer risk and non-cancer HI. The cancer risk in the urban air compartment alone was even higher than the  $10^{-6}$  risk management threshold value. Such difference in risk characterization demonstrates the need of regionalized LCI and the importance of identifying the HAPs emission locations.

**Table 10: Inhalation risks of non-site specific unit processes (Assume HAPs were emitted to the urban air compartment)**

<b>Environmental Compartment</b>	<b>Cancer Risk</b>	<b>Non-cancer HI</b>
Urban Air	$1.83 \times 10^{-6}$	$2.32 \times 10^{-2}$
Continental Air	$4.60 \times 10^{-10}$	$4.62 \times 10^{-6}$
Global Air	$2.13 \times 10^{-11}$	$1.52 \times 10^{-7}$

### 3.4.3 Relative unit process contribution to the inhalation risks

In the interpretation step of an LCA, the indicator results are often presented by unit process, so that high impact processes can be identified. However, since the human health LCIA is conducted at continental or global scale, such analysis fails to reveal the relative contribution of each unit process at different geographical locations. In this research, site-specific modeling results were analyzed to determine which unit processes contribute the most to the averaged county level inhalation risks (Figure 14). In this cradle-to-gate LCI, among the five unit processes modeled using AERMOD, only two unit processes (MDI and Cl<sub>2</sub>) emitted HAPs which have carcinogenic effect. All five unit processes contributed to the non-cancer HI. HAPs emitted from Cl<sub>2</sub> production contributed 100% to the cancer risk in 31 out of the 50 counties, and HAPs emitted from MDI production (gate-to-gate) contributed more than Cl<sub>2</sub> production in the remaining 19

counties. In terms of non-cancer HI, 14 out of 59 counties had at least two unit processes which contributed more than 10% of the overall inhalation risk. Most of the counties are located in the two relative high inhalation risk regions (Houston and Baton Rouge). In other regions, Cl<sub>2</sub> production had the highest impact which alone contributed more than 70% of the non-cancer HI in 36 counties. In this analysis, HEM-3/AERMOD enabled us to identify the top contributing unit processes in different regions. The results can guide decision makers to reduce the human health impacts of MDI supply chain with a focus on specific unit process in a high-risk region. For example, in the two counties with highest cancer risk (Ascension Parish, LA) and non-cancer HI (Iberville Parish, LA), HAPs reduction should focus on the unit process of Cl<sub>2</sub> and MDI since they were the highest contributing unit processes.

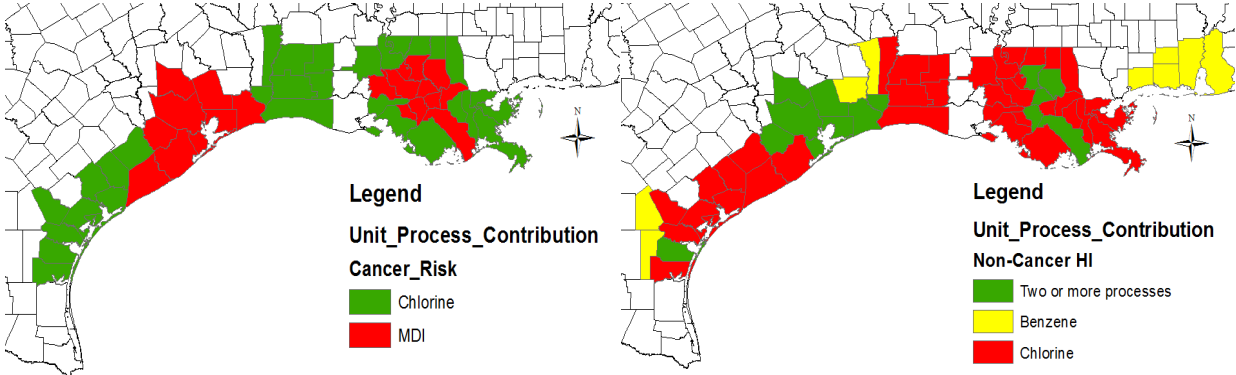


**Figure 14: Relative unit processes contribution to inhalation risks**

### **3.4.4 Limitation of this study**

The ACC MDI LCI was compiled by a third-party consulting firm, Franklin Associates, a division of ERG. Air, water and solid waste emissions were collected for each unit process by surveying representative plants. A standard emission survey form was used for all unit processes. For air emissions, this LCI only includes HAPs based on the USEPA's HAP list. However, there could be other air pollutants which may cause adverse health outcomes were not included. The reporting responsibilities of those air pollutants outside the USEPA's HAP list vary by states. Future work should be expanded to include those air pollutants which are in the state emission inventory but not the federal EPA's HAP list. In addition, data quality of this LCI relied on the plant engineers who filled the survey form. As indicated the LCI report, some professional judgements by the plant engineers were used for certain unit processes when measured values were not available. The site-specific air dispersion modeling conducted in this case study assumed that all HAPs emitted from a plant were point emissions from stacks, which modeling parameters were based on the unit process's SCC classification. However, a portion of the HAPs may be modeled as fugitive emissions. Future studies should separate the point vs. fugitive emissions in site-specific dispersion modeling when such data is available at unit process level in publicly available emission inventory databases.

USEtox results indicate that inhalation may not be the primary exposure pathway of certain chemicals. The steady state mass distribution of HAPs among different environmental compartments depends on chemical characteristics such as vapor pressure, octanol-water partition coefficient and degradation constant. Among the eleven HAPs modeled in USEtox, only five of them had the majority of mass partitioned in the air compartments at the steady state condition. Table 11 shows the mass distribution of HAPs when they were emitted to the continental air

compartment. Although Nickel (II) contributed significantly to the total inhalation risks (Figure 13), only a tiny amount of nickel stayed in the air compartment. Similar results can be found for other inorganics, which very little mass stayed in the air compartments at steady state while most mass was distributed into the soil compartment. Therefore, ingestion pathway should be included in future studies to evaluate the overall health risks of these inorganics in addition to the inhalation pathway.

This research evaluated the inhalation risks associated with cradle-to-gate MDI production but did not include downstream use of MDI. Future work should apply indoor fate and transport models to evaluate the health risks of downstream products which are made from MDI such as foam insulation.

**Table 11: HAPs mass distribution in different environmental compartments**

<b>HAPs</b>	<b>Air Compartments (%)</b>	<b>Water Compartments (%)</b>	<b>Soil Compartments (%)</b>
As (V)	$4.81 \times 10^{-3}$	6.57	93.4
<b>Benzene</b>	89.2	10.7	$5.59 \times 10^{-3}$
Cr (VI)	$4.41 \times 10^{-2}$	33.8	66.2
<b>Ethyl benzene</b>	98.0	1.88	0.152
<b>Ethylene Dibromide</b>	72.1	27.5	0.484
Hg (II)	$7.23 \times 10^{-4}$	$7.39 \times 10^{-2}$	99.9
Ni (II)	$6.53 \times 10^{-5}$	33.4	66.6
PAH as B(a)P	1.03	11.5	87.4
Sb (V)	$2.30 \times 10^{-2}$	46.9	53.1
<b>Toluene</b>	97.4	2.47	0.127
<b>Xylene</b>	97.6	2.12	0.256

Note: Bold fonts are those chemicals with the majority of mass distributed in the air compartment based on USEtox

### 3.5 CONCLUSIONS

Air dispersion modeling and LCA together can provide a holistic view of the human health risks of a chemical. Many current human health LCIA models assume environmental compartments are homogeneous and perform assessment under steady state conditions. However, such assumption lacks the ability to identify the geographical difference and pattern of human health risks which is an essential piece of information for decision makers to mitigate risk and improve manufacturing process. A current challenge is to increase the geographical relevance of HHIA without using confidential business information or proprietary data. This research demonstrates the development of a regionalized LCI using publicly available data and illustrates the application of site-specific air dispersion modeling together with USEtox to assess the inhalation risk of chemicals along the supply chain. This work derives the first regionalized LCI of a chemical for the industry using

publicly available data and evaluates inhalation risks along its cradle-to-gate production. With regionalized LCI, air dispersion modeling can be performed simultaneously for multiple facilities and unit processes in multi-facility HEM3. The case study uses MDI as an example but this method could be applied to any other chemicals or products to address the question often faced by decision makers: “Is manufacturing certain products along the life cycle adding unacceptable risk to the society?”

The case study results show that the conservative overall inhalation risk of cradle-to-gate MDI were three orders of magnitude lower than the EPA risk management threshold value. In addition, it was found that the highest inhalation risks occurred in two counties in LA where HAPs emitted from Cl<sub>2</sub> and MDI production (gate-to-gate) contributed the most. The advantage of employing site-specific air dispersion modeling is that geographical relevance in human health LCIA is increased by better understanding the spatial pattern of risks. As a result, pollution reduction and risk management actions can be implemented more efficiently.

This case study illustrates whenever feasible, site-specific air dispersion modeling should be considered. For many chemicals used as raw materials in the commerce, the production location and capacity can be obtained using publicly available data. However, such data for some other chemicals (e.g., crude oil and salt) are not always available. To improve the geographical relevance, emission inventory, manufacturer location and production capacity data should be continually collected and made publicly available.

In future studies, additional exposure pathways need to be evaluated for inorganic HAPs releases to the air. It will require regionalized or site-specific information on watersheds and agricultural production. Furthermore, downstream applications and disposal options should be included to assess the overall health risks along the rest of life cycle phases. In general, human

health assessment could benefit by embracing life cycle thinking and employing the site-specific modeling to increase geographical relevance.

#### **4.0 AN INDOOR AIR QUALITY EVALUATION IN A RESIDENTIAL RETROFIT PROJECT USING POLYURETHANE FOAM**

The following chapter contains material reproduced from an article published in the *Journal of Occupational and Environmental Hygiene* with the citation:

Tian, S., S. Ecoff, J. Sebroski, J. Miller, H. Rickenbacker and M. Bilec (2018). "An indoor air quality evaluation in a residential retrofit project using spray polyurethane foam." *Journal of Occupational and Environmental Hygiene* **15**(5): 363-375.

The article appears as published per the copyright agreement with Taylor & Francis, publisher of

*Journal of Occupational and Environmental Hygiene*

Portions of the Supporting Information submitted with *Journal of Occupational and Environmental Hygiene* appear in this chapter.

## 4.1 INTRODUCTION

### 4.1.1 Indoor air quality and spray polyurethane foam

Chemicals emitted to indoor environment can have more significant impacts to building occupants than outdoor emissions. Previous research has illustrated human intake of indoor chemicals can be three orders of magnitude higher than outdoor sources (Ilacqua, Hänninen et al. 2007, Nazaroff 2008). In order to reduce exposure to indoor chemicals, some previous IAQ studies have focused on quantifying emission rates of construction materials, as well as the absorption potential of chemicals in the built environment (Batterman and Burge 1995, Wolkoff 1995, Yu and Crump 1998, Wolkoff 1999, Meininghaus, Gunnarsen et al. 2000, Kemmlein, Hahn et al. 2003, Uhde and Salthammer 2007, Gunschera, Mentese et al. 2013, Liu, Allen et al. 2016a). Multiple research studies have also further described the human health impacts of chemicals emitted from building materials (Jones 1999, Bennett, Margni et al. 2002, Sundell 2004, Wenger, Li et al. 2012, Collinge, Landis et al. 2013, Jolliet, Ernstoff et al. 2015).

SPF is a “spray-applied plastic that can form continuous insulation and air sealing barriers on walls, roofs, around corners, and on contoured surfaces” (American Chemistry Council 2018). Though the energy savings have been documented (Spray Polyurethane Foam Alliance 2012), the potential health risk associated with SPF ingredients during and after spray application should be further investigated to ensure the protection of construction workers and building occupants (Manuel 2011, U.S. Environmental Protection Agency 2017a).

Existing literature on SPF and IAQ from a method perspective can be grouped into three categories: 1) field IH surveys to evaluate airborne chemical concentrations during and after spray application (Crespo and Galán 1999, Lesage, Stanley et al. 2007, Booth, Cummings et al.

2009, Poppendieck and Connor 2015, Ecoff, Tian et al. 2017, Wood 2017); 2) chamber studies (including spray booth) to evaluate chemical emissions during foam curing (Poppendieck, Schlegel et al. 2017, Sebroski, Miller et al. 2017, Wood 2017); and 3) mathematical modeling to study the fate and transport of chemicals (Bevington, Guo et al. 2017, Tian, Sebroski et al. 2017). However, each of the above research methods only reveals partial information on the relationship between SPF and IAQ. Field IH surveys use the “end-control” approach that measures the airborne concentrations during the sampling period but often neglects to collect information on the emission source such as SPF surface area and air velocity above the foam. Without measuring these parameters, IH surveys may not quantitatively link the emission source to airborne concentration and thus overlook emission sources required for the development of emission control strategies. Chamber studies use the “front-control” approach which documents the parameters that impact emission rates; however, without taking into account the field conditions (e.g., air movement and emission sinks in a building), chamber study results may not be extrapolated to predict airborne chemical concentrations in a real-world scenario. Mathematical modeling studies tend to bring the IH and chamber studies together, but they heavily rely on IH surveys to provide modeling input parameters. Without carefully planning the IH survey, mathematical modeling may not yield a reliable result to help decision-making. Therefore, a comprehensive approach is needed to integrate all three types of studies. A more comprehensive IAQ research on SPF should design its sampling plan to address key human exposure pathways. For example, in addition to measuring airborne chemical concentrations, SVOCs accumulation on indoor surfaces should also be measured since SVOCs could be re-emitted into the environment. Moreover, key mathematical modeling parameters should be

collected such as air changes per hour (ACH), temperature, particle size distribution and application time, so that models can be tested for their predictability.

This field study took place in a three-story, single-family house in New Martinsville, West Virginia. The spray application took 4 days to finish in August 2016. This research aimed to quantify the airborne concentrations of chemicals of interest during and after SPF application, especially MDI in the first 24 hours after spray. This research also measured the natural ACH on each floor, airborne particle size distribution and explored TCPP accumulation on to building materials such as carpet and drywall. We also compared our field study results to a recent chamber study to understand any differences between the two studies (Liu, Allen et al. 2016a).

#### **4.1.2 Chemicals evaluated and their criteria values**

The chemicals of interest in this study and their emission criteria values are listed in **Table 12**. In addition, chemicals which were analyzed and had concentration levels above their Limit of Quantification (LOQ) based on the analytical method used are listed in **Table 13**.

**Table 12: Criteria values for chemicals evaluated in this study, all units are in  $\mu\text{g}/\text{m}^3$**

Chemical	CAS Number	EPA Chronic Inhalation RfC	California OEHHA CREL (Office of Environmental Health Hazard Assessment 2016)	OSHA PEL (Occupational Safety and Health Administration 1998)	NIOSH REL (The National Institute for Occupational Safety and Health 2007)	ACGIH TLV (American Conference of Governmental Industrial Hygienists 2016)	USGBC LEED v4 (U.S. Green Building Council 2015)
4,4'-MDI	101-68-8	0.6 (Greenberg 1998)	0.08	200 (Ceiling)	50 (TWA) 200 (Ceiling)	51 (TWA)	N.V.
Formaldehyde	50-00-0	N.V.	9 (Chronic) 55 (Acute)	920 (TWA) 2,450 (STEL)	19.6 (TWA) 122 (Ceiling)	370 (Ceiling)	27
Acetaldehyde	75-07-0	9 (National Center for Environmental Assessment 1991)	140	360,000 (TWA)	N.V.	45,000 (Ceiling)	140
Propionaldehyde	123-38-6	8 (Stanek, Goldhaber et al. 2008)	N.V.	N.V.	N.V.	47,500 (TWA)	N.V.
TCPP	13674-84-5	N.V.	N.V.	N.V.	N.V.	N.V.	N.V.
Solstice™ LBA <sup>a</sup>	102687-65-0	N.V.	N.V.	N.V.	N.V.	N.V.	N.V.

LBA = Liquid Blowing Agent, CAS = Chemical Abstracts Service, RfC = Reference Concentration, N.V. = No Value, OEHHA = Office of Environmental Health Hazard Assessment, CREL = Chronic Reference Exposure Level, OSHA = Occupational Safety and Health Administration, PEL = Permissible Exposure Level, NIOSH = National Institute for Occupational Safety and Health, REL = Recommended Exposure Limit, TWA = Time Weighted Average, STEL = Short Term Exposure Limit, ACGIH = American Conference of Governmental Industrial Hygienists, TLV = Threshold Limit Value, USGBC = U.S. Green Building Council, LEED = Leadership in Energy and Environmental Design.

a. Solstice™ is a trade mark of Honeywell. University of Cincinnati Toxicology Excellence for Risk Assessment Center Workplace Environmental Exposure Level (8-hr TWA) is 4,240,000  $\mu\text{g}/\text{m}^3$  (800 ppm).(Occupational Alliance for Risk Science 2013)

**Table 13: Chemicals analyzed and were above LOQ**

<b>Chemical Name</b>	<b>CAS Number</b>	<b>Chemical Name</b>	<b>CAS Number</b>
1-propoxy-2-propanol	1569013	1,2-dichloroethane	107062
Ethylene Glycol Monobutyl Ether	111762	1,2-dichloropropane	78875
1,2-Dimethylimidazole (DMIAZ)	1739840	chlorobenzene	108907
Triethyl phosphate (TEP)	78400	1,2-dichlorobenzene	95501
Toluene	108883	Ethylene Glycol	107211

## **4.2 METHODS AND MATERIALS**

### **4.2.1 Building information and insulation material applied**

SPF was applied to the interior and exterior facade of a three-story, single-family house between August 15 and 18, 2016. The dimension of the house was approximately 9.15 m by 9.15 m with a 2.75 m ceiling on the first and second floors. The attic (third floor of the house) takes the shape of the adjacent roof and is a triangular pyramid with a ceiling of 3.66 m at the highest point.

The SPF used was a two-component system that contained polymeric methylene diphenyl diisocyanate (pMDI) (part A), and a mixture of polyhydroxy alcohol (polyol) and other additives (together as part B). Part A contains approximately 50% monomeric MDI and the rest is higher molecular weight oligoisocyanates (more than two rings). Part B often contains blowing agent (Solstice™ LBA in this study), flame retardant (TCPP in this study), catalysts, surfactants and other additives in addition to the polyol. During application, the two components are proportionally pumped towards the nozzle, heated, and mixed using Graco hydraulic spray foam equipment. As the mixture is sprayed, the chemical reactions occur, and SPF is applied to the

desired thickness (average 2~3 inches). The curing process (chemicals in the product are reacting to produce SPF (U.S. Environmental Protection Agency 2017a)) generally takes 24 to 48 hours to complete.

#### **4.2.2 Analytical methods and sampling procedure**

Multiple IAQ surveys were conducted over a three-month period between August and November of 2016. Instead of assuming the entire house is well mixed, samples were collected in four areas which were located on three floors of the house so that spatial variations within the building were captured. As shown in Figure 15, the sampling locations were in rooms A, G and H, plus the center of the attic (not shown in Figure 15). The finishing time of each room was tracked based on the specific time of SPF application at each sampling location. For example, rooms G and H were finished two days prior to the completion of the attic; therefore, post-application time zero for the attic was actually 48 hours post application for room G and H. This is an important step to later evaluate the decay rate of specific chemicals such as MDI, especially during the first few days, since MDI decays rapidly during the first few hours after spray (Ecoff, Tian et al. 2017, Sebroski, Miller et al. 2017, Wood 2017). The sampling schedule was also designed in this way to account for future indoor modeling scenarios where it is essential to factor in the differences of spray finishing time in each room.

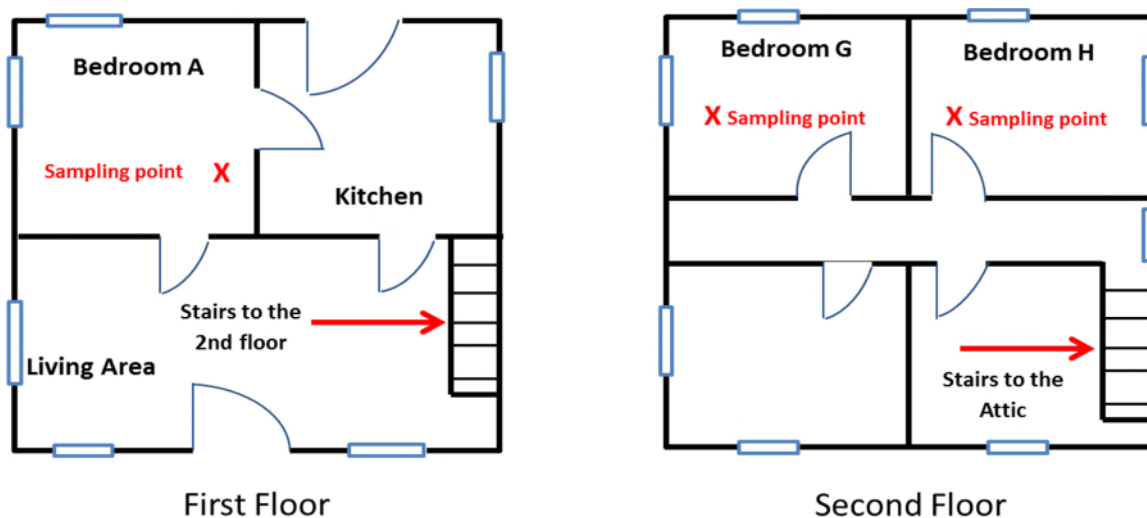


**Figure 15: First and second floor plan view of the residential home**

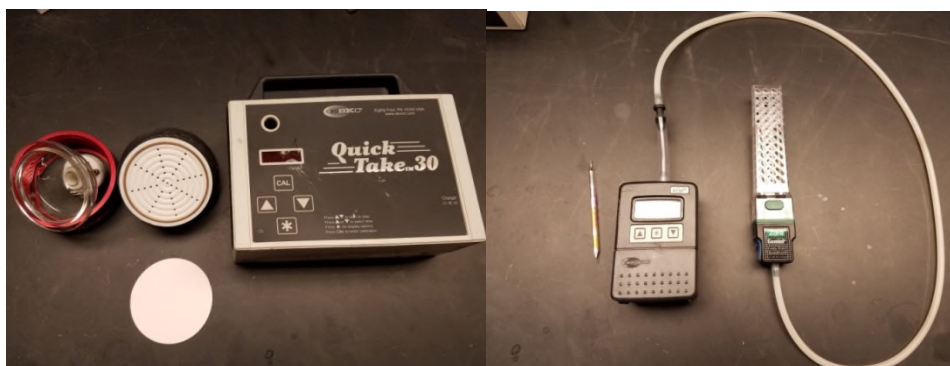
**4.2.2.1 Airborne MDI** Previous studies have shown that traditional IH sampling and analytical methods such as the Occupational Safety and Health Administration (OSHA) method 47 are suitable for assessing airborne MDI concentrations during SPF application. However, the method is not sensitive enough for post application period because airborne MDI concentrations decrease rapidly (Ecoff, Tian et al. 2017). OSHA method 47 recommends sampling 15 L at a flow rate of 1 L/min. The Reliable Quantitation Limit (RQL) ( $2.6 \mu\text{g}/\text{m}^3$ ) is not sufficient to determine the chronic threshold values listed in **Table 12**. This is due to the low quantities of MDI collected on the sampling filter (37-mm cassettes). As a result, sampling time should last longer than 12 hours so that the LOQ can at least reach the California Office of Environmental Health Hazard Assessment's (OEHHA) Chronic Reference Exposure Level (CREL) ( $0.08 \mu\text{g}/\text{m}^3$ ) during post application sampling periods. Previous research showed airborne MDI concentration decays rapidly after application (Ecoff, Tian et al. 2017, Wood 2017), so a shorter sampling time with a lower LOQ was required to capture the concentration changes, especially during the first 24

hours. Therefore, a modified method based on both OSHA method 47 (Occupational Safety and Health Administration 1989) and USEPA Conditional Testing Method (CTM) 036 (U.S. Environmental Protection Agency 2005a) was used to increase sampling volume and lower the LOQ. The RQL ( $0.01 \mu\text{g}/\text{m}^3$ ) in the revised method was two orders of magnitude lower than the RQL ( $2.6 \mu\text{g}/\text{m}^3$ ) in the OSHA method 47. The modifications were made to the following:

- 1) Rather than using a 37-millimeter (mm) sampling cassette as specified in the OSHA 47 method, a 90-mm glass fiber filter was placed in an open face holder in order to increase the sampling surface area. The 90-mm filter was treated with 1-(2-pyridyl piperazine) before collecting samples and desorbed in the field with 5 ml 90:10 Acetonitrile: Dimethyl Sulfoxide (DMSO). Field desorption can minimize isocyanate loss and potential underestimation comparing to laboratory desorption (Schaeffer, Sargent et al. 2013).
- 2) Instead of using a personal sampling pump at 1 L/min and a total sampling volume of 15 L, a SKC Quick Take 30 pump was used at 15 L/min for 1 hour. The total sampling volume is 900 L which is 60 times higher than that obtained in OSHA method 47.
- 3) Instead of using the High-Performance Liquid Chromatography (HPLC) with an ultraviolet or fluorescence detector in OSHA method 47, an Agilent 6400 series triple quadrupole liquid chromatography/Mass Spectrometry (MS) (Agilent Technologies, Santa Clara, CA, USA) was used to increase sensitivity and remove the possibility of interferences.

When airborne MDI was drawn through the filter, it was converted to a stable isocyanate urea derivative and then desorbed in the Acetonitrile/DMSO solution at the end of the sampling period. Then HPLC/MS was used to analyze the isocyanate urea and calculate the airborne MDI

concentration. Lesage et al. indicated that the 37-mm cassette used in OSHA method 47 has low particle capture efficiency due to large aerosol size during spray application (Lesage, Stanley et al. 2007). The improved sampling method was expected to improve capture efficiency because of the large sampling volume and higher velocity when particles reach the filter causing large particles to break into smaller particles. Compared to the personal samples collected by Lesage et al., this area sample (1.83 m from the applicator) should have fewer large particles because they tend to fall out in a short range from the applicator or are flushed out of the room by mechanical ventilation (fan with flexible ducts that exhaust air to the outside). Figure 16 illustrates the MDI sampling equipment. The filter and holder were mounted to a tripod at 1.5-meter height.



*(left: MDI, right: VOCs and blow agent thermal desorption tubes)*

**Figure 16: Sampling equipment**

**4.2.2.2 Aldehydes** This work identified three aldehydes including Formaldehyde, Acetaldehyde and Propionaldehyde. The sampling tubes (the tube left to the sampling pump as shown on the right picture of Figure 16) contained silica adsorbent coated with 2,4-Dinitrophenylhydrazine (DNPH). The DNPH reacts with aldehydes and then converts to hydrazone derivatives. The

derivatives were analyzed with an Agilent 1100 series HPLC using methodology based on ASTM D5197-09e1 (ASTM International 2009). The sampling volume was set to 0.25 L/min and the sampling time was 60 minutes.

**4.2.2.3 Blowing agent and flame retardant** Solstice™ LBA and TCPP were collected using the stainless-steel Thermal Desorption (TD) tubes (the tubes in the GEMINI® twin port sampler). Based on a previous study (Ecoff, Tian et al. 2017), a blowing agent should be collected at a lower flow rate to prevent TD tube break-through. The TD tube for collecting Solstice™ LBA contains Tenax® TA 35/60, Carbograph™ 1TD 40/60, Carboxen® 1003 40/60. While the other VOCs/SVOCs including TCPP were collected on TD tubes with 5mm Quartz Wool, Tenax® TA 35/60, Carbograph™ 5TD 40/60. Both TD tubes were manufactured by Markes International. The flow rate was set to 0.05 L/min for the blowing agent TD tube and 0.2 L/min for the other TD tube. The sampling time was 60 minutes. TD tubes were analyzed using an Agilent 7890/5975 GC/MS based on the method described in Sebroski et al (Sebroski, Miller et al. 2017).

**4.2.2.4 Airborne particles** Current research revealed that human exposure to SVOCs through the inhalation of airborne particles cannot be ignored and since have developed models to quantify SVOCs sorption onto particles (Xu and Little 2006, Weschler and Nazaroff 2008, Liu, Ye et al. 2013, Liu, Allen et al. 2016a). These studies have shown that SVOCs are first adsorbed onto and then migrate into the particles (Weschler and Nazaroff 2010, Guo 2014). Particle size distribution during and after application were measured to provide essential input parameters for future modeling work. Considering the potential high aerosol concentrations during SPF application that could damage the continuous monitoring equipment, a Marple style personal

cascade impactor (290 series, Tisch Environmental, Inc.) was placed in the middle of the attic to collect any indoor particles (background and introduced by spray). The flow rate was set to 2 L/min and sampled for 90 minutes. The corresponding cut-point particle diameter collected on each stage of the cascade can be found in the user manual (Tisch Environmental Inc. 2003). Instead of following the sprayer to measure personal exposure as in the Lesage study (Lesage, Stanley et al. 2007), the goal was to measure particle size distribution in the ambient environment during spray. After the application was completed and the spray area was swept (about 1 hour), a GrayWolf PC-3016A particle counter was placed in the middle of attic to monitor 6 particle sizes (0.3, 0.5, 1.0, 2.5, 5.0 and 10.0  $\mu\text{m}$ ) continuously. The particle counter had undergone annual National Institute of Standards and Technology (NIST) calibration to ensure data accuracy.

**4.2.2.5 TCPP accumulation onto building materials** Several previous studies have shown SVOCs absorbed onto indoor surfaces may be an important human exposure pathway (Weschler and Nazaroff 2008, Weschler and Nazaroff 2010, Xu and Zhang 2011, Liu, Morrison et al. 2012, Wenger, Li et al. 2012, Guo 2013). A recent study has quantified OPFRs sorption onto building materials and consumer products through chamber work (Liu, Allen et al. 2016a) and found gypsum wallboard (drywall) and carpet are two common building materials which have significant sorption capacity of SVOCs. This work was designed to test and quantify TCPP accumulation to these two materials. The drywall and carpet were purchased from a local store and had a thickness of 1.91 cm and 1.27 cm. They were cut into 5.08 cm by 5.08 cm pieces and put into aluminum trays (as shown in Figure 17). After SPF application stopped and spray debris was cleaned, seven sets of building materials (1 carpet and 1 drywall are 1 set) were placed in one aluminum tray and placed on the floors of room A and room H for a period of 7 weeks.

Eight sets of building materials were placed in the attic to accommodate a longer time period of 3 months due to the higher volume of SPF applied. After the samples were collected from the field, TCPF was analyzed using an Agilent 6890/5973 GC/MS with the analytical method developed by Liu et al. (Liu, Allen et al. 2016a).



**Figure 17: TCPF accumulation samplers**

**4.2.2.6 Air changes per hour** Blower door tests were conducted using a Minneapolis Blower Door System (Model 3, The Energy Conservatory). One whole house blower door test was conducted before SPF was installed, and three blower door tests were conducted after SPF was installed. The goal was to evaluate the ACH for each floor. The blower door test measured one  $ACH_{50}$  (ACH at 50 pascals of negative pressure) which was then converted into  $ACH_{natural}$  (ACH at natural ventilation) by dividing an adjustment factor (N). N is a function of local climate, number of stories, sheltering and crack size of the house (American Society of Heating Refrigerating and Air-Conditioning Engineers 1993, Reysa 2013). For the house studied, the

factor N was calculated as 10.5, about half of the typical value (N=20) (Reysa 2013) because this house was under major renovation and leakier than a typical residential building.

**4.2.2.7 Sampling schedule** The spray application process lasted 4 days: one day each for the first and second floor and two days for the attic. Post application hours were tracked by each floor. The sampling frequencies and schedules are listed in **Table 14**. MDI sampling was collected up to 24-hours after spray. The chemicals collected by TD tubes were sampled more frequently in the first 24-hours. The rest of samples were collected on Day 2, 3, 7; Week 2, 4, 7; and Month 3, after the application was complete on each floor. The drywall and carpet samples were tested more frequently in the first week. A duplicate set of samples was tested for the last testing period. One blank sample of MDI filter and TD tubes was tested during each sampling period. A total of four lab control sample sets (carpet and drywall) were also tested and the results were averaged. Starting during Week 2, all sampling activities were conducted at the same time on all floors, but time was tracked by floor, based on the actual hours after application.

**Table 14: Sampling media summary and sampling schedule**

Chemical	Sampling Media	Sampling Location	Sampling Time	
			During	After Spray
4,4'-MDI	Open face filter	First floor Living room, Second floor 2G and 2H, and the Attic	Yes	2hr, 4hr, 8hr, 12hr and 24hr
Aldehydes	DNPH tubes (0.25L/min)			4hr, 8hr, 12hr, 24hr, Day 2, 3, 7, Week 2, 4, 7 and Month 3
TCPP and other VOCs	TD tubes (0.2L/min)			4hr, 8hr, 12hr, 24hr, Day 2, 3, 7, Week 2, 4, 7 and Month 3
Solstice™ LBA	TD tubes (0.05L/min)			4hr, 8hr, 12hr, 24hr, Day 2, 3, 7, Week 2, 4, 7 and Month 3
TCPP accumulation	Dry wall /Carpet samples	First floor Living room, Second floor 2G, and the attic	No	Day 1, 3, 7, Week 2, 4, 7 and Month 3 (Attic only), a duplicate sample for each material at the last testing period
Particles	<b>During:</b> Impactor <b>After spray:</b> Gray Wolf particle counter	<b>Impactor:</b> First floor Living room and the attic <b>GrayWolf:</b> Attic only	Yes	<b>Impactor:</b> 4 hr and 24 hr <b>GrayWolf:</b> Every 10 mins until Week 4

## 4.3 RESULTS AND DISCUSSION

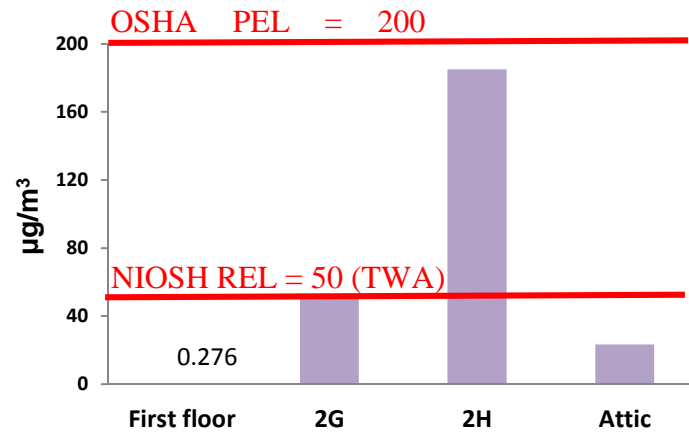
The sampling results presented in this section discuss the concentration and trend of airborne MDI, aldehydes, Solstice™ LBA, TCPP, and airborne particles during and after application. In addition, TCPP accumulation on to building materials was also measured and compared with a recent chamber study. Finally, ACHs before and after SPF application were reported.

### 4.3.1 Airborne MDI

During application, the airborne MDI concentration is a function of the relative location of the sampling point to the spray gun, ventilation rate, room volume, and amount of SPF applied per surface area. Figure 18 shows the locations of SPF installed. As expected, applying SPF on the exterior wall cavity resulted in a much lower indoor airborne MDI concentration on the first floor as shown in Figure 19 and Figure 20. Room H had a much higher concentration, since it is a smaller room and the sampling point was relatively closer to the spray gun than other rooms. During application, all measured airborne MDI concentrations were lower than the OSHA Permissible Exposure Level (PEL) ceiling level ( $200 \mu\text{g}/\text{m}^3$ ). The highest MDI concentration during application was  $185 \mu\text{g}/\text{m}^3$  in room H. The airborne MDI concentration was  $23.26 \mu\text{g}/\text{m}^3$  in the attic.

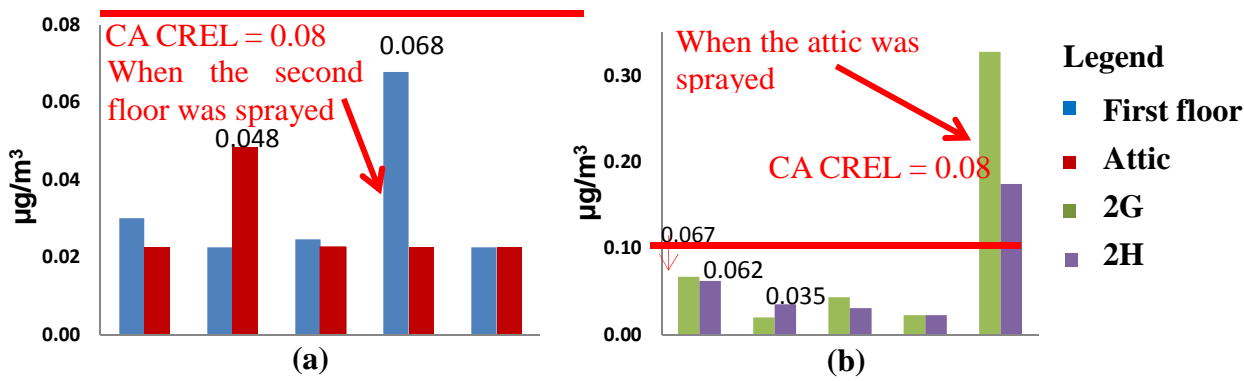


**Figure 18: SPF application first floor exterior façade (left) and second floor interior wall (right)**



*OSHA = Occupational Safety and Health Administration, PEL = Permissible Exposure Level, NIOSH = National Institute for Occupational Safety and Health, REL = Recommended Exposure Limit*

**Figure 19: Airborne MDI concentration during application**



CA CREL = California Chronic Reference Exposure Level

**Figure 20: Airborne MDI concentration after application**

When spray application was stopped and there was no active spraying in the building, the airborne MDI concentration decreased on all three floors. Two hours after SPF application, airborne MDI concentrations decreased to  $3.3 \times 10^{-4}$  % (room H)  $\sim$  0.11% (first floor) of the concentration measured during spray. As shown in Figure 20, after application, all measured values on the first floor and attic were less than the CA CREL – the most stringent of all standards listed in Table 12 - with two values higher than the LOQ. In the two second floor rooms, airborne MDI concentrations constantly decreased from the 2<sup>nd</sup> hour to the 18<sup>th</sup> hour with values exceeding the LOQ threshold for only the first four hours. However, a sharp increase did occur 24 hours after application on the second floor, which was influenced by the spray application in the attic. Intra-zonal flows allowed MDI fumes to disperse in the home; our study was able to capture this relationship further defining how chemical levels change over vertical

gradients. When the attic and second floor were sprayed, the airborne MDI concentration increased by a factor of 14, 8 and 3 on the second-floor rooms G, H and first floor, respectively.

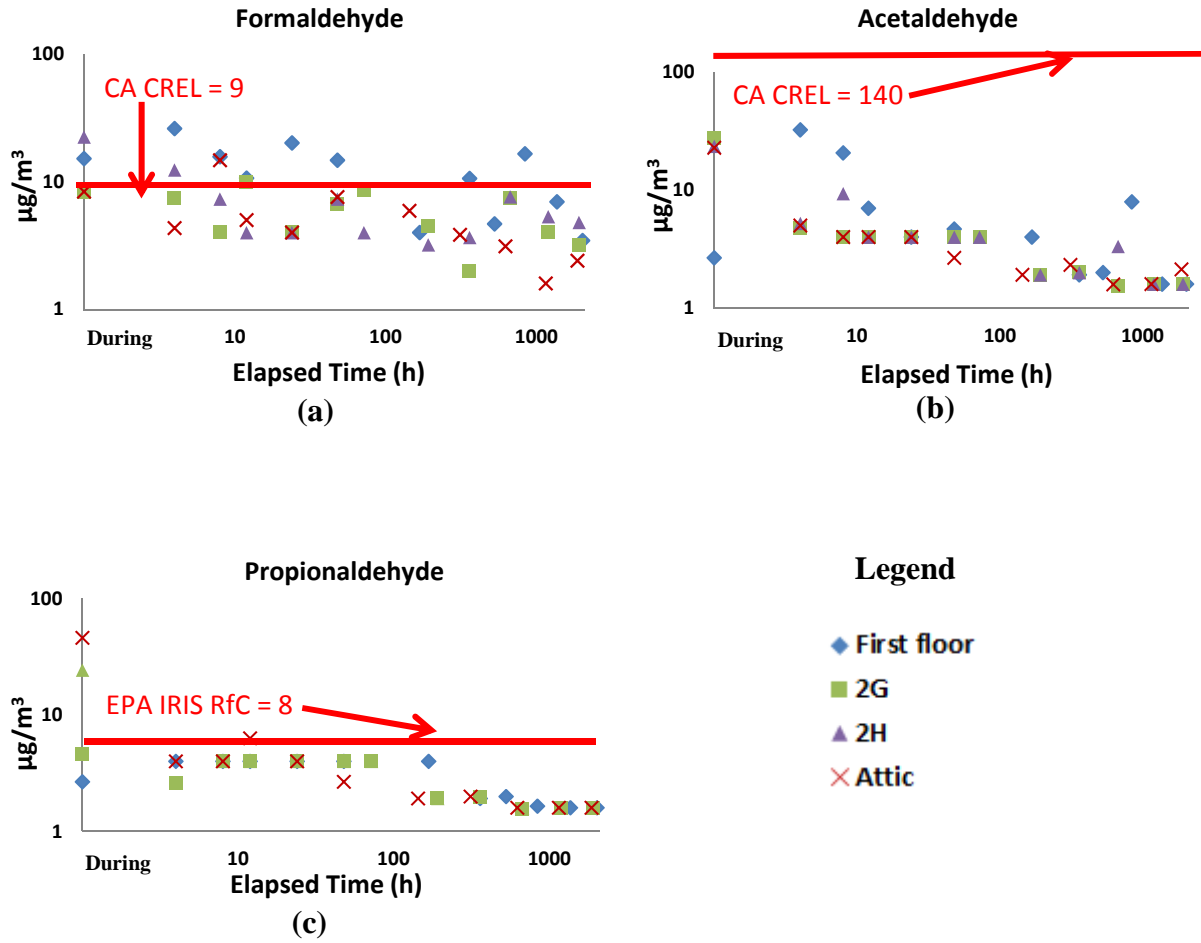
The results suggest a plausible association between the transport of chemicals and exposure at adjacent environments; based on these findings, workers should not occupy the building without proper protection equipment while active SPF application is in process. When the two-component high pressure SPF application is complete, the industry recommended re-entry time is 24 hours for unprotected applicators, helpers, other workers and building occupants such as home owners (Center for the Polyurethanes Industry 2017).

#### **4.3.2 Aldehydes**

Background concentrations of aldehydes were collected one week before the spray application. The first floor living area had relatively higher background Formaldehyde ( $12.8 \mu\text{g}/\text{m}^3$ ) and Acetaldehyde levels ( $16.7 \mu\text{g}/\text{m}^3$ ) than the second floor and attic (both less than the LOQ at  $3.1 \mu\text{g}/\text{m}^3$ ) attributed to the first floor being an active living area while the other two floors were unoccupied. Propionaldehyde concentrations were less than the LOQ ( $3.1 \mu\text{g}/\text{m}^3$ ) on all three floors.

In general, as shown in Figure 21, the aldehyde concentrations exceeded background levels (first floor) or LOQ (second floor and attic) during application and up to 48 hours after application. For example, the Formaldehyde level remained less than  $9 \mu\text{g}/\text{m}^3$  (CA CREL) starting from 24 hours in sampling areas except the first floor. For Propionaldehyde, the results were compared with EPA IRIS RfC due to the lack of CA CREL limits. Except during application, the airborne Propionaldehyde level was less than the RfC throughout the sampling period. Compared to MDI, the first and second floor aldehyde concentrations did not show an

increase, while other areas of the house were sprayed in the same house. Unlike MDI, aldehydes are not intentionally added into the SPF formulation and have much less mass available for emission. Therefore, migration of aldehydes in the house during spray was limited. In fact, Formaldehyde is a trace component in the raw materials used to produce polyol (part B of SPF) while Acetaldehyde and Propionaldehyde are formed during the foaming process on the application site.

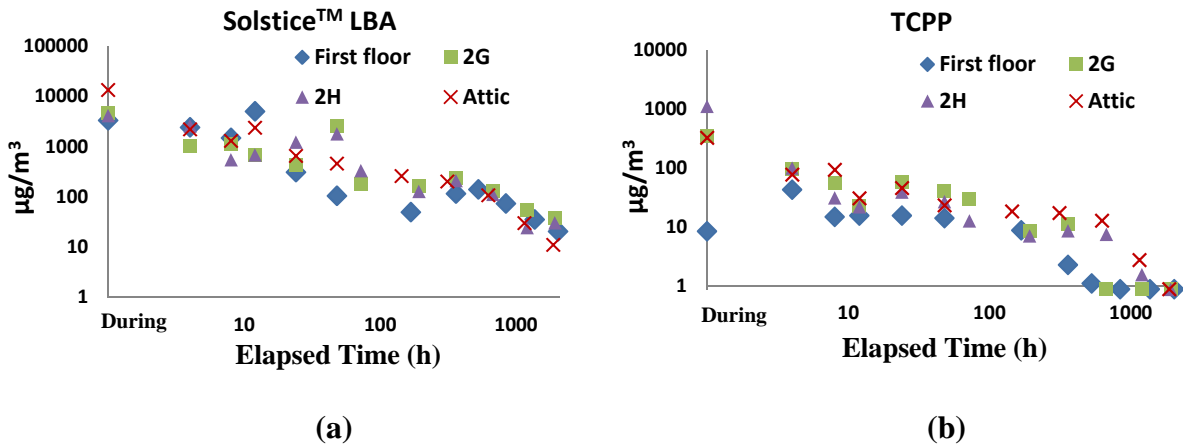


CA CREL = California Chronic Reference Exposure Level, IRIS = Integrated Risk Information System, RfC = Reference Concentration

**Figure 21: Airborne aldehydes concentration (during and after application)**

### 4.3.3 Blowing agent and flame retardant

The LOQ for Solstice™ LBA and TCPP were 9.8 and 2.2  $\mu\text{g}/\text{m}^3$  respectively during the background sampling, and none of the areas evaluated had concentrations greater than the LOQ before SPF was applied. Based on the literature review and to the best knowledge, no regulatory standards pertaining to the chemicals were identified. Both of the chemicals were generally detected at elevated levels during application, but decayed in the first 24 hours, as shown in Figure 22. Although the Solstice™ LBA concentration was still greater than the LOQ in all areas evaluated at the end of testing period, the decreasing trend was clear. TCPP concentration dropped to the LOQ around 15 days after application on the first floor while it did not reach below the LOQ until 48 days in the attic. The time series of Solstice™ LBA and TCPP can be best described in a log-log regression between airborne concentration ( $\mu\text{g}/\text{m}^3$ ) and time (hour) as shown in Table 15. These regression equations were used to calculate the time weighted average (TWA) airborne TCPP concentrations over the sampling period on each floor, since the total TCPP available in the gas phase is important to TCPP mass transfer rates from indoor air to sinks such as building interior materials, airborne particles and settled dusts.



LOQ during background sampling: Solstice™ LBA =  $9.8 \mu\text{g}/\text{m}^3$ , TCPP =  $2.2 \mu\text{g}/\text{m}^3$

**Figure 22: Airborne Solstice™ LBA (a) and TCPP (b) concentration (During and after application)**

**Table 15: Log-Log regression between airborne concentration and time.<sup>a</sup>**

Chemical	Room	A	B	R <sup>2</sup>	P
<b>Log (Concentration, <math>\mu\text{g}/\text{m}^3</math>) = A – B × log (Time, hr)</b>					
Solstice LBA	First fl. A	3.809	0.731	0.793	0.001
	Second fl. G	3.522	0.533	0.733	0.001
	Second fl. H	3.776	0.663	0.806	0.001
	Attic	3.985	0.784	0.922	0.001
TCPP	First fl. A	1.933	0.596	0.835	0.002
	Second fl. G	2.473	0.691	0.731	0.003
	Second fl. H	2.174	0.546	0.840	0.001
	Attic	2.234	0.479	0.828	0.001

a. Only post application airborne concentration higher than the LOQ was used in regression

#### 4.3.4 Airborne particles

On the first floor, all filters (during 4 hours and 24 hours) collected from the Marple 8-stage personal cascade impactor were either less than or at the LOQ which is 30  $\mu\text{g}/\text{filter}$ . During application in the attic, 3 filters out of the 8 stages (particle diameter between 10 and 15, 6 and 10, 1.5 and 3.5  $\mu\text{m}$ ) had particle mass higher than the LOQ. The total mass collected on all filters was 149  $\mu\text{g}$  (0.83  $\mu\text{g}/\text{m}^3$ ). At 4 hours and 24 hours after application, 1 filter out of the 8 stages (particle diameter above 20) had particle mass (160  $\mu\text{g}$  or 0.89  $\mu\text{g}/\text{m}^3$ ) higher than LOQ. Compared to during application particle concentration measured by Lesage et al. (Lesage, Stanley et al. 2007), our results were 20% lower. This was expected because the impactor was placed in the middle of the room rather than worn by the applicator as a personal sampler.

The airborne particle concentrations result (10 minutes average,  $N = 3,730$ ) obtained by the Gray Wolf PC-3016A particle counter is presented in Figure 23. When grouping the six particle sizes into  $\text{PM}_{2.5}$  and  $\text{PM}_{10}$ , the mean airborne concentrations were  $16.23 \pm 0.35$  and  $22.49 \pm 1.05$   $\mu\text{g}/\text{m}^3$ . These results will be used in Chapter 5 as input parameters in i-SVOC (version 1.0, USEPA, Research Triangle Park, NC) and IECCU (version 1.0, ICF-International, Research Triangle Park, NC) to study SVOCs sorption onto indoor particles.

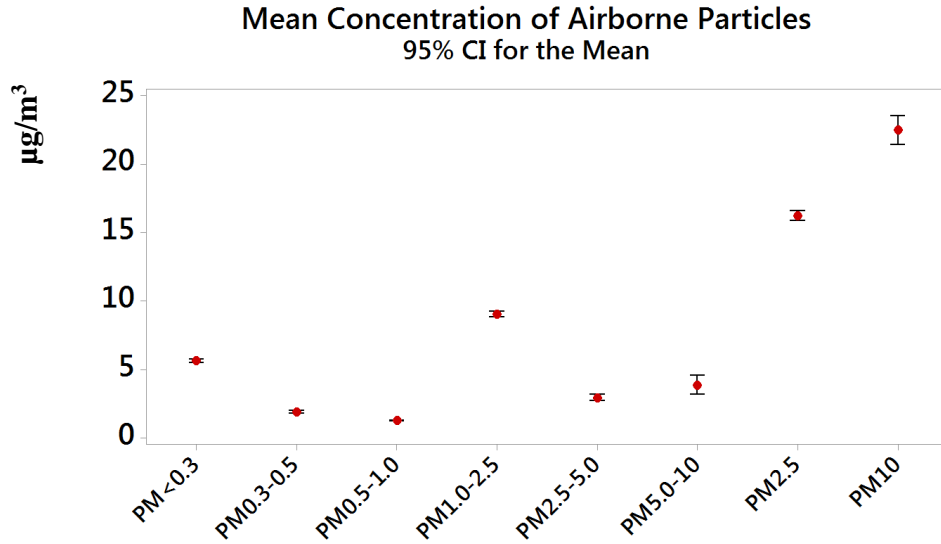


**Figure 23: Mean airborne concentration and confidence interval by particle**

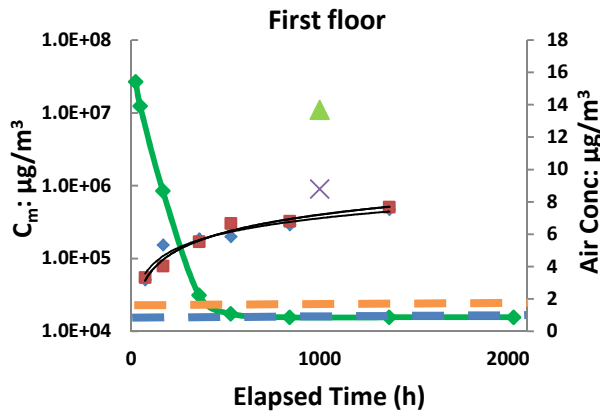
#### 4.3.5 TCPP accumulation onto building materials

The following indicators were used to evaluate the TCPP accumulation:

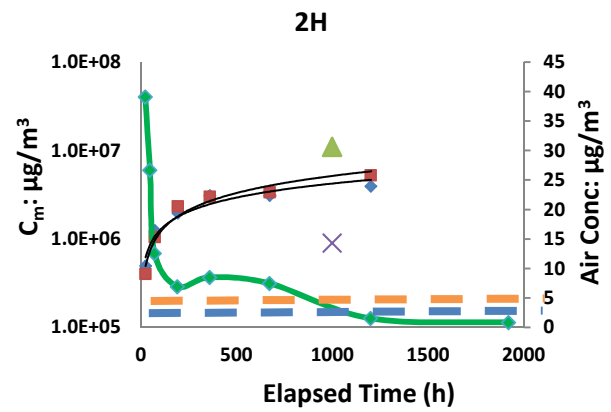
- 1) Concentration by volume ( $C_m$ :  $\mu\text{g}/\text{m}^3$ ): the total TCPP found on the material divided by material volume (Figure 24);
- 2) Concentration by exposed surface area ( $C_s$ :  $\mu\text{g}/\text{m}^2$ ): the total TCPP found on the material divided by the total exposed area (all sample surface area excluding the bottom) (**Figure 25**);
- 3) Volume specific time averaged accumulation rate ( $R_m$ :  $\mu\text{g}/\text{h}/\text{m}^3$ ) which was calculated as  $C_m$  divided by the amount of elapsed time between two measurements (**Figure 26**) and;
- 4) Surface specific time averaged accumulation rate ( $R_s$ :  $\mu\text{g}/\text{h}/\text{m}^2$ ) which was calculated as  $C_s$  divided by the amount of elapsed time between two measurements (Figure 27).

The total amount of TCPP on the samples ( $C_m$  and  $C_s$ ) increased over time on all three floors at a decreasing rate, while the accumulation rates ( $R_m$  and  $R_s$ ) decreased during the sampling period. Comparing among floors, all four indicators were one order of magnitude lower on the first floor than the other two floors, which was partially because airborne TCPP concentration was lower on the first floor. TWA airborne TCPP concentration was evaluated by integrating the regression curves listed in **Table 15** and divided by 1,000 hours, which was 11.86, 7.51 and 3.37  $\mu\text{g}/\text{m}^3$  for the attic, second floor and first floor, respectively.

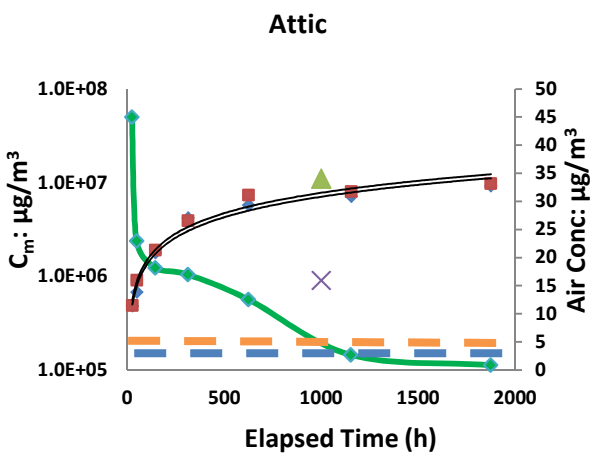
An attempt was made to compare the results of this study to a chamber study conducted by Liu et al. (Liu, Allen et al. 2016a). In general, the four indicators evaluated were within one order of magnitude between this study and Liu's study (Liu, Allen et al. 2016a) for most cases; there were a few exceptions that, mostly on the first floor. One significant difference is that instead of a relative constant sorption rate in the chamber study,  $R_m$  and  $R_s$  in the field decreased by roughly 70% to 90% along the sampling period, depending on the type of sorption material and sampling location. When the two types of material were compared, on all three floors, the field study revealed that TCPP per volume ( $C_m$ ) and per surface area ( $C_s$ ) were very close between carpet and drywall. However, in the chamber study, drywall contained more TCPP than carpet.



(a)



(b)



(c)

**Legend**

- ◆ Carpet (this study)
- Drywall (this study)
- ▲ Drywall (Liu, 2016)
- × Carpet (Liu, 2016)
- Air Conc. (Right Axis)
- - - TCPP conc. in sink chamber lower bond (Liu, 2016)
- - - TCPP conc. In sink chamber upper bond (Liu, 2016)

**Figure 24: TCPP concentration ( $C_m$ ,  $\mu\text{g}/\text{m}^3$ ) in carpet and drywall, compared with Liu's chamber study data (Liu, Allen et al. 2016a).**

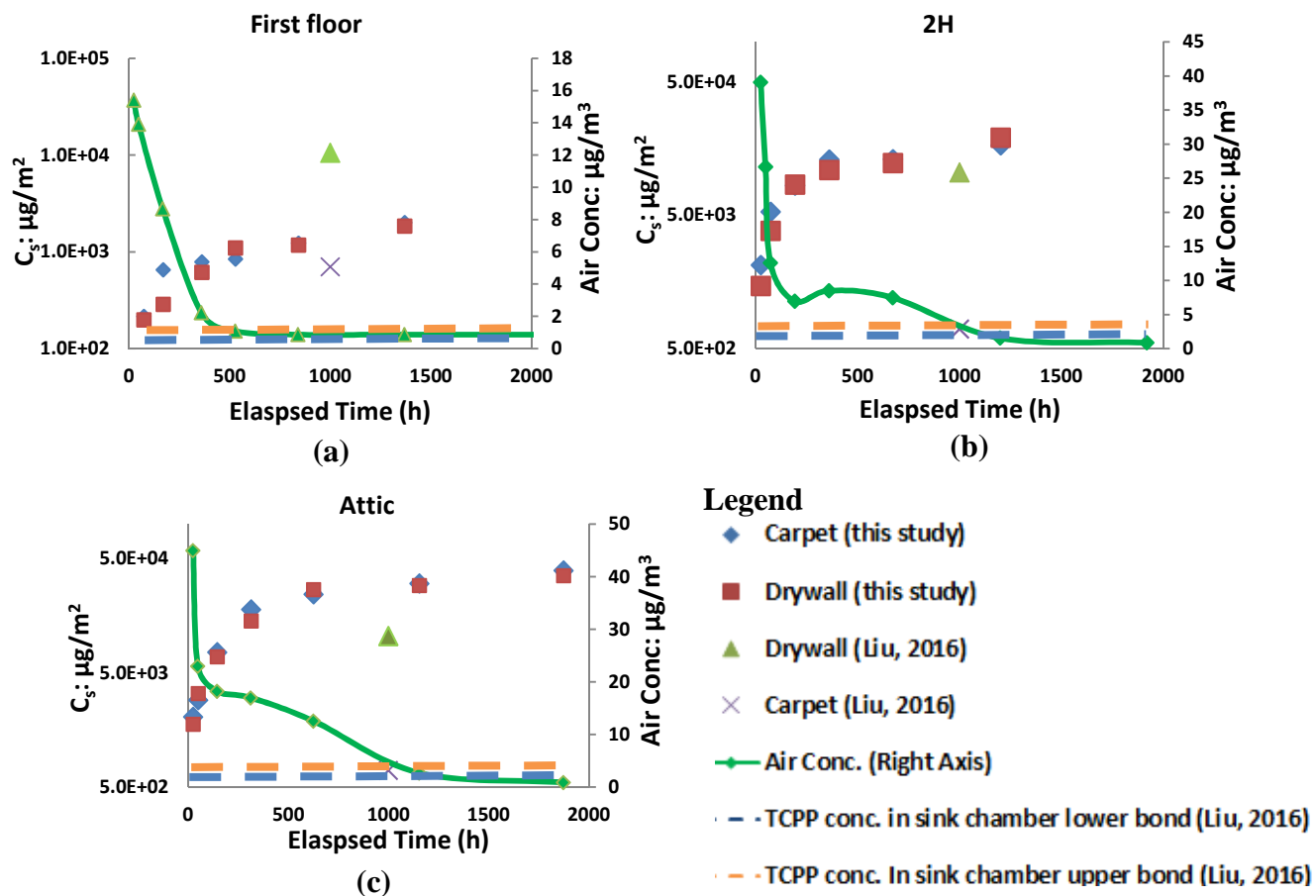
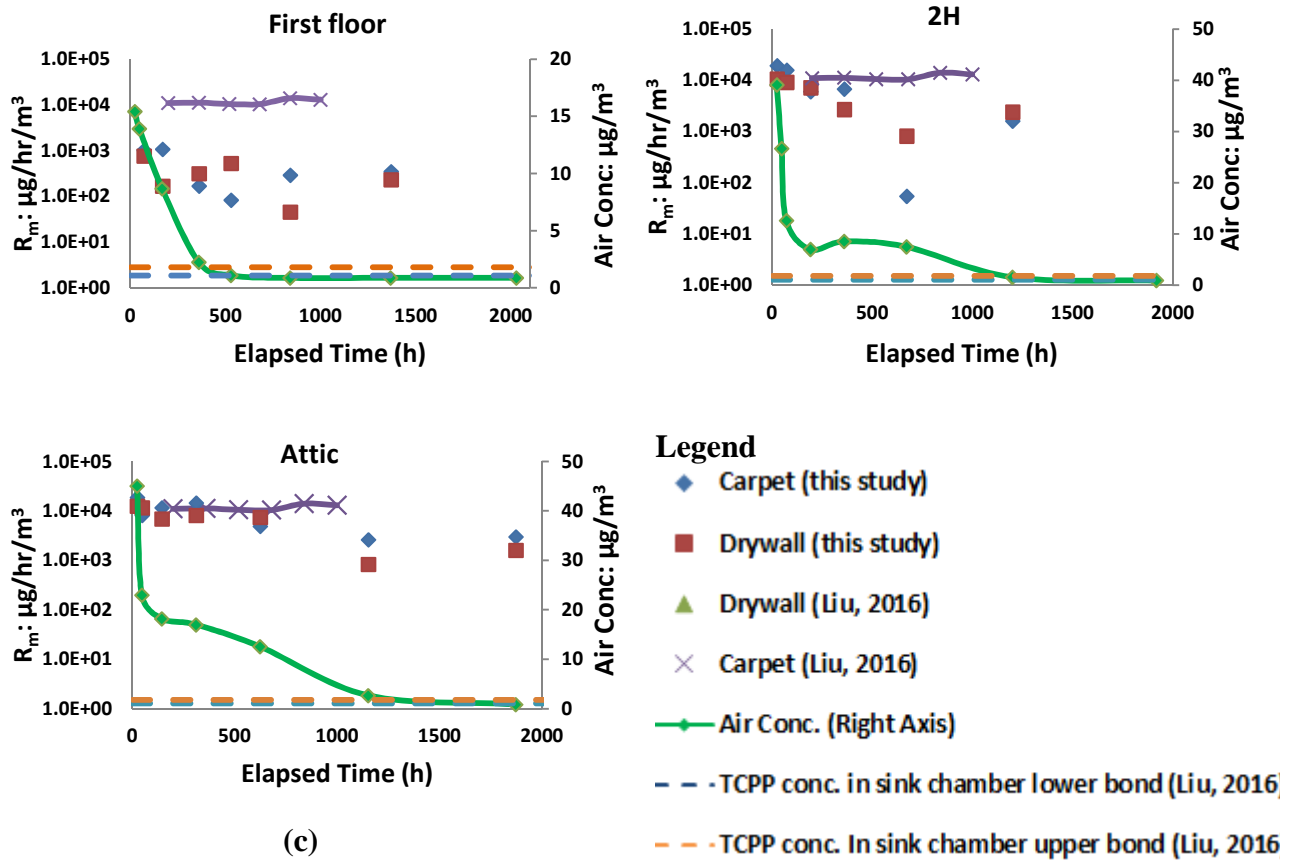


**Figure 25: TCPP concentration ( $C_s$ ,  $\mu\text{g}/\text{m}^2$ ) in carpet and drywall by total exposed area**

There are a few factors that explain the differences between the chamber and field studies. One of the most important factors was the presence of indoor particles in the ambient air. In the field study, TCPP can be absorbed onto indoor particles and then deposited onto other indoor building materials. While in the chamber study, clean air was used. Based on our observations, the carpet and drywall results were close to each other in the field study but were around one order of magnitude different in the chamber study with no particles in the air. This difference indicated that particle deposition could be a contributing factor to TCPP accumulation on the drywall and carpet samples. Another important factor that may impact the four indicators was the

airborne TCPP concentration. In the chamber study, it was relatively constant (1.08 to 1.80  $\mu\text{g}/\text{m}^3$ ), while in our field study, airborne TCPP concentrations were higher than the level of the chamber study in the first few days but reached a similar level after 7 weeks (~1,200 hours) into the sampling period on the second floor and attic. The TWA TCPP concentration in the field study was higher than the averaged TCPP concentration in chamber by a factor of 2 to 10. Furthermore, the gas phase mass transfer coefficient ( $H_g$ ) which is positively related  $R_m$  and  $R_s$  may also contribute to the differences between the two studies.  $H_g$  is negatively related to the characteristic length ( $L$ ) of sorption materials, which is defined as the square root of the sorption material surface area. Sorption materials used in the field study had a characteristic length of 5.1 cm, which was higher than materials used in the chamber study ( $L = 1.2$  cm). However, in order to quantify the impact of each factor on each indicator, advanced fate and transport modeling such as i-SVOC and IECCU should be employed in future studies, as illustrated in Chapter 5.

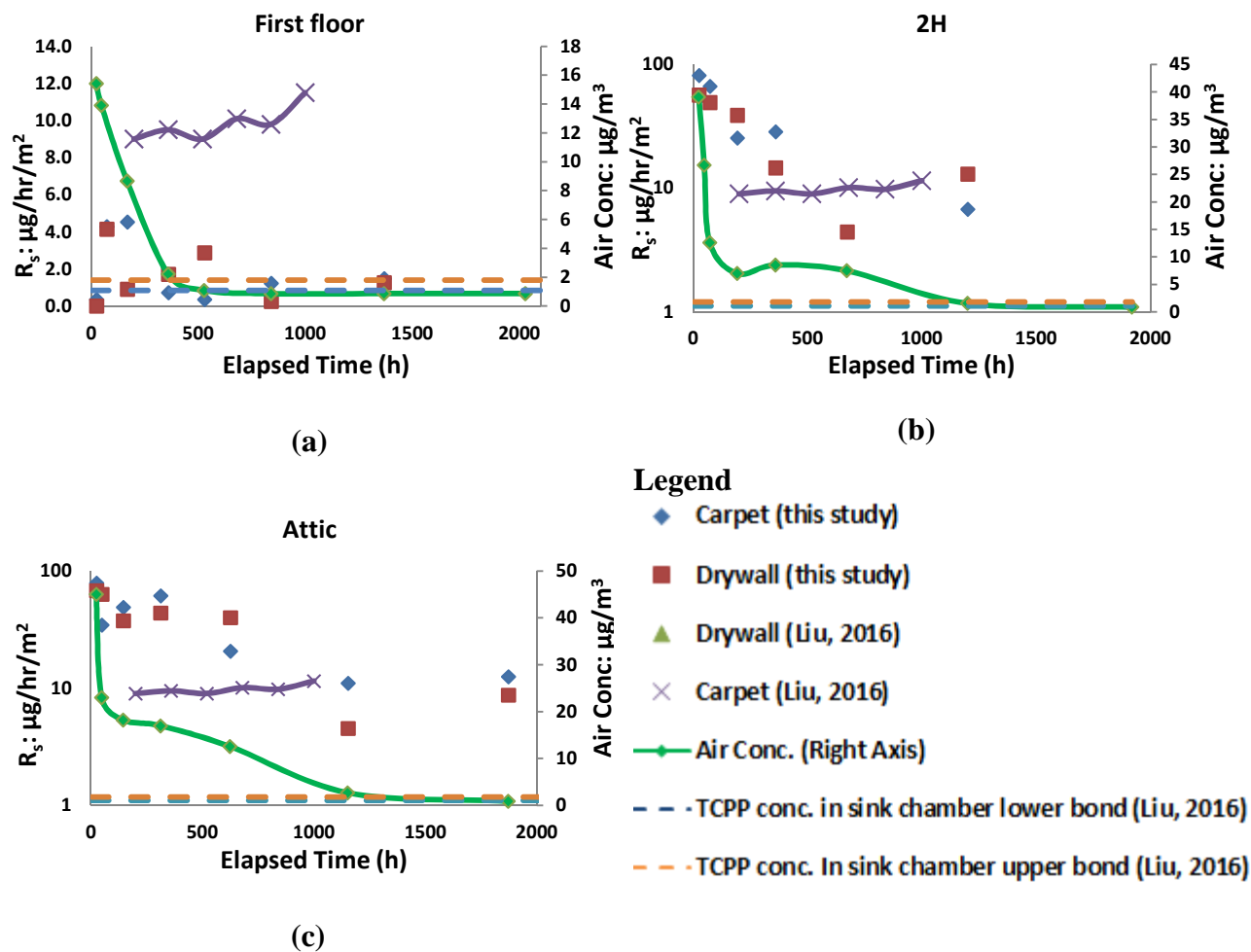


(c)

The two dotted lines on the bottom of each chart is the TCPP air concentration range in the sink chamber.

Carpet sorption rate was not reported by Liu (Liu, Allen et al. 2016a).

**Figure 26: Averaged TCPP accumulation rate ( $R_m$ :  $\mu\text{g}/\text{h}/\text{m}^3$ ), compared with Liu chamber study data.(Liu, Allen et al. 2016a)**



The two dotted lines on the of each chart is the TCPP air concentration range ( $\pm 1$  standard deviation) in the sink chamber of Liu (2016) (Liu, Allen et al. 2016a).

**Figure 27: TCPP surface specific averaged accumulation rate ( $R_s$ :  $\mu\text{g}/\text{h}/\text{m}^2$ ) and comparisons with data in Liu (2016) (Liu, Allen et al. 2016a)**

### 4.3.6 Air changes per hour

The measured  $ACH_{50}$  and calculated  $ACH_{natural}$  are listed in **Table 16**. Since the aged home was under major renovations, there were many places for air leakage and infiltration. For example, in order to spray on the exterior facade, outside sidings had to be removed leaving a large gap along the perimeter of the house between the first and second floor wall studs. SPF was used as wall insulation and not meant to be used for sealing such gaps. Due to the large areas for potential air leakage,  $ACH_{natural}$  was not significantly reduced after SPF application, and to note, this is not typical in most building renovation projects using SPF. Nonetheless, the measured ACH values are essential to quantify chemical decay rates in IAQ studies since they are predictive of dynamic and transient airflows (Bevington, Guo et al. 2017). Another blower door test is scheduled in the home when the entire renovation project has been completed.

**Table 16: Measured  $ACH_{50}$  and calculated  $ACH_{natural}$  on each floor**

	<b>Location</b>	<b><math>ACH_{50}</math></b>	<b><math>ACH_{natural}</math></b>
Before SPF installed	Whole House	32.52	3.09
	First floor	28.40	2.70
After SPF installed	Second floor	24.20	2.30
	Attic	43.87	4.16

## 4.4 LIMITATIONS AND FUTURE STUDIES

Human exposure to SVOCs can occur by inhaling vapor directly and through inhalable airborne particles which have SVOCs accumulated on the surface. Both exposure pathways are important

to understand the human health impacts of SVOCs. In this research, a Zefon inhalable dust sampler developed by the Institute of Occupational Medicine (IOM) was used to collect airborne particles for the analysis of TCPP on the filter. However, due to the low particle concentration, after sampling for 90 minutes at 2 L/min, only 4 out of the 15 IOMs had measurable weight difference ( $> 30\mu\text{g}$ ). In addition, because of the low particle mass difference on the IOM before and after sampling, the filter and particles had to be analyzed together. Therefore, the measured results from this analysis were the amount of vapor phase TCPP absorbed onto both filter and particles, which cannot be separated. Any traditional filter method to collect airborne particles would have the same issue if particles must be analyzed together with filter. Similarly, TCPP accumulated on the drywall and carpet samples could come from two sources: TCPP vapor absorbed onto the sample surface directly and settled particles that had TCPP absorbed on them. There is a possibility that some of those settled particles were generated during application as overspray. However, this effect should be reduced since most of overspray particles are large in diameter and have been removed by mechanical ventilation during room cleaning after spray. Future study should consider separating TCPP sorption onto particles from the TCPP absorbed on the sink materials (e.g., drywall and carpet) directly. For example, the authors set large pans made of aluminum foil for extended time to collect settled particles and analyzes TCPP sorption onto particles. In addition, future research may consider using cyclone to collect airborne particles.

The modified sampling and analytical method has improved the level of quantification of MDI for area samples. However, further research should compare this method with the impinger method to evaluate its accuracy.

Although chemical conversion is out of the scope of this research, future studies may consider to evaluate the potential creation of Methylenedianiline (MDA) in SPF application phase, especially for occupational exposure. MDA is a carcinogen which may be generated when MDI is hydrolyzed with water. The MDA concentration formed in the environment through MDI-water reaction is low (J. Sekizawa and Greenberg 2000). However, the human health risk of MDA in the indoor environment has not been well characterized.

#### 4.5 CONCLUSIONS

During a 3-month sampling period in a residential retrofit project, indoor airborne concentrations of MDI, aldehydes, a flame retardant (TCPP) and a blowing agent (Solstice™ LBA) were evaluated during and after SPF application. In this field study, the LOQ of MDI was improved by using a more sensitive sampling and analytical method, ACHs were valuated before and after SPF application, and TCPP accumulation on to building construction materials was measured and compared with a chamber study. The results showed when spray application was completed in the entire building, airborne concentration decreases over time for all measured chemicals. Four hours after application, the MDI airborne concentration was at least 50% lower than the most stringent standard (CA CREL) in all four measured areas. This study also demonstrated and quantified chemical migration among building compartments, especially for MDI. It is our recommendation that during SPF application, no one should return to the application site without proper personal protection equipment as long as there are active spray activities in the building. Although many factors may cause the differences between the field and chamber study, such differences were generally within one order of magnitude. In order to better

understand the fate and transport of SVOCs, such as TCPP, in the indoor environment, applying advanced IAQ models is planned to further evaluate how to extrapolate and use the chamber results to predict SVOCs behavior in the indoor environment.

#### **4.6 ACKNOWLEDGEMENT**

The authors appreciate the helpful comments given by Dr. Xiaoyu Liu at the USEPA and Dr. Dustin Poppendieck at NIST. We also thank Mr. Chris Hazen and Mr. Joe Hazen for allowing us to conduct sampling in their home and Mr. Richard Romero's coordination on this project. Shen Tian works at Covestro and is also a Ph.D. candidate at the University of Pittsburgh and Covestro supports his research through tuition payment. Covestro is a chemical raw material supplier of methylene diphenyl diisocyanate. Covestro also supplied raw materials to produce the two-component SPF system applied in this renovation project.

## **5.0 INDOOR FATE OF FLAME RETARDANTS IN A RESIDENTIAL BUILDING RENOVATED WITH SPRAY POLYURETHANE FOAM: MODEL PARAMETERIZATION AND RESULT INTERPRETATION**

### **5.1 INTRODUCTION**

#### **5.1.1 SVOCs and OPFRs**

SVOCs are considered to be organic chemicals with vapor pressure between  $10^{-9}$  to 10 Pa (Weschler and Nazaroff 2008). Due to their unique chemical and physical characteristics, SVOCs behave differently in the indoor environment than high vapor pressure VOCs. With lower vapor pressure and higher partition coefficient between solid materials and air than VOCs, SVOCs tend to be partitioned more into materials such as indoor surfaces, airborne particles and settled dusts. Therefore, SVOCs have a longer indoor residence time and higher exposure potential, even after the primary source is removed from the indoor environment (Mølhave, Clausen et al. 1997, Destailats, Maddalena et al. 2008, Weschler and Nazaroff 2008, Xu and Zhang 2011, Liu, Ye et al. 2013, Liu, Zhang et al. 2015). Many building and construction materials, consumer products and furnishings contain SVOCs. One type of SVOCs that has been studied in the past decades is the OPFRs. OPFRs are widely used as additives in industrial and consumer products such as polyurethane foam insulation, furniture, electrical products and

plastics (Van den Eede, Dirtu et al. 2011, Fromme, Lahrz et al. 2014, Tajima, Araki et al. 2014, Jayjock, Kroner et al. 2015, Tan, Peng et al. 2017, Zhou, Hiltcher et al. 2017). The USEPA has listed a few OPFRs including TCPP as Action Plan chemicals under the amended TSCA (U.S. Environmental Protection Agency 2015c).

### **5.1.2 TCPP in the indoor environment and multi-media models**

Human exposure to indoor chemicals can occur through various routes such as inhalation of gas phase pollutants and airborne particles, ingestion of settled dusts and direct dermal contact with contaminated surfaces. Extensive research has been conducted to evaluate TCPP concentration in the indoor environment (Carlsson, Nilsson et al. 1997, Sanchez, Ericsson et al. 2003, Marklund, Andersson et al. 2005, Saito, Onuki et al. 2007, Fromme, Lahrz et al. 2014, Yang, Ding et al. 2014, Liagkouridis, Cequier et al. 2017). Most of these studies use the “end control” approach which reveals TCPP concentration in each indoor environmental media, but do not study the mass transfer processes such as the emission mechanisms, sorption and desorption of TCPP from indoor surfaces and how TCPP interacts with indoor SVOC sinks such as flooring, carpet and settled dusts. Without a better understanding of these fundamental fate and transport processes, risk mitigation and pollution control may not be effective. A few research studies have been focused on measuring TCPP emission rates from consumer products and quantifying the migration pathways, such as sorption on indoor sinks through chamber testing (Kemmlin, Hahn et al. 2003, Liu, Allen et al. 2016a, Liu, Allen et al. 2016b, Liagkouridis, Lazarov et al. 2017, Liang, Liu et al. 2018a). However, such studies are often time and resource intensive resulting in a limited number of samples that could be collected and analyzed. An emerging need for IAQ

assessment of OPFRs is to derive chemical concentration in each indoor media in a cost-effective way (Tian, Sebroski et al. 2017, Tian, Ecoff et al. 2018).

Indoor mass transfer models are viable alternatives to chamber or field studies, since the modeling approach requires less time, resources and it does not limit to certain chemicals or indoor media, provided the required input parameters are available. In the past decades, many multi-media models have been developed and applied to study the fate, transport and distribution of SVOCs in the indoor environment, including pesticides, phthalates and OPFRs (Matoba, Yoshimura et al. 1998, Bennett and Furtaw 2004, Xu and Little 2006, Weschler and Nazaroff 2008, Xu, Cohen-Hubal et al. 2009, Zhang, Diamond et al. 2009, Clausen, Liu et al. 2010, Little, Weschler et al. 2012, Tian, Sebroski et al. 2017). These models are different in terms of modeling form (e.g., steady state or ordinary differential equations), representation of sources and sinks, and chemicals of focused. Two areas of future research were identified as: better representations of source and sink materials using diffusional models (Guo 2013) and the need of deriving key modeling input parameters to characterize SVOCs behavior in the indoor environment (Liu, Ye et al. 2013).

To advance SVOC indoor multi-media models to include diffusional sources and sinks, the USEPA has developed the i-SVOC (U.S. Environmental Protection Agency 2013b) and the IECCU (Guo 2017a) model to simulate SVOC emission, sorption and accumulation in the indoor media. The i-SVOC is a single zone mass transfer model which calculates SVOC mass fluxes of each environment media, while IECCU can model a multi-zone building and include temperature dependent partition and diffusion coefficients of various emission sources. Instead of an off-the-shelf tool, both of the two USEPA models require the users to provide extensive input parameters to ensure the modeling results are accurate and realistic as possible. Although a few

recent research studies provided measured (Liu, Allen et al. 2016a, Liu, Allen et al. 2016b, Liang, Liu et al. 2018a) or estimated (Weschler and Nazaroff 2010, Tian, Sebroski et al. 2017) modeling input parameters for TCPP such as the partition coefficients in building materials and consumer products, a comprehensive list of modeling parameters that include TCPP sources, sinks, settled dusts and airborne particles was not available. Multi-media models can bridge the gaps between field measurements and chamber testing studies so that indoor SVOC research can be conducted more efficiently, only if these models have been validated and provided with realistic material and chemical specific input parameters.

### **5.1.3 Objective and scope**

This research aimed to quantify the emission, fate and distribution of TCPP in a renovated residential building using SPF. A comprehensive list of input parameters required by IECCU was either measured or estimated. Based on the value range of key modeling parameters, eight scenarios were developed to evaluate the impact of each input parameter to the final modeling outcome such as TCPP airborne concentration. Field measurements were then compared with the modeling results to discuss the potential causes of the discrepancies. The exposure assessment conducted aimed to quantify building occupants' TCPP exposure through the inhalation and ingestion pathways only, averaged over a 100-day modeled period. The hazard index was calculated based on an USEPA provisional toxicity threshold.

This paper focuses on the approaches to derive key modeling input parameters for IECCU, modeled TCPP mass balance results in a residential building and the comparisons between field measurements and modeling results. Details about the field study and analytical methods can be found in a paper published by Tian et al. (Tian, Ecoff et al. 2018).

## 5.2 METHODS AND MATERIALS

### 5.2.1 Field measurements

A field IH survey was conducted in 2016 to measure TCPP airborne concentration and surface accumulation in a renovated residential building using SPF. Airborne TCPP concentration and TCPP accumulated onto sink materials were collected in various areas throughout the building during a three months period and analyzed by gas chromatograph – mass spectrometry (GC-MS). Details about the sample collection process, analytical methods and results were published previously (Tian, Ecoff et al. 2018).

### 5.2.2 Mass balance

Figure 28 shows the sources, sinks and ventilation pathways of the studied residential house. The mass balance of TCPP in the two zones of this house are written in Equation 3 and Equation 4.

$$V_1 \frac{dc_1}{dt} = \dot{m}_{source,t} - \dot{m}_{dust,t} - \dot{m}_{PM_{2.5},t} - \dot{m}_{PM_{10},t} - \dot{m}_{sink,t} + C_{2,t} \times Q_{21,t} + C_0 \times Q_{01,t} - C_{1,t} \times Q_{10,t} - C_{1,t} \times Q_{12,t} \quad \text{Equation 3}$$

$$V_2 \frac{dc_2}{dt} = \dot{m}_{source,t} - \dot{m}_{dust,t} - \dot{m}_{PM_{2.5},t} - \dot{m}_{PM_{10},t} - \dot{m}_{sink,t} + C_{1,t} \times Q_{12,t} + C_0 \times Q_{02,t} - C_{2,t} \times Q_{20,t} - C_{2,t} \times Q_{21,t} \quad \text{Equation 4}$$

Where  $V_1$  and  $V_2$  are the volume of living area and attic ( $m^3$ );  $\dot{m}_{source,t}$ ,  $\dot{m}_{dust,t}$ ,  $\dot{m}_{PM_{2.5},t}$ ,  $\dot{m}_{PM_{10},t}$ ,  $\dot{m}_{sink,t}$  are the TCPP source emission rate, TCPP mass change rate of dust,

PM<sub>2.5</sub>, PM<sub>10</sub> and the sink materials, respectively ( $\mu\text{g}/\text{hr}$ );  $C_0$  is the TCPP concentration in the outdoor air ( $\mu\text{g}/\text{m}^3$ );  $C_{1,t}$  and  $C_{2,t}$  are TCPP airborne concentration in the living area and attic at time  $t$  ( $\mu\text{g}/\text{m}^3$ );  $Q_{01,t}$  and  $Q_{02,t}$  are the air flow rates from the outdoor environment to the living area and attic at hour  $t$  ( $\text{m}^3/\text{hr}$ );  $Q_{10,t}$  and  $Q_{12,t}$  are the air flow rates from the living area to the outdoor environment and attic at hour  $t$  ( $\text{m}^3/\text{hr}$ );  $Q_{20,t}$  and  $Q_{21,t}$  are the air flow rates from the attic to the outdoor environment and the living area at hour  $t$  ( $\text{m}^3/\text{hr}$ ).

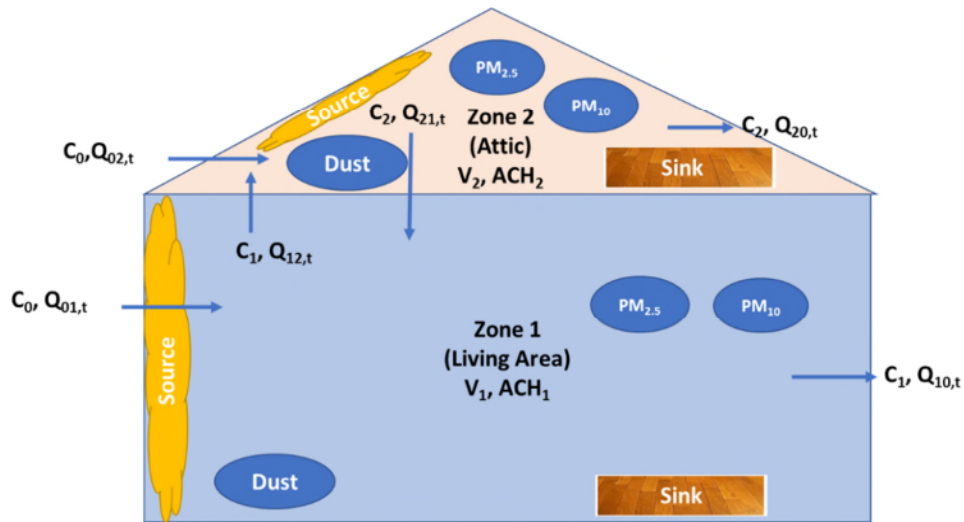


**Figure 28: Schematic of the studied residential house**

### 5.2.3 IECCU model

IECCU was developed by USEPA to study chemical fate, transport and exposure in buildings with multiple zones, chemicals, sources and sinks (Guo 2017a). One application of IECCU is to study SPF applied in unconditioned zones such as attic, basement and crawlspaces. In our prior field study (Tian, Ecoff et al. 2018), SPF was sprayed in both conditioned zones (living area) and

unconditioned zones (attic). Therefore, modeling parameters were adjusted accordingly based on the field conditions.

IECCU combined two existing models, IAQx and i-SVOC. IAQx is an IAQ simulation model that calculates the pollutant concentration as a function of time using simple mass transfer models (Guo 2000, U.S. Environmental Protection Agency 2000). i-SVOC is a mass transfer model specifically built to study the fate and transport of SVOCs in a single zone environment (U.S. Environmental Protection Agency 2013b). The key mass transfer theory in i-SVOC is the modified state space (MSS) method (Yan, Zhang et al. 2009, Guo 2013). The advantage of MSS method is that instead of solving partial differential equations, it converts the process of SVOC diffusion into a series of ordinary differential equations by dividing the source or sink materials into a finite number of slices. The computational process has been greatly improved. The details of MSS application for indoor sinks such as settled dusts have been thoroughly described by Guo (Guo 2014) and only the key equations are repeated here for the purpose of explaining results found in this research.

In the MSS method (as shown in Figure 29), a local two-phase theory (Lewis and Whitman 1924, Guo 2014) is used to describe the chemical mass transfer process between the solid material (e.g. sinks and settled dusts) and the ambient air as shown in Equation 5 to Equation 7.

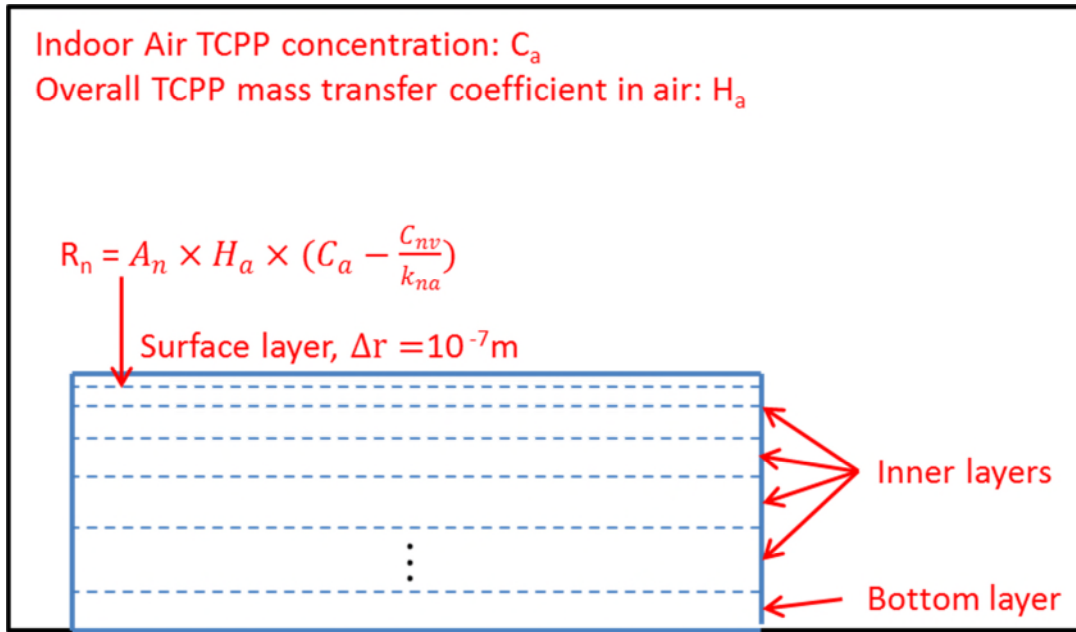


**Figure 29: Schematic diagram for the MSS method and the local two-phase mass transfer theory**

$$R_n = A_n \times H_a \times \left( C_a - \frac{C_{nv}}{k_{na}} \right) \quad \text{Equation 5}$$

$$\frac{1}{H_a} = \frac{1}{k_{na} \times h_n} + \frac{1}{h_{an}} \quad \text{Equation 6}$$

$$h_n = \frac{2D_n}{\Delta r} \quad \text{Equation 7}$$

Where  $R_n$  ( $\mu\text{g/h}$ ) is the chemical mass transfer rate from air to the top surface layer of the sink materials,  $A_n$  ( $\text{m}^2$ ) is the top surface area of the sink material,  $H_a$  ( $\text{m/h}$ ) is the overall gas-phase mass transfer coefficient from Equation 6.  $C_a$  ( $\mu\text{g}/\text{m}^3$ ) is the airborne TCPP concentration in the indoor environment or a chamber,  $C_{nv}$  ( $\mu\text{g}/\text{m}^3$ ) is the concentration in the top surface layer of the sink material,  $k_{na}$  (unitless) is the sink-air partition coefficient,  $h_n$  ( $\text{m/h}$ ) is the solid phase sink material mass transfer coefficient from Equation 7,  $h_{an}$  ( $\text{m/h}$ ) is gas phase sink material mass

transfer coefficient,  $D_n$  ( $m^2/h$ ) is the sink material diffusion coefficient and  $\Delta r$  (m) is the thickness of the top surface layer which is defaulted to be  $10^{-7}$  m. Beside sink materials, this theory also applies to sources, airborne particles and settled dusts. For settled dusts, Equation 5 to Equation 7 can be written as Equation 8 to Equation 10. The only difference is that those parameters related to sink materials ( $R_n$ ,  $A_n$ ,  $C_{nv}$ ,  $k_{na}$ ,  $h_n$ ,  $h_{an}$  and  $D_n$ ) are changed to settled dusts ( $R_d$ ,  $A_d$ ,  $C_{dv}$ ,  $k_{da}$ ,  $h_d$ ,  $h_{ad}$  and  $D_d$ ).

$$R_d = A_d \times H_a \times \left( C_a - \frac{C_{dv}}{k_{da}} \right) \quad \text{Equation 8}$$

$$\frac{1}{H_a} = \frac{1}{k_{da} \times h_d} + \frac{1}{h_{ad}} \quad \text{Equation 9}$$

$$h_d = \frac{2D_d}{\Delta r} \quad \text{Equation 10}$$

We have generated key modeling input parameters for i-SVOC to study TCPP emission from SPF and TCPP surface sorption on indoor sink materials. Part of the parameters generated in our prior study was adopted in this IECCU modeling (Tian, Sebroski et al. 2017).

## 5.2.4 Chamber testing

IECCU modeling parameters required for sources and sinks were previously estimated in our prior study (Tian, Sebroski et al. 2017). However, parameters related to settled dust have not been reported in the literature and therefore need to be developed. A chamber testing was conducted to estimate TCPP diffusion coefficient ( $D_d$ ) in settled dusts.

### 5.2.4.1 House dusts collection and preparation

House dust samples were collected from five homes in Pittsburgh, PA area using household vacuum machines. The samples were combined and sieved into two diameter sizes (25-90  $\mu m$  and 90-150  $\mu m$ ) in order to investigate the

differences of TCPP accumulation quantity and rate on settled dusts based on their diameters. It is expected smaller dusts should have higher accumulation rate due to larger surface area per unit volume. For each diameter size, a total of 12 samples were placed in a small chamber (36 Liter, shown in Figure 30). Each sample contained  $0.258 \pm 0.002$  g (Mettler Toledo, Columbus, OH) of dust which was spread out on a filter paper (Whatman 1004-110 Grade 4 Qualitative Circles) as much as possible. A blank filter was also added to test the amount of TCPP accumulated onto the filters. To minimize direct surface migration of TCPP from the chamber wall to the dust samples, a stainless-steel wire net (Blue Hawk, from a local store) was placed on the bottom of the chamber as a holder for all dust samples. The 1-inch space between the chamber bottom and the dust samples prevented direct contact of dust samples to chamber wall and may also increase air circulation and mixing so that the airborne TCPP in the chamber can be more evenly distributed.



**Figure 30: Dust samples and blank filter placed in the small chamber**

**5.2.4.2 Chamber testing systems** The dust sorption test was conducted in a two stainless steel chambers system as shown in Figure 31. The micro-chamber (0.114 Liter, left picture in Figure 32) was used as a source chamber to provide a continuous TCPP flow into the small chamber (36 Liter, right picture in Figure 32) where dust samples were placed. Liquid TCPP was weighed and placed into the three small cavities pre-drilled into Teflon blocks that were sized to fit tightly into the micro-chamber cavities. There was enough TCPP in the source chamber during the testing period to maintain a relative constant TCPP flow into the test chamber. Before dust samples were placed into the test chamber, clean air was used to flow through the system for a total of 47 days. During the first 19 days, the micro-chamber was heated to 35 °C and then the temperature was reduced to 23 °C for the rest of 28 days. The goal of this step was to generate a TCPP gas flow to coat the inner surfaces of connection tubes and the test chamber so TCPP sorption onto these surfaces could be reduced after dust samples were introduced. During this period, air samples were periodically collected for both chambers using thermal desorption (TD) tubes which contained 5-mm quartz wool, Tenax<sup>®</sup> TA 35/60, Carbograph<sup>™</sup> 5TD 40/60 (Markes International). Airborne TCPP in both chambers constantly decayed but reached to a relative steady concentration before dust samples were placed. After dust samples were placed, clean air flowed through the system at 0.20 liter/minute which resulted an air change rate of 0.33 ACH in the test chamber. There were two identical chamber testing systems used in this study, one for each dust diameter size.

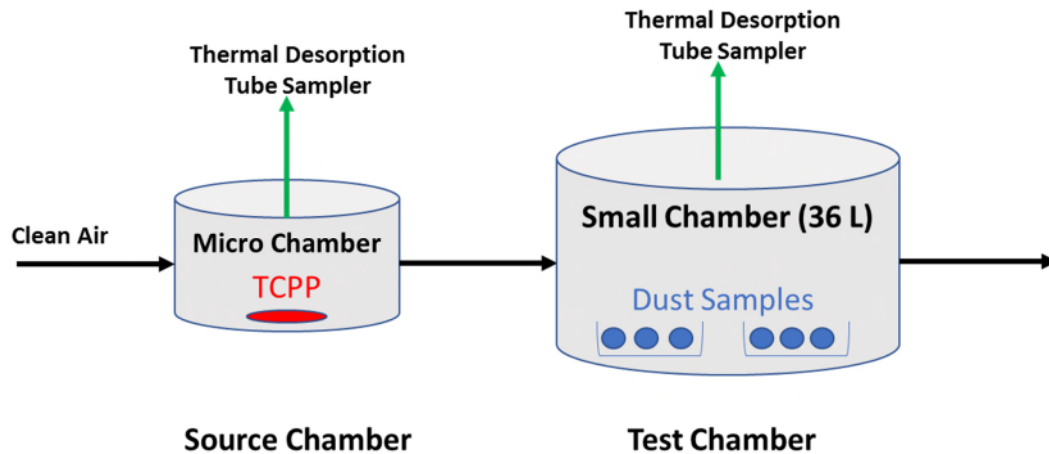


**Figure 31: Schematic of the two-chamber testing system**

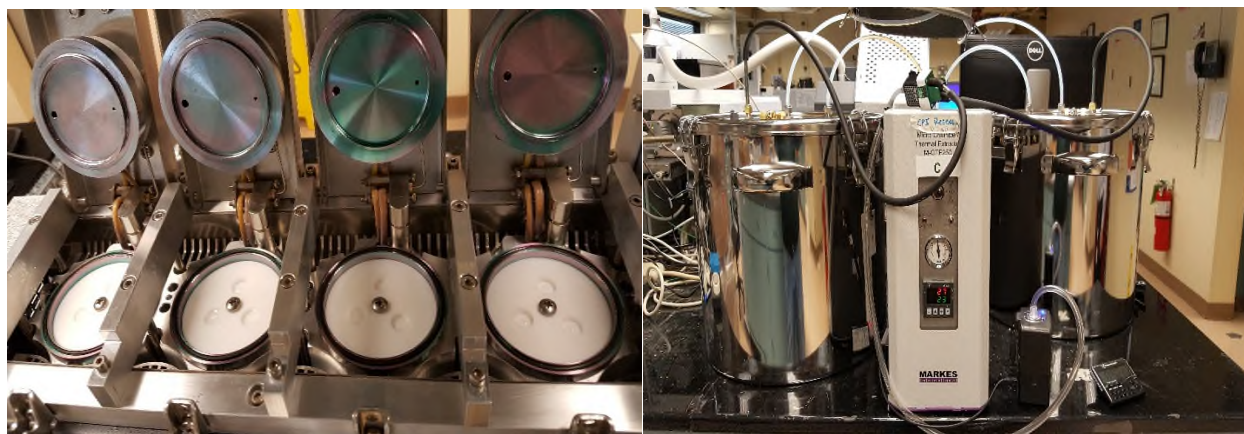


**Figure 32: Micro-chambers (Source) and small chambers (connected with micro-chambers)**

**5.2.4.3 Sampling schedule and procedure** The sorption testing was conducted between 12/15/17 and 01/19/18 for 35 days, including 6 sampling days on day 3, 7, 14, 21, 28 and 35. On each sampling day, before dust samples were taken out, a 60 mins TD tube sample (0.1 liter/minute) was collected from each test chamber to measure airborne TCP concentration. When TD tube sampling was finished, the lid of each test chamber was opened, two dust samples were collected and the lid was closed within 3 minutes. The collected dust samples were weighed, placed into a glass jar (0.1 Liter) and refrigerated immediately for future extraction.

**5.2.4.4 Extraction and analytical methods** To evaluate the concentration of TCP in the chambers, TD tubes were analyzed using a Markes International TD-100 thermal desorber connected to Agilent Technologies 7890A gas chromatography (GC) and 5975C Inert XL mass selective detector (MSD) as described in Sebroski et al (Sebroski, Miller et al. 2017) and ASTM D8142-17 (ASTM International 2017b). The dust samples were extracted with 50 ml of 50/50 methylene chloride/ethyl acetate and then sonicated for 30 minutes with a Branson PC620 Sonicator. The extracts were filtered and then 100 ng/ml of tributylphosphate-d27 was added as an internal standard prior to analysis with an Agilent 6890/5973 GC/MS using GC/MS conditions reported by Liu et al (Liu, Allen et al. 2016a).

**5.2.4.5 Quality assurance and control** Daily calibration checks were analyzed for the TD/GC/MS and GC/MS methods to verify that the instruments were within 20% of the reference standards. The extraction method was evaluated alongside the dust samples to demonstrate that the extraction efficiency was greater than 90%. Method blanks were also performed with each sample batch to verify that there was no significant background contamination.

**5.2.4.6 SVOC modeling parameterization and TCPP mass balance in the test chamber A**

mass transfer model (i-SVOC) designed to study the emission, transport and sorption of SVOCs in the indoor environment was used to estimate TCPP sorption onto settled dusts and the chamber gas phase TCPP concentration. The chamber study results of this research and a similar research conducted by USEPA were compared with the i-SVOC modeling results. Least square curve fitting was performed to estimate one of the key modeling parameters for TCPP sorption onto settled dusts: diffusion coefficient ( $D_d$ ). The key i-SVOC modeling parameters are listed in **Table 17**.

**Table 17: i-SVOC modeling parameters**

<b>Input Parameters</b>	<b>This Research</b>		<b>Liu's Study (Liu, Allen et al. 2016b)</b>
Chamber volume (L)	36.0		53.0
ACH (1/hr)	0.333		1.10
Equivalent TCPP flow concentration into the test chamber ( $C_{in}$ ) ( $\mu\text{g}/\text{m}^3$ )	74.7 <sup>(1)</sup>	83.1 <sup>(1)</sup>	2.50
Settled dusts geometric mean diameter ( $\mu\text{m}$ )	47.4 (25~90)	116 (90~150)	67.9
Gas phase mass transfer coefficient ( $h_g$ ) (m/h) <sup>(7)</sup>	568	232	397
Particle density ( $\rho_{dust}$ ) ( $\text{g}/\text{cm}^3$ )	0.938 <sup>(8)</sup>		0.938
Mass of dusts in chamber ( $\mu\text{g}$ ) <sup>(9)</sup>	1.26	1.26	0.530
Number of particles (#) <sup>(10)</sup>	$2.40 \times 10^7$	$1.64 \times 10^6$	$6.84 \times 10^6$
Octanol/air partition coefficient ( $k_{oa}$ ) (-)	$1.60 \times 10^{8(2)}$ , $9.75 \times 10^{8(3)}$ , $3.09 \times 10^{9(4)}$ , $4.80 \times 10^{9(5)}$		
Dust/air partition coefficient ( $k_{da}$ ) (-) <sup>(6)</sup>	$3.41 \times 10^7$ , $2.08 \times 10^8$ , $6.59 \times 10^8$ , $8.70 \times 10^8$		
Diffusion coefficient in settled dusts ( $D_d$ ) ( $\text{m}^2/\text{h}$ )	To be determined by curve fitting		
<b>Outputs</b>			
TCPP flow concentration out of the test chamber ( $C_{out}$ ) ( $\mu\text{g}/\text{m}^3$ )	To be calculated		
TCPP on settled dusts ( $\mu\text{g}/\text{g}$ )	To be calculated		

(1) Calculated based on mass balance equation; (2) (U.S. Environmental Protection Agency 2012b); (3) (Liagkouridis, Cousins et al. 2015); (4) (European Commissions 2008); (5) (Wang, Zhao et al. 2017); (6) Calculated as  $k_{da} = \frac{f_{om\_dust}}{\rho_{dust}} \times k_{oa}$ ,  $f_{om\_dust}$  is the volume fraction of organic matter associated with settled dust, which is assumed to be 0.2 (Weschler and Nazaroff 2008, Weschler and Nazaroff 2010); (7) Calculated based on equations in (Tian, Sebroski et al. 2017) ; (8) Assumed to the same as the value measured by Liu et al (Liu, Allen et al. 2016b); (9) Time weighted average dust mass based on the amount of hours each sample (one filter tray in this study and one tray in Liu et al. (Liu, Allen et al. 2016b)) stayed in the testing chamber. A weighted average dust mass is need because samples were taken out in sequence during the testing period; (10) Calculated in i-SVOC based on particle density, size and mass.

The mass balance of TCP in the test chamber during the testing period can be expressed as Equation 11.

$$M_{in} + E_{chamber\ wall} (or - S_{chamber\ wall}) = M_{air} + M_{settled\ dust} + M_{out} + M_{paper\ filter} \quad \text{Equation 11}$$

$M_{in}$  ( $\mu\text{g}$ ) is the amount of TCP intake from the source chamber to the test chamber.  $E_{chamber\ wall}$  and  $S_{chamber\ wall}$  are the amount of TCP emitted and absorbed from the test chamber wall;  $M_{in} + E_{chamber\ wall} (or - S_{chamber\ wall}) - M_{paper\ filter}$  can be expressed as  $C_{in} \times ACH \times 0.036\ \text{m}^3$ , where  $C_{in}$  is the equivalent TCP flow concentration into the test chamber;  $M_{air}$  is the TCP in the chamber air;  $M_{settled\ dust}$  and  $M_{paper\ filter}$  are the amount of TCP accumulated onto the settled dusts;  $M_{out}$  is the amount of TCP released from the test chamber in outflow gas.  $M_{out} = C_{out} \times ACH \times 0.036\ \text{m}^3$ .  $M_{in}$ ,  $M_{settled\ dust}$ ,  $M_{paper\ filter}$  and  $M_{out}$  were measured directly in this study, assuming TCP loss in connecting tubes is minimal,  $C_{in}$  and  $E_{chamber\ wall}$  or  $S_{chamber\ wall}$  can be calculated.

A significant range of values were reported in literature for  $k_{oa}$ , USEPA's EPISuite software has the lowest estimate of  $1.60 \times 10^8$  while an experimental study using gas chromatograph with a flame ionization detector measured the highest value of  $4.80 \times 10^9$ . In the existing literature,  $k_{da}$  and  $D_d$  have been demonstrated to be two of the important parameters that determine TCP sorption onto settled dusts (Weschler and Nazaroff 2008, Guo 2014, Tian, Sebroski et al. 2017).  $k_{da}$  is a function of  $k_{oa}$ ,  $f_{om\_dust}$  and  $\rho_{dust}$ . Diffusion coefficient ( $D_d$ ) is determined by particle morphologies and only limited literature data exists for VOCs such as benzene, toluene, ethylbenzene, and o-xylene (BTEX) (Theis, Waldack et al. 2001, Liu, Shi et al. 2013, Tian, Sebroski et al. 2017).  $D_d$  of these VOCs are significantly higher than SVOCs (Odum, Yu et al. 1994). In this research,  $D_d$  was estimated by least square curve fitting the i-SVOC modeling results with the measured data in chamber studies.

After parameterization was completed, i-SVOC was run to simulate the chamber testing for a period of 1,000 hours. In addition, airborne TCPP concentration in the test chamber was also calculated in i-SVOC and compared with measured data.

## 5.2.5 IECCU Modeling software and parameterization

IECCU requires the user to collect parameters related to the studied building, sources and sink materials, settled dusts and airborne particles. For this work, these parameters were either collected in the field or calculated using empirical equations reported in the literature. The key modeling parameters are listed in **Table 18** to **Table 22** and discussed in detail in this section. Additional modeling parameters are provided in Appendix B. For those parameters which are not a single value but a range, the highest and lowest values were selected to derive eight different modeling scenarios listed in **Table 23**.

**5.2.5.1 Building and environment** The building dimensions and air flow rates are reported in **Table 18**. The air flow rates were calculated based on the ACH of both zones reported in our prior study (Tian, Ecoff et al. 2018) for the building shown in Figure 28. The air flow balance in each zone can be written as Equation 12 and Equation 13.

$$\text{Living area (zone 1)} \quad Q_{01,t} + Q_{21,t} + Q_m = Q_{12,t} + Q_{10,t} \quad \text{Equation 12}$$

$$\text{Attic (zone 2)} \quad Q_{02,t} + Q_{12,t} + Q_m = Q_{21,t} + Q_{20,t} \quad \text{Equation 13}$$

Where the added mechanical ventilation  $Q_m$  (4,537 m<sup>3</sup>/hr) only applies to the zone during SPF application. The rest of air flows rates were explained in Equation 3 and Equation 4. Within each zone, the total air flow rate was calculated by multiplying the measured ACH and the volume of each zone, then it was allocated by surface area of each zone to derive the air flow

rates between the zones. For example, when the living area was sprayed, the total air flow in zone 1 was  $1,150 \text{ m}^3/\text{hr}$  (2.5 ACH multiplied by zone volume of  $460 \text{ m}^3$ ) plus  $Q_m$ . The ratios of  $Q_{01}:Q_{21}$  and  $Q_{10}:Q_{12}$  were 3.4 based on the surface area of  $285 \text{ m}^2$  (all surface of the living area which is exposed to outdoor air) vs.  $84 \text{ m}^2$  (ceiling of the living area which is the floor of attic). At the same time, in the attic,  $Q_{12}$  and  $Q_{21}$  were calculated from Equation 12.  $Q_{02}$  was calculated based on the natural ventilation rate of  $424 \text{ m}^3/\text{hr}$  (4.16 ACH) (Tian, Ecoff et al. 2018) multiplied by zone volume of  $102 \text{ m}^3$  and the surface area percentage of the attic which is exposed to the outdoor air (56%).  $Q_{20}$  was calculated using Equation 13 since all other air flow rates were known.

**Table 18: IECCU modeling parameters of building and environment**

Parameter	Value		
Living area volume ( $\text{m}^3$ )	460		
Attic volume ( $\text{m}^3$ )	102		
Temperature ( $^{\circ}\text{C}$ )	Hourly field measurement		
Air flow rates	During SPF was sprayed in living area	During SPF was sprayed in attic	After SPF application in the entire house
$Q_{01} (\text{m}^3/\text{hr})$	5,426	889	889
$Q_{02} (\text{m}^3/\text{hr})$	238	4,775	238
$Q_{10} (\text{m}^3/\text{hr})$	4,395	2,880	964
$Q_{12} (\text{m}^3/\text{hr})$	1,293	186	186
$Q_{20} (\text{m}^3/\text{hr})$	1,269	2,783	163
$Q_{21} (\text{m}^3/\text{hr})$	261	2,178	261

**5.2.5.2 Sources** A total of seven pieces of foam (one piece is from one wall or roof cavity) was sprayed in the building and their modeling parameters are reported in **Table 19**. SPF was sprayed at roughly 6.3 cm (2.5 in). The lowest and highest TCPP partition coefficient between sources and air ( $k_{sa}$ ) and TCPP diffusion coefficient in sources ( $D_s$ ) values at  $23 \text{ }^{\circ}\text{C}$  were adopted from

our prior study (Tian, Sebroski et al. 2017). These parameters are temperature dependent; therefore, the field measured temperature was used to adjust  $k_{sa}$  and  $D_s$  values using Equation B1 and Equation B2 in Appendix B. The mass transfer coefficient in ( $h_{as}$ ) air is a function of air density, viscosity, velocity, TCPP diffusivity in air and the characteristic length of the source materials.  $h_{as}$  values were calculated based on the Sparks method available in the PARAMS 1.1 software (Sparks, Tichenor et al. 1996, Guo 2017b). More details can be found in Appendix B. The initial TCPP concentration in the foam was calculated based on 4% (as in the safety data sheets) of the closed cell foam which has a density of 32 kg/m<sup>3</sup> (2 lb/ft<sup>3</sup>).

**Table 19: IECCU modeling parameters of sources**

Parameter	Value	
# of pieces of foam modeled	Living area: four	Attic: three
Areas sprayed (m <sup>2</sup> )	10.9, 12.1, 17.6, 17.2	7.8, 70.0, 24.8
Thickness (m)	6.3 × 10 <sup>-2</sup>	
$k_{sa}$ (unitless), temperature dependent (Tian, Sebroski et al. 2017)	At 296 K, range from 1.3 × 10 <sup>7</sup> to 9.4 × 10 <sup>7</sup>	
$D_s$ (m <sup>2</sup> /hr), temperature dependent (Tian, Sebroski et al. 2017)	At 296 K, range from 6.3 × 10 <sup>-11</sup> to 1.3 × 10 <sup>-10</sup>	
$h_{as}$ (m/hr), characteristic length dependent	1.25, 1.23, 1.16, 1.16 for the four pieces sprayed	1.32, 0.92, 1.09 for the three pieces sprayed
Initial TCPP concentration in sources ( $C_{s0}$ ) (µg/m <sup>3</sup> )	1.3 × 10 <sup>9</sup>	

**5.2.5.3 Sinks** Gypsum board and wood flooring are two main sink materials in the tested house.

Indoor sink materials are very important for TCPP indoor fate and transport because when airborne concentration is high, TCPP could be absorbed and diffused into sink materials and removed from the indoor air. However, when airborne concentration decreases, TCPP in the sink

materials could be released back to the air. Five pieces of gypsum board, one piece of wood floor in the living area and one piece of wood floor in the attic were modeled as shown in **Table 20**. PARAMS 1.1 was used to estimate the range of TCPP partition coefficient between sinks and air ( $k_{na}$ ) and TCPP diffusion coefficient in sinks ( $D_n$ ). It is worth to note that the correlations to derive  $k_{na}$  and  $D_n$  of sink materials were developed based on a broader group of VOCs which may not be applicable for SVOCs. However, the calculated  $k_{na}$  and  $D_n$  of gypsum board in **Table 20** were within one order of magnitude from the measured values reported by Liu et al (Liu, Allen et al. 2016a). The gas phase mass transfer coefficient of sinks ( $h_{an}$ ) was also estimated by the Sparks method in PARAMS 1.1. The initial TCPP concentration in the sink materials was assumed to be zero.

**Table 20: IECCU modeling parameters of sinks**

Parameter	Value
Thickness (m)	Gypsum board: 0.03, Wood floor: 0.05
$k_{na}$ (unitless) (Tian, Sebroski et al. 2017)	Gypsum board: range from $1.1 \times 10^7$ to $5.6 \times 10^7$ Wood floor: range from $8.8 \times 10^7$ to $6.8 \times 10^8$
$D_n$ ( $m^2/hr$ ), $h_{an}$ (m/hr) (Tian, Sebroski et al. 2017)	Gypsum board: $4.1 \times 10^{-9}$ , Wood: $7.4 \times 10^{-9}$ In the living area: Gypsum board: 0.72, 0.79, 1.09, 1.04, 1.36 Wood floor: 0.79 In the attic: Wood floor: 0.89
Initial TCPP concentration in sinks ( $C_{n0}$ ) ( $\mu g/m^3$ )	0

**5.2.5.4 Settled dusts** Settled dust is another potential sink of TCPP in the indoor environment. The key modeling parameters are listed in **Table 21**. The TCPP partition coefficient between settled dusts and air ( $k_{da}$ ) and TCPP diffusion coefficient in settled dusts ( $D_d$ ) were derived from

the chamber testing and curve fitting discussed in section 5.2.4.  $k_{da}$  is expressed as  $\frac{f_{om\_dust}}{\rho_{dust}} \times k_{oa}$ , in which  $f_{om\_dust}$  was assumed to be 0.2 (Weschler and Nazaroff 2008, Weschler and Nazaroff 2010) and  $\rho_{dust}$  was measured at 0.94 g/cm<sup>3</sup>. For each calculated  $k_{da}$  value, a best fit  $D_d$  value was estimated using the least square curve fitting method. The results of the 90~150  $\mu$ m dusts were selected in this modeling work. Appendix B gives the particle numbers in each zone calculated by IECCU and the gas phase mass transfer coefficient of settled dusts ( $h_{ad}$ ).

**Table 21: IECCU modeling parameters of settled dusts**

Parameter	Value
Geometric mean diameter ( $\mu$ m)	116
Density (g/cm <sup>3</sup> )	$9.4 \times 10^{-1}$
$k_{oa}$ (unitless) (U.S. Environmental Protection Agency 2012b, Wang, Zhao et al. 2017)	Range from $1.6 \times 10^8$ to $4.8 \times 10^9$
$k_{da}$ (unitless)	Range from: $3.4 \times 10^7$ to $8.7 \times 10^8$
$D_d$ (m <sup>2</sup> /hr)	Range from: $9.0 \times 10^{-14}$ to $6.0 \times 10^{-16}$
Initial TCPP concentration in settled dusts ( $C_{d0}$ ) ( $\mu$ g/m <sup>3</sup> )	0

**5.2.5.5 Airborne particles** Airborne particle concentration was measured using a GrayWolf PC-3016A particle counter and aggregated into two particle sizes: PM<sub>2.5</sub> and PM<sub>10</sub>. Airborne particle density and TCPP partition coefficient between airborne particles and air ( $k_{pa}$ ) were assumed to the same as the settled dusts and had a zero initial TCPP concentration ( $C_{p0}$ ). Airborne particles can be removed from the indoor air by either ventilation or deposition. The deposition rate is affected by indoor air speed and furnishings. Thatcher et al. measured airborne particle deposition rate in an isolated room with different air flow conditions and furnishing levels (Thatcher, Lai et al. 2002). The corresponding deposition rates (**Table 22**) reported under bare

room surfaces and fully furnished room were adopted for the attic and living area in the studied building.

**Table 22: IECCU modeling parameters of airborne particles**

Parameter	Value	
Particle size ( $\mu\text{m}$ )	2.5	10
Density ( $\text{g}/\text{cm}^3$ )	$9.4 \times 10^{-1}$	
Indoor concentration ( $\mu\text{g}/\text{m}^3$ )	9.1	15.4
Deposition rate (1/hr) (Thatcher, Lai et al. 2002)	Living area: $9.3 \times 10^{-1}$ Attic: $7.8 \times 10^{-1}$	Living area: 5.3 Attic: 4.1
$C_{p0}$ ( $\mu\text{g}/\text{m}^3$ )	0	
$k_{pa}$ (unitless)	Range from: $3.4 \times 10^7$ to $8.7 \times 10^8$	

**5.2.5.6 Modeling scenarios** Key modeling parameters associated with TCPP sources and sinks were estimated as a range, instead of a single value. For example,  $k_{sa}$  was estimated based on a correlation between  $k_{sa}$  and chemical vapor pressure specific to polyurethane foam (Holmgren, Persson et al. 2012). Since TCPP vapor pressure in the literature was a range,  $k_{sa}$  estimated was also a range. A total of eight scenarios were modeled and compared as shown in **Table 23**. The three letters in the scenario names are based on the selection of partition coefficient value for sources, sinks and airborne particles/settled dusts, respectively. For example, the HHH scenario selects the highest  $k_{sa}$ ,  $k_{na}$ ,  $k_{da}/k_{pa}$  values while the LLL scenario selects the lowest partition coefficients values.

**Table 23: IECCU modeling scenarios**

Scenario	Sources		Sinks		Particles/Settled Dusts	
	$k_{sa}$ (-)	$D_s$ (m <sup>2</sup> /hr)	$k_{na}$ (-)	$D_s$ (m <sup>2</sup> /hr)	$k_{pa}, k_{da}$ (-)	$D_{da}^*$ (m <sup>2</sup> /hr)
HHH			Wood floor: $6.8 \times 10^8$ Gypsum board: $5.6 \times 10^7$		$8.7 \times 10^8$	$6.0 \times 10^{-16}$
HHL	$9.4 \times 10^7$	$1.3 \times 10^{-10}$			$3.4 \times 10^7$	$9.0 \times 10^{-14}$
HLH			Wood floor: $8.8 \times 10^7$ Gypsum board: $1.1 \times 10^7$	Wood floor: $7.4 \times 10^{-9}$ Gypsum board: $4.1 \times 10^{-9}$	$8.7 \times 10^8$	$6.0 \times 10^{-16}$
HLL					$3.4 \times 10^7$	$9.0 \times 10^{-14}$
LHH			Wood floor: $6.8 \times 10^8$ Gypsum board: $5.6 \times 10^7$		$8.7 \times 10^8$	$6.0 \times 10^{-16}$
LHL	$1.3 \times 10^7$	$6.3 \times 10^{-11}$			$3.4 \times 10^7$	$9.0 \times 10^{-14}$
LLH			Wood floor: $8.8 \times 10^7$ ; Gypsum board: $1.1 \times 10^7$		$8.7 \times 10^8$	$6.0 \times 10^{-16}$
LLL					$3.4 \times 10^7$	$9.0 \times 10^{-14}$

\*  $D_{da}$  was estimated by least square curve fitting based on  $k_{pa}/k_{da}$  selected.

### 5.3 RESULTS AND DISCUSSION

This section presents results of both chamber testing and IECCU modeling. In section 5.3.1, a mass balance evaluation was conducted to confirm that the chamber wall did not behave as a major source or a sink during the testing period. Figure 33 to Figure 35 gave the least square curve fitting results to derive the best TCPP diffusion coefficient in settled dusts, based on the two chamber tests in this study and one conducted by USEPA. Table 25 gives the best fit  $D_d$  values for each  $k_{da}$  value and diameter size. Figure 36 plots two measured TCPP sorption rates ( $R_D$ ) (25-90  $\mu\text{m}$  and 90-150  $\mu\text{m}$ ) on the settled dusts normalized by airborne TCPP concentration

in the chamber. Figure 37 and Figure 38 present the modeled  $R_D$  for the two chamber tests in this study and one conducted by USEPA.

The whole house modeling using IECCU is discussed in section 5.3.2 to 5.3.4. First, Figure 39 and Figure 40 describe the dynamic mass balance in the studied building. Based on Equation 3 and Equation 4, each TCPP mass flow (e.g. source emission rate, sink sorption rate) was plotted for those hours when field samples were taken in the living area and attic. Second, Figure 41 and Figure 43 illustrate the modeled total accumulated mass of TCPP in each environmental media. Figure 42 and Figure 44 present the percentage distribution of TCPP in those environment media which building residents may be exposed to TCPP by inhalation or ingestion exposure pathway. Third, IECCU modeling and field measurement results were compared for TCPP airborne concentration (Figure 45) and TCPP accumulation on indoor sink materials and settled dusts (Figure 47). Only the two extreme scenarios (HHH and LLL) which generate the lowest and highest airborne TCPP concentrations are presented in this section and the rest six scenarios are presented in Appendix B. Based on the modeling results, averaged TCPP exposure by age groups are presented in section 5.3.5 (in Figure 47) for both inhalation and ingestion pathways.

### 5.3.1 Chamber testing

**5.3.1.1 Chamber wall effects** A mass balance calculation was conducted (Equation 11) to examine whether the test chamber walls were successfully coated with TCPP during the 47 days period prior placing any dust samples. In **Table 24**,  $M_{in}$ ,  $M_{air}$  and  $M_{out}$  were calculated using time

weighted average airborne TCPP concentration measured by TD tubes on the sampling days. Considering the variations of airborne TCPP concentration in both source and test chambers during sampling days, the small positive values under the chamber wall column indicate chamber wall is neither a major source nor sink in the test chambers.

**Table 24: TCPP mass balance in the 36 Liter test chamber**

Dust Diameter ( $\mu\text{m}$ )	$M_{\text{in}}$ ( $\mu\text{g}$ )	$M_{\text{settled dust +}} +$ $M_{\text{paper filter}}$ ( $\mu\text{g}$ )	$M_{\text{air +}} + M_{\text{out}}$ ( $\mu\text{g}$ )	$E_{\text{chamber wall (+)}} +$ $\text{or } S_{\text{chamber wall (-)}}$ ( $\mu\text{g}$ )
25~90	1,031	826	233	28
90~150	1,255	1,166	166	77

**5.3.1.2 TCPP diffusion coefficient in settled dusts ( $D_d$ )** To estimate  $D_d$ , least squares curve fitting was performed for the sorption quantity ( $\mu\text{g TCCP /g dust}$ ) vs. time (hours) curves. Figure 33, Figure 34 and Figure 35 are sorption curves for the 25-90  $\mu\text{m}$ , 90-150  $\mu\text{m}$  diameter ranges tested in this study and the house dusts tested in Liu et al.'s study (Liu, Allen et al. 2016b), respectively. **Table 25** gives the best fit  $D_d$  values for each  $k_{\text{da}}$  value and diameter size. The details of this curve fitting are listed in the Appendix B. The highest  $D_d$  estimated was  $9.00 \times 10^{-14} \text{ m}^2/\text{h}$  for the 90-150  $\mu\text{m}$  dust with a  $k_{\text{da}}$  of  $3.41 \times 10^7$ , while the lowest  $D_d$  estimated was  $7.00 \times 10^{-18} \text{ m}^2/\text{h}$  for the 25-90  $\mu\text{m}$  dust with a  $k_{\text{da}}$  of  $8.70 \times 10^7$ . The difference was more than four orders of magnitude.

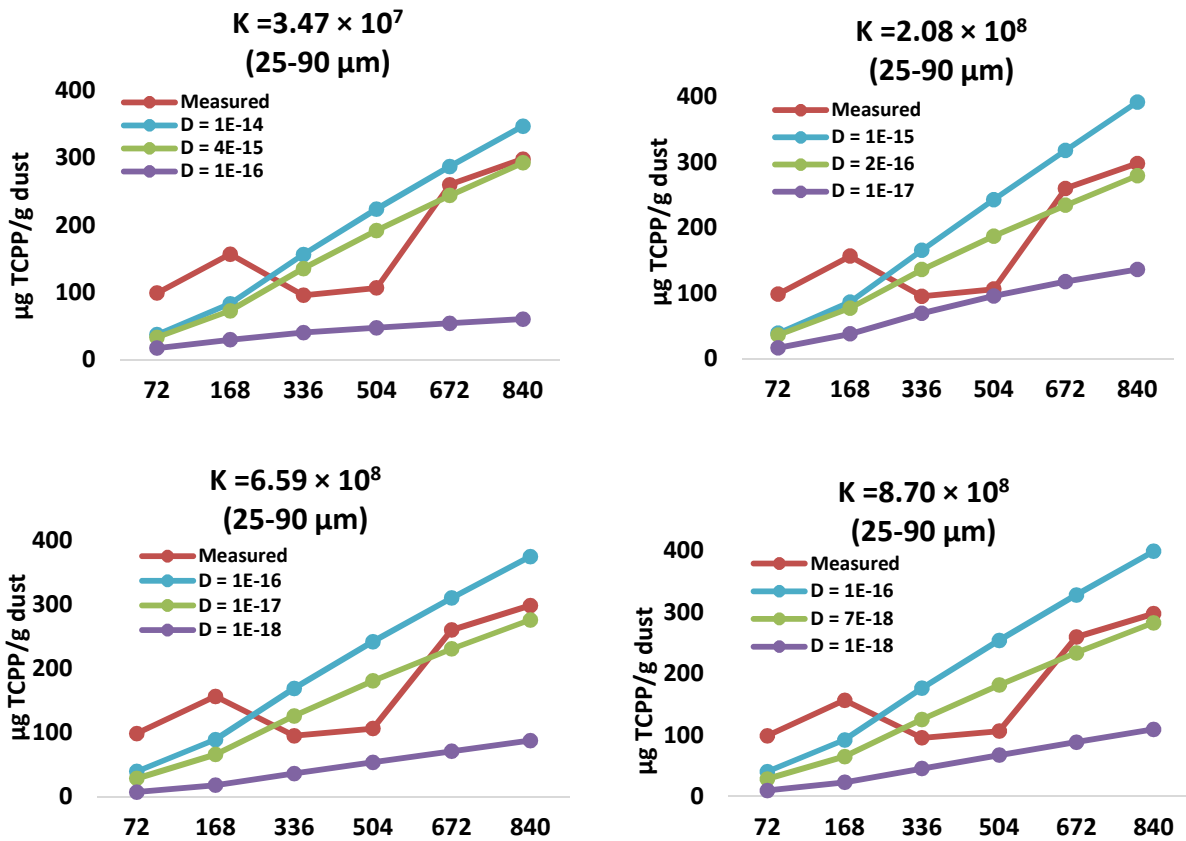


Figure 33: Comparison between i-SVOC modeling and measured results for 25-90  $\mu\text{m}$  dust

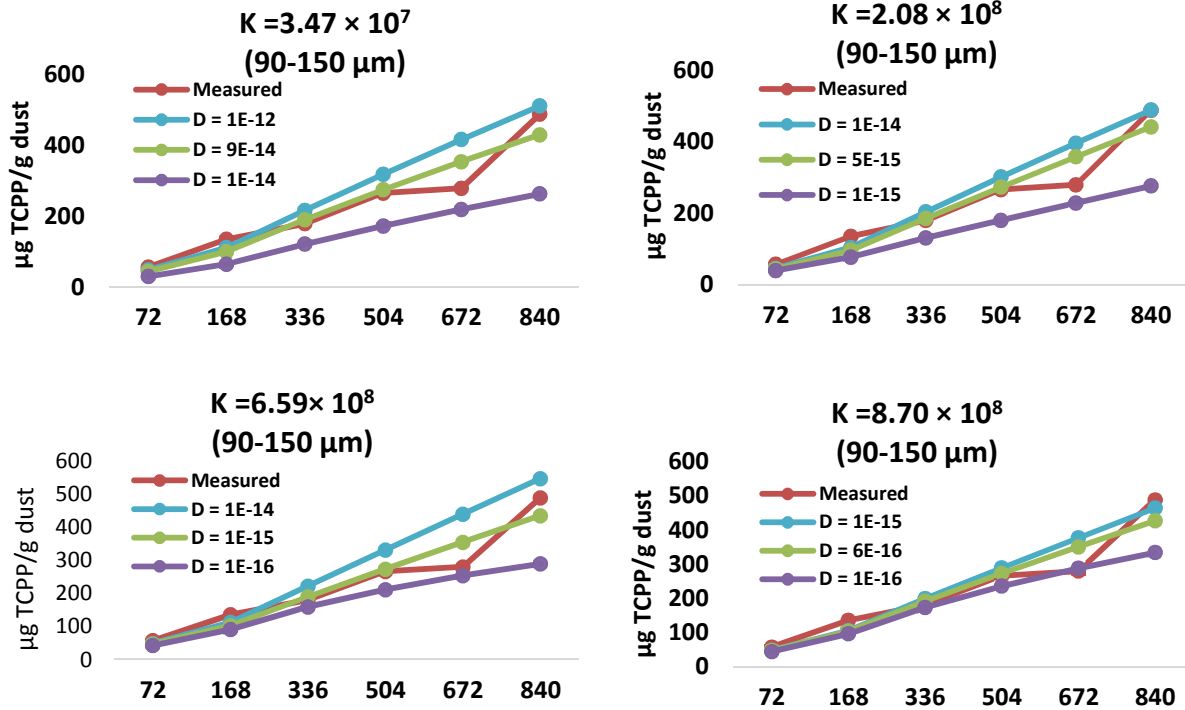


Figure 34: Comparison between i-SVOC modeling and measured results for 90-150 μm dust

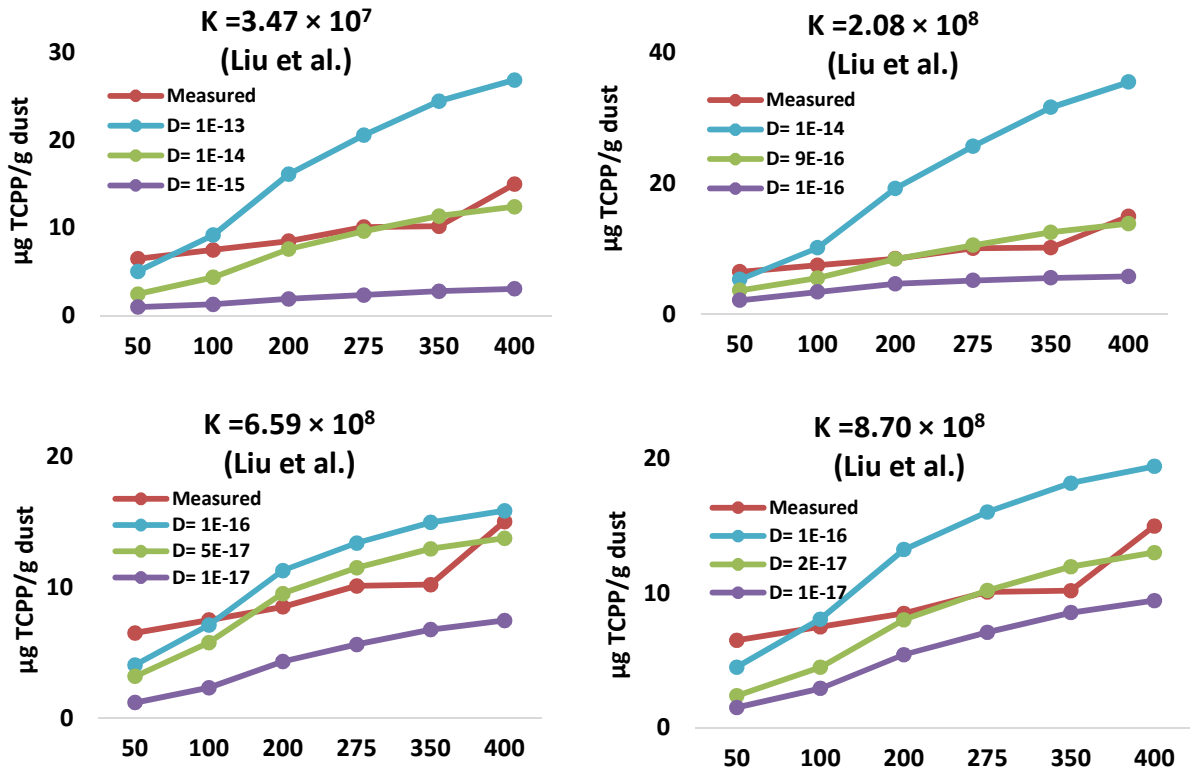


Figure 35: Comparison between i-SVOC modeling and measured results in Liu et al (Liu, Allen et al. 2016b)

Table 25: Best fit TCPP diffusion coefficient (D<sub>a</sub>) within settled dusts

k <sub>da</sub> (unitless)	D <sub>a</sub> (m <sup>2</sup> /h) This study		D <sub>a</sub> (m <sup>2</sup> /h) Liu et al.
	25-90 μm (GM = 47.43 μm)	90-150 μm (GM = 116.19 μm)	(Liu, Allen et al. 2016b) (Mean diameter = 67.88 μm)
3.41 × 10 <sup>7</sup>	4.00 × 10 <sup>-15</sup>	9.00 × 10 <sup>-14</sup>	1.00 × 10 <sup>-14</sup>
2.08 × 10 <sup>8</sup>	2.50 × 10 <sup>-16</sup>	5.00 × 10 <sup>-15</sup>	9.00 × 10 <sup>-16</sup>
6.59 × 10 <sup>8</sup>	1.00 × 10 <sup>-17</sup>	1.00 × 10 <sup>-15</sup>	5.00 × 10 <sup>-17</sup>
8.70 × 10 <sup>8</sup>	7.00 × 10 <sup>-18</sup>	6.00 × 10 <sup>-16</sup>	2.00 × 10 <sup>-17</sup>

GM = geometric mean

Within one dust diameter, when  $k_{da}$  increases, the best fit  $D_d$  decreases. This trend can be explained by Equation 8 to Equation 10. When the sorption process started, since  $C_{dv}$  is relatively small, the determining factor for  $R_d$  is  $H_a$ . Combine Equation 9 and Equation 10,  $H_a$  is determined by two terms:  $\frac{2k_{da} \times D_d}{\Delta r}$  and  $h_a$ . In the MSS method,  $\Delta r$  is defaulted to  $10^{-7}$  m. For TCPP,  $k_{da}$  is in the range of  $10^7$  to  $10^8$  and  $D_d$  is in the range of  $10^{-14}$  to  $10^{-18}$  m<sup>2</sup>/h. Therefore, the smaller one of the two terms has a higher impact to the overall mass transfer coefficient  $H_a$ . For most cases,  $\frac{2k_{da} \times D_d}{\Delta r}$  was two to three orders of magnitude lower than  $h_a$  (except the 90-150  $\mu$ m dusts). The highest  $\frac{2k_{da} \times D_d}{\Delta r}$  value obtained was 61.4 m/h (90-150  $\mu$ m) which is still less than  $h_a$  at 232 m/h. As a result, the product of  $k_{da}$  and  $D_d$  determines the TCPP mass transfer rate at the beginning of the testing period. This range of  $k_{da}$  and  $D_d$  values indicates the importance of estimating  $k_{da}$  and  $D_d$  together because TCPP surface accumulation process is determined by both of them. When curve fitting was performed, a higher  $k_{da}$  leads to a lower  $D_d$ . Practically speaking, with a higher  $k_{da}$ , TCPP has a higher tendency to be partitioned onto settled dusts and “requires” less  $D_d$  to reach the same amount of TCPP sorption onto settled dusts.

Among the three dust diameters, with the same  $k_{da}$ , settled dusts with the largest diameter had the highest  $D_d$  estimates. This trend is because the larger dusts had a larger  $R_D$  during the testing period and accumulated more TCPP (e.g., Figure 34 vs. Figure 33). A larger  $R_D$  was resulted from a higher  $H_a$  which was due to a higher  $\frac{2k_{da} \times D_d}{\Delta r}$  value. Since  $k_{da}$  and  $\Delta r$  were constants, the estimated  $D_d$  was higher. In addition, mass transfer rate within the settled dusts depends only on  $D_d$  regardless  $k_{da}$  and  $h_a$ . A higher  $D_d$  means TCPP transfers faster from dust surface to inner core and therefore the outer surface layer can absorb more TCPP from the chamber air.

**5.3.1.3 TCPP sorption rate** Chamber air normalized TCPP sorption rates ( $R_D$ ) are presented in Figure 36 for all three measurements (two in this study and one in Liu et al (Liu, Allen et al. 2016b)). At 168 and 336 hours, the sorption rate of the 25 - 90  $\mu\text{m}$  dusts was negative so it was defaulted to zero. Figure 37 give the i-SVOC modeled dusts  $R_D$  for two dust diameters (25-90  $\mu\text{m}$  and 90-150  $\mu\text{m}$ ). The modeled  $R_D$  using chamber parameters in Liu et al. (2016) is presented in Figure 38.

$R_D$  measures how much TCPP is accumulated onto the settled dusts during time period  $t$ , at a given test chamber airborne TCPP concentration. It is calculated as

$$R_D = \frac{\Delta \dot{m}_t}{\bar{c}_{air}} = A_d H_a \left(1 - \frac{C_{dv}}{\bar{c}_{air} \times k_{da}}\right) \quad \text{Equation 14}$$

Where  $R_D$  is the normalized sorption rate ( $\mu\text{g TCPP/g dust/h}$ )/( $\mu\text{g TCPP/m}^3$  chamber air),  $\Delta \dot{m}_t$  is the incremental mass flow rate of TCPP on a unit mass of settled dusts during time period  $t$  ( $\mu\text{g TCPP/g dust/h}$ ),  $\bar{c}_{air}$  is the time weighted average airborne TCPP concentration in the chamber air during time period  $t$  ( $\mu\text{g TCPP/m}^3$  chamber air),  $A_d$  is the surface area of the settled dusts ( $\text{m}^2$ ),  $H_a$  is the overall TCPP mass transfer coefficient in the air ( $\text{m/h}$ ),  $C_{dv}$  is the TCPP concentration in the top layer of the settled dusts ( $\mu\text{g TCPP/m}^3$  settled dusts) and  $k_{da}$  is the partition coefficient between the settled dusts and air (unitless).

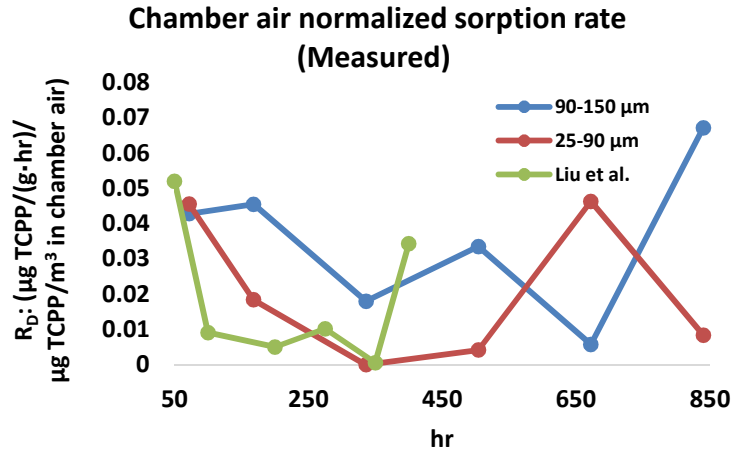


Figure 36: Measured chamber air normalized TCPP sorption rates on settled dusts

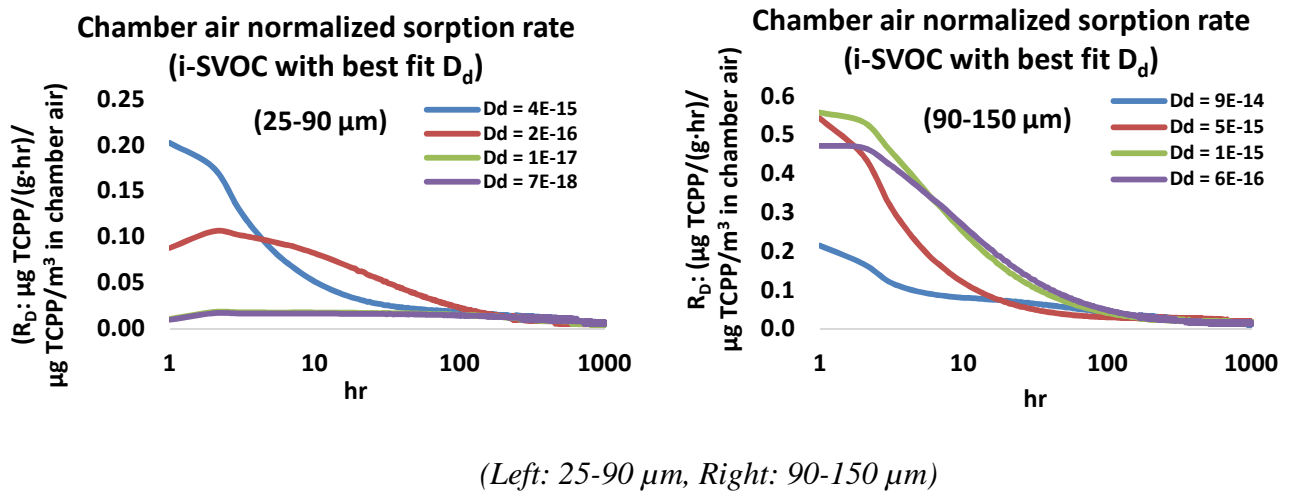
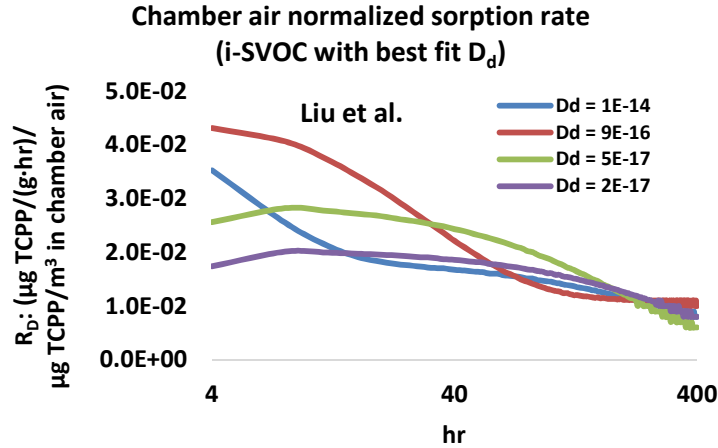


Figure 37: Modeled chamber air normalized TCPP sorption rates on settled dusts



**Figure 38: Modeled chamber air normalized TCPP sorption rates on settled dusts tested by Liu et al. (Liu, Allen et al. 2016b)**

It can be found that  $R_D$  values predicted by model (Figure 37) are at the same order of magnitude as the measured values (Figure 36). The first measured  $R_D$  value was at hour 50. Within the modeling scenarios using different  $k_{da}$  and  $D_d$  pairs derived from the least square curve fitting, the predicted  $R_D$  values are very similar after the first day (24 hours) which again demonstrate the combination of  $k_{da}$  and  $D_d$  determines TCPP sorption onto the settled dusts. The local two-phase theory (Lewis and Whitman 1924, Guo 2014) can explain the results found in Figure 36 to Figure 38. As shown in Equation 14, for all three measurements, at the beginning of the testing period, TCPP concentration in the outer hollow sphere ( $C_{dv}$ ) of the settled dusts increased. Since  $C_a$  is relatively constant and  $k_{da}$  is a constant,  $1 - \frac{C_{dv}}{C_a \times k_{da}}$  decreases and therefore  $R_D$  starts to decrease. As shown in Figure 36, the general trend of  $R_D$  for all three measurements was decreasing during the testing period except the last one or two samples. This trend matches the decreasing  $R_D$  as shown in Figure 37 and Figure 38. The increasing  $C_{dv}$  and decreasing  $R_D$

also revealed that SVOCs diffusion within dusts is important for their sorption onto settled dusts. SVOCs sorption rate at the material/air interface is known to be controlled by external air conditions. In another word, for SVOC sorption on sink materials (Equation 5), the first term  $\frac{1}{k_{na} \times h_{an}}$  is usually small enough for SVOC that  $H_a$  is dominated by  $\frac{1}{h_a}$  and therefore,  $R_d$  is independent of  $D_d$ . In the contrast, SVOC mass transfer within the dusts is different than sink materials and it is controlled by  $D_d$  which impacts how fast SVOCs can be transported from the outer hollow sphere to the inner hollow sphere and dust core. An increasing  $C_{dv}$  and decreasing  $R_D$  indicates that inner dust diffusion is not fast enough that there is an accumulation of SVOCs in the top hollow sphere. Unlike the emission process which the overall mass transfer rate is limited by how fast SVOC can “escape” the top layer, the absorption process overall mass transfer rate is controlled by how fast SVOC can diffuse through the dust.

In terms of different dust diameters, all three measurements initially had a similar  $R_D$  but the largest dusts (90-150  $\mu\text{m}$ ) had a slower decay of  $R_D$  than the smaller ones. Especially for those settled dusts in the 25-90  $\mu\text{m}$  diameter range, the amount of TCPD accumulated on the dusts decreased between 168 and 504 hours which resulted a negative  $R_D$ . This result is counter intuitive and opposite to previous studies that fine particles should have a higher SVOC concentration than coarse particles (Lewis, Fortune et al. 1999, Vorhees, Cullen et al. 1999). When particles with low or no permeability to SVOCs exist, smaller particles have greater surface to volume ratio should have more surface adsorption of SVOCs. One of the reasons which may result such difference is the assumption that airborne TCPD was evenly distributed in the test chamber, which may not valid. For the 25-90  $\mu\text{m}$  dusts, the negative  $R_a$  was observed on those samples directly below the chamber inlet and outlet while other samples were away from the airflows. The TCPD airborne concentration may have less variation for those samples that

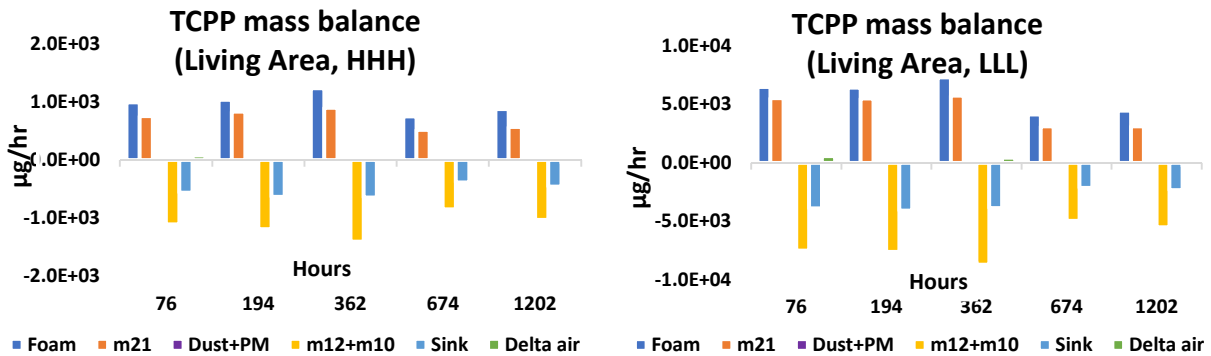
were not directly impacted by the chamber inlet and outlet. Another possible reason is that surface absorption is more dominant than adsorption for the dusts we tested. Since smaller dusts have a higher surface area and smaller volume of the top hollow sphere,  $C_{dv}$  increases more rapidly for smaller dusts than larger dusts, which results  $R_D$  decreases more quickly.

**5.3.1.4 Direct contact with chamber wall** Previous research has indicated when indoor dusts are settled on SVOC sources, SVOC can migrate rapidly from the source material to the dusts through direct contact (Takigami, Suzuki et al. 2008, Guo, Liu et al. 2012b). To prevent direct migration from the chamber surfaces to settled dusts, clean paper filter was used to hold the sample dust and a steel wire holder was placed in the test chamber so all dusts samples were about one inch from the chamber bottom. Although paper filter also accumulated TCPP during the testing period, the direct migration should be even more if the settled dusts were placed directly onto the chamber surfaces, which are coated with TCPP. The amount of TCPP accumulated on each filter was calculated based on the blank paper filter proportional to the amount of time each dust sample stayed in the test chamber.

### **5.3.2 TCPP mass balance in the tested house**

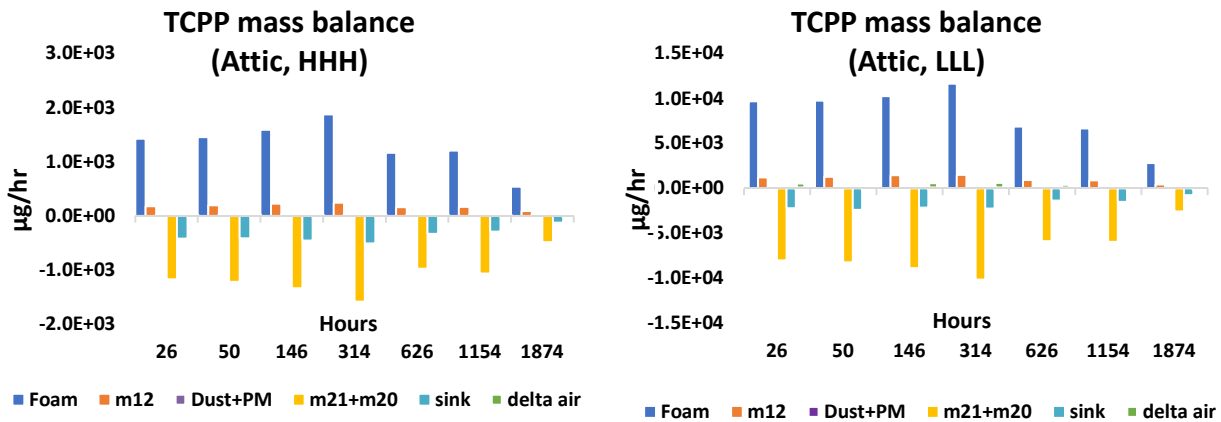
TCPP mass flow rates ( $\mu\text{g/hr}$ ) of the sources, sinks, settled dusts together with airborne particles, and interzone air flows are presented in Figure 39 and Figure 40 to illustrate TCPP mass balance for the two extreme modeling scenarios. TCPP emission rate was modeled using the i-SVOC model with the same parameters used in IECCU since IECCU does not report emission rate. Except the sink mass flow rate which was calculated using Equation 3 and Equation 4, the rest of

TCPP mass flow rates (settled dusts, airborne particles and interzone air flows) were derived using the results calculated in IECCU.



HHH and LLL are modeling scenarios based on partition and diffusion coefficient selections listed in Table 23. H and L denote the higher and lower values are selected for that parameter.

**Figure 39: TCPP mass balance in the living area during the sampling period**



HHH and LLL are modeling scenarios based on partition and diffusion coefficient selections listed in Table 23. H and L denote the higher and lower values are selected for that parameter.

**Figure 40: TCPP mass balance in the attic during the sampling period**

In a real-world residential building, TCPP airborne concentration fluctuated over time. In Figure 39 and Figure 40,  $\Delta$  air represents the mass change of airborne TCPP;  $m_{21}$ ,  $m_{12}$ ,  $m_{10}$  and  $m_{20}$  are the TCPP mass flow rates among the attic, living area and outdoor environment. TCPP removal from the air was primarily through ventilation and the inter-zone air flows, while absorption on sink materials also contributed to the removal. TCPP accumulation to settled dusts and airborne particles were relatively negligible.

TCPP emission rate ( $\mu\text{g/hr}$ ) of foam was higher in the attic than the living area since there was more foam applied ( $\sim 103 \text{ m}^2$  in attic vs.  $58 \text{ m}^2$  in living area) and temperature was higher in the attic. For example, at 674 hours after application, the attic was about 4 degrees Celsius higher than the living area. Temperature has a significant impact on  $k_{sa}$  which ultimately determines the TCPP emission rate from the foam. As shown in Equation B1, when temperature is higher,  $k_{sa}$  decreases and emission rate increases.

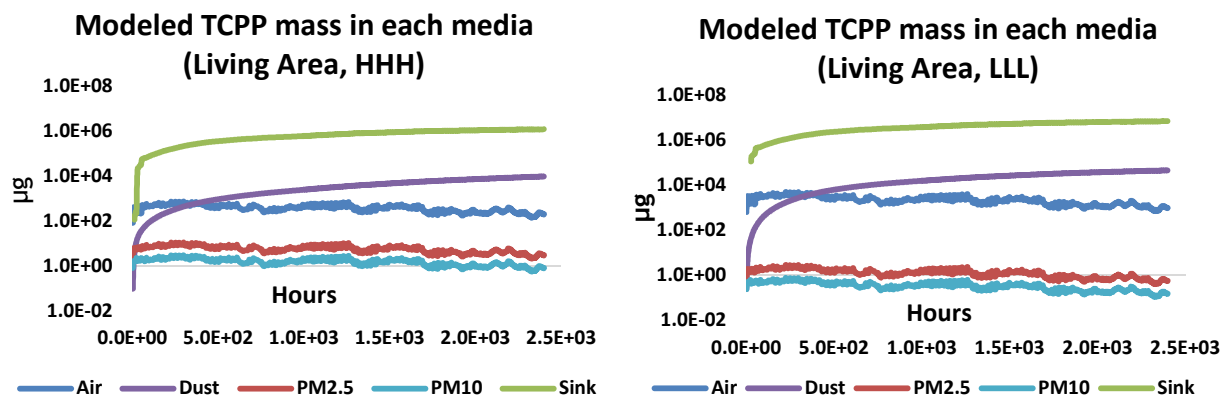
Air change is another factor to determine TCPP mass flow rate. The attic had a higher ACH than the living area; therefore, although there were more TCPP emitted in the attic, TCPP removal by ventilation was also higher in the attic, which led to a lower sink sorption rate.

### **5.3.3 Modeled TCPP mass distribution in the tested house**

TCPP is distributed in four media in the indoor environment: air, settled dusts, airborne particles and sink materials. Human exposure to TCPP can occur through multiple exposure pathways. The vapor phase TCPP in the air and TCPP accumulated on airborne particles can be inhaled, while settled dusts can be ingested, especially for young children who often crawl on the floor. Dermal exposure could also occur by direct dermal contact with settled dusts or sink materials on

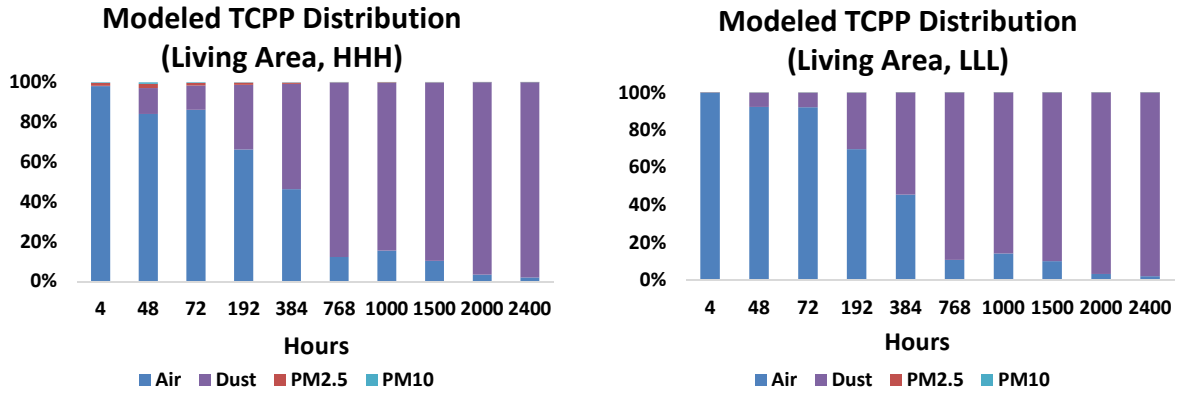
which TCPP is absorbed. This work evaluated the total amount of TCPP available in this modeled residential house and focused on the inhalation and ingestion exposure pathways only.

Figure 41 and Figure 43 illustrate TCPP accumulation in each environmental media over the modeled period. Regardless of modeling scenarios and indoor zones, TCPP accumulated on sink materials accounts for more than 99% of the total TCPP in the indoor environment except for the first few hours. Indoor air has the second highest TCPP accumulation until about two weeks (living area) and one week (attic) after SPF application, then it is surpassed by the settled dusts. Airborne particles have negligible contribution since they are more rapidly ventilated out of the indoor environment and the new particles from the outdoor environment are assumed to have zero background TCPP. Compared to the attic, the living area has about twice of the total TCPP in all environmental media than the attic due to a lower ACH rate in the living area, even though the attic has more foam. Among the modeling scenarios, scenarios using lower  $k_{sa}$  and  $D_s$  have higher modeled total TCPP in the indoor environment.



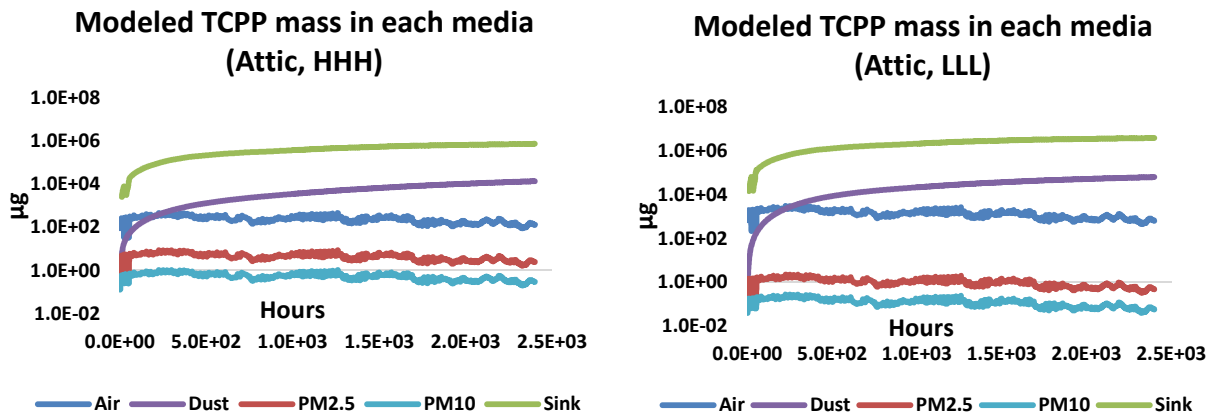
*HHH and LLL are modeling scenarios based on partition and diffusion coefficient selections listed in Table 23. H and L denote the higher and lower values are selected for that parameter.*

**Figure 41: TCPP mass accumulated in each environmental media in the living area**



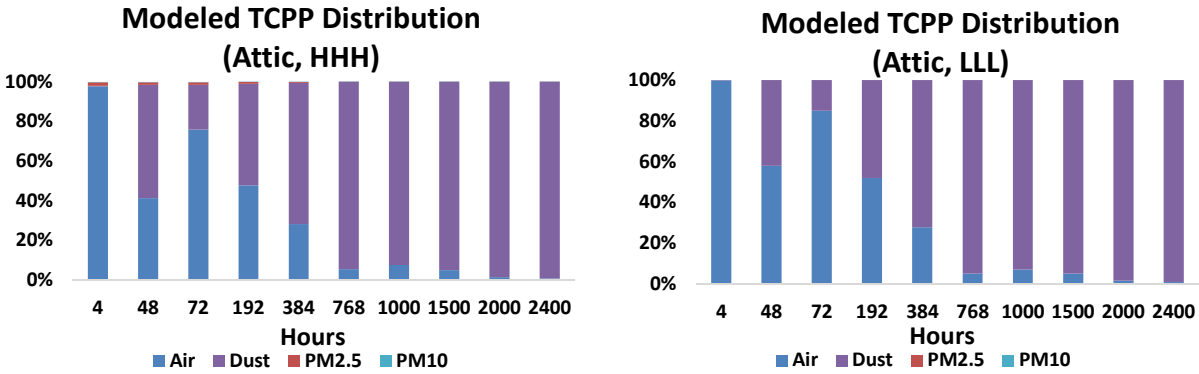
*HHH and LLL are modeling scenarios based on partition and diffusion coefficient selections listed in Table 23. H and L denote the higher and lower values are selected for that parameter.*

**Figure 42: TCPP mass distribution percentage in living area relevant to inhalation and ingestion exposure**



*HHH and LLL are modeling scenarios based on partition and diffusion coefficient selections listed in Table 23. H and L denote the higher and lower values are selected for that parameter.*

**Figure 43: TCPP mass accumulated in each environmental media in the attic**



*HHH and LLL are modeling scenarios based on partition and diffusion coefficient selections listed in Table 23. H and L denote the higher and lower values are selected for that parameter.*

**Figure 44: TCPP mass distribution percentage in attic relevant to inhalation and ingestion exposure**

When TCPP distribution percentage is evaluated for the environmental media relevant to inhalation and ingestion pathway, Figure 42 and Figure 44 illustrate the change of percentage contribution between air and settled dusts. After SPF application, during the first two weeks in the living area and one week in the attic, the majority of TCPP is in the air, while after the initial period, more TCPP is accumulated in the settled dusts. The primary reason is because of ventilation; the vapor phase TCPP in the air was constantly removed from the indoor environment, and there was no cleaning of settled dusts during the modeled 100-day period. Settled dusts become the largest TCPP distribution media quicker in the attic than the living area due to a larger ACH rate. Among the eight modeling scenarios, TCPP distribution in each media is relatively constant within each indoor zone.

### 5.3.4 Comparison between field measurements and IECCU modeling results

**5.3.4.1 Airborne TCPH concentration** When IECCU modeling results are compared with field measurements, it is found that field measurements have a higher TCPH airborne concentration than all modeling scenarios during the first two to three days after SPF application (as shown in Figure 45). Then, field measurements eventually decay lower than the modeling results in the attic at the 710 hours and 1,872 hours for the LLL and HHH scenarios. In the living area, measured TCPH airborne concentration is lower than the LLL scenarios after 672 hours but still higher than the HHH scenario at the end of sampling period. However, it is worth to note at the end of sampling period (1,920 hours) in the living area, the measured TCPH airborne concentration is lower than the level of quantification (LOQ).

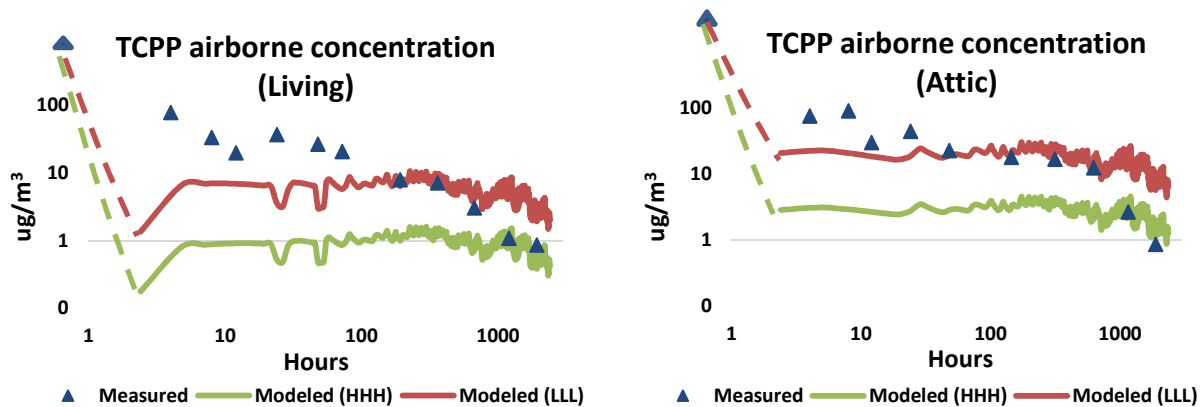


**Figure 45: TCPH airborne concentration: modeled vs. measured**

The higher measured TCPH concentration during the first few days and a much more rapid decay rate than modeling results indicate IECCU may underestimate TCPH airborne

concentration at the beginning of the post application period. A few possibilities that can explain such differences include overspray aerosol generated during application, concentration variations within each room and potential underestimate of initial source emission rate. First, the field study used a TD tube which aimed to collect gas phase TCPF only. However, even after SPF application, overspray aerosols may still be present in the indoor environment and collected by the TD tubes. Although the overspray aerosols contributed less to the area samples since they were relatively further away from the SPF sources (Tian, Ecoff et al. 2018), enhanced ventilation during spray application may not be effective enough to ventilate all overspray aerosols that a higher measured concentration occurred. The field measured TCPF airborne concentration during application was used in modeling as the initial concentration but it was quickly decayed due to the high ACH rate in these rooms. Second, IECCU assumes each room is well mixed and vapor phase TCPF is uniformly distributed in the rooms. However, field measurements were highly dependent on the sampling location and may be influenced by the unevenly distributed air flows (Ecoff, Tian et al. 2017). Third, as shown Figure 39 and Figure 40, the modeled source emission rates are relatively constant during the entire sampling period but previously literature shows that SPF emission rate is much higher during the initial hours after spray due to the high foam temperature which is much higher than the room temperature (Sebroski, Miller et al. 2017).

Among the eight modeled scenarios, as shown in Figure 46, TCPF airborne concentration is predominantly impacted by the modeling parameters associated with sources but is minimally impacted by the parameters associated with sinks, settled dusts and airborne particles. In those modeling scenarios with higher source parameters (a factor of 8 for  $k_{sa}$  and a factor of 2 for  $D_s$ ), source emission rates and the modeled airborne concentration are lower (a factor of 5 to 7 during the 100 days modeled).

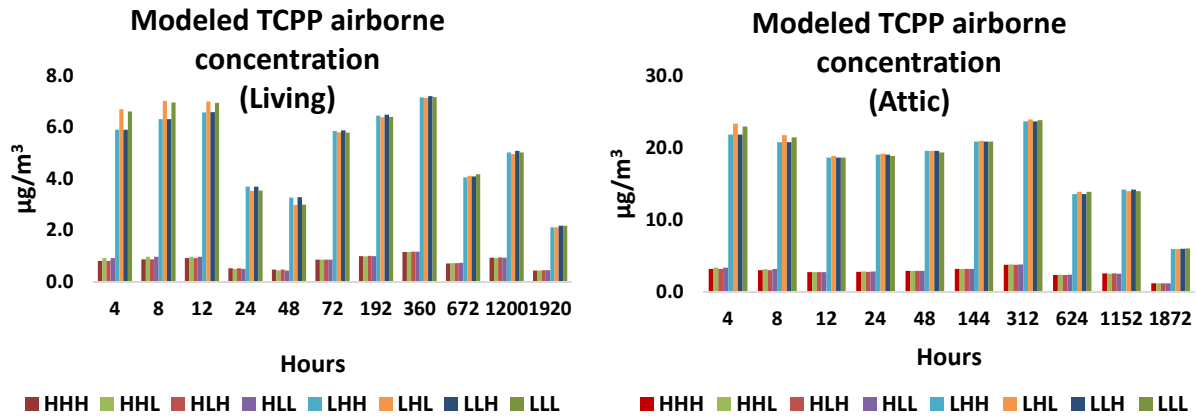


**Figure 46: Modeled TCPP airborne concentration**

**5.3.4.2 TCPP surface accumulation** Figure 47 and Figure B2 present the field vs. model comparison for TCPP surface accumulation on indoor sink materials and settled dusts. A similar trend can be found that IECCU estimates lower surface accumulation at the beginning of the testing period but such differences decrease in most cases towards the end of the sampling period, especially for the attic since it has a longer testing period. For the last sample collected in the attic (at 1,874 hour), the measured total TCPP accumulation is  $4.9 \times 10^6 \mu\text{g}$  while the modeled value is  $3.5 \times 10^6 \mu\text{g}$ . The overspray aerosol could be the main cause for IECCU underestimates TCPP accumulation at the initial period. Although the application site was swept before sink materials were placed, remaining overspray aerosols in the room may be resuspended and settled onto samples during the first few days. After the initial days, with constant air movements throughout the test period, less overspray aerosols were presented and therefore the differences between measurements and model decreased.

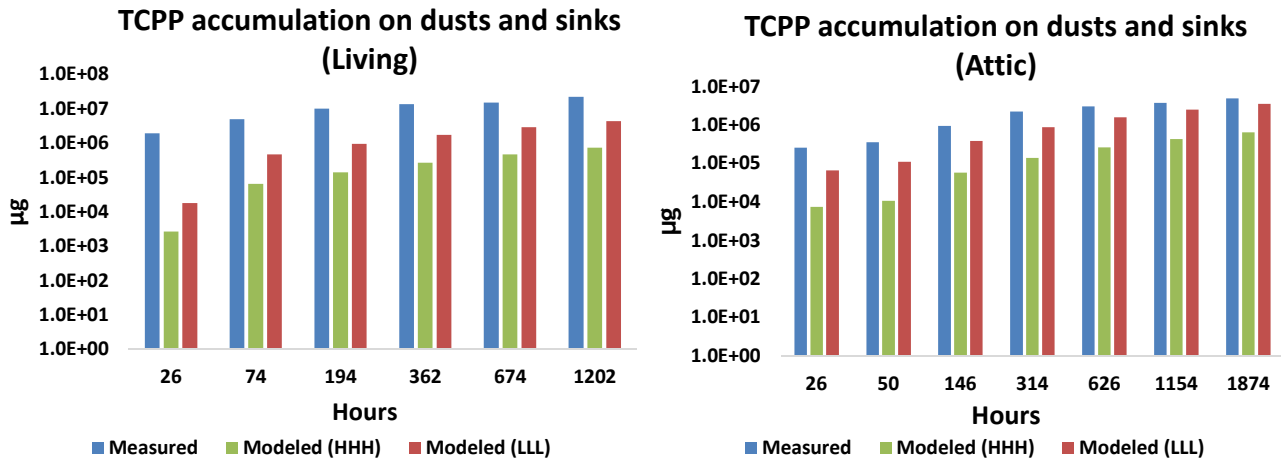


**Figure 47: TCPP accumulation on settled dusts and sinks: modeled vs. measured**

Comparing among the modeling scenarios, as shown in Figure 48, the amount of TCPP accumulated on sinks and settled dusts is determined by the parameters associated with sources, rather than those associated with sinks or settled dusts. Since sinks accumulate about two orders of magnitude more TCPP than settled dusts during the testing period, discussions on modeling parameters are focused on sinks. The local two-phase theory (Lewis and Whitman 1924, Guo 2014) can explain why the amount of TCPP accumulated on sinks is only impacted by source modeling parameters regardless sink parameters.

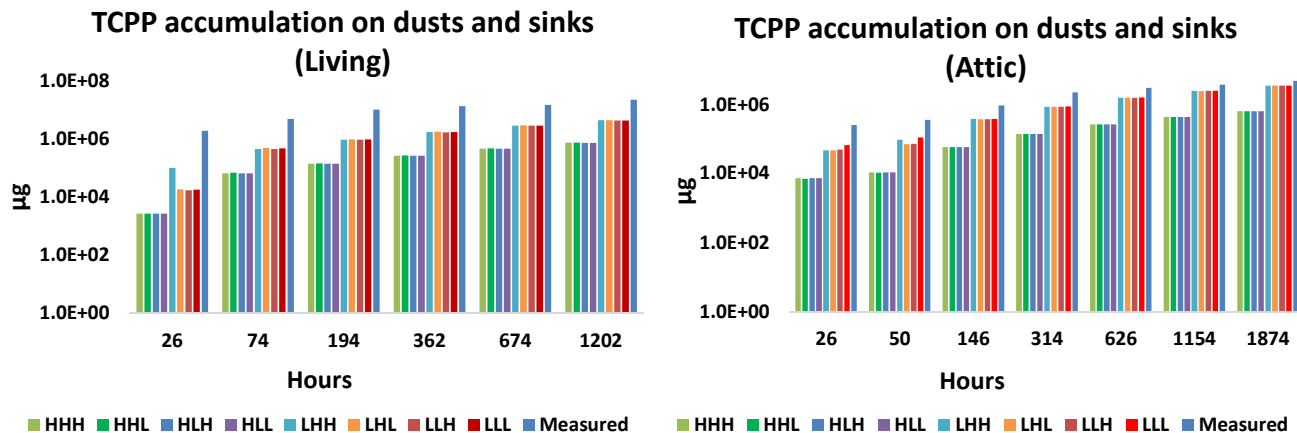


**Figure 48: Modeled TCPP surface accumulations (sink + settled dusts)**

In Equation 6, based on the  $k_{na}$  and  $D_n$  selected for sink materials,  $\frac{1}{k_{na} \times h_n}$  is small enough ( $1 \times 10^{-8} \sim 1 \times 10^{-7}$  m/h) that  $H_a$  is dominated by  $\frac{1}{h_{an}}$  ( $\sim 1$  m/h). Therefore, Equation 5 can be rewritten as  $R_n = A \times h_{an} \times (C_a - \frac{C_{nv}}{k_{na}})$  which is independent of  $D_n$ . For both living area and attic,  $C_a$  is much larger than  $\frac{C_{nv}}{k_{na}}$  during the entire modeled period. Therefore,  $R_n$  is linearly related to  $A$ ,  $h_{an}$  and  $C_a$ , which  $A$  and  $h_a$  are constant and  $C_a$  is determined by source parameters. Therefore,  $R_n$  is independent of  $k_{na}$  and  $D_n$  during the modeled 100 days.

### 5.3.5 Averaged TCPP exposure and risk characterization

Metabolism and Toxicokinetic studies indicated that TCPP is primarily removed by excretion as opposed to bio-accumulative (Minegishi, Kurebayashi et al. 1988, OECD (Organisation for Economic Co-operation and Development) 2000). The averaged TCPP exposure during the

modeled 100-day period is presented in Figure 49 for both inhalation and ingestion pathways. The lowest and highest exposure scenarios out of the eight modeling scenarios plus an additional scenario using reduced ACH were presented. The inhalation exposure was calculated using the modeled airborne TCPP concentration plus the concentration in the airborne particles in the air of the living area, multiplied the age specific inhalation rate and divided by age specific body weight reported in the USEPA's exposure handbook (U.S. Environmental Protection Agency 2011a). It was assumed that building occupants between 6 and 71 years old spend 16 hours while other age groups spend the entire day in the building. Similarly, the ingestion exposure was calculated using the modeled TCPP concentration in the settled dusts, multiplied by the age specific indoor settled dust ingestion rate reported by USEPA's exposure handbook. The same assumption of age specific hours spent in the building also applied to ingestion exposure.

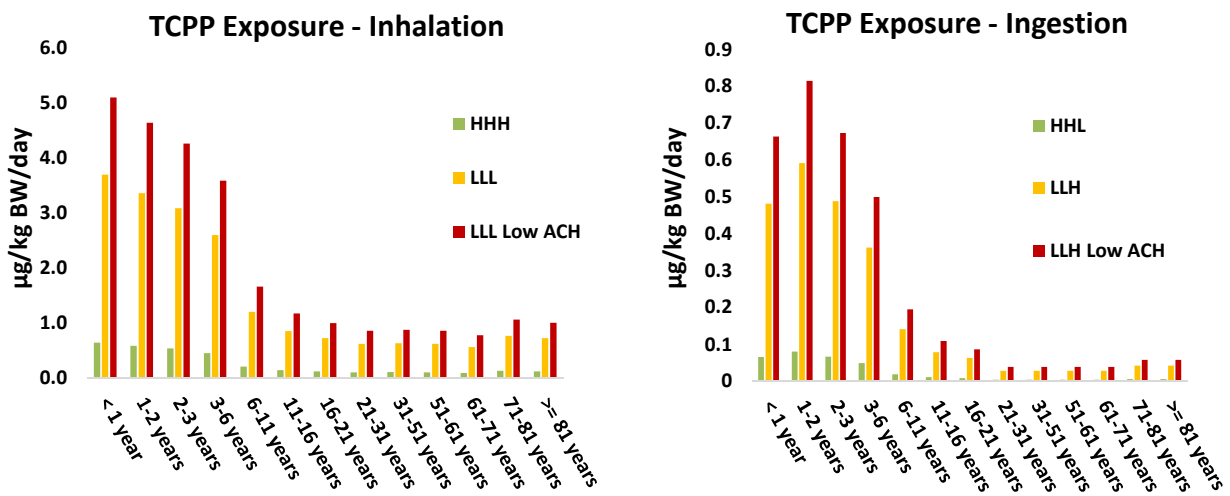


**Figure 49: The averaged TCPP exposure level of different age groups**

Due to the lower body weight (BW), infants and young children have a higher exposure level than adults, especially the working age population. Exposure assessment was first conducted for the eight previously modeled scenarios, excluding the one using reduced ACH. During the 100-day period, the averaged TCPP inhalation exposure ranges from 3.7 (0.6)  $\mu\text{g}/\text{kg BW}/\text{day}$  for less than one-year old infants to 0.6 (0.1)  $\mu\text{g}/\text{kg BW}/\text{day}$  for 21-31 years old adults in the LLL (HHH) scenario. Within the inhalation pathway, over 99% was from inhaling gas phase TCPP in the air and the inhalation exposure from airborne particles was negligible. The averaged ingestion exposure ranges from 0.6 (0.08)  $\mu\text{g}/\text{kg BW}/\text{day}$  for one to two years old children to 0.03 (0.005)  $\mu\text{g}/\text{kg BW}/\text{day}$  for age between 21 to 71 years old adult. The additional scenario assumed 50% of the ACH values used in the previous eight modeling scenarios in order to simulate a tighter home. The highest inhalation exposure is 5.1  $\mu\text{g}/\text{kg BW}/\text{day}$  for less than one-year old infants and highest ingestion exposure is 0.8  $\mu\text{g}/\text{kg BW}/\text{day}$  for one to two years old children. Although variations of TCPP exposure exist in different modeling scenarios, the trend is clear that children have a higher TCPP exposure than adult.

For cancer risk, TCPP was identified as “inadequate information to assess carcinogenic potential;” therefore, no cancer risk slope factor was developed (U.S. Environmental Protection Agency 2012c). For non-cancer risk, there is no RfD, RfC or cancer assessment for TCPP in the EPA’s IRIS database (U.S. Environmental Protection Agency 2018a). Only a screening level chronic provisional RfD was established at 10  $\mu\text{g}/\text{kg BW}/\text{day}$  for oral ingestion pathway (U.S. Environmental Protection Agency 2012c). Due to the lack of inhalation TCPP toxicology studies, no provisional RfC was established for inhalation pathway. Using the most conservative modeled exposure dose (0.6  $\mu\text{g}/\text{kg BW}/\text{day}$  at the LLH scenario for one to two years old children), the RCR (HI) is 0.06 for ingestion pathway, which is below the risk management

threshold of one (National Research Council 1994). Since the tested house was under major renovation, the reduced ACH modeling scenario is more representative for a typical house renovated with SPF. This scenario demonstrates the impact of indoor-outdoor ventilation to TCPP exposure of building occupants. The time weighted average exposure increases roughly 30% with a 50% ACH reduction.

#### **5.4 CONCLUSIONS AND FUTURE STUDIES**

This research compiled all the required modeling parameters of IECCU, either through measurements or literature empirical correlations. Based on the value ranges of key input parameters, a total of eight modeling scenarios were developed. In the modeling work, the emission, fate and distribution of TCPP emitted from SPF applied in a residential building were modeled during a 100-day period. The mass balance shows that ventilation removed the most TCPP out of the indoor air, followed by indoor sink TCPP sorption. For the TCPP that remained in the indoor environment, the majority of TCPP was distributed in the indoor sink materials, followed by settled dusts which had about two orders of magnitude lower than the amount TCPP on indoor sink materials.

Compared to the field measurements, the modeled TCPP airborne concentration remained relatively constant after SPF application but field measurement showed a more rapid decay. One possible explanation is that IECCU does not take into account the overspray TCPP vapor and aerosol generated during SPF application, which could remain in the indoor environment longer than the model prediction. For TCPP surface accumulation, the LLL modeling scenario

which predicts the highest TCPP emission is closer to the measured values than any other scenarios.

Based on the modeling result, the averaged TCPP inhalation exposure dose ranges from 3.7  $\mu\text{g}/\text{kg BW}/\text{day}$  for less than one-year old infants to 0.6  $\mu\text{g}/\text{kg BW}/\text{day}$  for 21-31 years old adults in the LLL scenario. However, there is no established inhalation RfC to derive the HI. The highest averaged oral ingestion exposure dose is 0.6  $\mu\text{g}/\text{kg BW}/\text{day}$  for one to two years old children and the corresponding HI (0.06) is lower than the risk management threshold of one.

Future studies should extend the field sampling time to more than 100 days, especially for the sink materials. In addition, toxicological threshold values should be established for inhalation exposure pathway so risk characterization can be performed.

## **6.0 CONCLUSIONS**

This research is centered on how to improve the HHIA of a product and conduct product safety and sustainability assessment from a life cycle perspective. To accomplish this objective, a method was developed to use publicly available life cycle emission inventory data and high-resolution air dispersion modeling in cradle-to-gate product HHIA. Chemical emissions and the associated human health risks were also addressed when a product is installed or used in an indoor environment by conducting industrial hygiene field measurements in a residential house renovated with SPF. In a laboratory chamber sorption study, the sorption mechanism of an OPFR, TCPP, onto the household settled dusts was researched. Data collected from the field and laboratory studies were used to develop a comprehensive list of modeling parameters in a state-of-the-art multi-media mass transfer model to evaluate the emission, transport and distribution of TCPP in the indoor environment.

### **6.1 INTEGRATION OF HIGH-RESOLUTION ENVIRONMENTAL MODELING TOOLS INTO LCA**

A method was proposed to improve the current HHIA in LCA by conducting more regionalized impact assessment using high-resolution air dispersion modeling. In this proposed method, a

regionalized LCI was developed with publicly available emission inventory data which avoid the challenge faced by many LCA practitioners: regionalized impact assessment is relied on proprietary information. With the regionalized LCI, a site-specific air dispersion model (HEM3-AERMOD) and a site-generic fugacity based multi-media model (USEtox) were implemented to quantify the far-field human health impacts of chemical products along their supply chain. This approach improved current HHIA in LCA by quantifying and identifying the geographical variations and patterns of human health risks in the far-field environment resulted from chemical manufacturing processes. In this case study, the results were visualized using GIS which helps environmental managers and process engineers to mitigate human health risks around the manufacturing facilities and improve the production processes. Risk mitigation priorities should be given to those unit processes located in the risk hotspot areas. Ultimately, this method can help corporations to quantify human health risks associated with cradle-to-gate manufacturing of a product and ensure the additional risk added to a society by making a product is acceptable and below the regulatory threshold.

## **6.2 CHEMICAL EMISSIONS IN PRODUCT USE PHASE**

Besides the human health risks resulted from far-field chemical exposure, professionals and consumers are also exposed to chemicals emitted from product application and use phase. A field industrial hygiene study was conducted to evaluate chemicals emitted during and after SPF was installed in a residential building. During a three months sampling period, we used an improved sample collection technique to measure the airborne concentration of MDI, aldehydes, a flame retardant (TCPP) and a blowing agent emitted from SPF. Results showed certain chemicals

decayed quickly in airborne concentration after it was introduced to the environment such as MDI and aldehydes but others can be present for longer time such as TCPP. Due to the inter-compartment migration, it is recommended that everyone should wear proper personal protection equipment when entering an active spraying site, regardless the actual spray location in the same building. In addition to airborne chemical concentration, surface accumulation of TCPP was measured and compared with a recent chamber study. Although there are differences on TCPP accumulation rates on indoor surfaces, the airborne TCPP concentration normalized surface sorption rates are within one order of magnitude between the field and chamber studies.

To further explore chemical emission, fate and distribution in the indoor environment, parameters needed for a multi-media mass transfer model, IECCU, such as ACH, temperature, airborne particle concentration and settle dusts accumulation were collected in the tested house. With the actual values collected from the field, the IECCU model can be used with higher confidence so that the model can be used to predict TCPP indoor behavior and conduct risk assessment.

### **6.3 INDOOR MULTI-MEDIA MASS TRANSFER MODELING IN HUMAN HEALTH RISK ASSESSMENT**

Field testing and measurement is one of the methods to evaluate product emissions and their human health impacts during the use phase. However, field testing is often time and resource intensive. In addition, due to the complexity of the indoor environment and limited data points one field testing can collect, results from field studies are highly influenced by environmental conditions such as temperature, ventilation rates and humidity which all impact chemical

emissions from a product. Therefore, field studies may have limited value in product HHRA since one field study conducted in an indoor environment may not be representative for another environment. Chamber studies aim to measure product emission rates in a more controlled environment. However, environmental conditions in a test chamber can be quite different than an actual indoor environment (Office of Chemical Safety and Pollution Prevention 2017). The chamber testing results may not be extrapolated to real world indoor environment and therefore also limits its use in product HHRA.

As an alternative and complimentary to field testing and chamber studies, multi-media mass transfer modeling has the advantage to be applied in any environment to evaluate many chemical emissions from indoor use products. This research collected indoor environment conditions in a field study and also conducted chamber testing to estimate the diffusion coefficient of a flame retardant, TCPP. With additional literature search, for the first time, we provided a comprehensive list of input parameters needed to model TCPP emission, fate and distribution in the indoor environment, using a state-of-the-art multi-media mass transfer model (IECCU) developed by USEPA. The case study revealed the possible reasons which cause IECCU underestimates chemical exposure during the first few days after SPF was installed. How to better characterize the overspray aerosol should be the focus for future model improvements. Nevertheless, multi-media mass transfer modeling has its advantages in conducting product HHRA due to its flexibility, efficiency and universal application in many indoor environment and chemicals. In the case study, TCPP exposure level through oral ingestion pathway in this renovated house is 0.6  $\mu\text{g}/\text{kg BW}/\text{day}$  for one to two years old children at the modeled worst-case scenario during the first 100 days after SPF is installed. Although this exposure level is about one order of magnitude higher than the time weighted average life time TCPP exposure for

the toddlers living in the US (0.062  $\mu\text{g}/\text{kg BW}/\text{day}$ ) (Stapleton, Klosterhaus et al. 2009), the corresponding RCR is still below the threshold value of 1 (0.06). In the case study, we demonstrated the uncertainties associated with the key modeling parameters, primarily caused by the uncertainties in chemical and physical properties (such as vapor pressure) of the interested chemicals. In order to increase the confidence of using multi-media mass transfer modeling in product safety and HHRA, we should improve measurements or estimates of the key modeling input parameters. The outcomes of this research reveal two types of risk reduction strategies for product indoor chemical exposure: 1) develop “non-emissive” flame retardants and other product functional additives which can be built into the product matrix. For example, a possible approach is to develop a flame retardant with hydroxyl groups so it can be reacted with isocyanates and built into the SPF structure; 2) reduce inhalation exposure by keeping good ventilation after SPF is installed, reduce ingestion exposure to settled dusts by removing them through regular cleaning and reduce dermal exposure to indoor sink surfaces by avoiding walking on barefoot. It is also important to keep good ventilation or wear facial mask while vacuuming to reduce inhalation exposure to resuspended dusts.

## **6.4 SUMMARY**

The novel and practical method proposed in this work allows environmental managers, product safety and sustainability professionals to evaluate the human health impacts of a product from a life cycle approach, with higher geographical relevance and including chemical emissions in the product use phase. As the chemical industry looks towards more sustainable manufacturing processes and products, a comprehensive product safety and sustainability assessment method

and associated tools with focus on human health impacts and risks is essential to move the industry towards the direction of more sustainable development. Results in the case studies demonstrate how current product HHIA can be improved. Although illustrated using SPF and its associated chemical, the approach proposed in this work can be expanded to any other products.

## **6.5 RECOMMENDATIONS FOR FUTURE WORK**

The human health impacts of products, along their life cycle phases, is an important aspect in product safety and sustainability assessment. The HHIA of consumer products has been involved from evaluating inherent chemical hazards to include chemical exposure (Wambaugh, Setzer et al. 2013, Isaacs, Glen et al. 2014) so decisions regarding if a product is safe to use can be made based on chemical human health risk characterization instead of hazard assessment only. Based on the life cycle stages of a product and where the product emissions occur, different tools and methods should be used to quantify the human health impacts of products. Existing efforts have been focused on improve current methods such as LCA and HHRA.

To improve current practice in product human health assessment, this dissertation illustrated how to derive regionalized LCI and apply a site-specific air dispersion model to characterize far-field chemical emissions from a chemical's cradle-to-gate life cycle stages. This proposed method relies on publicly available emission inventory databases such as the TRI. However, only limited chemical emissions are reported to these public databases. For example, the federal HAPs list only contains 187 chemicals but many more chemicals emitted from the cradle-to-gate chemical manufacturing processes may have adverse effects to human health. There is an emerging need to include more chemicals into the mandated reporting programs so more

complete and comprehensive LCI can be derived. The reporting requirements vary across different states. For instance, Michigan rule R336.1120(f) define toxics air contaminant (TAC) as any air contaminant which may become harmful to public health or environment when present in the outdoor atmosphere in sufficient quantities and duration, except the 41 exempted chemicals (Air Quality Division 2008). This list is much longer than the federal HAPs list. Besides expanding the reportable chemicals in the federal mandatory reporting programs, production capacity information should be developed for more background unit process such as salt mining, crude oil and natural gas processing so regionalized LCI can be derived. For far-field chemical emissions from cradle-to-gate life cycle stages, future work should expand the proposed method beyond inhalation pathway to oral ingestion and dermal contact pathways since for certain chemicals such as heavy metal, the majority of chemical mass is not present in the air compartment. To include other exposure pathways, regionalized emission inventory and other site-specific models to address chemical fate, transport and distribution in watersheds and food production system will be needed. This proposed regionalized method has the potential to be expanded to study the life cycle human health impacts of emerging chemicals and products such as nanomaterials and OPFRs. However, emissions associated with manufacturing, using and disposing these materials must be reported in publicly available databases first so that regionalized LCI can be derived. Researchers and regulatory agencies should work together to bridge the gap of data scarcity and promote regionalized human health impact assessment along a product's life cycle.

For the near-field indoor product emission, this dissertation utilized field measurement, chamber testing and multi-media mass transfer models to evaluate chemical emissions from SPF during its installation and use phase. This work proposed a novel open filter approach to reduce

MDI LOQ which should be further validated by comparing its results with traditional MDI liquid impinger method. In addition to airborne chemical concentration and surface accumulation, future field measurement studies should consider to increase the airborne particle mass concentration in the tested indoor environment to collect enough airborne particles for chemical absorption analysis. Furthermore, future field measurement may consider to conduct tests in a more air tight residential building with controlled ventilation and compare results with this study.

Multi-media mass transfer modeling is the cost-effective alternative to field measurement and chamber testing. However, intensive modeling input parameters are needed to apply these models to product HHIA. Without accurate measurement or estimate of input parameters, multi-media mass transfer models may not be able to provide meaningful results to characterize the human health risks associated with product chemical emissions in the indoor environment. Our study provided a comprehensive list of modeling input parameters for TCPP emitted from SPF. Future research should expand this list to other chemicals and products. Empirical relationship to estimate material-air partition coefficient and diffusion coefficients in sources and sinks need to be available for more chemical-product pairs. This effort requires more accurate measurements of key chemical and physical properties such as the vapor pressure and octanol-air partition coefficient of the interested chemicals. In terms chemical exposure pathway, this dissertation focused on inhalation and oral ingestion but we also calculated how much TCPP is absorbed to indoor sinks such as flooring. Future study can adopt such results and apply dermal exposure model to quantify TCPP exposure through dermal contact pathway and characterize its human health risks. In order to make the final decision to determine if residents are over exposed to TCPP emitted from SPF through inhalation pathway, additional toxicological studies should be conducted to derive RfC or cancer risk slope factors for TCPP so the RCR can be calculated.

## APPENDIX A

### CALCULATION EXAMPLE IN SECTION 3.2.4

**Unit process (benzene) emits Cl<sub>2</sub> at the benzene manufacturing facility (gate-to-gate)**

**Equation:** Equation 2 in the manuscript;

**Plant (j):** Channel View, TX;

**Unit Process (k):** Benzene;

**HAP (i):** Cl<sub>2</sub>;

**Production Capacity (PC<sub>k,j</sub>)** of plant j: 7.11% of total Benzene production in the U.S.;

**Annual MDI production in the U.S. (P<sub>MDI</sub>):** 1.27 Million mt;

**Emission Factor (EF<sub>i,k</sub>):** the amount of HAP (Cl<sub>2</sub>) emitted from unit process k (Benzene) per function unit (1 mt MDI) produced. This is a two-step process. First, 407 kg Benzene is needed per 1 mt of MDI and 0.0001 kg Cl<sub>2</sub> is emitted per 1 mt benzene produced (gate-to-gate). Therefore, the EF<sub>i,k</sub> is  $4.07 \times 10^{-5}$ , which is  $4.07 \times 10^{-5}$  kg/1 mt MDI produced.

**AERMOD modeling:** at this plant with Standard Classification Code specific stack parameters and site specific meteorological and terrain profiles, for 1 ton of Cl<sub>2</sub> released per year, at census block number 482014112001004, the AERMOD calculated airborne concentration (C<sub>i,j</sub>) is  $1.79 \times 10^{-4}$  µg/m<sup>3</sup>.

**Hazard Index (HI):**

$$\text{Hazard Index (HI)} = \frac{(\sum_k^p \sum_j^n \sum_i^m C_{i,j} \times EF_{i,k} \times PC_{k,j}) \times P_{MDI}}{RfC_i}$$

$$\text{HI} = \frac{1.79 \times 10^{-4} \mu\text{g}/\text{m}^3 \times 4.07 \times 10^{-5} \frac{\text{kg}}{1 \text{ mt MDI}} \times 1.27 \times 10^6 \text{ mt MDI}/\text{year} \times 7.11\% \times \frac{1 \text{ ton}}{909 \text{ kg}}}{RfC_i} = \frac{7.23 \times 10^{-7} \mu\text{g}/\text{m}^3}{RfC_i}$$

**RfC of Cl<sub>2</sub>:** 0.15 μg/m<sup>3</sup>.

$$\text{HI} = 4.83 \times 10^{-6}.$$

Finally, at one receptor (census block) the HI can be summed across all HAPs (i), plants (j) and unit process (k). The averaged risk characterization values (cancer risk and non-cancer HI) can be calculated at the census tract and county level.

## APPENDIX B

### ADDITIONAL MODELING PARAMETERS AND RESULTS IN SECTION 5.2.5 AND 5.3

**Table B1: Curve fitting residuals for all three tests**

<b>k<sub>da</sub> (unitless)</b>	<b>Dust</b>		<b>Chamber air</b>	
	<b>(<math>\mu\text{g TCPP/g dust}</math>)<sup>2</sup></b>		<b>(<math>\mu\text{g TCPP/m}^3\text{ air}</math>)<sup>2</sup></b>	
	<b>25-90 <math>\mu\text{m}</math></b>	<b>90-150 <math>\mu\text{m}</math></b>	<b>25-90 <math>\mu\text{m}</math></b>	<b>90-150 <math>\mu\text{m}</math></b>
	<b>(GM = 47.43 <math>\mu\text{m}</math>)</b>	<b>(GM = 116.19 <math>\mu\text{m}</math>)</b>	<b>(GM = 47.43 <math>\mu\text{m}</math>)</b>	<b>(GM = 116.19 <math>\mu\text{m}</math>)</b>
$3.41 \times 10^7$	$2.1 \times 10^4$	$1.1 \times 10^4$	$1.3 \times 10^3$	$6.2 \times 10^2$
$2.08 \times 10^8$	$1.9 \times 10^4$	$1.0 \times 10^4$	$2.0 \times 10^3$	$2.3 \times 10^2$
$6.59 \times 10^8$	$2.1 \times 10^4$	$9.7 \times 10^3$	$1.5 \times 10^3$	$4.8 \times 10^2$
$8.70 \times 10^8$	$2.1 \times 10^4$	$1.0 \times 10^4$	$1.3 \times 10^3$	$7.0 \times 10^2$

**Table B2: Other IECCU modeling parameters**

<b>Parameter</b>	<b>Value</b>		
<b>Sources</b>			
Application phase	Living area	Attic day 1	Attic day 2
<i>Start time (hr)</i>	0	24	46.5
<i>End time (hr)</i>	3.5	28	53
<i>Total area sprayed (m<sup>2</sup>)</i>	57.8	51.4	51.4
<i>Emission factor</i>	948		
( $\mu\text{g/m}^2/\text{hr}$ ) <sup>3</sup>			
<i>1<sup>st</sup> order decay rate</i>	0.0001 (essentially no decay)		

<b>Temperature dependent <math>k_{sa}</math></b>		
<i>Slope a (unitless) (Tian, Sebroski et al. 2017)</i>	$7.5 \times 10^{-1}$	
<i>TCPP evaporation enthalpy (J) (Tian, Sebroski et al. 2017)</i>	81,000	
<b>Temperature dependent <math>D_s</math></b>		
<i>TCPP activation energy (J) (Tian, Sebroski et al. 2017)</i>	95,800	
<b>Parameters to calculate <math>h_{as}</math></b>		
<i>Density of air (<math>kg/m^3</math>)</i>	1.2	
<i>Viscosity of air (<math>kg/m/s</math>)</i>	$1.9 \times 10^{-5}$	
<i>TCPP diffusivity in air (<math>m^2/s</math>)</i>	$4.7 \times 10^{-6}$	
<i>Characteristic length (m)</i>	Four pieces in the living area: 3.3, 3.5, 4.2 and 4.1 Three pieces in the attic: 2.8, 8.4 and 5.0	
<b>Sinks</b>		
<i>Area (<math>m^2</math>)</i>	Living area: 6 pieces modeled Gypsum board: 301.4, 167, 25.1, 32.7, 6.7 Wood floor: 167.4	Attic: 1 piece modeled Wood: 83.7
<i>Characteristic length (m)</i>	Living area Gypsum board: 17.3, 12.9, 5.0, 5.7, 2.6 Wood floor: 12.9	Attic Wood: 9.2
<b>Settled dusts</b>		
<i>Particle number (#)</i>	Living area $5.6 \times 10^8$	Attic $2.5 \times 10^8$
<i><math>h_{ad}</math> (m/hr)</i>	232	
<i><math>D_g</math> (<math>m^2/s</math>)</i>	$6.4 \times 10^{-6}$	
<i><math>R_2</math> (m)</i>	$5.8 \times 10^{-5}$	
<i><math>K_n</math> (unitless)</i>	$1.4 \times 10^{-3}$	
<i><math>\lambda</math> (m)</i>	$8.1 \times 10^{-8}$	
<i>c (m/s)</i>	138	
<i>R (J/K/mol)</i>	8.314	
<i>T (K)</i>	296	
<i>M (kg/mol)</i>	$3.3 \times 10^{-1}$	
<b>Simulation conditions</b>		
<i>Initial TCPP concentration in air (<math>\mu g/m^3</math>)</i>	0	
<i>Simulation time (hours)</i>	2400	
<i>Number of data points</i>	200	

Equation B1 calculates temperature dependent  $k_{sa}$ .

$$\ln\left(\frac{k_{sa1}}{k_{sa2}}\right) = \ln\left(\frac{P_2}{P_1}\right) = \frac{\Delta H_v}{R}\left(\frac{1}{T_1} - \frac{1}{T_2}\right) \quad \text{Equation B1}$$

Where,  $k_{sa}$  is the partition coefficient between source materials (unitless),  $P$  is the vapor pressure (Pa) of TCPP at temperature  $T$ ,  $\Delta H_v$  is the Evaporation enthalpy (J),  $R$  is the ideal gas constant (J/k/mol) and  $T$  is the absolute temperature (K).

Equation B2 calculates temperature dependent  $D_s$ .

$$\ln\left(\frac{D_{s2}}{D_{s1}}\right) = \frac{\Delta E}{R}\left(\frac{1}{296} - \frac{1}{T}\right) \quad \text{Equation B2}$$

Where  $D_{s2}$  is the diffusion coefficient of source materials ( $m^2/hr$ ) at temperature  $T$  (K),  $D_{s1}$  is the diffusion coefficient at 23 °C and  $\Delta E$  is TCPP's activation energy calculated as 95.8 kJ/mol (Tian, Sebroski et al. 2017).

Equation B3 calculates  $h_{as}$ .

$$h_{as} = 0.33D_a L^{-\frac{1}{3}} \left(\frac{u\rho}{\mu}\right)^{\frac{2}{3}} \quad \text{Equation B3}$$

Where,

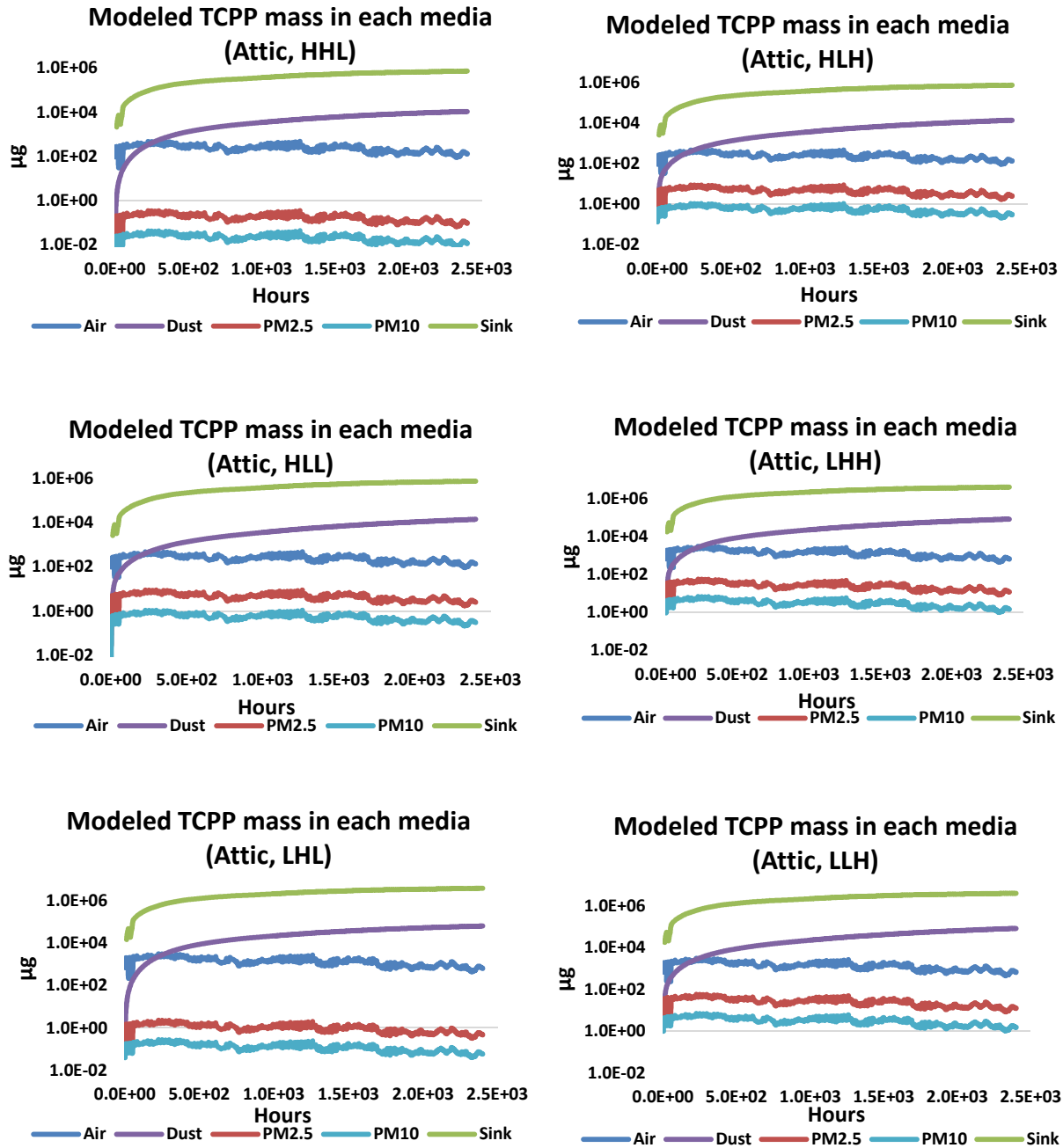
$D_a$  is the TCPP diffusivity in air ( $m^2/s$ ),  $L$  is the characteristic length of a source (m), calculated as the square root of the source area,  $u$  is the air velocity (m/s),  $\rho$  is the air density ( $kg/m^3$ ) and  $\mu$  is the viscosity of air ( $kg/m/s$ ).

Equation B4 and Equation B5 calculate the mass transfer coefficient in air of settled dusts ( $h_d$ ) (Li and Davis 1996, Liu, Shi et al. 2013).

$$h_d = \frac{D_g}{R_2} \times \frac{1 + K_n}{1 + 1.71K_n + 1.333K_n^2} \quad \text{Equation B4}$$

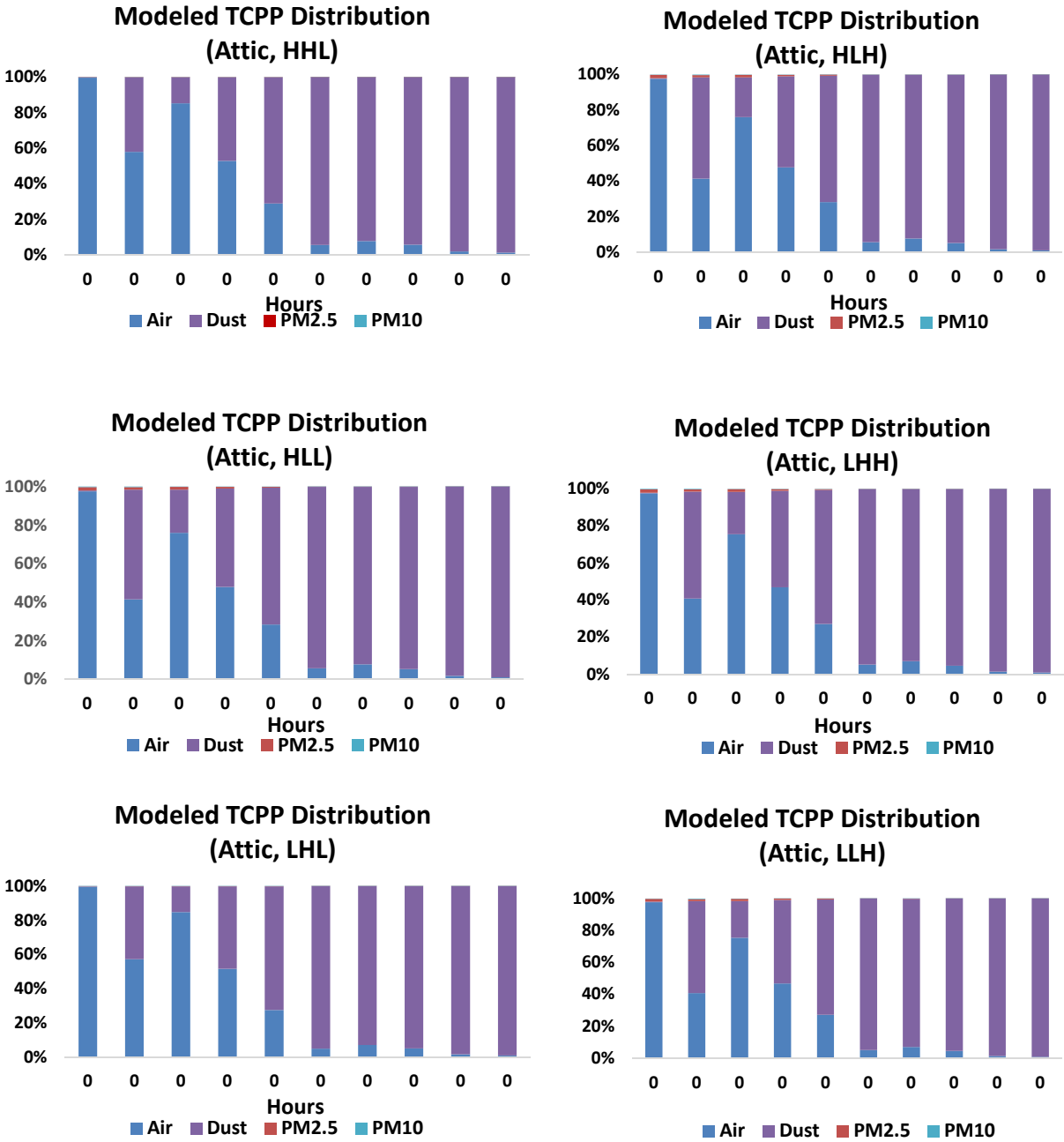
$$K_n = \frac{\lambda}{R_2}, \lambda = 3 \frac{D_g}{C}, c = \sqrt{\frac{8RT}{\pi M}} \quad \text{Equation B5}$$

Where  $D_g$  ( $m^2/s$ ) is the diffusion coefficient of SVOCs in air determined by Sparc Performs Automated Reasoning in Chemistry (SPARC) (Automated Reasoning in Chemistry 2015),  $R_2$  is the outer radius of dust or airborne particle,  $K_n$  is Knudsen number,  $\lambda$  (m) is the mean free path of SVOCs,  $c$  (m/s) is the mean molecular speed of SVOCs,  $R$  (J/K/mol) is the ideal gas constant,  $T$  (K) is the temperature and  $M$  (kg/mol) is the molecular weight of SVOCs.



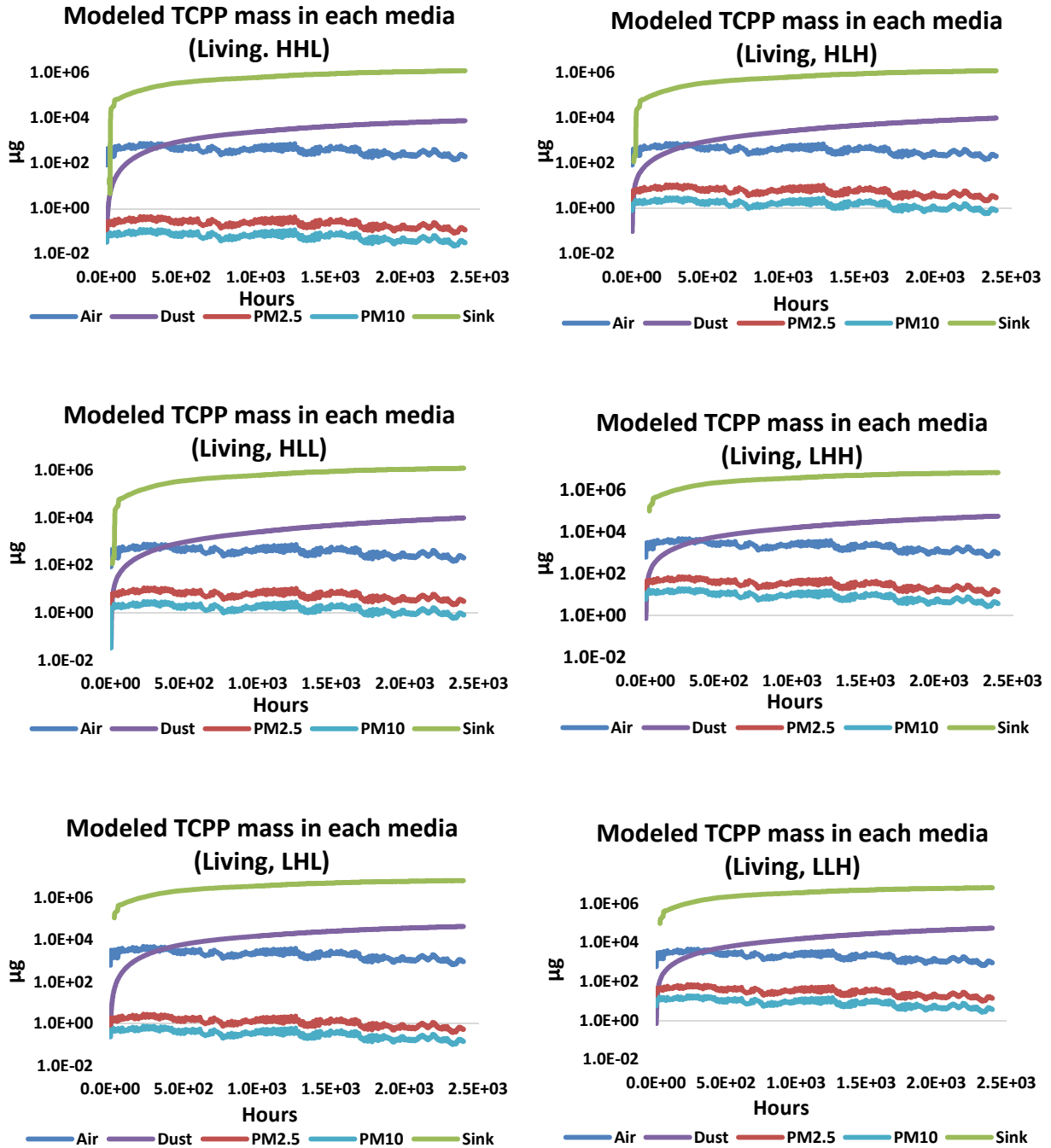
*HHL, HLH, HLL, LHH, LHL, LLH are modeling scenarios based on partition and diffusion coefficient selections listed in Table 23 of the main text. H and L denote the higher and lower values are selected for that parameter.*

**Figure B1: Modeled TCPP mass distribution in each indoor media in attic (HHH and LLL scenarios are listed in Figure 43)**



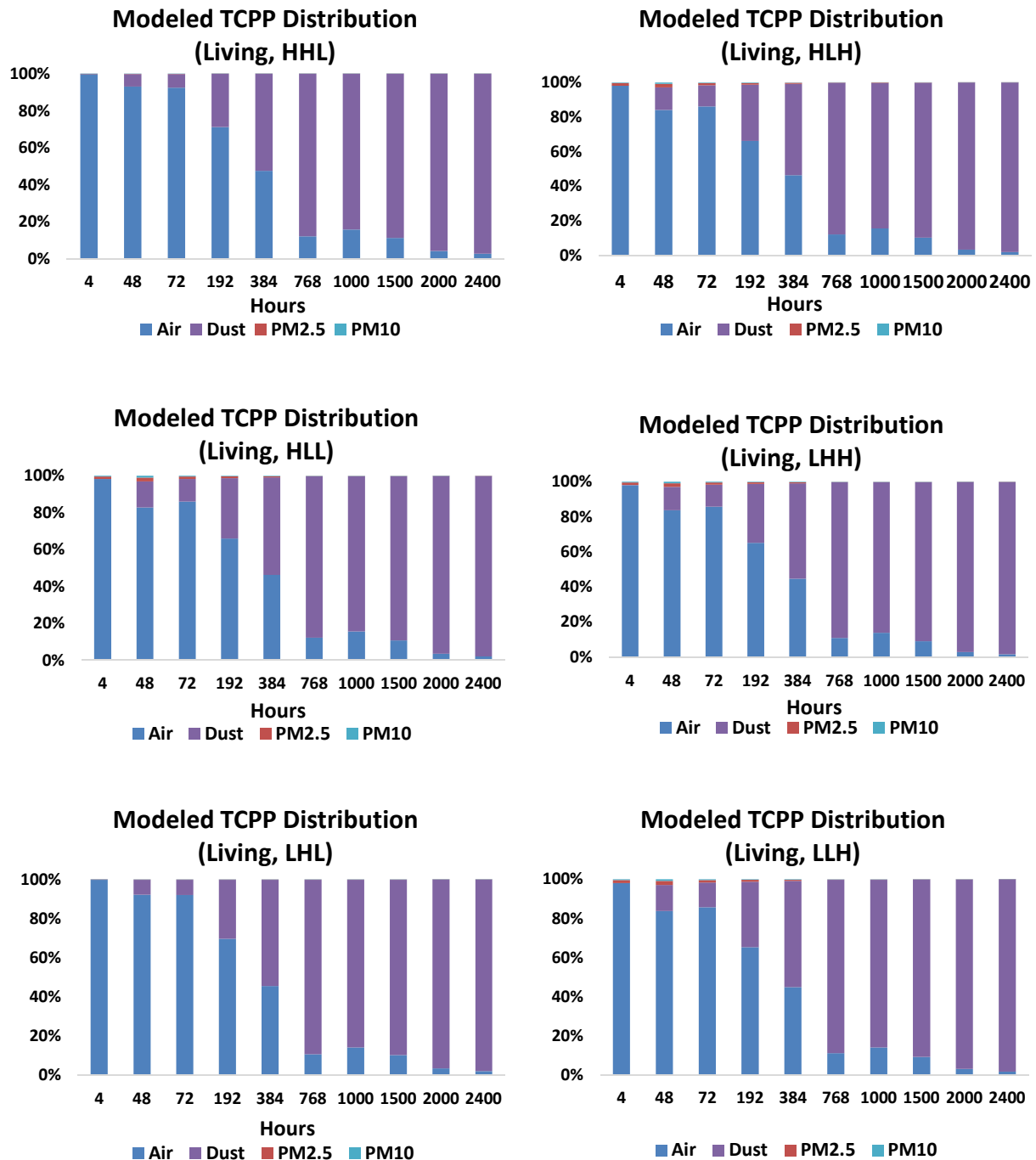
*HHL, HLH, HLL, LHH, LHL, LLH are modeling scenarios based on partition and diffusion coefficient selections listed in Table 23 of the main text. H and L denote the higher and lower values are selected for that parameter.*

**Figure B2: Modeled TCPP mass distribution percentage in attic relevant to inhalation and ingestion exposure (HHH and LLL scenarios are listed in Figure 44)**



*HHL, HLH, HLL, LHH, LHL, LLH are modeling scenarios based on partition and diffusion coefficient selections listed in Table 23 of the main text. H and L denote the higher and lower values are selected for that parameter.*

**Figure B3: Modeled TCPP mass distribution in each indoor media in living area (HHH and LLL scenarios are listed in Figure 41)**



*HHL, HLH, HLL, LHH, LHL, LLH are modeling scenarios based on partition and diffusion coefficient selections listed in Table 23 of the main text. H and L denote the higher and lower values are selected for that parameter.*

**Figure B4: Modeled TCPP mass distribution percentage in living area relevant to inhalation and ingestion exposure (HHH and LLL scenarios are listed in Figure 42)**

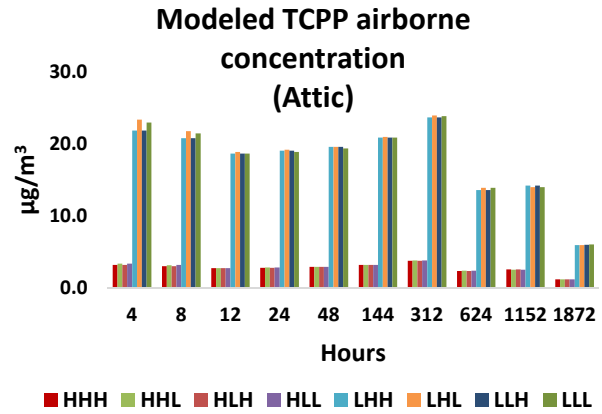
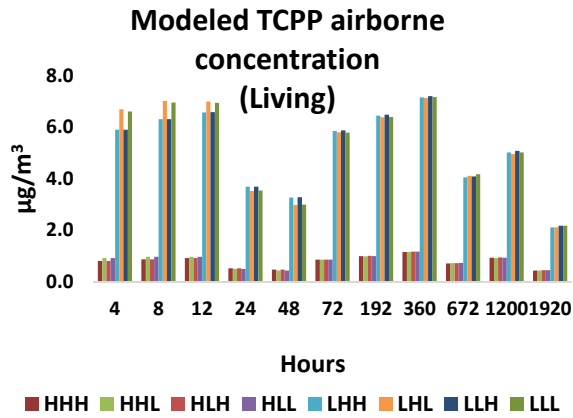


**Figure B5: Modeled TCPP airborne concentration**

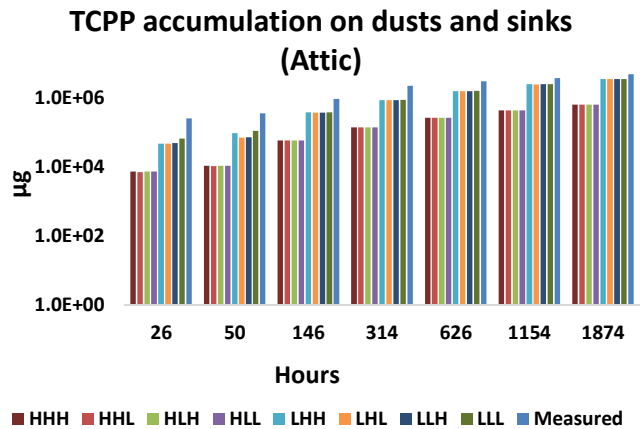
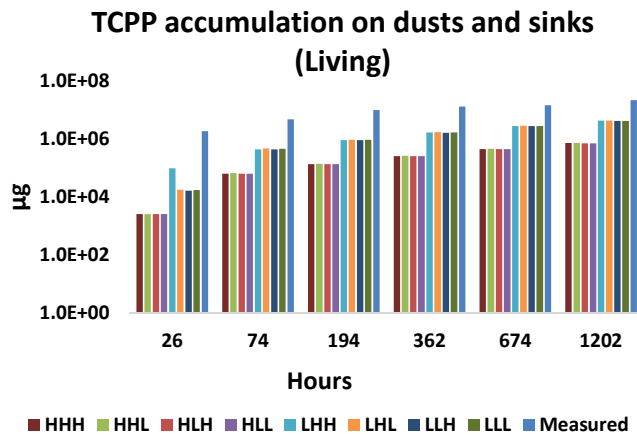


**Figure B6: Modeled TCPP surface accumulations (sink + settled dusts)**

## BIBLIOGRAPHY

Abdallah, M. A.-E. and A. Covaci (2014). "Organophosphate Flame Retardants in Indoor Dust from Egypt: Implications for Human Exposure." Environmental Science & Technology **48**(9): 4782-4789.

Afshar, A. A. (2014). "Chemical Profile: Methylene Diphenyl Diisocyanate." Retrieved March 23, 2018, from [http://www.chemplan.biz/\(X\(1\)S\(r05csalpuogmwlo1c3mrhj4g\)\)/chemplan\\_demo/sample\\_reports/MDI\\_Profile13.pdf](http://www.chemplan.biz/(X(1)S(r05csalpuogmwlo1c3mrhj4g))/chemplan_demo/sample_reports/MDI_Profile13.pdf).

Agency for Toxic Substances and Disease Registry (ATSDR) (2009). Toxicological Profile for Phosphate Ester Flame Retardants. Atlanta, GA, U.S. Department of Health and Human Services.

Air Quality Division (2008). Air Pollution Control Rules Part 1. General Provisions. Department of Environmental Quality of the State of Michigan. Lansing, MI. **R336.1120(f)**.

Ali, N., L. Ali, T. Mehdi, A. C. Dirtu, F. Al-Shammari, H. Neels and A. Covaci (2013). "Levels and profiles of organochlorines and flame retardants in car and house dust from Kuwait and Pakistan: Implication for human exposure via dust ingestion." Environment International **55**: 62-70.

American Chemistry Council (2011a). ACC Prioritization Screening Approach. Washington, D.C., American Chemistry Council.

American Chemistry Council (2011b). Cradle-to-gate Life Cycle Inventory of Nine Plastic Resins and Four Polyurethane Precursors. Washington, DC, American Chemistry Council.

American Chemistry Council. (2015). "What Are Diisocyanates?" Retrieved March 21, 2018, from <http://dii.americanchemistry.com/Diisocyanates-Explained/What-Are-Diisocyanates>.

American Chemistry Council. (2016). "American Chemistry: The Cornerstone of our Economy." Retrieved March 21, 2018, from <https://www.americanchemistry.com/Jobs/EconomicStatistics/American-Chemistry-The-Cornerstone-of-our-Economy.pdf>.

American Chemistry Council. (2017). "The business of chemistry by the numbers." Retrieved Aug 22<sup>nd</sup>, 2018, from <https://www.americanchemistry.com/Business-of-Chemistry-by-the-Numbers/>.

American Chemistry Council. (2018). "Why Spray Foam." Retrieved October 6<sup>th</sup>, 2018, from <https://www.whysprayfoam.org/spray-foam/>.

American Conference of Governmental Industrial Hygienists (2016). 2016 TLVs and BEIs Based on the Documentation of the Threshold Limit Values for Chemical Substances and Physical Agents & Biological Exposure Indices. Cincinnati, OH, ACGIH: 272.

American Society of Heating Refrigerating and Air-Conditioning Engineers (1993). Standard 136-1993 (RA 2006) -- A Method of Determining Air Change Rates in Detached Dwellings. Ann Arbor, MI, ASHRAE. **ASHRAE 136**.

Andersson, M., R. T. Ottesen and T. Volden (2004). "Building materials as a source of PCB pollution in Bergen, Norway." Science of The Total Environment **325**(1): 139-144.

Andresen, J. A., A. Grundmann and K. Bester (2004). "Organophosphorus flame retardants and plasticisers in surface waters." Science of The Total Environment **332**(1): 155-166.

Araki, A., I. Saito, A. Kanazawa, K. Morimoto, K. Nakayama, E. Shibata, M. Tanaka, T. Takigawa, T. Yoshimura, H. Chikara, Y. Saijo and R. Kishi (2014). "Phosphorus flame retardants in indoor dust and their relation to asthma and allergies of inhabitants." Indoor Air **24**(1): 3-15.

Arnot, J. (2009). Mass Balance Models for Chemical Fate, Bioaccumulation, Exposure and Risk Assessment. Exposure and Risk Assessment of Chemical Pollution — Contemporary Methodology. L. Simeonov and M. Hassanien, Springer Netherlands: 69-91.

ASTM International (2009). ASTM D5197-09e1, Standard Test Method for Determination of Formaldehyde and Other Carbonyl Compounds in Air (Active Sampler Methodology). West Conshohocken, PA., ASTM.

ASTM International (2017a). Standard Practice for Rapid Screening of VOC Emissions from Products Using Micro-Scale Chambers. West Conshohocken, PA, 2017, ASTM International,. **ASTM D7706-17**.

ASTM International (2017b). Standard Test Method for Determining Chemical Emissions from Spray Polyurethane Foam (SPF) Insulation using Micro-Scale Environmental Test Chambers. West Conshohocken, PA, ASTM International. **ASTM D8142-17**.

ASTM International (2017c). Standard Guide for Small-Scale Environmental Chamber Determinations of Organic Emissions from Indoor Materials/Products. West Conshohocken, PA, ASTM International,. **ASTM D5116-17**.

ASTM International (2018). Standard Practice for Full-Scale Chamber Determination of Volatile Organic Emissions from Indoor Materials/Products. West Conshohocken, PA, ASTM International,. **ASTM D6670-18**.

Automated Reasoning in Chemistry. (2015). "SPARC Performs Automated Reasoning in Chemistry." Retrieved March 14<sup>th</sup>, 2015, from <http://archemcalc.com/contact-us.html>.

Bare, J. (2011). "TRACI 2.0: the tool for the reduction and assessment of chemical and other environmental impacts 2.0." Clean Technologies and Environmental Policy **13**(5): 687-696.

Bare, J. C. (2002). "TRACI, The Tool for the Reduction and Assessment of Chemical and Other Environmental Impacts." Journal of Industrial Ecology **6**(3-4): 49-78.

Batterman, S. and H. Burge (1995). "HVAC Systems As Emission Sources Affecting Indoor Air Quality: A Critical Review." HVAC&R Research **1**(1): 61-78.

Bennett, D. H. and E. J. Furtaw (2004). "Fugacity-Based Indoor Residential Pesticide Fate Model." Environmental Science & Technology **38**(7): 2142-2152.

Bennett, D. H., M. D. Margni, T. E. McKone and O. Jolliet (2002). "Intake Fraction for Multimedia Pollutants: A Tool for Life Cycle Analysis and Comparative Risk Assessment." Risk Analysis **22**(5): 905-918.

Bergh, C., R. Torngrip, G. Emenius and C. Östman (2011). "Organophosphate and phthalate esters in air and settled dust – a multi-location indoor study." Indoor Air **21**(1): 67-76.

Bevington, C., Z. Guo, T. Hong, H. Hubbard, E. Wong, K. Sleasman and C. Hetfield (2017). A Modeling Approach for Quantifying Exposures from Emissions of Spray Polyurethane Foam Insulation in Indoor Environments. Developing Consensus Standards for Measuring Chemical Emissions from Spray Polyurethane Foam (SPF) Insulation. J. Sebroski and M. Mason. Anaheim, CA, ASTM International: 199-227.

Bilan, R. A., W. O. Hafladson and D. J. McVittie (1989). "Assessment of Isocyanate Exposure during the Spray Application of Polyurethane Foam." American Industrial Hygiene Association Journal **50**(6): 303-306.

Biryol, D., C. I. Nicolas, J. Wambaugh, K. Phillips and K. Isaacs (2017). "High-throughput dietary exposure predictions for chemical migrants from food contact substances for use in chemical prioritization." Environment International **108**: 185-194.

Björklund, J., S. Isetun and U. Nilsson (2004). "Selective determination of organophosphate flame retardants and plasticizers in indoor air by gas chromatography, positive-ion chemical ionization and collision-induced dissociation mass spectrometry." Rapid Communications in Mass Spectrometry **18**(24): 3079-3083.

Bonnell, M. A., A. Zidek, A. Griffiths and D. Gutzman (2018). "Fate and exposure modeling in regulatory chemical evaluation: new directions from retrospection." Environmental Science: Processes & Impacts **20**(1): 20-31.

Booth, K., B. Cummings, W. J. Karoly, S. Mullins, W. P. Robert, M. Spence, F. W. Lichtenberg and J. Banta (2009). "Measurements of Airborne Methylene Diphenyl Diisocyanate (MDI) Concentration in the U.S. Workplace." Journal of Occupational and Environmental Hygiene **6**(4): 228-238.

Bradman, A., R. Castorina, F. Gaspar, M. Nishioka, M. Colón, W. Weathers, P. P. Egeghy, R. Maddalena, J. Williams, P. L. Jenkins and T. E. McKone (2014). "Flame retardant exposures in California early childhood education environments." Chemosphere **116**: 61-66.

Brommer, S., S. Harrad, N. Van den Eede and A. Covaci (2012). "Concentrations of organophosphate esters and brominated flame retardants in German indoor dust samples." Journal of Environmental Monitoring **14**(9): 2482-2487.

Brown, L. (2012). "LCA: Getting It Right." Retrieved September 27<sup>th</sup>, 2018, from [http://www.sustainablebrands.com/news\\_and\\_views/supplychain/lca-getting-it-right](http://www.sustainablebrands.com/news_and_views/supplychain/lca-getting-it-right).

Bureau of Economic Analysis. (2016). "Gross-Domestic-Product-(GDP)-by-Industry Data." Retrieved March 21, 2018, from [http://www.bea.gov/industry/gdpbyind\\_data.htm](http://www.bea.gov/industry/gdpbyind_data.htm).

Bureau of Economic Analysis. (2018). "Industry data - GDP by industry: value added by industry." Retrieved Aug 22<sup>nd</sup>, 2018, from <https://apps.bea.gov/iTable/iTable.cfm?ReqID=51&step=1>.

Cadogan, D. F. and C. J. Howick (2000). Plasticizers. Kirk - Othmer Encyclopedia of Chemical Technology. C. Ley. Hoboken, NJ, John Wiley & Sons, Inc: 1-30.

Carlsson, H., U. Nilsson, G. Becker and C. Östman (1997). "Organophosphate Ester Flame Retardants and Plasticizers in the Indoor Environment: Analytical Methodology and Occurrence." Environmental Science & Technology **31**(10): 2931-2936.

Carter, W., D. Luo and I. Malkina (1999). Investigate of the Atmospheric Ozone Formation Potential of Para Toluene Isocyanate and Methylene Diphenylene Diisocyanate. Riverside, California 92521, Center for Environmental Research and Technology, University of California.

Cellarius, D. (2014). "Toxic Loopholes in LEED and Environmental Product Declarations." Retrieved September 27<sup>th</sup>, 2018, from <https://content.sierraclub.org/grassrootsnetwork/documents/toxic-loopholes-leed-and-environmental-product-declarations>.

Center for the Polyurethanes Industry. (2017). "Spray Polyurethane Foam Health and Safety - Reoccupancy." Retrieved June 14<sup>th</sup>, 2017, from <https://spraypolyurethane.org/Reoccupancy>.

Centers for Disease Control and Prevention. (2012). "The Different Types of Health Assessments." Retrieved March 21, 2018, from [https://www.cdc.gov/healthylives/types\\_health\\_assessments.htm](https://www.cdc.gov/healthylives/types_health_assessments.htm).

Ciroth, A., M. Hagelüken, G. Sonnemann, F. Castells and G. Fleischer (2002a). "Geographical and technological differences in life cycle inventories shown by the use of process models for waste incinerators part I. technological and geographical differences." The International Journal of Life Cycle Assessment **7**(5): 295-300.

Ciroth, A., M. Hagelüken, G. Sonnemann, F. Castells and G. Fleischer (2002b). "Geographical and technological differences in Life Cycle Inventories shown by the use of process models for waste incinerators part II. technological and geographical differences." The International Journal of Life Cycle Assessment **7**(6): 363-368.

Civit, B., A. Arena and D. Allende (2012). "Determination of regional acidification factors for Argentina." The International Journal of Life Cycle Assessment: 1-11.

Clausen, P. A., Z. Liu, V. Kofoed-Sørensen, J. Little and P. Wolkoff (2012). "Influence of Temperature on the Emission of Di-(2-ethylhexyl)phthalate (DEHP) from PVC Flooring in the Emission Cell FLEC." Environmental Science & Technology **46**(2): 909-915.

Clausen, P. A., Z. Liu, Y. Xu, V. Kofoed-Sørensen and J. C. Little (2010). "Influence of air flow rate on emission of DEHP from vinyl flooring in the emission cell FLEC: Measurements and CFD simulation." Atmospheric Environment **44**(23): 2760-2766.

Clausen, P. A., Y. Xu, V. Kofoed-Sørensen, J. C. Little and P. Wolkoff (2007). "The influence of humidity on the emission of di-(2-ethylhexyl) phthalate (DEHP) from vinyl flooring in the emission cell "FLEC"." Atmospheric Environment **41**(15): 3217-3224.

Collinge, W., A. E. Landis, A. K. Jones, L. A. Schaefer and M. M. Bilec (2013). "Indoor environmental quality in a dynamic life cycle assessment framework for whole buildings: Focus on human health chemical impacts." Building and Environment **62**(0): 182-190.

- Cowell, W. J., H. M. Stapleton, D. Holmes, L. Calero, C. Tobon, M. Perzanowski and J. B. Herbstman (2017). "Prevalence of historical and replacement brominated flame retardant chemicals in New York City homes." Emerging Contaminants **3**(1): 32-39.
- Crespo, J. and J. Galán (1999). "Exposure to MDI during the process of insulating buildings with sprayed polyurethane foam." The Annals of Occupational Hygiene **43**(6): 415-419.
- De Haes, U., G. Finnveden, M. Goedkoop, M. Hauschild, E. Hertwich, P. Hofstetter, O. Jolliet, W. Klöpffer, W. Krewitt, E. Lindeijer, R. Müller-Wenk, S. Olsen, D. W. Pennington, J. Potting and B. Steen (2002). Life-Cycle Impact Assessment: Striving Towards Best Practice.
- Destailats, H., R. L. Maddalena, B. C. Singer, A. T. Hodgson and T. E. McKone (2008). "Indoor pollutants emitted by office equipment: A review of reported data and information needs." Atmospheric Environment **42**(7): 1371-1388.
- Dodson, R. E., L. J. Perovich, A. Covaci, N. Van den Eede, A. C. Ionas, A. C. Dirtu, J. G. Brody and R. A. Rudel (2012). "After the PBDE Phase-Out: A Broad Suite of Flame Retardants in Repeat House Dust Samples from California." Environmental Science & Technology **46**(24): 13056-13066.
- Dresen, B. and M. Jandewerth (2012). "Integration of spatial analyses into LCA—calculating GHG emissions with geoinformation systems." The International Journal of Life Cycle Assessment **17**(9): 1094-1103.
- Dressler, D., A. Loewen and M. Nelles (2012). "Life cycle assessment of the supply and use of bioenergy: impact of regional factors on biogas production." The International Journal of Life Cycle Assessment **17**(9): 1104-1115.
- EC/R Incorporated (2014). The HEM-3 User's Guide: Instructions for using the Human Exposure Model Version 1.3.1 (AERMOD version) for Single Facility Modeling. Research Triangle Park, NC, U. S. Environmental Protection Agency.
- Ecoff, S., S. Tian and J. Sebroski (2017). Prioritizing Chemical Emissions from Closed-Cell Spray Polyurethane Foam: Utilizing Micro-Scale Chamber Emission Factors and Field Measurement Data Developing Consensus Standards for Measuring Chemical Emissions from Spray Polyurethane Foam (SPF) Insulation. J. Sebroski and M. Mason. West Conshohocken, PA, ASTM International. **STP1589**: 98-118.
- Egeghy, P. P., D. A. Vallero and E. A. Cohen Hubal (2011). "Exposure-based prioritization of chemicals for risk assessment." Environmental Science & Policy **14**(8): 950-964.
- Environmental Systems Research Institute (2015). ArcGIS Desktop
- European Centre for Ecotoxicology and Toxicology of Chemicals (2004). Targeted Risk Assessment - Technical Report No. 93. Brussels, December 2004: 223.
- European Centre for Ecotoxicology and Toxicology of Chemicals. (2014). "TARGETED RISK ASSESSMENT (TRA)." Retrieved September 27<sup>th</sup>, 2018, from <http://www.ecetoc.org/tools/targeted-risk-assessment-tra/>.

European Commissions (2008). European Union Risk Assessment Report, TRIS(2-CHLORO-1-METHYLETHYL) PHOSPHATE (TCPP). Luxembourg, Office for Official Publications of the European Communities.

Finnvedcn, G. and L.-G. Lindfors (1996). "On the nordic guidelines for life cycle assessment." The International Journal of Life Cycle Assessment **1**(1): 45-48.

Freudenthal, R. I. and R. T. Henrich (1999). "A Subchronic Toxicity Study of Fyrol PCF in Sprague-Dawley Rats." International Journal of Toxicology **18**(3): 173-176.

Fromme, H., T. Lahrz, M. Kraft, L. Fembacher, C. Mach, S. Dietrich, R. Burkardt, W. Völkel and T. Göen (2014). "Organophosphate flame retardants and plasticizers in the air and dust in German daycare centers and human biomonitoring in visiting children (LUPE 3)." Environment International **71**: 158-163.

Gallego, A., L. Rodríguez, A. Hospido, M. Moreira and G. Feijoo (2010). "Development of regional characterization factors for aquatic eutrophication." The International Journal of Life Cycle Assessment **15**(1): 32-43.

García, M., I. Rodríguez and R. Cela (2007). "Microwave-assisted extraction of organophosphate flame retardants and plasticizers from indoor dust samples." Journal of Chromatography A **1152**(1): 280-286.

Georgopoulos, P. G. and P. J. Lioy (2006). "From a Theoretical Framework of Human Exposure and Dose Assessment to Computational System Implementation: The Modeling ENvironment for TOtal Risk Studies (MENTOR)." Journal of Toxicology and Environmental Health, Part B **9**(6): 457-483.

Geyer, R., J. P. Lindner, D. M. Stoms, F. W. Davis and B. Wittstock (2010). "Coupling GIS and LCA for biodiversity assessments of land use: Part 2: Impact assessment." The International Journal of Life Cycle Assessment **15**(7).

Geyer, R., D. Stoms, J. Lindner, F. Davis and B. Wittstock (2010). "Coupling GIS and LCA for biodiversity assessments of land use: Part I Inventory Modeling." The International Journal of Life Cycle Assessment **15**(5): 454-467.

Global Market Insights Inc. (2017). "Spray Polyurethane Foam Market will surpass \$2.5bn by 2024: Global Market Insights, Inc." Retrieved September 25<sup>th</sup>, 2018, from <https://globenewswire.com/news-release/2017/09/19/1124607/0/en/Spray-Polyurethane-Foam-Market-will-surpass-2-5bn-by-2024-Global-Market-Insights-Inc.html>.

Goedkoop, M., R. Heijungs, M. Huijbregts, A. De Schryver, J. Struijs and R. Van Zelm (2008). ReCiPE 2008: A life cycle impact assessment method which comprises harmonised category indicators at the midpoint and the endpoint level.

Goedkoop, M. and R. Spriensma (2001). The Eco-indicator 99, A damage oriented method for Life Cycle Impact Assessment: Methodology Annex. Utrecht, The Netherlands, PRe Consultants: 87.

Greenberg, M. M. (1998). Toxicological Review of Methylene Diphenyl Diisocyanate (monomeric MDI) and polymeric MDI (PMDI). Washington, D.C., U.S. Environmental Protection Agency, : 54.

Guinée, J. and R. Heijungs (1993). "A proposal for the classification of toxic substances within the framework of life cycle assessment of products." Chemosphere **26**(10): 1925-1944.

Guinée, J. B., M. Gorrée, R. Heijungs, G. Huppes and R. Kleijn (2001). Handbook on Life Cycle Assessment, Operational Guide to the ISO Standards, Centre of Environmental Science – Leiden University.

Guinee, J. B. and R. Heijungs (1992). Classification factors for toxic substances within the framework of life cycle assessment of products. Leiden, The Netherlands, Centre of Environmental Science Leiden University.

Gunnarsen, L., P. A. Nielsen and P. Wolkoff (1994). "Design and Characterization of the CLIMPAQ, Chamber for Laboratory Investigations of Materials, Pollution and Air Quality\*." Indoor Air **4**(1): 56-62.

Gunschera, J., S. Mentese, T. Salthammer and J. R. Andersen (2013). "Impact of building materials on indoor formaldehyde levels: Effect of ceiling tiles, mineral fiber insulation and gypsum board." Building and Environment **64**: 138-145.

Guo, Z. (2000). "Development of a Windows-based indoor air quality simulation software package." Environmental Modelling & Software **15**(4): 403-410.

Guo, Z. (2013). "A Framework for Modelling Non-Steady-State Concentrations of Semivolatile Organic Compounds Indoors – I: Emissions from Diffusional Sources and Sorption by Interior Surfaces." Indoor and Built Environment **22**(4): 685-700.

Guo, Z. (2014). "A framework for modelling non-steady-state concentrations of semivolatile organic compounds indoors – II. Interactions with particulate matter." Indoor and Built Environment **23**(1): 26-43.

Guo, Z. (2017a). IECCU- Indoor Environmental Concentrations in Buildings with Conditioned and Unconditioned Zones. Washington, D.C., U.S. Environmental Protection Agency.

Guo, Z. (2017b). Parameters (PARAMS) Program User's Guide, Version 1.0, for indoor emission source modeling. Research Triangle Park, NC, U.S. Environmental Protection Agency.

Guo, Z., X. Liu, K. A. Krebs and D. J. Greenwell (2012a). Laboratory study of polychlorinated biphenyl (PCB) contamination and mitigation in buildings – Part 1. emissions from selected primary sources. Research Triangle Park, NC, U.S. Environmental Protection Agency: 127.

Guo, Z., X. Liu, K. A. Krebs and D. J. Greenwell (2012b). Laboratory study of polychlorinated biphenyl (PCB) contamination and mitigation in buildings – Part 2. Transport from primary sources to building materials and settled dust. Research Triangle Park, NC, U.S. Environmental Protection Agency: 166.

Harder, R., H. Holmquist, S. Molander, M. Svanstrom and G. M. Peters (2015). "Review of Environmental Assessment Case Studies Blending Elements of Risk Assessment and Life Cycle Assessment." Environ. Sci. Technol. **49**(22): 13083-13093.

Hartmann, P. C., D. Bürgi and W. Giger (2004). "Organophosphate flame retardants and plasticizers in indoor air." Chemosphere **57**(8): 781-787.

Hauschild, M. (2006). "Spatial Differentiation in Life Cycle Impact Assessment: A decade of method development to increase the environmental realism of LCIA." The International Journal of Life Cycle Assessment **11**(1): 11-13.

- Hauschild, M. and J. Potting (2005). Spatial differentiation in Life Cycle impact assessment - The EDIP2003 methodology. Denmark, Danish Ministry of the Environment.
- Hauschild, M. Z., M. Huijbregts, O. Jolliet, M. Macleod, M. Margni, D. van de Meent, R. K. Rosenbaum and T. E. McKone (2008). "Building a Model Based on Scientific Consensus for Life Cycle Impact Assessment of Chemicals: The Search for Harmony and Parsimony." Environmental Science & Technology **42**(19): 7032-7037.
- Hazardous Substance Data Bank (HSDB) (2013). Tris(chloropropyl)phosphate (TCPP), CASRN: 26248-87-3. A TOXNET database. Bethesda, MD, U.S. National Library of Medicine,.
- Health and Environmental Sciences Institute. (2017). "About RISK21." Retrieved Aug 28<sup>th</sup>, 2018, from <http://risk21.org/about-risk21/>.
- Hellweg, S., E. Demou, R. Bruzzi, A. Meijer, R. K. Rosenbaum, M. A. J. Huijbregts and T. E. McKone (2009). "Integrating Human Indoor Air Pollutant Exposure within Life Cycle Impact Assessment." Environmental Science & Technology **43**(6): 1670-1679.
- Herrick, R. F., M. D. McClean, J. D. Meeker, L. K. Baxter and G. A. Weymouth (2004). "An Unrecognized Source of PCB Contamination in Schools and Other Buildings." Environmental Health Perspectives **112**(10): 1051-1053.
- Holdren, M. W., C. W. Spicer and R. M. Riggin (1984). "Gas Phase Reaction of Toluene Diisocyanate with Water Vapor." American Industrial Hygiene Association Journal **45**(9): 626-633.
- Holmgren, T., L. Persson, P. L. Andersson and P. Haglund (2012). "A generic emission model to predict release of organic substances from materials in consumer goods." Science of The Total Environment **437**: 306-314.
- Hsu, T. (2018). "Johnson & Johnson Told to Pay \$4.7 Billion in Baby Powder Lawsuit." Retrieved Aug 22<sup>nd</sup>, 2018, from <https://www.nytimes.com/2018/07/12/business/johnson-johnson-talcum-powder.html>.
- Hu, D. and K. C. Hornbuckle (2010). "Inadvertent Polychlorinated Biphenyls in Commercial Paint Pigments." Environmental Science & Technology **44**(8): 2822-2827.
- Hugo, J., S. Fishman, C. Zu and M. LaFramboise (2016). MDI hydrolysis on surfaces, The Dow Chemical Company.
- Humbert, S., R. Manneh, S. Shaked, C. Wannaz, A. Horvath, L. Deschênes, O. Jolliet and M. Margni (2009). "Assessing regional intake fractions in North America." Science of The Total Environment **407**(17): 4812-4820.
- Humbert, S., J. D. Marshall, S. Shaked, J. V. Spadaro, Y. Nishioka, P. Preiss, T. E. McKone, A. Horvath and O. Jolliet (2011). "Intake Fraction for Particulate Matter: Recommendations for Life Cycle Impact Assessment." Environmental Science & Technology **45**(11): 4808-4816.
- ICF International (2011). An Overview of Methods for EPA's National-Scale Air Toxics Assessment. P. Office of Air Quality, and Standards,. Research Triangle Park, North Carolina, U.S. Environmental Protection Agency,.

- Ilacqua, V., O. Hänninen, N. Kuenzli and M. F. Jantunen (2007). "Intake fraction distributions for indoor VOC sources in five European cities." Indoor Air **17**(5): 372-383.
- Ingerowski, G., A. Friedle and J. Thumulla (2001). "Chlorinated Ethyl and Isopropyl Phosphoric Acid Triesters in the Indoor Environment - An Inter - Laboratory Exposure Study." Indoor Air **11**(3): 145-149.
- International Agency for Research on Cancer (2015). Evaluation of five organophosphate insecticides and herbicides. The IARC Monographs Programme. Lyon, France, World Health Organization. **112**.
- International Isocyanate Institute (2003). MDI and TDI: Safety, Health and the Environment: A Source Book and Practical Guide. West Sussex, England, John Wiley & Sons Ltd.
- International Programme for Chemical Safety (1998). Flame retardants: Tris(chloropropyl) phosphate and tris(2-chloroethyl) phosphate. . Environmental Health Criteria 209. Geneva, Switzerland: 106.
- International Standard Organization (2006a). Environmental management — Life cycle assessment — Principles and framework. Switzerland, International Standard Organization. **ISO 14040**.
- International Standard Organization (2006b). Environmental management — Life cycle assessment — Requirements and guidelines. Switzerland, International Standard Organization. **ISO 14044**.
- International Trade Administration. (2018). "Chemical spotlight - The chemical industry in the United States." Retrieved Aug 22<sup>nd</sup>, 2018, from <https://www.selectusa.gov/chemical-industry-united-states>.
- Ionas, A. C., A. C. Dirtu, T. Anthonissen, H. Neels and A. Covaci (2014). "Downsides of the recycling process: Harmful organic chemicals in children's toys." Environment International **65**: 54-62.
- Isaacs, K. K., W. G. Glen, P. Egeghy, M.-R. Goldsmith, L. Smith, D. Vallero, R. Brooks, C. M. Grulke and H. Özkaynak (2014). "SHEDS-HT: An Integrated Probabilistic Exposure Model for Prioritizing Exposures to Chemicals with Near-Field and Dietary Sources." Environmental Science & Technology **48**(21): 12750-12759.
- J. Sekizawa and M. M. Greenberg (2000). Concise International Chemical Assessment Document 27 - DIPHENYLMETHANE DIISOCYANATE (MDI). Geneva, Switzerland, World Health Organization: 32.
- Jayjock, M., O. Kroner, D. Lee, A. Parker, J. Patterson, J. Reichard and A. Willis (2015). Environmental Concentrations and Consumer Exposure Data for Selected Flame Retardants (TDCPP, TCPP, TEP, TPP). J. Patterson and A. Parker. Cincinnati, OH, Toxicology Excellence for Risk Assessment.
- Jolliet, O. (2014). "The life cycle impact assessment (LCIA) method IMPACT World+." Retrieved July, 3rd, 2014, from The life cycle impact assessment (LCIA) method IMPACT World+.
- Jolliet, O., A. S. Ernstoff, S. A. Csiszar and P. Fantke (2015). "Defining Product Intake Fraction to Quantify and Compare Exposure to Consumer Products." Environmental Science & Technology.
- Jolliet, O., M. Margni, R. Charles, S. Humbert, J. Payet, G. Rebitzer and R. Rosenbaum (2003). "IMPACT 2002+: A new life cycle impact assessment methodology." The International Journal of Life Cycle Assessment **8**(6): 324-330.
- Jones, A. P. (1999). "Indoor air quality and health." Atmospheric Environment **33**(28): 4535-4564.

Kajiwara, N., Y. Noma and H. Takigami (2011). "Brominated and organophosphate flame retardants in selected consumer products on the Japanese market in 2008." Journal of Hazardous Materials **192**(3): 1250-1259.

Kalberlah, F., M. Schwarz, J. Oltmanns, E. Schmincke and B. Grahl (2015). ProScale: Basics of the Approach. Workshop: Toxicity performance assessment in sustainable construction. Brussels, Belgium.

Kanazawa, A., I. Saito, A. Araki, M. Takeda, M. Ma, Y. Saijo and R. Kishi (2010). "Association between indoor exposure to semi-volatile organic compounds and building-related symptoms among the occupants of residential dwellings." Indoor Air **20**(1): 72-84.

Katsumata, H., S. Murakami, S. Kato, K. Hoshino and Y. Ataka (2008). "Measurement of semi-volatile organic compounds emitted from various types of indoor materials by thermal desorption test chamber method." Building and Environment **43**(3): 378-383.

Kawasaki, H., T. Murai and S. Kanoh (1982). Studies on the toxicity of insecticides and food additives in pregnant rats. V. Fetal toxicity of tris-(chloropropyl)phosphate (TCPP).

Kemmlin, S., O. Hahn and O. Jann (2003). "Emissions of organophosphate and brominated flame retardants from selected consumer products and building materials." Atmospheric Environment **37**(39): 5485-5493.

Kim, S. and B. Dale (2009). "Regional variations in greenhouse gas emissions of biobased products in the United States—corn-based ethanol and soybean oil." The International Journal of Life Cycle Assessment **14**(6): 540-546.

Klepeis, N. E., W. C. Nelson, W. R. Ott, J. P. Robinson, A. M. Tsang, P. Switzer, J. V. Behar, S. C. Hern and W. H. Engelmann (2001). "The National Human Activity Pattern Survey (NHAPS): a resource for assessing exposure to environmental pollutants." Journal Of Exposure Analysis And Environmental Epidemiology **11**: 231.

Kohler, M., J. Tremp, M. Zennegg, C. Seiler, S. Minder-Kohler, M. Beck, P. Lienemann, L. Wegmann and P. Schmid (2005). "Joint Sealants: An Overlooked Diffuse Source of Polychlorinated Biphenyls in Buildings." Environmental Science & Technology **39**(7): 1967-1973.

Krone, C. A. and T. D. Klingner (2005). "Isocyanates, polyurethane and childhood asthma." Pediatric Allergy and Immunology **16**(5): 368-379.

Larry Barnthouse, J. F., Ken Humphreys, Robert Hunt, Larry Laibson, Scott Noesen, Gregory Norris, James Owens, Joel Todd, Bruce Vigon, Keith Weitz, John Young, (1997). Life-Cycle Impact Assessment: The State of the Art, 2nd edition: 145.

Lazarov, B., R. Swinnen, D. Poelmans, M. Spruyt, E. Goelen, A. Covaci and M. Stranger (2016). "Influence of suspended particles on the emission of organophosphate flame retardant from insulation boards." Environmental Science and Pollution Research **23**(17): 17183-17190.

Lesage, J., J. Stanley, W. J. Karoly and F. W. Lichtenberg (2007). "Airborne Methylene Diphenyl Diisocyanate (MDI) Concentrations Associated with the Application of Polyurethane Spray Foam in Residential Construction." Journal of Occupational and Environmental Hygiene **4**(2): 145-155.

- Lewis, R. G., C. R. Fortune, R. D. Willis, D. E. Camann and J. T. Antley (1999). "Distribution of pesticides and polycyclic aromatic hydrocarbons in house dust as a function of particle size." Environmental Health Perspectives **107**(9): 721-726.
- Lewis, W. K. and W. G. Whitman (1924). "Principles of Gas Absorption." Industrial & Engineering Chemistry **16**(12): 1215-1220.
- Li, W. and E. J. Davis (1996). "Aerosol Evaporation in the Transition Regime." Aerosol Science and Technology **25**(1): 11-21.
- Liagkouridis, I., E. Cequier, B. Lazarov, P. Cousins, C. Thomsen, M. Stranger and I. Cousins (2017). "Relationships between estimated flame retardant emissions and levels in indoor air and house dust." Indoor Air **27**(3): 650-657.
- Liagkouridis, I., A. P. Cousins and I. T. Cousins (2015). "Physical–chemical properties and evaluative fate modelling of ‘emerging’ and ‘novel’ brominated and organophosphorus flame retardants in the indoor and outdoor environment." Science of The Total Environment **524-525**: 416-426.
- Liagkouridis, I., B. Lazarov, G. Giovanoulis and I. T. Cousins (2017). "Mass transfer of an organophosphate flame retardant between product source and dust in direct contact." Emerging Contaminants **3**(3): 115-120.
- Liang, Y., O. Caillot, J. Zhang, J. Zhu and Y. Xu (2015). "Large-scale chamber investigation and simulation of phthalate emissions from vinyl flooring." Building and Environment **89**: 141-149.
- Liang, Y., X. Liu and M. R. Allen (2018a). "Measuring and modeling surface sorption dynamics of organophosphate flame retardants on impervious surfaces." Chemosphere **193**: 754-762.
- Liang, Y., X. Liu and M. R. Allen (2018b). "Measurements of Parameters Controlling the Emissions of Organophosphate Flame Retardants in Indoor Environments." Environmental Science & Technology **52**(10): 5821-5829.
- Liang, Y. and Y. Xu (2014). "Improved Method for Measuring and Characterizing Phthalate Emissions from Building Materials and Its Application to Exposure Assessment." Environmental Science & Technology **48**(8): 4475-4484.
- Liang, Y. and Y. Xu (2015). "The influence of surface sorption and air flow rate on phthalate emissions from vinyl flooring: Measurement and modeling." Atmospheric Environment **103**: 147-155.
- Lippiatt, B. C., A. L. Greig and P. D. Lavappa (2010). BEES Online: Life Cycle Analysis for Building Products. Gaithersburg, MD, National Institute of Standards and Technology.
- Little, J. C., C. J. Weschler, W. W. Nazaroff, Z. Liu and E. A. Cohen Hubal (2012). "Rapid Methods to Estimate Potential Exposure to Semivolatile Organic Compounds in the Indoor Environment." Environmental Science & Technology **46**(20): 11171-11178.
- Liu, C., G. C. Morrison and Y. Zhang (2012). "Role of aerosols in enhancing SVOC flux between air and indoor surfaces and its influence on exposure." Atmospheric Environment **55**: 347-356.
- Liu, C., S. Shi, C. Weschler, B. Zhao and Y. Zhang (2013). "Analysis of the Dynamic Interaction Between SVOCs and Airborne Particles." Aerosol Science and Technology **47**(2): 125-136.

- Liu, C., Y. Zhang, J. L. Benning and J. C. Little (2015). "The effect of ventilation on indoor exposure to semivolatile organic compounds." Indoor Air **25**(3): 285-296.
- Liu, X., M. R. Allen and N. F. Roache (2016a). "Characterization of organophosphorus flame retardants' sorption on building materials and consumer products." Atmospheric Environment **140**: 333-341.
- Liu, X., M. R. Allen and N. F. Roache (2016b). Sorption of Organophosphorus Flame Retardants on Settled Dust. 14<sup>th</sup> International Conference on Indoor Air Quality and Climate. Ghent, Belgium.
- Liu, X., Z. Guo, K. A. Krebs, D. J. Greenwell, N. F. Roache, R. A. Stinson, J. A. Nardin and R. H. Pope (2016a). "Laboratory study of PCB transport from primary sources to building materials." Indoor and Built Environment **25**(4): 635-650.
- Liu, X., Z. Guo, K. A. Krebs, D. J. Greenwell, N. F. Roache, R. A. Stinson, J. A. Nardin and R. H. Pope (2016b). "Laboratory study of PCB transport from primary sources to settled dust." Chemosphere **149**: 62-69.
- Liu, X., Z. Guo, K. A. Krebs, R. A. Stinson, J. A. Nardin, R. H. Pope and N. F. Roache (2015). "Chamber study of PCB emissions from caulking materials and light ballasts." Chemosphere **137**: 115-121.
- Liu, X., Z. Guo and N. F. Roache (2014). "Experimental method development for estimating solid-phase diffusion coefficients and material/air partition coefficients of SVOCs." Atmospheric Environment **89**: 76-84.
- Liu, Z. and J. C. Little (2012). Semivolatile organic compounds (SVOCs): phthalates and flame retardants. Toxicity of Building Materials. F. Pacheco-Torgal, S. Jalali and A. Fucic, Woodhead Publishing: 122-137.
- Liu, Z., W. Ye and J. C. Little (2013). "Predicting emissions of volatile and semivolatile organic compounds from building materials: A review." Building and Environment **64**: 7-25.
- Lucattini, L., G. Poma, A. Covaci, J. de Boer, M. H. Lamoree and P. E. G. Leonards (2018). "A review of semi-volatile organic compounds (SVOCs) in the indoor environment: occurrence in consumer products, indoor air and dust." Chemosphere **201**: 466-482.
- Mackay, D. (2001). Multimedia Environmental Models: The Fugacity Approach, Second edition. Boca Raton, FL, CRC Press.
- MacLeod, M., D. Woodfine, D. Mackay, T. McKone, D. Bennett and R. Maddalena (2001). "BETR North America: A regionally segmented multimedia contaminant fate model for North America." Environmental Science and Pollution Research **8**(3): 156-163.
- Mäkinen, M. S. E., M. R. A. Mäkinen, J. T. B. Koistinen, A.-L. Pasanen, P. O. Pasanen, P. J. Kalliokoski and A. M. Korpi (2009). "Respiratory and Dermal Exposure to Organophosphorus Flame Retardants and Tetrabromobisphenol A at Five Work Environments." Environmental Science & Technology **43**(3): 941-947.
- Manuel, J. (2011). "Avoiding health pitfalls of home energy-efficiency retrofits." Environ Health Perspect **119**(2): A76-79.
- Marć, M., B. Zabiegała and J. Namieśnik (2012). "Testing and sampling devices for monitoring volatile and semi-volatile organic compounds in indoor air." TrAC Trends in Analytical Chemistry **32**: 76-86.

- Markes International. (2018). "Micro-Chamber/Thermal Extractor." Retrieved September 24<sup>th</sup>, 2018, from <https://www.markes.com/Products/Instrumentation/Micro-Chamber-Thermal-Extractor.aspx>.
- Marklund, A., B. Andersson and P. Haglund (2003). "Screening of organophosphorus compounds and their distribution in various indoor environments." Chemosphere **53**(9): 1137-1146.
- Marklund, A., B. Andersson and P. Haglund (2005). "Organophosphorus flame retardants and plasticizers in air from various indoor environments." Journal of Environmental Monitoring **7**(8): 814-819.
- Matoba, Y., J.-i. Ohnishi and M. Matsuo (1993). "A simulation of insecticides in indoor aerosol space spraying." Chemosphere **26**(6): 1167-1186.
- Matoba, Y., J.-i. Ohnishi and M. Matsuo (1994). "Indoor simulation of insecticides supplied with an electric vaporizer by the fugacity model." Chemosphere **28**(4): 767-786.
- Matoba, Y., J.-i. Ohnishi and M. Matsuo (1995). "Indoor simulation of insecticides in broadcast spraying." Chemosphere **30**(2): 345-365.
- Matoba, Y., J. Yoshimura, J.-i. Ohnishi, N. Mikami and M. Matsuo (1998). "Development of the Simulation Model InPest for Prediction of the Indoor Behavior of Pesticides." Journal of the Air & Waste Management Association **48**(10): 969-978.
- McKone, T. E., D. Hall and W. E. Kastenberg (1997). CalTOX Version 2.3 - Description of Modifications and Revisions. Sacramento, California, The Office of Environmental Health Hazard Assessment, California Environmental Protection Agency.
- Meijer, A., M. Huijbregts, E. G. Hertwich and L. Reijnders (2006). "Including Human Health Damages due to Road Traffic in Life Cycle Assessment of Dwellings." The International Journal of Life Cycle Assessment **11**(1): 64-71.
- Meijer, A., M. Huijbregts and L. Reijnders (2005a). "Human Health Damages due to Indoor Sources of Organic Compounds and Radioactivity in Life Cycle Impact Assessment of Dwellings - Part 1: Characterisation Factors." The International Journal of Life Cycle Assessment **10**(5): 309-316.
- Meijer, A., M. Huijbregts and L. Reijnders (2005b). "Human Health Damages due to Indoor Sources of Organic Compounds and Radioactivity in Life Cycle Impact Assessment of Dwellings - Part 2: Damage Scores." The International Journal of Life Cycle Assessment **10**(6): 383-392.
- Meininghaus, R., L. Gunnarsen and H. N. Knudsen (2000). "Diffusion and Sorption of Volatile Organic Compounds in Building Materials—Impact on Indoor Air Quality." Environmental Science & Technology **34**(15): 3101-3108.
- Minegishi, K., H. Kurebayashi, S. Nambaru, K. Morimoto, T. Takahashi and T. Yamaha (1988). "Comparative Studies on Absorption, Distribution, and Excretion of Flame Retardants Halogenated Alkyl Phosphate in Rats." Eisei kagaku **34**(2): 102-114.
- Mølhave, L., G. Clausen, B. Berglund, J. Ceaurriz, A. Kettrup, T. Lindvall, M. Maroni, A. C. Pickering, U. Risse, H. Rothweiler, B. Seifert and M. Younes (1997). "Total Volatile Organic Compounds (TVOC) in Indoor Air Quality Investigations." Indoor Air **7**(4): 225-240.

- Morello - Frosch., R. A., T. J. Woodruff, D. A. Axelrad and J. C. Caldwell (2000). "Air Toxics and Health Risks in California: The Public Health Implications of Outdoor Concentrations." Risk Analysis **20**(2): 273-292.
- Moriguchi, Y. and A. Terazono (2000). "A simplified model for spatially differentiated impact assessment of air emissions." The International Journal of Life Cycle Assessment **5**(5): 281.
- Mutel, C. L. and S. Hellweg (2009). "Regionalized Life Cycle Assessment: Computational Methodology and Application to Inventory Databases." Environmental Science & Technology **43**(15): 5797-5803.
- Mutel, C. L., S. Pfister and S. Hellweg (2011). "GIS-Based Regionalized Life Cycle Assessment: How Big Is Small Enough? Methodology and Case Study of Electricity Generation." Environmental Science & Technology **46**(2): 1096-1103.
- Nagase, M., M. Toba, H. Kondo, A. Yasuhara and K. Hasebe (2003). "Estimation of Organophosphoric Acid Triesters in Soft Polyurethane Foam Using a Concentrated Sulfuric Acid Dissolution Technique and Gas Chromatography with Flame Photometric Detection." Analytical Sciences **19**(12): 1617-1620.
- National Center for Environmental Assessment (1991). Integrated Risk Information System Chemical Assessment Summary - Acetaldehyde. Washington, D.C., U.S. Environmental Protection Agency,.
- National Research Council (1994). Science and Judgment in Risk Assessment. Washington D.C., National Academies Press.
- National Research Council (2000). Toxicological Risks of Selected Flame-Retardant Chemicals. Washington, DC, The National Academies Press.
- Nazaroff, W. W. (2008). "Inhalation intake fraction of pollutants from episodic indoor emissions." Building and Environment **43**(3): 269-277.
- Neumann, C. M., D. L. Forman and J. E. Rothlein (1998). "Hazard screening of chemical releases and environmental equity analysis of populations proximate to toxic release inventory facilities in Oregon." Environmental Health Perspectives **106**(4): 217-226.
- Occupational Alliance for Risk Science (2013). Workplace Environmental Exposure Levels (WEELs) - Trans-1-Chloro-3,3,3-Trifluoropropene (1233zd(E)). Cincinnati, OH, Toxicology for Risk Assessment.
- Occupational Safety and Health Administration (1989). Sampling and Analytical Method 47: Methylene Bisphenyl Isocyanate (MDI). Washington, D.C., OSHA.
- Occupational Safety and Health Administration (1998). Permissible Exposure Limits – Annotated Tables. Washington, D.C., Department of Labor.
- Odum, J. R., J. Yu and R. M. Kamens (1994). "Modeling the Mass Transfer of Semivolatile Organics in Combustion Aerosols." Environmental Science & Technology **28**(13): 2278-2285.
- OECD (Organisation for Economic Co-operation and Development) (2000). Tris(1-chloro2-propyl)phosphate. Screening Information Data Set (SIDS). Geneva, Switzerland.
- Office Of Air Quality Planning and Standards (1999). Residual Risk Report to Congress 1999. Research Triangle Park, NC 27711, U.S. Environmental Protection Agency: 225.

Office of Air Quality Planning and Standards (2015). Technical Support Document EPA's 2011 National-scale Air Toxics Assessment. Research Triangle Park, NC 27711, U.S. Environmental Protection Agency: 361.

Office of Chemical Safety and Pollution Prevention (2017). Indoor Exposure Product Testing Protocols Version 2.0. Washington, D.C., U.S. Environmental Protection Agency,.

Office of Energy Efficiency & Renewable Energy. (2011). "Chemical industry profile." Retrieved Aug 22<sup>nd</sup>, 2018, from <https://www.energy.gov/eere/amo/chemicals-industry-profile>.

Office of Environmental Health Hazard Assessment. (2016, Jun 28<sup>th</sup>, 2016). "OEHHA Acute, 8-hour and Chronic Reference Exposure Level (REL) Summary." Retrieved Feb 28<sup>th</sup>, 2017, from <https://oehha.ca.gov/air/general-info/oehha-acute-8-hour-and-chronic-reference-exposure-level-rel-summary>.

Office of Pollution Prevention and Toxics (2013). ChemSTEER User Guide: Chemical Screening Tool for Exposures and Environmental Releases. Washington, D.C., U.S. Environmental Protection Agency,.

Olsen, S. I., F. M. Christensen, M. Hauschild, F. Pedersen, H. F. Larsen and J. Tørsløv (2001). "Life cycle impact assessment and risk assessment of chemicals — a methodological comparison." Environmental Impact Assessment Review **21**(4): 385-404.

Owens, J. W. (1997). "Life-Cycle Assessment in Relation to Risk Assessment: An Evolving Perspective." Risk Analysis **17**(3): 359-365.

Pierce, D. (2014). Expanding LEED V4 Material Health Transparency: The Lack of Toxin Reporting in ISO EPDs + LCAs is in Conflict with Truth in Advertising Law Perkins+Will and AREA Research White Paper Chicago, IL: 8.

Pizzol, M., P. Christensen, J. Schmidt and M. Thomsen (2011). "Impacts of "metals" on human health: a comparison between nine different methodologies for Life Cycle Impact Assessment (LCIA)." Journal of Cleaner Production **19**(6-7): 646-656.

Poppendieck, D. and A. Connor (2015). Measuring Flame Retardant Emissions from Spray Polyurethane Foam in a Home. U.S. Department of Commerce. Gaithersburg, MD, National Institute of Standards and Technology.

Poppendieck, D., M. Schlegel, A. Connor and A. Blickley (2017). Flame Retardant Emissions from Spray Polyurethane Foam Insulation," Developing Consensus Standards for Measuring Chemical Emissions from Spray Polyurethane Foam (SPF) Insulation. Developing Consensus Standards for Measuring Chemical Emissions from Spray Polyurethane Foam Insulation. J. Sebroski and M. Mason. Anaheim, CA, ASTM International: 57-76.

Potting, J. and M. Hauschild (1997). "Predicted Environmental Impact and Expected Occurrence of Actual Environmental Impact. Part II: spatial differentiation in life-cycle assessment via the site-dependent characterisation of environmental impact from emissions." The International Journal of Life Cycle Assessment **2**(4): 209-216.

Potting, J., M. Hauschild and H. Wenzel (1999). "'Less is better" and "only above threshold": Two incompatible paradigms for human toxicity in life cycle assessment?" The International Journal of Life Cycle Assessment **4**(1): 16-24.

Potting, J., O. Hertel, W. Schöpp and A. Bastrup-Birk (2006). "Spatial Differentiation in the Characterisation of Photochemical Ozone Formation: The EDIP2003 Methodology." The International Journal of Life Cycle Assessment **11**(1): 72-80.

Potting, J., W. Schöpp, K. Blok and M. Hauschild (1998). "Comparison of the acidifying impact from emissions with different regional origin in life-cycle assessment." Journal of Hazardous Materials **61**(1-3): 155-162.

ReportsnReports. (2018). "Polyurethane Foam Market to Grow at 8.0% Growth Rate and Projected to Reach US\$ 79.77 Billion by 2023." Retrieved September 25<sup>th</sup>, 2018, from <https://www.prnewswire.com/news-releases/polyurethane-foam-market-to-grow-at-8-0-growth-rate-and-projected-to-reach-us-79-77-billion-by-2023-829701816.html>.

Reuters. (2018). "Monsanto Ordered to Pay \$289 Million in Roundup Cancer Trial." Retrieved Aug 22<sup>nd</sup>, 2018, from <https://www.nytimes.com/2018/08/10/business/monsanto-roundup-cancer-trial.html>.

Reysa, G. (2013). "Homemade Blower Door -- Estimating Flow Rates, 50 Pa Flow, Natural Infiltration, Heat Loss, Fuel Costs, and Carbon Emissions." Retrieved March, 5<sup>th</sup>, 2017, from <http://www.builditsolar.com/Projects/Conservation/BlowerDoor/FlowRates.htm>.

Robson, M., L. Melymuk, S. A. Csiszar, A. Giang, M. L. Diamond and P. A. Helm (2010). "Continuing sources of PCBs: The significance of building sealants." Environment International **36**(6): 506-513.

Rosenbaum, R., M. J. Huijbregts, A. Henderson, M. Margni, T. McKone, D. Meent, M. Hauschild, S. Shaked, D. Li, L. Gold and O. Jolliet (2011). "USEtox human exposure and toxicity factors for comparative assessment of toxic emissions in life cycle analysis: sensitivity to key chemical properties." The International Journal of Life Cycle Assessment **16**(8): 710-727.

Rosenbaum, R. K., T. M. Bachmann, L. S. Gold, M. A. J. Huijbregts, O. Jolliet, R. Juraske, A. Koehler, H. F. Larsen, M. MacLeod, M. Margni, T. E. McKone, J. Payet, M. Schuhmacher, D. van de Meent and M. Z. Hauschild (2008). "USEtox—the UNEP-SETAC toxicity model: recommended characterisation factors for human toxicity and freshwater ecotoxicity in life cycle impact assessment." The International Journal of Life Cycle Assessment **13**(7): 532-546.

Rosenbaum, R. K., A. Meijer, E. Demou, S. Hellweg, O. Jolliet, N. L. Lam, M. Margni and T. E. McKone (2015). "Indoor Air Pollutant Exposure for Life Cycle Assessment: Regional Health Impact Factors for Households." Environmental Science & Technology **49**(21): 12823-12831.

Saad, R., M. Margni, T. Koellner, B. Wittstock and L. Deschênes (2011). "Assessment of land use impacts on soil ecological functions: development of spatially differentiated characterization factors within a Canadian context." The International Journal of Life Cycle Assessment **16**(3): 198-211.

Saito, I., A. Onuki and H. Seto (2007). "Indoor organophosphate and polybrominated flame retardants in Tokyo." Indoor Air **17**(1): 28-36.

Sala, S., D. Marinov and D. Pennington (2011). "Spatial differentiation of chemical removal rates from air in life cycle impact assessment." The International Journal of Life Cycle Assessment **16**(8): 748-760.

Salthammer, T. and T. Schripp (2015). "Application of the Junge- and Pankow-equation for estimating indoor gas/particle distribution and exposure to SVOCs." Atmospheric Environment **106**: 467-476.

Sanchez, C., M. Ericsson, H. Carlsson and A. Colmsjö (2003). "Determination of organophosphate esters in air samples by dynamic sonication-assisted solvent extraction coupled on-line with large-volume injection gas chromatography utilizing a programmed-temperature vaporizer." Journal of Chromatography A **993**(1): 103-110.

SC&A Incorporated (2017). Risk Assessment and Modeling - Human Exposure Model (HEM). Washington, D.C., U.S. Environmental Protection Agency.

Schaeffer, J. W., L. M. Sargent, D. R. Sandfort and W. J. Brazile (2013). "A Comparison of Two Sampling Methods for the Detection of Airborne Methylene Bisphenyl Diisocyanate." Journal of Occupational and Environmental Hygiene **10**(4): 213-221.

Sebroski, J., J. Miller, C. Thompson and E. Roeske (2017). Evaluation of Micro-Scale Chambers for Measuring Chemical Emissions from Spray Polyurethane Foam Insulation. Developing Consensus Standards for Measuring Chemical Emissions from Spray Polyurethane Foam (SPF) Insulation. J. Sebroski and M. Mason. West Conshohocken, PA, ASTM International. **STP1589**: 1-26.

Shah, V. and R. Ries (2009). "A characterization model with spatial and temporal resolution for life cycle impact assessment of photochemical precursors in the United States." The International Journal of Life Cycle Assessment **14**(4): 313-327.

Shin, H.-M., T. E. McKone, N. S. Tulve, M. S. Clifton and D. H. Bennett (2013). "Indoor Residence Times of Semivolatile Organic Compounds: Model Estimation and Field Evaluation." Environmental Science & Technology **47**(2): 859-867.

Skarping, G., D. Karlsson and M. Dalene (2011). Investigation of Wall Effects of MDI/MDA in Emission Chamber Testing. Hässleholm, Sweden, Institutet för Kemisk Analys Norden AB.

Sleeswijk, A. (2011). "Regional LCA in a global perspective. A basis for spatially differentiated environmental life cycle assessment." The International Journal of Life Cycle Assessment **16**(2): 106-112.

Sonnemann, G., F. Castells and M. Schuhmacher (2004). Integrated Life-Cycle and Risk Assessment for Industrial Processes. USA, Lewis Publishers.

Spadaro, J. V. and A. Rabl (1999). "Estimates of real damage from air pollution: Site dependence and simple impact indices for LCA." International Journal of Life Cycle Assessment **4**(4): 229.

Sparks, L. E., B. A. Tichenor, J. Chang and Z. Guo (1996). "Gas-Phase Mass Transfer Model for Predicting Volatile Organic Compound (VOC) Emission Rates from Indoor Pollutant Sources." Indoor Air **6**(1): 31-40.

Spray Polyurethane Foam Alliance (2012) "Life Cycle Assessment of Spray Polyurethane Foam Insulation for Residential & Commercial Building Applications."

Staaf, T. and C. Östman (2005). "Organophosphate triesters in indoor environments." Journal of Environmental Monitoring **7**(9): 883-887.

Stanek, J., S. Goldhaber, F. Stack and E. Zeiger (2008). Toxicological Review of Propionaldehyde. National Center for Environmental Assessment. Research Triangle Park, NC 27211, U.S. Environmental Protection Agency, : 78.

Stanford Research Institute (2011). Directory of chemical producers: United States of America. Menlo Park, CA, Chemical Information Services, Stanford Research Institute.

Stapleton, H. M., S. Klosterhaus, S. Eagle, J. Fuh, J. D. Meeker, A. Blum and T. F. Webster (2009). "Detection of Organophosphate Flame Retardants in Furniture Foam and U.S. House Dust." Environmental Science & Technology **43**(19): 7490-7495.

Stapleton, H. M., S. Klosterhaus, A. Keller, P. L. Ferguson, S. van Bergen, E. Cooper, T. F. Webster and A. Blum (2011). "Identification of Flame Retardants in Polyurethane Foam Collected from Baby Products." Environmental Science & Technology **45**(12): 5323-5331.

Stapleton, H. M., S. Sharma, G. Getzinger, P. L. Ferguson, M. Gabriel, T. F. Webster and A. Blum (2012). "Novel and High Volume Use Flame Retardants in US Couches Reflective of the 2005 PentaBDE Phase Out." Environmental Science & Technology **46**(24): 13432-13439.

Sundell, J. (2004). "On the history of indoor air quality and health." Indoor Air **14 Suppl 7**: 51-58.

Tajima, S., A. Araki, T. Kawai, T. Tsuboi, Y. Ait Bamai, E. Yoshioka, A. Kanazawa, S. Cong and R. Kishi (2014). "Detection and intake assessment of organophosphate flame retardants in house dust in Japanese dwellings." Science of The Total Environment **478**: 190-199.

Takigami, H., G. Suzuki, Y. Hirai, Y. Ishikawa, M. Sunami and S.-i. Sakai (2009). "Flame retardants in indoor dust and air of a hotel in Japan." Environment International **35**(4): 688-693.

Takigami, H., G. Suzuki, Y. Hirai and S.-i. Sakai (2008). "Transfer of brominated flame retardants from components into dust inside television cabinets." Chemosphere **73**(2): 161-169.

Tam, B. N. and C. M. Neumann (2004). "A human health assessment of hazardous air pollutants in Portland, OR." J Environ Manage **73**(2): 131-145.

Tan, H., C. Peng, Y. Guo, X. Wang, Y. Wu and D. Chen (2017). "Organophosphate Flame Retardants in House Dust from South China and Related Human Exposure Risks." Bulletin of Environmental Contamination and Toxicology **99**(3): 344-349.

Thatcher, T. L., A. C. K. Lai, R. Moreno-Jackson, R. G. Sextro and W. W. Nazaroff (2002). "Effects of room furnishings and air speed on particle deposition rates indoors." Atmospheric Environment **36**(11): 1811-1819.

The 61<sup>st</sup> United States Congress (1910). Federal Insecticide Act. U.S.C. United States. **6**.

The 80<sup>th</sup> United States Congress (1947). Federal Insecticide, Fungicide, and Rodenticide Act. U.S.C. **6**.

The 94<sup>th</sup> United State Congress (1976). Toxic Substances Control Act of 1976. U.S.C. **53**.

The 114<sup>th</sup> United State Congress (2016). Frank R. Lautenberg Chemical Safety for the 21st Century Act. U.S.C. Washington, D.C. **53**.

The National Institute for Occupational Safety and Health (1978). Criteria for a Recommended Standard: Occupational Exposure to Diisocyanates. DHHS (NIOSH) Publication Number 78-215. Atlanta, GA, US Department of Health, Education and Welfare.

The National Institute for Occupational Safety and Health (1996). Preventing asthma and death from diisocyanate exposure. NIOSH Alert. Morgantown, WV Centers for Disease Control and Prevention.

The National Institute for Occupational Safety and Health (2007). The NIOSH Pocket Guide to Chemical Hazards. Cincinnati, Ohio, NIOSH Publications: 2, 148, 208.

Theis, A. L., A. J. Waldack, S. M. Hansen and M. A. Jeannot (2001). "Headspace Solvent Microextraction." Analytical Chemistry **73**(23): 5651-5654.

Thinkstep. (2014). "GaBi LCA Databases." Retrieved March 21, 2018, from <http://www.gabi-software.com/databases/gabi-databases/>.

Tian, S. and M. Bilec (2018). "Integrating site-specific dispersion modeling into life cycle assessment, with a focus on inhalation risks in chemical production." Journal of the Air & Waste Management Association: 1-15.

Tian, S., S. Ecoff, J. Sebroski, J. Miller, H. Rickenbacker and M. Bilec (2018). "An indoor air quality evaluation in a residential retrofit project using spray polyurethane foam." Journal of Occupational and Environmental Hygiene **15**(5): 363-375.

Tian, S., J. Sebroski and S. Ecoff (2017). Predicting TCPP Emissions and Airborne Concentrations from Spray Polyurethane Foam Using USEPA i-SVOC Software: Parameter Estimation and Result Interpretation. Developing Consensus Standards for Measuring Chemical Emissions from Spray Polyurethane Foam (SPF) Insulation. J. Sebroski and M. Mason. West Conshohocken, PA, ASTM International. **STP1589**: 167-198.

Tisch Environmental Inc. (2003). Marple Style Personal Cascade Impactors 290 Series Operators Manual 145 S. Miami Ave. Cleves, Ohio 45002, Tisch Environmental, Inc.

Tollbäck, J., S. Isetun, A. Colmsjö and U. Nilsson (2010). "Dynamic non-equilibrium SPME combined with GC, PICI, and ion trap MS for determination of organophosphate esters in air." Analytical and Bioanalytical Chemistry **396**(2): 839-844.

Tolle, D. (1997). "Regional scaling and normalization in LCIA." The International Journal of Life Cycle Assessment **2**(4): 197-208.

Toose, L., D. G. Woodfine, M. MacLeod, D. Mackay and J. Gouin (2004). "BETR-World: a geographically explicit model of chemical fate: application to transport of  $\alpha$ -HCH to the Arctic." Environmental Pollution **128**(1-2): 223-240.

TSA Group Delft bv (2008). EUSES-the European Union System for the Evaluation of Substances EUSES 2.1.1 User Manual. Brussels, Belgium, Joint Research Center: 41.

Tury, B., D. Pemberton and R. E. Bailey (2003). "Fate and Potential Environmental Effects of Methylene-diphenyl Diisocyanate and Toluene Diisocyanate Released into the Atmosphere." Journal of the Air & Waste Management Association **53**(1): 61-66.

U.S. Environmental Protection Agency (1989). Risk Assessment Guidance for Superfund, Volume I, Human Health Evaluation Manual (Part A). Office of Emergency and Remedial Response. Washington, D.C.

U.S. environmental Protection Agency. (1996). "Technology Transfer Network: 1996 National-Scale Air Toxics Assessment - Unit Risk Estimate (URE)." Retrieved October 7<sup>th</sup>, 2018, from <https://archive.epa.gov/airtoxics/nata/web/html/gload.html>.

U.S. Environmental Protection Agency. (1999). "Estimate of Stack Heights and Exit Gas Velocities for TRI Facilities in OPPT's Risk-Screening Environmental Indicators Model, June 1999." Retrieved October 6<sup>th</sup>, 2018, from <https://www.epa.gov/rsei/estimate-stack-heights-and-exit-gas-velocities-tri-facilities-oppts-risk-screening>.

U.S. Environmental Protection Agency (2000). Simulation Tool Kit for Indoor Air Quality and Inhalation Exposure (IAQX). National Risk Management Research Laboratory. Research Triangle Park, NC: 76.

U.S. Environmental Protection Agency (2005a). Conditional Test Method 036. Washington, D.C.: 9.

U.S. Environmental Protection Agency (2005b). Human Health Risk Assessment Protocol. Office of Solid Waste and Emergency Response. Washington, D.C., U.S. Environmental Protection Agency.

U.S. Environmental Protection Agency (2011a). Exposure Factors Handbook: 2011 Edition. Office of Research and Development. Washington D.C., U.S. EPA.

U.S. Environmental Protection Agency (2011b). Methylene Diphenyl Diisocyanate (MDI) and Related Compounds Action Plan. Washington, D.C.

U.S. Environmental Protection Agency (2012a). Addendum: User's Guide for The AMS/EPA Regulatory Model - AERMOD. Office of Air Quality Planning and Standards. Research Triangle Park, NC.

U.S. Environmental Protection Agency (2012b). Estimation Programs Interface Suite™ for Microsoft® Windows, v 4.11. Washington, D.C., U.S. Environmental Protection Agency,.

U.S. Environmental Protection Agency (2012c). Provisional Peer-Reviewed Toxicity Values for Tris(1-chloro-2-propyl)phosphate (CASRN 13674-84-5). Cincinnati, OH, National Center for Environmental Assessment, Office of Research and Development.

U.S. Environmental Protection Agency. (2013a). "Polybrominated diphenylethers (PBDEs) Significant New Use Rules (SNUR)." Retrieved September 8<sup>th</sup>, 2018, from <https://www.epa.gov/assessing-and-managing-chemicals-under-tsca/polybrominated-diphenylethers-pbdes-significant-new-use>.

U.S. Environmental Protection Agency (2013b). Simulation program i-SVOC user's guide. Cincinnati, Ohio, U.S. Environmental Protection Agency.

U.S. Environmental Protection Agency. (2015a). "Assessing and Managing Chemicals under TSCA: Methylene Diphenyl Diisocyanate (MDI) and Related Compounds." Retrieved October 7<sup>th</sup>, 2018, from <https://www.epa.gov/assessing-and-managing-chemicals-under-tsca/methylene-diphenyl-diisocyanate-mdi-and-related>.

U.S. Environmental Protection Agency (2015b). PCBs in building materials - questions and answers. Washington, D.C.: 18.

U.S. Environmental Protection Agency (2015c). TSCA Work Plan Chemical Technical Supplement - Use and Exposure of the Brominated Phthalates Cluster (BPC) Chemicals Brominated Phthalates Cluster Flame Retardants. Office of Chemical Safety and Pollution Prevention. Washington, D.C.

U.S. Environmental Protection Agency. (2016a). "Human Health Risk Assessment." Retrieved September 27<sup>th</sup>, 2018, from <https://www.epa.gov/risk/human-health-risk-assessment>.

U.S. Environmental Protection Agency. (2016b). "Modifications To The 112(b)1 Hazardous Air Pollutants." Retrieved October 7<sup>th</sup>, 2018, from <https://www3.epa.gov/airtoxics/pollutants/atwsmod.html>.

U.S. Environmental Protection Agency. (2017a). "Potential Chemical Exposures From Spray Polyurethane Foam." Retrieved October 7<sup>th</sup>, 2018, from <https://www.epa.gov/saferchoice/potential-chemical-exposures-spray-polyurethane-foam#curing>.

U.S. Environmental Protection Agency (2017b). Procedures for Chemical Risk Evaluation under the Amended Toxic Substances Control Act. 40 CFR Part 702. U. S. E. P. Agency. Washington, D.C., Federal Register. **2017-01224**: 19.

U.S. Environmental Protection Agency (2017c). Technical Fact Sheet – Polybrominated Diphenyl Ethers (PBDEs). Office of Land and Emergency Management. Washington, D.C.

U.S. Environmental Protection Agency. (2018a). "Integrated risk information system (IRIS)." Retrieved August 17<sup>th</sup> 2018, from <https://www.epa.gov/iris>.

U.S. Environmental Protection Agency. (2018b). "Risk Evaluations for Existing Chemicals under TSCA." Retrieved Aug 29<sup>th</sup>, 2018, from <https://www.epa.gov/assessing-and-managing-chemicals-under-tsca/risk-evaluations-existing-chemicals-under-tsca>.

U.S. Environmental Protection Agency. (2018c). "Toxicity Forecasting: advancing the next generation of chemical safety evaluation." Retrieved September 27<sup>th</sup>, 2018, from <https://www.epa.gov/chemical-research/toxicity-forecasting>.

U.S. Environmental Protection Agency. (2018d). "Toxics Release Inventory (TRI) Program." Retrieved October 6<sup>th</sup>, 2018, from <https://www.epa.gov/fera/human-exposure-modeling-overview>.

U.S. Green Building Council (2015). Indoor air quality assessment. LEED BD+C: New Construction. Washington, D.C., USGBC.

Uhde, E. and T. Salthammer (2007). "Impact of reaction products from building materials and furnishings on indoor air quality—A review of recent advances in indoor chemistry." Atmospheric Environment **41**(15): 3111-3128.

United States Census Bureau. (2015). "Census Blocks." Retrieved March 21, 2018, from <https://www.census.gov/geo/reference/webatlas/blocks.html>.

United States Government Accountability Office (2013). Chemical Regulation: Observations on the Toxic Substances Control Act and EPA Implementation. United States Government Accountability Office. Washington, DC 20548.

Van den Eede, N., A. C. Dirtu, H. Neels and A. Covaci (2011). "Analytical developments and preliminary assessment of human exposure to organophosphate flame retardants from indoor dust." Environment International **37**(2): 454-461.

van der Veen, I. and J. de Boer (2012). "Phosphorus flame retardants: Properties, production, environmental occurrence, toxicity and analysis." Chemosphere **88**(10): 1119-1153.

Versar, I. (2007). Exposure and Fate Assessment Screening Tool (E-FAST) Version 2.0: Documentation Manual. Washington, D.C., U.S. Environmental Protection Agency,.

Vorhees, D. J., A. C. Cullen and L. M. Altshul (1999). "Polychlorinated Biphenyls in House Dust and Yard Soil near a Superfund Site." Environmental Science & Technology **33**(13): 2151-2156.

Walser, T., R. Juraske, E. Demou and S. Hellweg (2014). "Indoor Exposure to Toluene from Printed Matter Matters: Complementary Views from Life Cycle Assessment and Risk Assessment." Environmental Science & Technology **48**(1): 689-697.

Wambaugh, J. F., R. W. Setzer, D. M. Reif, S. Gangwal, J. Mitchell-Blackwood, J. A. Arnot, O. Joliet, A. Frame, J. Rabinowitz, T. B. Knudsen, R. S. Judson, P. Egeghy, D. Vallero and E. A. Cohen Hubal (2013). "High-Throughput Models for Exposure-Based Chemical Prioritization in the ExpoCast Project." Environmental Science & Technology **47**(15): 8479-8488.

Wambaugh, J. F., A. Wang, K. L. Dionisio, A. Frame, P. Egeghy, R. Judson and R. W. Setzer (2014). "High Throughput Heuristics for Prioritizing Human Exposure to Environmental Chemicals." Environmental Science & Technology **48**(21): 12760-12767.

Wang, J., Y. Wang, Z. Shi, X. Zhou and Z. Sun (2018). "Legacy and novel brominated flame retardants in indoor dust from Beijing, China: Occurrence, human exposure assessment and evidence for PBDEs replacement." Science of The Total Environment **618**: 48-59.

Wang, Q., H. Zhao, Y. Wang, Q. Xie, J. Chen and X. Quan (2017). "Determination and prediction of octanol-air partition coefficients for organophosphate flame retardants." Ecotoxicology and Environmental Safety **145**: 283-288.

Wegener Sleeswijk, A. and R. Heijungs (2010). "GLOBOX: A spatially differentiated global fate, intake and effect model for toxicity assessment in LCA." Science of The Total Environment **408**(14): 2817-2832.

Wei, G.-L., D.-Q. Li, M.-N. Zhuo, Y.-S. Liao, Z.-Y. Xie, T.-L. Guo, J.-J. Li, S.-Y. Zhang and Z.-Q. Liang (2015). "Organophosphorus flame retardants and plasticizers: Sources, occurrence, toxicity and human exposure." Environmental Pollution **196**: 29-46.

Weidema, B. P., C. Bauer, R. Hischer, C. Mutel, T. Nemecek, J. Reinhard, C. O. Vadenbo and G. Wernet (2013). The ecoinvent database: Overview and methodology, Data quality guideline for the ecoinvent database version 3. Ecoinvent Report 1(v3). St. Gallen, Swiss Centre for Life Cycle Inventories

Wenger, Y., D. Li and O. Joliet (2012). "Indoor intake fraction considering surface sorption of air organic compounds for life cycle assessment." The International Journal of Life Cycle Assessment **17**(7): 919-931.

Wensing, M., E. Uhde and T. Salthammer (2005). "Plastics additives in the indoor environment—flame retardants and plasticizers." Science of The Total Environment **339**(1): 19-40.

Weschler, C. J. (2009). "Changes in indoor pollutants since the 1950s." Atmospheric Environment **43**(1): 153-169.

Weschler, C. J. and W. W. Nazaroff (2008). "Semivolatile organic compounds in indoor environments." Atmospheric Environment **42**(40): 9018-9040.

Weschler, C. J. and W. W. Nazaroff (2010). "SVOC partitioning between the gas phase and settled dust indoors." Atmospheric Environment **44**(30): 3609-3620.

Wolkoff, P. (1995). "Volatile Organic Compounds Sources, Measurements, Emissions, and the Impact on Indoor Air Quality." Indoor Air **5**(S3): 5-73.

Wolkoff, P. (1996). A Micro Emission Cell for Measurements of Volatile Organic Compounds Emitted from Building Materials for Indoor Use - The Field and Laboratory Emission Cell ("FLEC").

Wolkoff, P. (1999). "How to measure and evaluate volatile organic compound emissions from building products. A perspective." Science of The Total Environment **227**(2-3): 197-213.

Wolkoff, P., P. Clausen, P. Nielsen, H. Gustafsson, B. Johnson and E. Rasmusen (1991). Field and Laboratory Emission Cell: FLEC. IAQ '91 Healthy Buildings. Washington, D.C., American Society of Heating, Refrigerating and Air Conditioning Engineers, Inc: 160-165.

Wolkoff, P., P. A. Clausen, P. A. Nielsen and L. Gunnarsen (1993). "Documentation Of Field And Laboratory Emission Cell "FLEC": Identification Of Emission Processes From Carpet, Linoleum, Paint, And Sealant By Modeling." Indoor Air **3**(4): 291-297.

Wood, R. D. (2017). "Center for the Polyurethanes Industry summary of unpublished industrial hygiene studies related to the evaluation of emissions of spray polyurethane foam insulation." Journal of Occupational and Environmental Hygiene **14**(9): 681-693.

World Health Organization (1989). Indoor air quality: organic pollutants. EURO Reports and Studies 111. Copenhagen, World Health Organization Regional Office for Europe.

World Health Organization. (2018). "Metrics: Disability-Adjusted Life Year (DALY)." Retrieved September 27<sup>th</sup>, 2018, from [http://www.who.int/healthinfo/global\\_burden\\_disease/metrics\\_daly/en/](http://www.who.int/healthinfo/global_burden_disease/metrics_daly/en/).

Xu, Y., E. Cohen-Hubal and C. Little John (2010). "Predicting Residential Exposure to Phthalate Plasticizer Emitted from Vinyl Flooring: Sensitivity, Uncertainty, and Implications for Biomonitoring." Environmental Health Perspectives **118**(2): 253-258.

Xu, Y., E. A. Cohen-Hubal, P. A. Clausen and J. C. Little (2009). "Predicting Residential Exposure to Phthalate Plasticizer Emitted from Vinyl Flooring: A Mechanistic Analysis." Environmental Science & Technology **43**(7): 2374-2380.

Xu, Y. and J. C. Little (2006). "Predicting Emissions of SVOCs from Polymeric Materials and Their Interaction with Airborne Particles." Environmental Science & Technology **40**(2): 456-461.

Xu, Y., Z. Liu, J. Park, P. A. Clausen, J. L. Benning and J. C. Little (2012). "Measuring and Predicting the Emission Rate of Phthalate Plasticizer from Vinyl Flooring in a Specially-Designed Chamber." Environmental Science & Technology **46**(22): 12534-12541.

Xu, Y. and J. Zhang (2011). "Understanding SVOCs." ASHRAE Journal **53**(12): 2-5.

Yan, W., Y. Zhang and X. Wang (2009). "Simulation of VOC emissions from building materials by using the state-space method." Building and Environment **44**(3): 471-478.

Yang, F., J. Ding, W. Huang, W. Xie and W. Liu (2014). "Particle Size-Specific Distributions and Preliminary Exposure Assessments of Organophosphate Flame Retardants in Office Air Particulate Matter." Environmental Science & Technology **48**(1): 63-70.

Yu, C. and D. Crump (1998). "A review of the emission of VOCs from polymeric materials used in buildings." Building and Environment **33**(6): 357-374.

Yu, C. W. F. and D. R. Crump (2003). "Small Chamber Tests for Measurement of VOC Emissions from Flooring Adhesives." Indoor and Built Environment **12**(5): 299-310.

Yurika, N., L. J. I., N. G. A., W. Andrew, H. Patrick and S. J. D. (2002). "Integrating Risk Assessment and Life Cycle Assessment: A Case Study of Insulation." Risk Analysis **22**(5): 1003-1017.

Zelm, R., M. J. Huijbregts and D. Meent (2009). "USES-LCA 2.0—a global nested multi-media fate, exposure, and effects model." The International Journal of Life Cycle Assessment **14**(3): 282-284.

Zhang, X., M. L. Diamond, C. Ibarra and S. Harrad (2009). "Multimedia Modeling of Polybrominated Diphenyl Ether Emissions and Fate Indoors." Environmental Science & Technology **43**(8): 2845-2850.

Zhou, L., M. Hiltcher, D. Gruber and W. Püttmann (2017). "Organophosphate flame retardants (OPFRs) in indoor and outdoor air in the Rhine/Main area, Germany: comparison of concentrations and distribution profiles in different microenvironments." Environmental Science and Pollution Research **24**(12): 10992-11005.